DISTAV
Dipartimento di Scienze della Terra, dell'Ambiente e della Vita
Università degli Studi di Genova

Ph.D. course of Science and technology for environment and territory
Curriculum: Marine Science
XXXIII Cycle

Vibrio interactions with bivalve hemocytes and analysis of the *Crassostrea gigas* microbiota

Coordinator: Prof. Luigi Vezzulli, Prof.ssa Carla Pruzzo

Candidate: Dott. Alessio Borello

INDEX

Summary and Objectives

My PhD project aimed at investigating the molecular mechanisms at the basis of the interaction between *Vibrio* bacteria and shellfish in the bivalve models *Crassotrea gigas* and *Mytilus galloprovincialis* and to study the composition and dynamics of bivalve microbiota.

Previous studies suggested that persistence of entrapped bacteria inside bivalve tissues depends, at least in part, on their capacity to survive to the hemolymph bactericidal activity, that is exerted by both hemocytes and serum soluble factors. In the first part of my PhD work, hemocytes of *M. galloprovincialis* were challenged with different pathogenic *Vibrio* strains (*V. aestuarianus* 01/032, *V. aestuarianus* 02/041, *V. tasmaniensis* LGP32, *V. harveyi* VH2, *V. tapetis* CECT 4600 and *V. coralliilyticus* ATCC BAA 450) in the presence or in the absence of the extrapallial protein present in *M. galloprovincialis* serum (MgEP), and of the whole hemolymph serum. In addition, *C. gigas* hemocytes were exposed to the bivalve pathogens *V. aestuarianus* 01/032 and *V. aestuarianus* 02/041 under the same conditions to better understand molecular basis of bacteria-hemolymph interactions in oysters. We observed that MgEP promotes D- mannose sensitive adhesion to and killing by hemocytes of the bivalve pathogens *V. aestuarianus* 01/032, *V. aestuarianus* 02/041, *V. tasmaniensis* LGP32 and *V. coralliilyticus* ATCC BAA 450. In addition, in the presence of *M. galloprovincialis* EP protein (MgEP), *C. gigas* haemocytes killed *V. aestuarianus* 01/032 and *V. aestuarianus* 02/041 almost as efficiently as mussel phagocytes. These findings suggest that the different sensitivity of *Vibrio* strains to the antibacterial activity of oyster (susceptible to *Vibrio* infection) and mussel (resistant to *Vibrio* infection) haemolymph might partly depend on the fact that *C. gigas* serum lacks MgEP-like opsonins. These results may have important implications for improving bivalve depuration strategies and prevent diseases affecting bivalve production worldwide.

In the second part of my thesis work, I studied the microbial communities associated to contrasting *C. gigas* samples collected during mortality episodes in different European sites. Real-time PCR targeting oyster pathogens (e.g. Ostreid herpesvirus 1 [OshV-1] and *V. aestuarianus*) and 16SrRNA gene-based microbial profiling were applied on a large number of *C. gigas* samples (n=525 and n=101 for qPCR and 16SrRNA gene profiling analysis, respectively) to extensively investigate the patterns and dynamics of oyster microbiota during mortality events. Comparative analysis of contrasting (e.g. infected vs not infected) *C. gigas*

samples conducted using these methods revealed that oyster experiencing mortality outbreaks displayed signs of microbiota disruption associated with the presence of previously undetected potential pathogenic microbial species mostly belonging to genus Vibrio and Arcobacter. This represents to our knowledge, the largest study conducted so far to determine the composition and dynamics of farmed oyster microbiota.

1. INTRODUCTION

1.1 The *Vibrio* genus

The genus name *Vibrio* was coined by Pacini in 1854 during his study on cholera disease and it comes from these bacteria movement that appears like a vibration at microscope (Farmer III *et al.*, 2006). Vibrios are Gram-negative bacteria ubiquitary of the marine and estuarine waters, curved rod-shape 1.4-2.6 µm wide and motile by a single polar flagellum. They are facultative anaerobe capable of fermentative and respiratory metabolism, oxidase-positive, chiefly halophic and grow well at neutral and alkaline pH values up to 9 (Tantillo *et al.*, 2004; Igbinosa *et al.*, 2008). *Vibrio* species keep 2 chromosomes each of them with a distinct and independent origin of replication (Rasmussen et al., 2007). They are not able to form spore but they can enter the "Viable But Not Culturable" state (VBNC) as a survival strategy in the environment also for years (Colwell *et al.*, 1994; Lipp *et al.*, 2002). VBNC cells are in a dormant stage, are still alive but do not replicate (not culturable); however, they can re-growth if exposed to appropriate stimuli (Oliver *et al.*, 1991; Gauthier, 2000). An important aspect of this state is the possibility to maintain some virulence aspects: VBNC *Vibrio cholerae* O1 cells retain the ability to adhere to intestinal cells and, after reactivation, can cause disease (Colwell *et al.*, 1994).

Vibrio genus includes more than 100 species, some of them are pathogenic for humans (*V. cholerae*, *Vibrio vulnificus*, *Vibrio parahaemolyticus*) others for marine invertebrates and vertebrates (*e.g.*, *Vibrio coralliilyticus* for corals, *Vibrio aestuarianus* for oysters, *Vibrio tapetis* for clams) (Austin 2005; Paillard *et al.*, 2004; Thompson *et al.*, 2004a; Chakraborty *et al.*, 1997).

Several *Vibrio* species have been isolated as natural component of some mollusc's microbiota, nevertheless they may also act as opportunistic pathogens e.g., when environmental

conditions are not optimal or when they infect an immune-compromised host (Saulnier *et al*., 2010). *V. aestuarianus* and some species of *Splendidus* clade, ubiquitous in different geographic areas, such as USA, Europe, China and New Zealand (Tison and Seidler, 1983; Eiler *et al*., 2006; Garnier *et al*., 2008; Zhang *et al*., 2011; Keeling *et al*., 2014; Romero *et al*., 2014; Scarano *et al*., 2014), are associated with oyster mortality outbreaks; however, they have been also found in healthy and moribund *Crassostrea gigas* (EFSA 2015).

The bacterial disease brown ring disease (BRD) was caused by *Vibrio tapetis,* appeared in moribund clams exhibited a brown conchiolin deposit on the inner face of the shell, within the extrapallial space.

The *Vibrio* spp concentration in the aquatic environment is related to different environmental variables, such as temperature, salinity, pH and presence of planktonic organisms. Most Vibrios prefer warm temperatures for growth as it is evident during Summer when their concentration drastically increases. Optimal salinity values are usually between 5 and 25/00, but the tolerance can change between species (*V. cholerae* can survive from 0 and 45/00 salt concentration) (Singleton *et al*., 1982, Lipp *et al*., 2002). Others environmental factors operate as limiting factors. For instance, iron is a fundamental nutrient for bacteria and algae in the water environment; *V. cholerae* can produce an iron-chelanting siderophores to take up insoluble iron from the environment (Payne and Finkelstein 1976).

A relevant feature that influences survival and concentration of Vibrios in the environment is the capability to interact with living and non-living substrates (Pruzzo *et al*., 2008). As usual for bacteria, Vibrios adhering to these substrates can survive longer in hostile environment (*e.g*., in the presence of antibacterial factors or facing bivalve immunity system) than free-living form. Adhering bacteria can also participate to biofilm formation.

1.2 *Vibrio* species pathogenic for bivalves

Diseases caused by infectious agents pose threats to aquaculture worldwide. Cultivated oysters represent the main aquacultural production species of France and China and are at risk to such infections in their rearing environment. Many oyster diseases have been reported to be caused by protozoa, fungi, viruses (Elston, 1993, McGladdery, 1999) as well as by bacteria, which were initially described mainly in larval stages of hatchery-produced oysters (Sinderman, 1990).

Among the different biotic factors with incidence on massive oyster mortalities, Vibrios are one of the main biotic factors of these outbreaks. Several species have been isolated during these events and associated to mortalities: *V. aestuarianus* and the different species of *V. splendidus* clade were the most common, although other Vibrio spp. were isolated such as *Vibrio harveyi*, *Vibrio tubiashii and Vibrio alginolyticus* (summarized in Alfaro *et al*., 2018). *Vibrio aestuarianus* is a naturally occurring gram-negative bacterium, widely spread in marine ecosystems (Tison *et al*., 1983). Recent epidemiological studies conducted during recurrent summer mortality events of *Crassostrea gigas* oysters along the French Atlantic coast have also documented the predominance of this bacterial species in the hemolymph of diseased animals and have demonstrated its pathogenicity to *C. gigas* by experimental challenge (Garnier *et al*., 2007; Labreuche *et al*., 2006).

Some *V. aestuarianus* strains were identified as the main bacteria pathogens causing *C. gigas* mortalities in different European aquaculture settings.

V. aestuarianus has frequently been associated with massive mortality events in *C. gigas* oysters occurring during summer. These events often occur when seawater temperatures reach 19 °C on the French Atlantic coast and affect mainly young individuals of 1 to 2 years in age (Garnier *et al*., 2007). Previous studies designed to understand *V. aestuarianus* pathogenicity mechanisms have shown that one of the isolated strains, named 01/32, secretes extracellular products (ECPs) which induce immunosuppressant activities on *C. gigas* hemocyte functions in vitro and display lethality to oysters in vivo (Labreuche *et al*., 2006).

This *V. aestuarianus* strain (01/32) was shown to impair the function and survival of immuno-competent cells, known as hemocytes, by producing toxins.

Treatment of hemolymph in vitro with extracellular products produced by this pathogenic strain was shown to induce a significant inhibition of both hemocyte adhesive properties and phagocytosis, and an enhancement of reactive oxygen species (Labreuche *et al*., 2006a). Similar results were found with an in vivo approach performed by experimental infection using the 01/32 bacterial strain, which also demonstrated a deregulation in the hemocyte oxidative metabolism (Labreuche *et al*., 2006b).

During the time course of infection, this bacterial isolate was also reported to circumvent the host cellular immune defenses (Labreuche *et al*., 2006). However, the mechanisms and bacterial effector(s) responsible for these immunomodulatory and toxic effects remain poorly understood.

Among the 12 virulent strains found, one of the highly virulent strains resulted *V. aestuarianus* subsp. *francensis* (02/041) with 80% of mortalities by injection of 100 bacteria/animal (Goudenège et al., 2015).

As reported above and shown in Figure 1, *Vibrio* spp., including species associated to *C. gigas* outbreaks, can adhere and accumulate on both chitin surfaces and marine organisms (Vezzulli *et al.,* 2014). These aquatic substrates, like marine snow (a shower of organic material falling from upper waters to the deep ocean), chitin particles and zoo/phytoplankton, may accumulate large communities of bacteria including oyster pathogens (*e.g*., *V. aestuarianus* or *Splendidus* clade spp.). Inside the community, pathogens can increase their virulence potential by quorum sensing, enhancing gene expression of virulence factors. In addition, colonized substrates when filtered by the bivalve may introduce inside the animal high amount of pathogens favouring the infection.

It has been demonstrated that the human pathogen *V. cholerae* can reach concentration of 10^3 – 10^5 on a single copepod; since the requisite infectious dose for clinical cholera is 10^6 bacteria/ml, ingestion of untreated water containing colonized copepods could initiate the disease (Cash *et al.,* 1974; Colwell *et al.,* 1992).

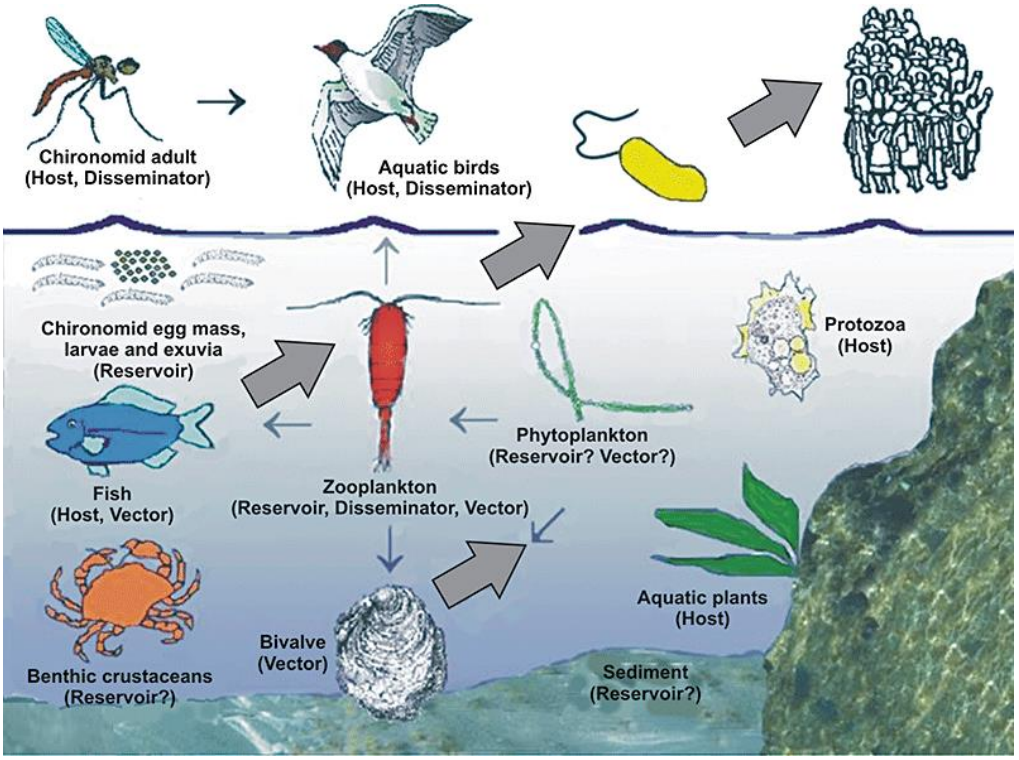

Figure 1. Variety of reservoir and vector of V. cholerae in the marine environment (Vezzulli et al., 2010)

1.3 Farmed Bivalves used as model to study *Vibrio* infections

Bivalvia is the second largest class of *Mollusca* and it counts 9200 species of filter feeders. This class includes clams, oysters, cockles, mussels, scallops and numerous other families that live in saltwater, as well as a number of families that live in freshwater. The shell is made of calcium carbonate and enclose the animal body. The name *Bivalvia* comes from the division of the shell in two valves joined together along one edge (the hinge line) by a flexible ligament that, usually in conjunction with interlocking "teeth" on each of the valves, forms the hinge.

Bivalve farming has become one of the largest aquaculture activities in the world and represents a major contribution to the socioeconomic development of coastal regions (Renault, 1996; Paillard *et al*., 2004). During the development of this activity, several countries have been faced with infectious diseases of varying severity and duration affecting farmed animals. Involved aetiological agents include *Vibrio* species, which are present in large numbers in coastal waters and are accumulated inside bivalves as a consequence of their filter-feeding habit.

1.4 Mytilus galloprovincialis

Mytilus galloprovincialis is a species of bivalve, a marine mollusc in the family Mytilidae. This animal grows up to 140 mm in length. It is a smooth-shelled mussel with a slightly broader base than that of the black mussel (*Choromytilus meridionalis*), with which it is often confused in South Africa. Its shell is blue-violet or black, but may shade to light brown. The morphology is extremely variable in shape and colour because some shells have a pattern of radiating striae on a pale, often olive background. Most shells are smooth and relatively thin, but some populations have a rough surface due to heavy growth lines. These shells can be fairly thick. The periostracum is often intact, but in some conditions it may be absent, leaving the blue shell unprotected against erosion. Mediterranean specimens are usually large, flat, and have more concave basal line, giving the shell a rounded shape and may regard a separate species, a subspecies or a form of *Mytilus edulis* (fao.org) (Figure 2).

Figure 2. Mytilus galloprovincialis shell (fao.org).

The exact range of *M. galloprovincialis* is not known because of the confusion with other, very similar *Mytilus*. In Europe it lives on all coasts that have hard substrates. Intertidal to 40 m deep attached by byssus threads to rocks and piers, within sheltered harbours and estuaries and on rocky shores of the open coast, sometimes living in dense masses wherever there are suitable surfaces for attachment. The diet of mussels consists of phytoplankton and detritus filtered from the surrounding water. The dimensions of the species is greatly influenced by its biotope: intertidal shells often remain small, rarely exceding 6 cm, while deep-water shells easily measure 9 cm.

Mytilus galloprovincialis is mainly cultured in coastal waters from Galicia (NW Spain) to the northern shores of the Mediterranean Sea. However, production has also been reported from some southern Mediterranean countries, the Russian Federation, Ukraine, and South Africa. This species is also cultured in China.

1.5 Crassostrea gigas

Crassostrea gigas is an oyster native to the Pacific coast of Asia. It has become an introduced species in North America, Australia, Europe, and New Zealand; it has solid shell, inequivalve and extremely fluted. As showed in Figure 3, the left or lower valve is deeply cupped and this distinctive tract granted it the name of Pacific cupped oyster (FAO 2014).

Figure 3. Oyster Crassostrea gigas shell. The right valve is flat while the left one is concave (Wikipedia)

As reported in 2014 FAO document, this oyster usually lives attached to rocks, debris or other oyster shells in different type of bottoms: from lower intertidal zone 40m to mud or sand-muds bottoms. *C. gigas* is a resilient animal that can survive in different environmental conditions: it can survive in a wider salinity spectrum from 10 to 35‰ salinities. Likewise, the Pacific cupped oyster has a wide temperature range of survivability, from -1.8°C to 35°C.

Pacific oysters are protandrous hermaphrodites, most commonly maturing first as males. In areas with good food supply the sex ratio in older oysters shows a predominance of females, whereas the reverse is true in areas of low food supply; females can revert back to male when food supply is limiting.

The molluscs cultivation is a worldwide economic activity, among them the main bivalve species cultured in the world are clam (36%), oyster (35%), scallop (14.6%) and mussel (14.4%). Global bivalve aquaculture production has increased over the last 20 years, recently slowed, reaching to 13 million tons per year that represents for a total value of US$13.8 billion. Along with fisheries, aquaculture ensures the income of 10–12% of the world's population (Rees J. *et al*., 2010, FAOSTAT 2012).

Among oyster species, *C. gigas* is the most important cultured spp. that was introduced in west coast of United States from Japan in the 1920s and in France in 1966 (FAO 2014). The aquaculture of this spp. represents 97% of the oyster worldwide production (mainly from China, Japan, Republic of Korea and France) followed by *Ostrea edulis*.

1.6 Bivalve Haemolymph and interactions with in*fecting vibrios*

Vibrio strains belonging to *Vibrio aestuarianus* and *Vibrio harveyi* species and Splendidus clade, together with the ostreid herpes virus designed OsHV-1, are the most common microorganisms associated to the syndrome known as 'summer mortality' (Figure 4) affecting production of *Crassostrea gigas* oyster worldwide (Lacoste *et al*., 2001; Waechter *et al*., 2002; Gay *et al*., 2004; Garnier *et al*., 2007; Segarra *et al*., 2010; Schikorski *et al*., 2011; Aboubaker *et al*., 2013; Wendling *et al*., 2014).

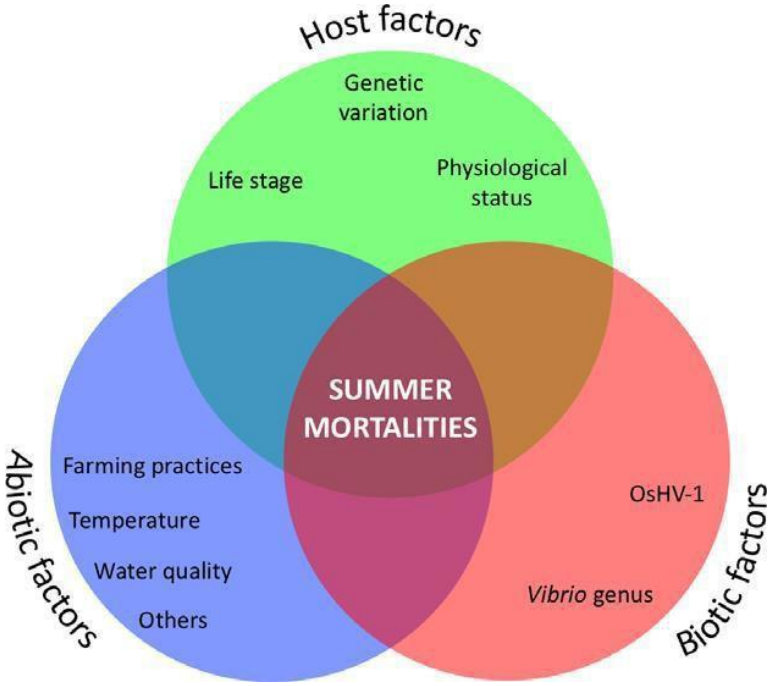

Figure 4. Venn diagram of main factors that contribute to mass mortality (Alfaro et al., 2018)

In particular, epidemiological studies conducted during recurrent summer mortality events of *C. gigas* along the French Atlantic coast documented the predominance of *V. aestuarianus* in

the haemolymph of diseased animals; moreover, its pathogenicity to *C. gigas* has been demonstrated by experimental challenge (Labreuche *et al*., 2010).

In contrast to the oyster *C. gigas*, the mussel *Mytilus* spp is considered to be particularly resistant to microbial infection (Labreuche *et al*., 2006). For example, *V. aestuarianus* isolates were only moderately pathogenic to *Mytilus galloprovincialis* compared with *C. gigas* (Garnier *et al*., 2007; Romero *et al*., 2014). The different sensitivity to infection exhibited by the two bivalve species may depend, at least in part, on their different capability to kill invading pathogens through the action of cellular (haemocytes) and soluble (e.g. enzymes, opsonizing molecules) components of their blood, the haemolymph (Mitta *et al*., 2000; Canesi *et al*., 2002; Pruzzo *et al*., 2005).

In bivalves, immunity involves both cell-mediated and humoral systems that operate in a co-ordinated way to provide protection from invading microorganisms. Cellular responses are carried out by circulating haemocytes that can kill microbes through phagocytosis and various cytotoxic reactions, such as the release of lysosomal enzymes and anti-microbial peptides and the respiratory burst which involves the production of oxygen metabolites (Cheng, 1975; 1984; Fryer and Bayne, 1996; Hine, 1999; Canesi *et al*., 2002a). The fluid portion, or haemolymph serum, contains a low amount of proteins including soluble lectins, lysosomal enzymes (e.g. acid phosphatase, lysozyme) and various anti-microbial peptides (Sminia *et al*., 1979; Leippe and Renwrantz, 1988; Pipe, 1990a; Leclerc, 1996; Carballal *et al*., 1997; Tunkijjanukij *et al*., 1998; Mitta *et al*., 2000). Microbial killing results from the combined action of the haemocytes and humoral defence factors.

There are two elements involved in this system: the hemocytes, cells responsible for cellular defense mechanism (*i.e.* phagocytosis, production of reactive oxygen intermediates and release of lysosomal enzymes) and humoral defense factors, such as opsonin and hydrolytic enzymes (Olafsen *et al.*, 1993) (Figure 5).

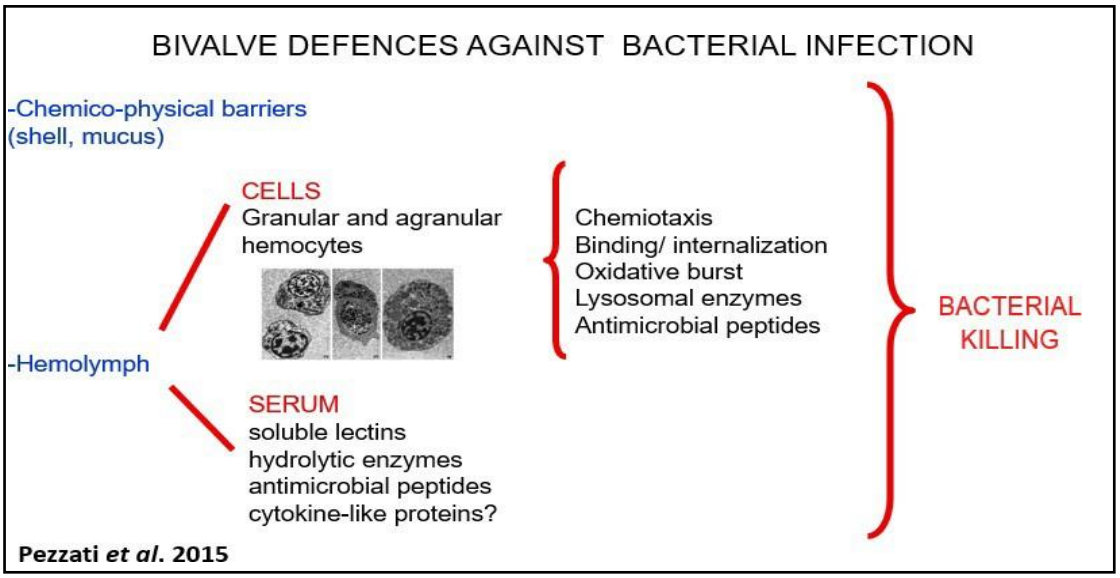

Figure 5. Persistence of bacteria in bivalves largely depends on their sensitivity to the hemolymph bactericidal activity.

Bivalves are filter feeding organisms that can concentrate high amount of particles present in ambient water, including microorganisms. Bacteria have different capability to persist inside bivalves; if they are capable to persist they can reach concentrations dangerous for humans if mussels are ingested raw or partially cooked (Pezzati *et al.*, 2015).

Different factors affect bacterial persistance inside bivalve. One of the most important is sensitivity to the hemolymph bactericidal activity (Pezzati *et al.*, 2015; Canesi *et al*., 2016).

Bivalve molluscs have an open circulatory system where the hemolymph, passing out the open end or arteries, bathes all organs before returning to the heart. Hemolymph blood cells (hemocytes) and soluble factors operate in a co-ordinated way to provide protection from invading micro-organisms. Microbial killing results from the combined action of the hemocytes and humoral defence factors (Canesi *et al*., 2002).

Bacteria show different capacities to survive hemocyte phagocytosis as consequence of the different ability to attract phagocytes, interact with opsonizing molecules, bind hemocytes and survive intracellular killing (Canesi *et al.*, 2002).

2. RESULTS

2.1 Vibrio interactions with bivalve hemocytes and role of the MgEP protein

2.1.1 Introduction

Vibrio species, which are present in large numbers in large numbers in coastal waters, are accumulated inside bivalves as a consequence of their filter-feeding habit.

In contrast to the oyster *C. gigas*, the mussel *Mytilus* spp., is considered to be particularly resistant to microbial infection (Labreuche *et al*., 2006). The different sensitivity to infection exhibited by the two bivalve species may depend, at least in part, on their different capability to kill invading pathogens through the action of cellular (haemocytes) and soluble (e.g. enzymes, opsonizing molecules) components of their blood, the haemolymph (Mitta *et al*., 2000; Canesi *et al*., 2002; Pruzzo *et al*., 2005). However, comparative studies on these aspects are still scarce.

A more recent study showed that *V. aestuarianus* 01/032 was efficiently internalized by *M. galloprovincialis* haemocytes, without inducing stressful conditions and stimulating the release of hydrolytic enzymes (lysozyme) as a rapid antibacterial response (Balbi *et al*., 2013). In contrast, in *C. gigas* haemocytes, this strain induced severe lysosomal destabilization and did not elicit lysozyme release (Balbi *et al.*, 2013). In order to partly decipher the cellular and molecular mechanisms underlying the different capability of bivalve species to resist infection, a comparative study was performed on both the capability of this bacterium and other vibrios to interact with haemocytes from *M. galloprovincialis* mussel and *C. gigas* oyster and the role played by haemolymph soluble factors in such interactions. Given that previous studies showed that *M. galloprovincialis* serum soluble factors specifically bind mannose-sensitive bacterial ligands (e.g. mannose-sensitive haemagglutinin (MSHA) pilus of *Vibrio cholerae*), particular attention was given to the role of mannose-sensitive interactions in vibrios adhesion to and sensitivity to killing by bivalve haemocytes. In this work, the adhesion and the sensistivity to killing of Vibrio strains of interest involved in bivalve

diseases (*V. aestuarianus* 02/041, *V. harveyi* VH2, V. *tasmaniensis* LGP 32, *V. tapetis* CECT 4600 and *V. coralliilyticus* ATCC BAA 450) to hemocytes of *M. galloprovincialis.* After these preliminary experiments, Vibrio strains that gave more interesting results (such as *V. aestuarianus* 02/041) were tested *in vitro* with *C. gigas*. To this aim, hemocytes were exposed to bacteria in the presence and in the absence of hemolymph serum and the purified opsonin MgEP (*Mytilus galloprovincialis* extrapallial protein) from mussels hemolymph. The adhesion was measured by quantifying bacteria cells through Real Time PCR specific protocols for each bacteria strain, and the sensitivity of bacteria to killing by hemocytes was evaluated by counting of CFU on agar plates.

2.1.2 Experimental procedures

Bacteria and culture conditions

Vibrio strains tested for the killing and adhesion experiments (*Vibrio aestuarianus* 02/041, *Vibrio tapetis* CECT 4600, *Vibrio harveyi* VH2, V. *tasmaniensis* LGP 32 and *Vibrio coralliilyticus* ATCC BAA 450) were kindly provided by IFREMER Institute (La Tremblade, France).

Bacteria were cultured overnight under constant shaking at 20°C in Zobell medium broth (Scharlau, Italy). Cells were harvested after centrifugation at 4500 x g for 10 min and the resulting pellet was washed twice and resuspended in Artificial Sea Water (ASW) (35 ppt or 31 ppt salinity) to the concentration of about $1x10^9$ CFU/ml. Thiosulfate Citrate Bile salts Sucrose (TCBS) agar and Marine agar medium (Scharlau, Italy) were also used for isolation of Vibrio colonies.

Bivalve stabulation

Mussels (*M. galloprovincialis* Lam), 4–5 cm long, originating from an aquaculture farm (Arborea, OR, Italy) and taken from a local market. The bivalves were well cleaned from any epibionts and washed with fresh ASW (salinity 35 ppt) at 18°C, and were kept for 24 hours in static tanks containing aerated ASW, salinity 35 ppt (1 l mussel−1) at 18°C.

Adult oysters (*C. gigas* oysters), originating from Bay of Biscay (La Rochelle, France) length 8-10 cm and weight 71.7-116.4 gr, were taken from local market. The bivalves were well cleaned from any epibionts and washed with fresh ASW (salinity 31 ppt) at 18°C. After the cleaning, the oysters were stabulated for 24 hours in static tanks containing aerated ASW, salinity 31 ppt (2 l oyster−1) at 18°C.

Haemolymph collection, serum and haemocytes preparation

Haemolymph was extracted from the posterior adductor muscle using a sterile 1 ml of syringe with an 18 G1/200 needle. With the needle removed, haemolymph was filtered through a sterile gauze and pooled in 50 ml Falcon tubes at 18°C. Haemolymph serum was obtained by centrifugation of whole haemolymph at 100 × g for 10 min, and the supernatant was sterilized through a 0.22 mm pore filter.

To prepare haemocyte monolayers, haemolymph aliquots (approximately 500 µl, containing about 2–5 × 10^6 cells) were seeded onto the wells of 24 well microtitre plates. The plates were incubated at 18°C for 40 min. Non-adherent haemocytes were removed by gently washing the preparations three times with 500 µl of ASW (Zampini *et al.*, 2003). Haemolymph sampling and preparation of haemocyte monolayers for mussels, oysters and clams were performed as described above.

Purification of mussel serum component(s) by ConA-sepharose affinity column

The protocol of purification of mussel serum component(s) was the same as described in Pezzati *et al*., 2015. Haemolymph serum (30 ml) was concentrated 10-folds using Amicon Ultra centrifugal filters (molecular mass cut-off 10 kDa; Millipore Corporation, MA, USA) and added with 13 ml of binding buffer (phosphate buffer 0.1 M, NaCl 0.3 M, $MnCl_2$ 0.76 mM, $CaCl_2$ 0.4 mM, pH 7.2). The sample was applied to a ConA-sepharose affinity column (Ge Healthcare, Italy) previously washed with binding buffer (Figure 6).

The column was washed with wash buffer and bound material then eluted with 0.5 M D-mannose in 0.2 M NaCl.

Figure 6. Purification system of mussel serum by using ConA-sepharose affinity column. The tube containing the concentrated mussel serum (about 2 ml) and 13ml of binding buffer ml of Haemolymph serum is applied to the ConA-sepharose affinity column by using a pump (the flow was setted at a constant speed of 0,5 ml/min).

The resulting eluate was passed through a PD-10 desalting column (Ge Healthcare), lyophylized and resuspended in PBS (0.1 M KH_2PO_4, 0.1 M Na_2HPO_4, 0.15 M NaCl, pH 7.3) in order to obtain the same protein concentration as that of native serum sample. This concentration was utilized for all subsequent experiments. Samples were subjected to 10% sodium dodecyl sulfate-polyacrylamide gel electrophoresis (SDS-PAGE) (Laemli, 1970) (Figure 7). Proteins were visualized by blue Comassie.

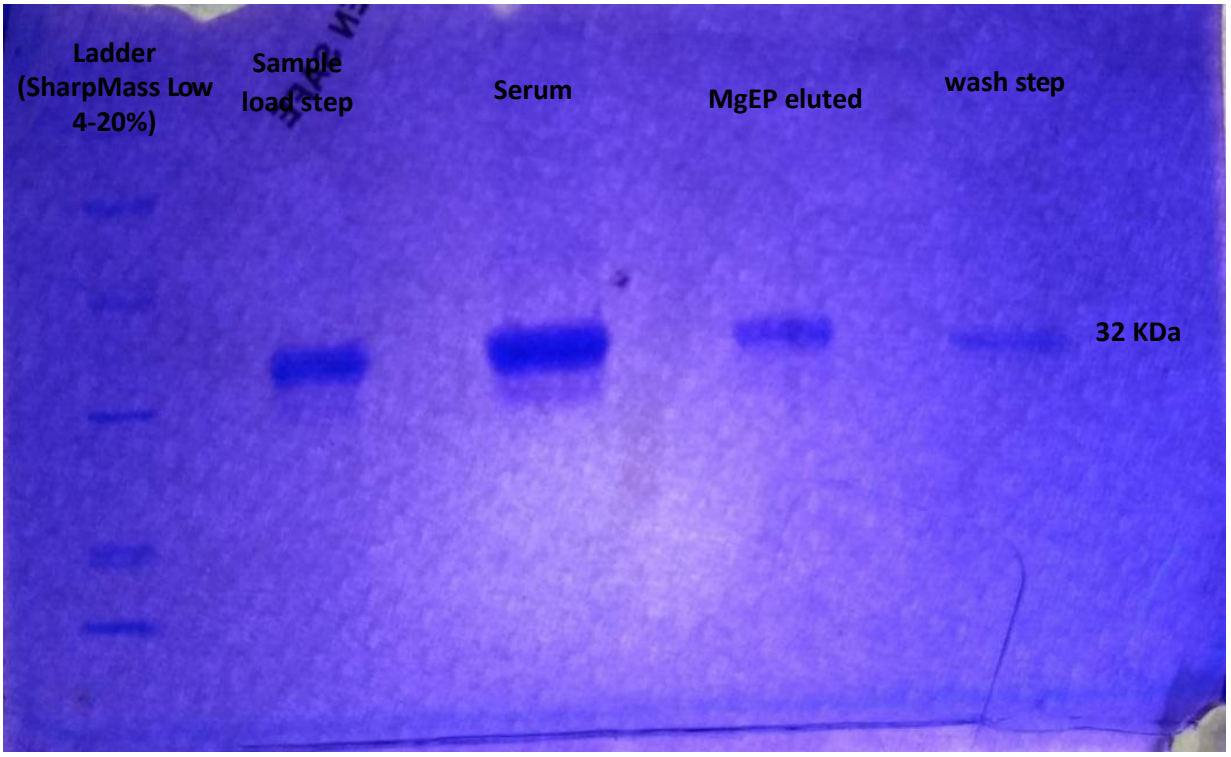

Figure 7. SDS Page gel of mussel serum (serum), serum passed through ConA-sepharose affinity column ("load" step), sample collected from ConA-sepharose affinity column after the washing step ("wash step") and MgEP (bound material eluted with 0.5 M D-mannose in 0.2 M NaCl). Proteins were visualized by blue Comassie.

Bacterial adhesion to haemocyte monolayers

10 µl of resuspended bacteria in Artificial Sea Water (ASW) (35 ppt or 31 ppt salinity) at the concentration of about $1x10^9$ CFU/ml were added to Aliquots (500 µl) of different conditions (as described in Figure 8):

- ASW + haemocytes monolayers
- whole haemolymph serum + haemocytes monolayers
- ASW + MgEP (at the concentration of 0,5 µg $µl^{-1}$) + haemocytes monolayers
- ASW + MgEP (at the concentration of 0,5 µg $µl^{-1}$) + haemocytes monolayers + D-Mannose (at the final concentration of 60 mg ml-1 for each well).

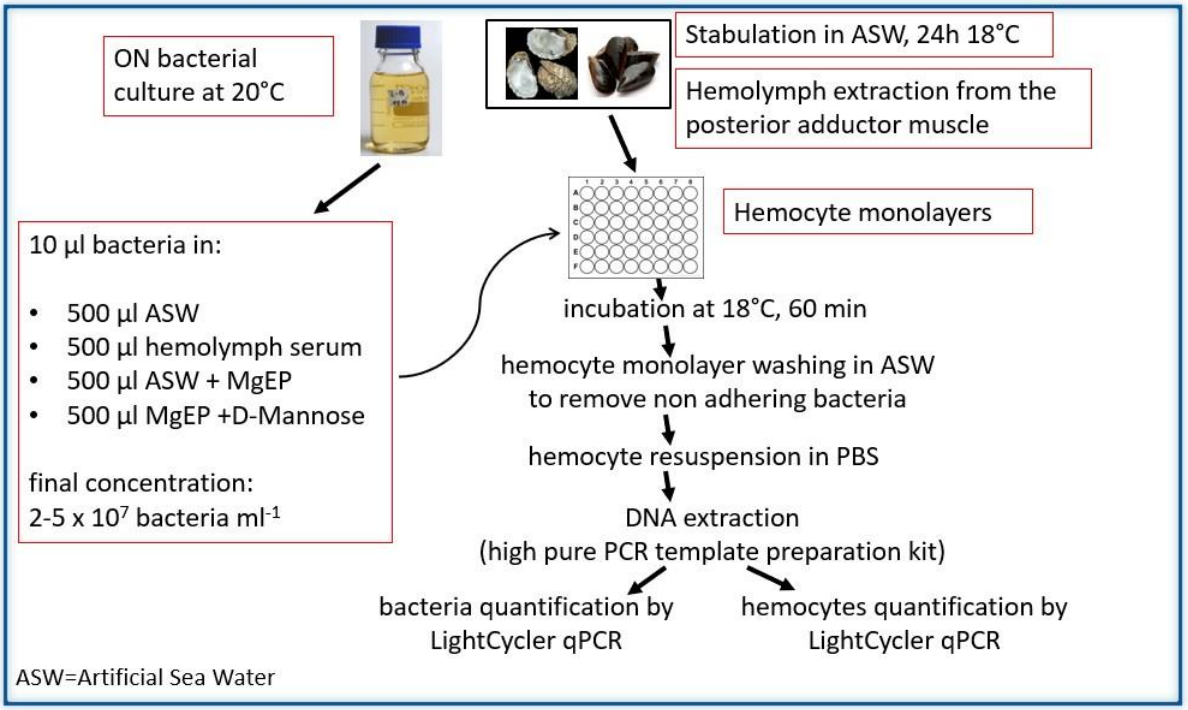

Figure 8. Adhesion assay workflow

Bacterial suspension was added to haemocyte monolayers rinsed twice with ASW to remove haemolymph serum. Bacterial concentration in each well was 2–5 × 10^7 bacteria ml−1 in order to obtain a bacteria:haemocyte ratio of 10:1.

Adhesion assay was performed by incubating haemocyte monolayers with bacteria for 60 min at 18°C (as described in Canesi *et al.*, 2001). After incubation and 3 washing steps with ASW to remove non-adherent bacteria, haemocytes were lysed with 300 µl of PBS 0.1 M KH_2PO_4, 0.1 M Na_2HPO_4, 0.15 M NaCl, pH 7.3) and DNA was extracted with the High Pure PCR Template Preparation Kit (Roche Diagnostics, Mannheim, Germany), according to the manufacturer's instructions. Enumeration of each bacterial strain was performed using the Real Time PCR instrument LightCycler 1.5 (Roche Diagnostics) using the following specific primers (Figure 9):

Bacteria	Target Gene	Primers and probes sequence
Vibrio aestuarianus clade	DNAj	DNA j F: GTATGAAATTTTAACTGACCCACAA
		DNA j R: CAATTTCTTTCGAACAACCAC
		Probe: DNA j FAM-TGGTAGCGCAGACTTCGGCGAC-BHQ2
Vibrio coralliilyticus ATCC BAA 450	zinc-metalloprotease VcpART	VcpARTF: AGCTACGACTGCCGCCCTTAC
		VcpARTR: GGAGCCCTTTCACTTACGATGTTG
Vibrio tapetis CECT 4600	virB4	virB4-F3: TTA-AAA-GTG-GCG-GAG-GAA-TG
		virB4-R3: AAG-CTC-TGC-ATC-GGT-TAG-GA
		Probe virB4-P1: CGA-GTA-CCA-ACA-TGC-CTT-CCC-GT
V. *tasmaniensis* LGP32 (splendidus clade)	16S	SPF2: ATC ATG GCT CAG ATT GAA CG
		SPR2: CAA TGG TTA TCC CCC ACA TC
		16S Probe: 6FAM-CCC ATT AAC GCA CCC GAA GGA TTG--BHQ1

Figure 9. primers and probes used in Real-Time PCR protocols. Accurately quantified copy number genomic DNA of V. tasmaniensis LGP32, *V. aestuarianus* 01/32, *V. aestuarianus* 02/041, *V. coralliilyticus* ATCC BAA 450 *and V. tapetis* CECT 4600 *strains were used as a standard.*

For all the real-time PCR were added five microliters of DNA template to the reaction mixture. For quantification, the log of the number of genome units of a dilution series of the sample was plotted versus the cycle number at which the fluorescent signal increased above background or threshold (Ct value). To evaluate the presence of endogenous bacteria in hemocytes, we included controls consisting of hemocyte monolayers without additional bacteria. To quantify hemocytes, specific primers were used for each bivalve as shown in figure 10.

Enumeration of hemocytes for each bivalve tested was performed using the Real Time PCR instrument LightCycler 1.5 (Roche Diagnostics) using the following specific primers (Figure 10):

Bivalve	Target Gene	Primers sequence
Mytilus galloprovincialis	Cytochrome Oxidase	CO.M.g. F: 5'-GTTCGCCCTTTAAAATCTAACA-3’
		CO.M.g. R: 5'-GGCGTGAGCTAGTTCAGTTTCTA-3'
Crassostrea gigas	Cytochrome Oxidase (S4)	CCGS4 F: 5'-TATTCgTTggAgACTTTATTACCCT -3’
		CCGS4 R: 5'-AAggCTTAgAATTgCAAggTCTATA -3’

Figure 10. primers and probes used in Real-Time PCR protocols. Accurately quantified copy number genomic DNA of M. galloprovincialis and C. gigas hemocytes were used as a standard.

Bacterial sensitivity to haemocyte killing

For each bacterial strain tested, bacterial sensitivity to antibacterial activity by haemocyte monolayers was evaluated at 18°C by adding bacteria suspension (about $1x10^9$ CFU/ml) to haemocyte monolayers at timed intervals (0, 60 and 90 min) at different conditions:

- ASW + haemocytes monolayers
- whole haemolymph serum + haemocytes monolayers
- ASW + MgEP (at the concentration of 0,5 µg $µl^{-1}$) + haemocytes monolayers

Triplicate preparations were made for each sampling time. The collected monolayers supernatants and hemocytes lysates were tenfold serial diluted in ASW and were plated onto Marine Agar and LB agar 3% NaCl to evaluate the number of CFU per hemocytes monolayers. Percentages of killing were determined in comparison to values obtained at zero time. To evaluate the presence of endogenous bacteria in hemocytes, we included controls consisting of hemocyte monolayers without additional bacteria. The experimental design was described in figure 11.

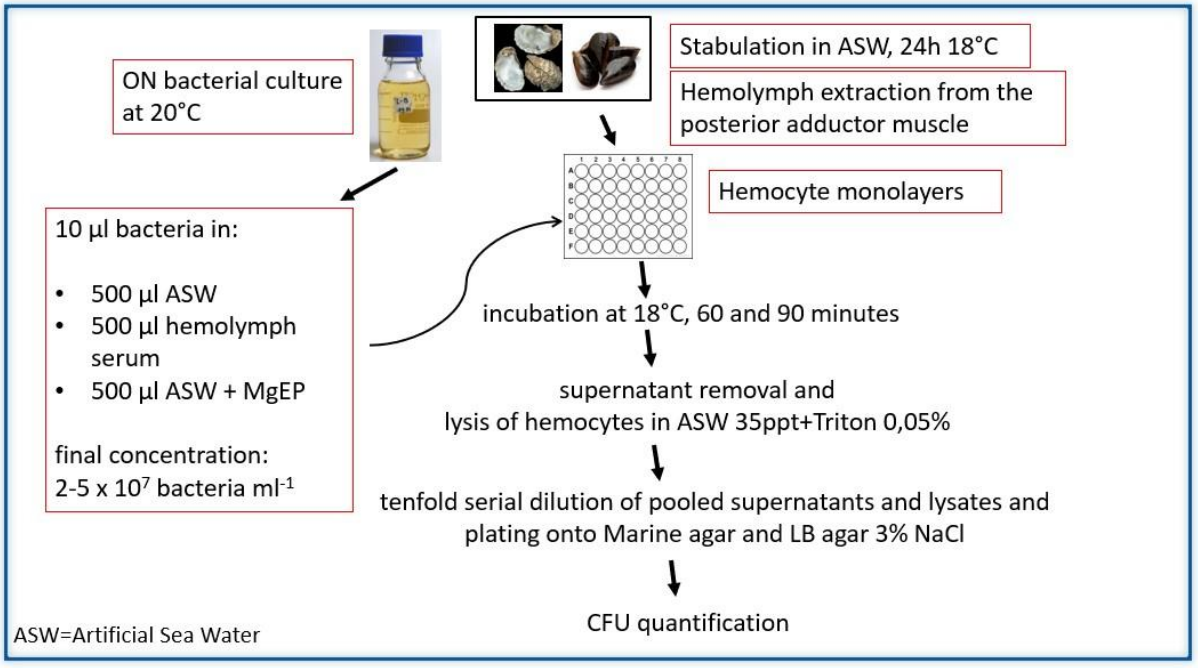

Figure 11. Killing test workflow.

Determination of LMS in C. gigas haemocytes

Haemocyte monolayers were pre-incubated for 30 min with suspensions of *V. aestuarianus* 02/041 (2–3 × 10^7 bacteria ml−1) in ASW, haemolymph serum obtained from oysters or from mussels and LMS was evaluated by the NRRT assay (Ciacci *et al.*, 2010).

Briefly, hemolymph from 3-5 oysters was pooled, hemocyte monolayers, after 20 minutes of incubation at 18°C, were prepared on glass slides, washed out and incubated with 30 ml of a neutral red (NR) solution (final concentration 40 mg/ml from a stock solution of NR 20 mg/ml dimethylsulfoxide). After 15 min, excess dye was washed out, 30 ml of ASW was added, and slides were sealed with a coverslip. Every 15 min, slides were examined under optical microscope and the percentage of cells showing loss of dye from lysosomes in each field was evaluated (an example is shown in Figure 12). For each time point, 10 fields were randomly observed, each containing 8 -10 cells.

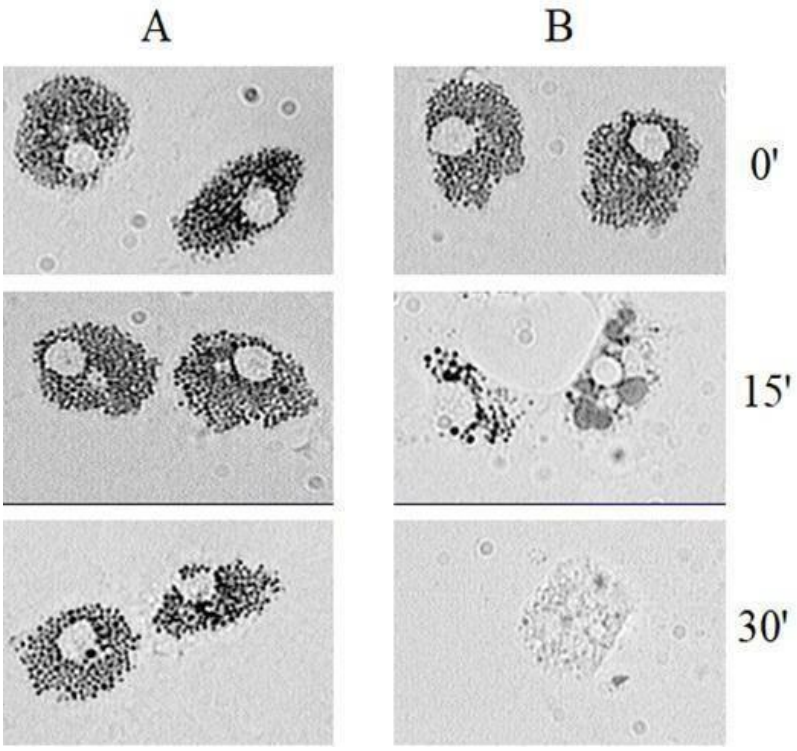

Figure 12. M. galloprovincialis hemocyte health status as shown by LMS assay. A: control hemocytes; B: hemocytes treated with a stressful agent. After 15 min incubation, neutral red (black dots) is released by stressed hemocytes while control cells keep the dye.

The end-point of the assay was defined as the time at which 50% of the cells showed sign of lysosomal leaking (the cytosol becoming red and the cells rounded). All incubations were carried out at 18°C. In this work, experimental conditions were:

- Control (Hemocytes monolayers in ASW)
- Vibrio + MgEP (conc. 40µg/ml) in ASW
- Vibrio + Oyster serum

- Vibrio + Mussel serum

Data analysis

All experiments were carried out in triplicate and were repeated three times. Statistical analysis was performed by ANOVA followed by Tukey's post-hoc test using the GRAPHPAD PRISM 6 software.

2.1.3 Results

Vibrio strains adhesion and sensitivity to killing of *Mytilus galloprovincialis* hemocytes
Experiments were conducted to study adhesion and sensitivity to killing of *Vibrio aestuarianus* 01/032, *Vibrio tasmaniensis* LGP 32, *Vibrio aestuarianus* 02/041, *Vibrio tapetis* CECT 4600, *Vibrio harveyi* VH2 and *Vibrio coralliilyticus* ATCC BAA 450 strains to *M. galloprovincialis* hemocytes. To this end, hemocytes were exposed to bacteria in the presence and in the absence of hemolymph serum and MgEP protein. Bacteria cells were quantified by Real-Time PCR.

V. aestuarianus 01/032

Adhesion: In Figure 13 is shown that, in comparison to the condition with ASW, adhesion of *V. aestuarianus* 01/032 cells to hemocytes monolayers significantly increased in the presence of hemolymph serum and also in the presence of MgEP protein. Moreover, adhesion of *V. aestuarianus* 01/032 to *M. galloprovincialis* hemocytes significantly decreases MgEP and D-Mannose.

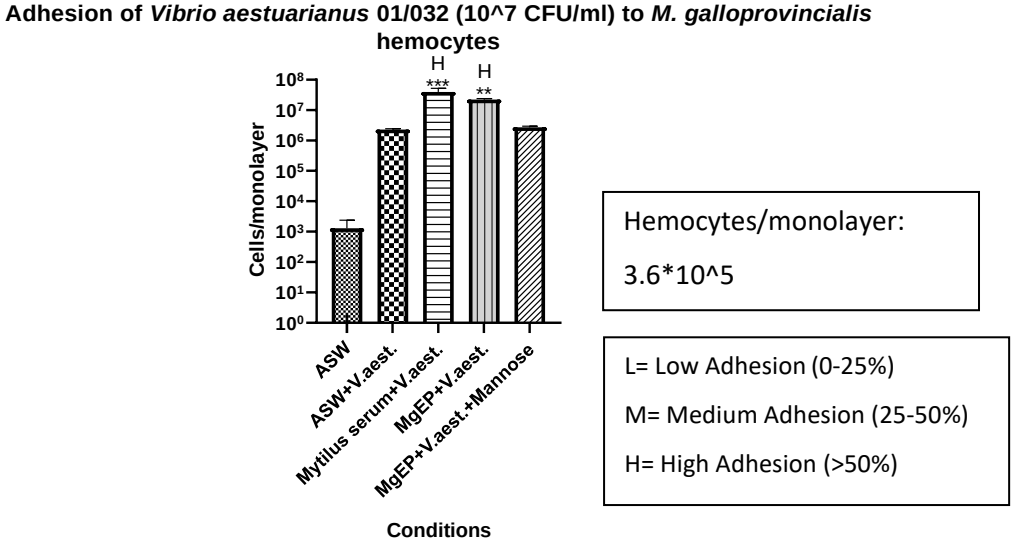

Figure 13. Adhesion of V. aestuarianus 01/032 (expressed as cells per monolayers) to M. galloprovincialis hemocytes significantly increases in the presence of serum and MgEP. Adhesion of V. aestuarianus 01/032 to M. galloprovincialis hemocytes significantly decreases in the presence MgEP and D-Mannose.

Killing: In Figure 14 is shown that, in comparison to the condition with ASW, killing (expressed as decreasing of CFU/ml in each condition) of *V. aestuarianus* 01/032 cells by hemocytes monolayers significantly increased in the presence of serum and MgEP protein at the time point of 60 minutes. A high and significant killing of *V. aestuarianus* 01/032 by hemocytes is shown after 90 minutes.

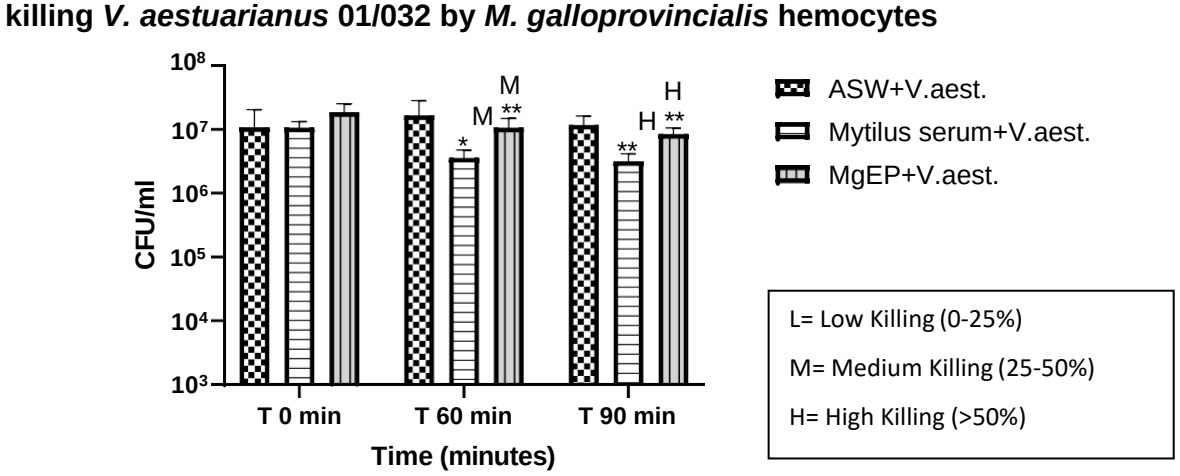

Figure 14. Killing of V. aestuarianus 01/032 by M. galloprovincialis hemocytes significantly increases in the presence of hemolymph and MgEP. The killing is shown as decreasing of viable bacteria, expressed as CFU/ml.

Vibrio tasmaniensis LGP 32

Adhesion: In Figure 15 is shown that, in comparison to the condition with ASW, adhesion of *V. tasmaniensis* LGP 32 cells to hemocytes monolayers significantly increased in the presence of hemolymph serum and also in the presence of MgEP protein. Adhesion of *V. tasmaniensis* LGP 32 to *M. galloprovincialis* doesn't decrease significantly in the presence of MgEP and D-Mannose.

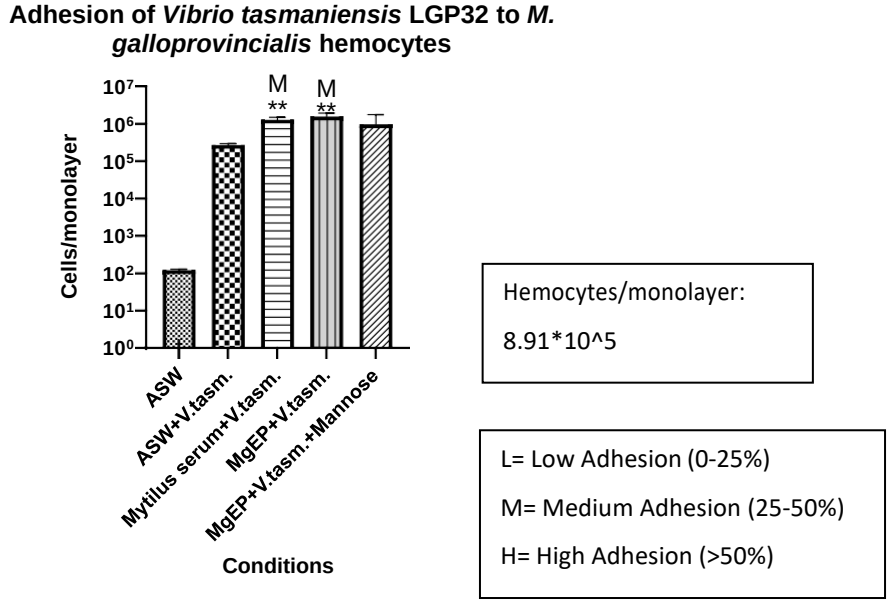

Figure 15. Adhesion of V. tasmaniensis LGP 32 (expressed as cells per monolayers) to M. galloprovincialis hemocytes significantly increases in the presence of serum and MgEP. No decrease in adhesion of V. tasmaniensis LGP 32 to M. galloprovincialis hemocytes was observed in the presence of MgEP and D-Mannose.

Killing: In Figure 16 is shown that, in comparison to the condition with ASW, killing (expressed as decreasing of CFU/ml in each condition) of *V. tasmaniensis* LGP 32 cells by

hemocytes monolayers significantly increased in the presence of MgEP protein at the time point 90 minutes. A low killing in the presence of serum was also shown after 60 and 90 minutes.

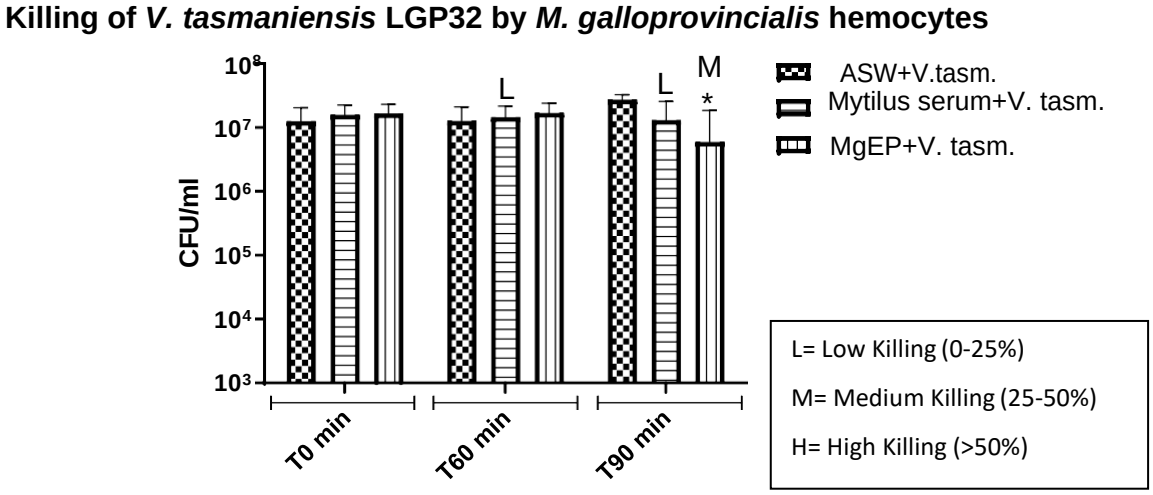

Figure 16. Killing of V. tasmaniensis LGP 32 *by M. galloprovincialis hemocytes significantly increases in the presence of MgEP after 90 minutes. A low killing is shown in the presence of serum after 60 and 90 minutes. The killing is shown as decreasing of viable bacteria, expressed as CFU/ml.*

V. aestuarianus 02/041

Adhesion: In Figure 17 is shown that, in comparison to the condition with ASW, adhesion of *V. aestuarianus,* cells to hemocytes monolayers significantly increased in the presence of hemolymph serum and also in the presence of MgEP protein. Moreover, adhesion of *V. aestuarianus* 02/041 to *M. galloprovincialis* hemocytes significantly decreases MgEP and D-Mannose.

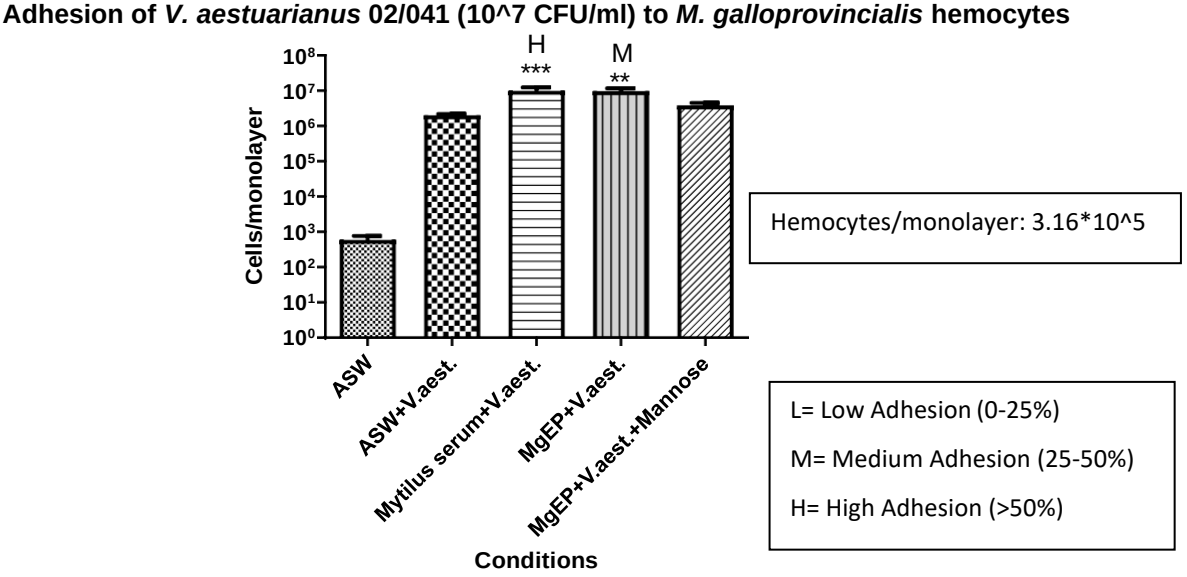

Figure 17. Adhesion of V. aestuarianus 02/041 (expressed as cells per monolayers) to M. galloprovincialis hemocytes significantly increases in the presence of serum and MgEP. Adhesion

of V. aestuarianus 02/041 to M. galloprovincialis hemocytes significantly decreases in the presence of MgEP and D-Mannose.

Killing: In Figure 18 is shown that, in comparison to the condition with ASW, killing (expressed as decreasing of CFU/ml in each condition) of *V. aestuarianus* 02/041 cells by hemocytes monolayers significantly increased in the presence of MgEP protein at the time point of 60 and 90 minutes. A low killing of *V. aestuarianus* 02/041 by hemocytes is shown after 90 minutes.

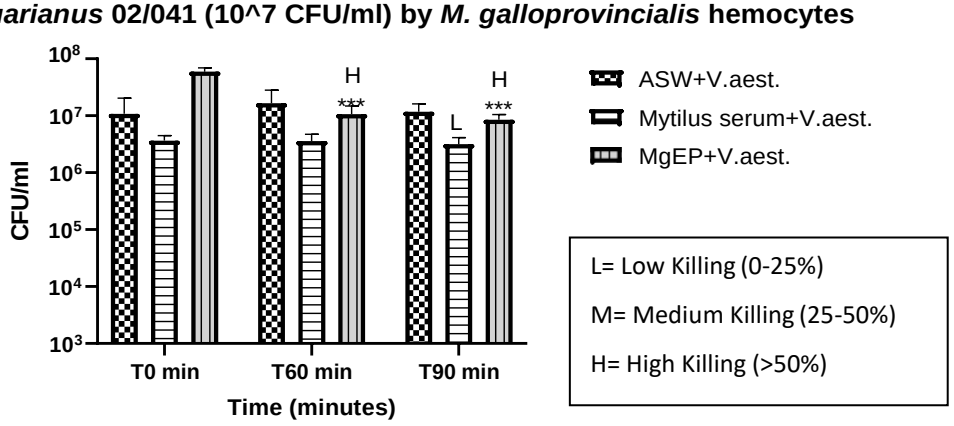

Figure 18. Killing of V. aestuarianus 02/041 by M. galloprovincialis hemocytes significantly increases in the presence of MgEP. A low killing by Mussel serum is shown after 90 minutes The killing is shown as decreasing of viable bacteria, expressed as CFU/ml.

V. tapetis CECT 4600

Adhesion: In Figure 19 is shown that, in comparison to the condition with ASW, adhesion of *V. tapetis* CECT4600 cells to hemocytes monolayers significantly increased in the presence of hemolymph serum and also in the presence of MgEP protein, but adhesion didn't decrease in the presence of MgEP and D- Mannose.

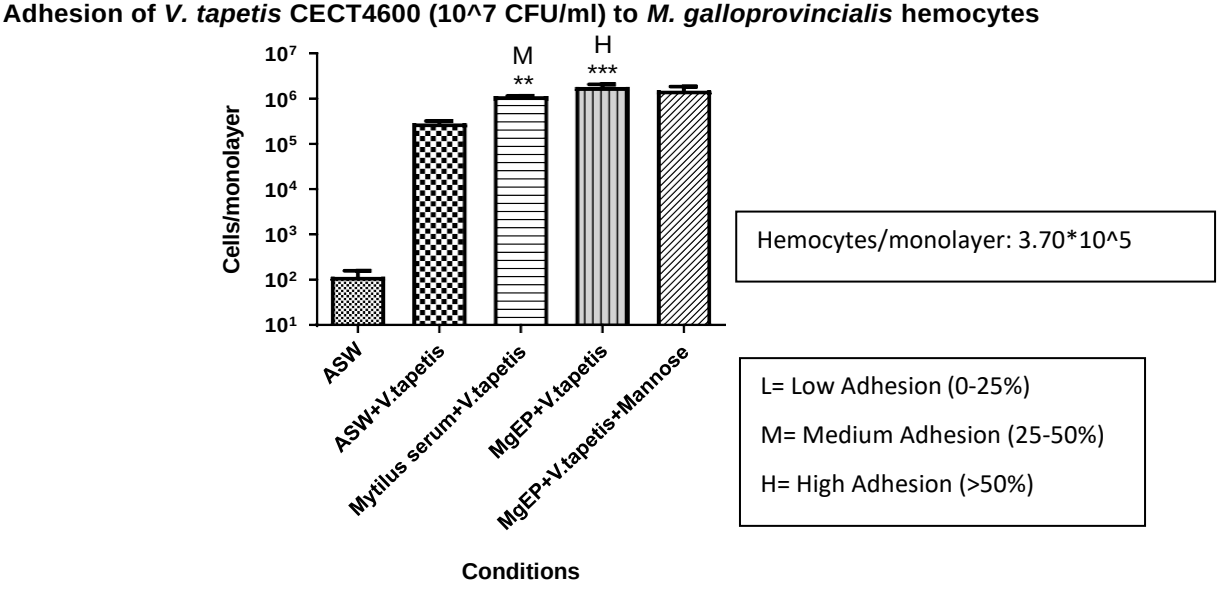

Figure 19. Adhesion of V. tapetis CECT 4600 *to M. galloprovincialis hemocytes significantly increases in the presence of hemolymph serum and in the presence of MgEP. No decreasing of adhesion in the presence of MgEP and D-Mannose.*

Killing: In Figure 20 is shown that, in comparison to the condition with ASW, killing (expressed as decreasing of CFU/ml in each condition) of *V. tapetis* CECT 4600 cells by hemocytes monolayers significantly increased in the presence of serum at the time points of 60 and 90 minutes. No killing was observed in the presence of MgEP.

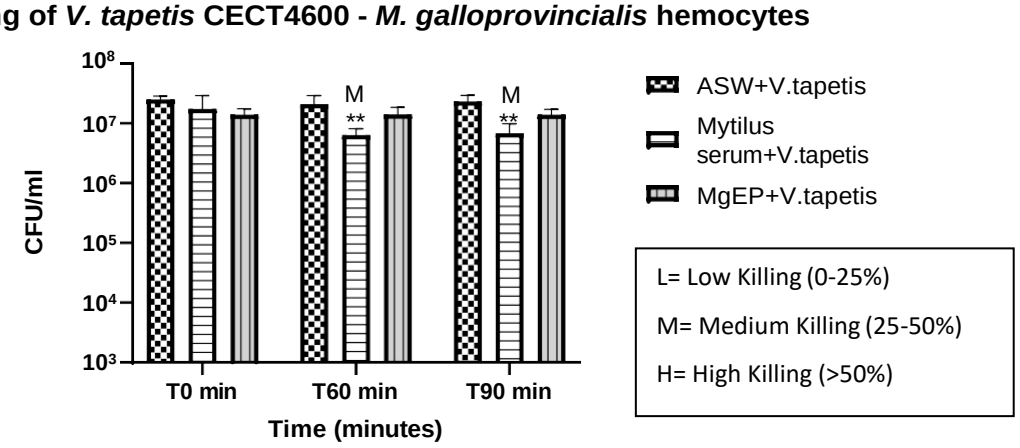

Figure 20. Killing of V. tapetis CECT 4600 *by M. galloprovincialis hemocytes significantly increases in the presence of hemolymph serum, but not in the presence of MgEP. The killing is shown as decreasing of viable bacteria, expressed as CFU/ml.*

Vibrio harveyi VH2

Adhesion: In Figure 21 is shown that, in comparison to the condition with ASW, adhesion of *V. harveyi* VH2 cells to hemocytes monolayers didn't increase significantly in the presence of hemolymph serum and also in the presence of MgEP protein.

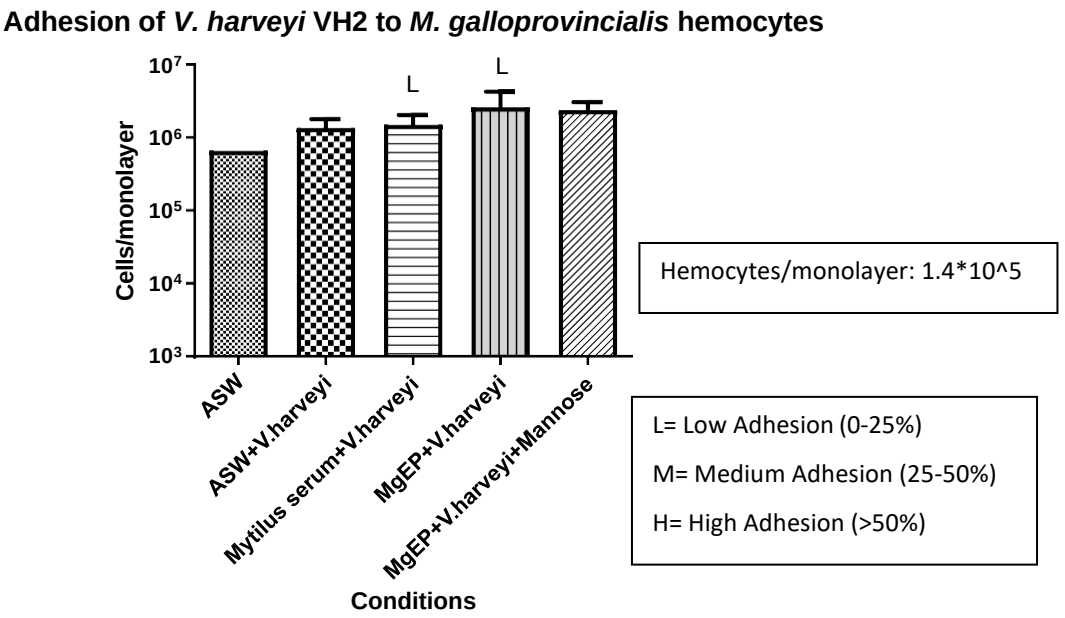

Figure 21. Adhesion of V. harveyi VH2 *by M. galloprovincialis doesn't increase significantly in the presence of hemolymph serum and also in the presence of MgEP.*

Killing: In Figure 22 is shown that, in comparison to the condition with ASW, killing (expressed as decreasing of CFU/ml in each condition) of *V. harveyi* VH2 cells by hemocytes monolayers significantly increased in the presence of serum at the time points of 60 and 90 minutes. No killing was observed in the presence of MgEP.

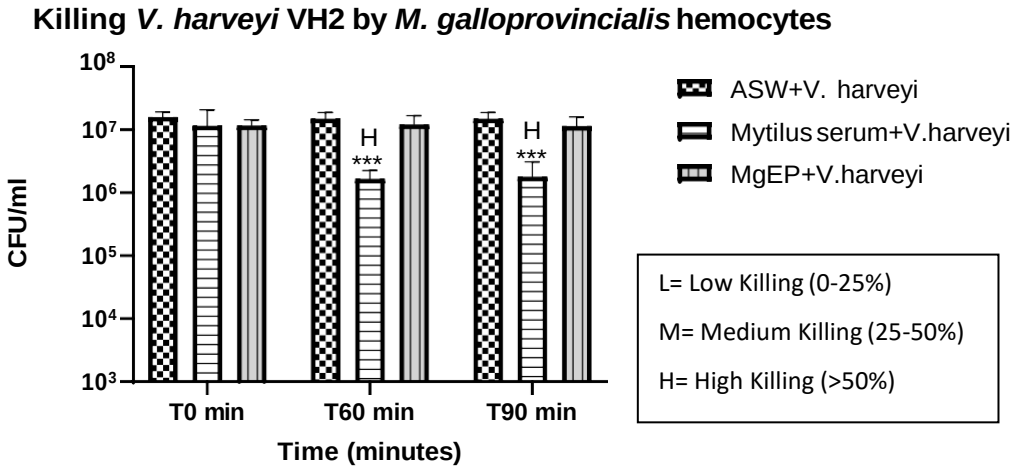

Figure 22. Killing of V. harveyi VH2 *by M. galloprovincialis hemocytes significantly increases in the presence of hemolymph serum, but not in the presence of MgEP. The killing is shown as decreasing of viable bacteria, expressed as CFU/ml.*

V. coralliilyticus ATCC BAA 450

Adhesion: In Figure 23 is shown that, in comparison to the condition with ASW, adhesion of *V. coralliilyticus* ATCC BAA 450 cells to hemocytes monolayers significantly increased in the presence of hemolymph serum and also in the presence of MgEP protein. Adhesion of *V. coralliilyticus* ATCC BAA 450 to *M. galloprovincialis* didn't decrease in the presence of MgEP and D-Mannose.

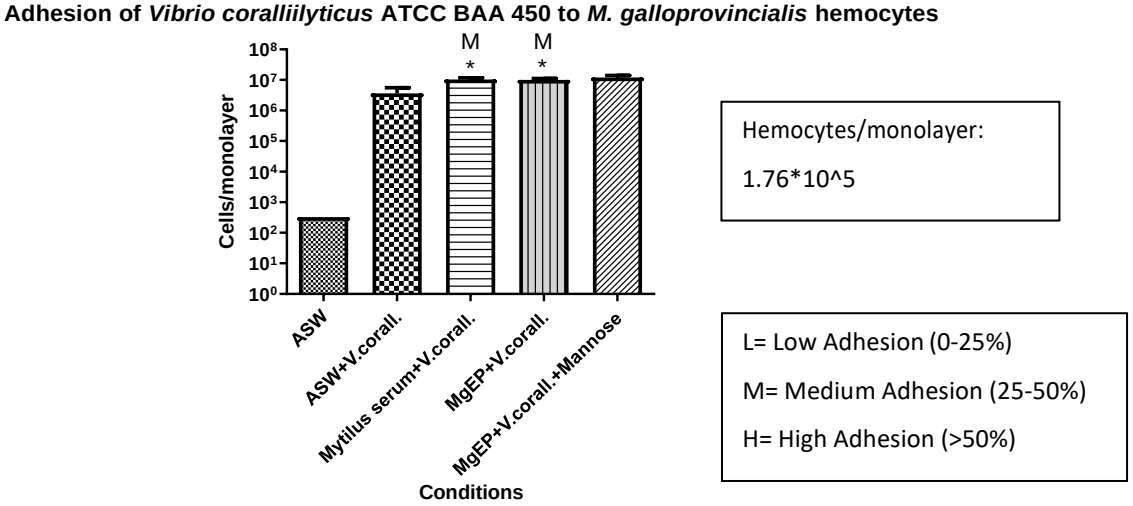

Figure 23. Adhesion of V. coralliilyticus ATTCC BAA 450 (expressed as cells per monolayers) to M. galloprovincialis hemocytes significantly increases in the presence of serum and MgEP. No decrease in adhesion of V. coralliilyticus ATTCC BAA 450 to M. galloprovincialis hemocytes was observed in the presence of MgEP and D-Mannose.

Killing: In Figure 24 is shown that, in comparison to the condition with ASW, killing (expressed as decreasing of CFU/ml in each condition) of *V. coralliilyticus* ATCC BAA 450 cells by hemocytes monolayers significantly increased in the presence of MgEP protein at the time points of 60 and 90 minutes. A significative killing in the presence of serum was also shown after 60 and 90 minutes. No killing was observed by hemocytes in the presence of MgEP and D-Mannose.

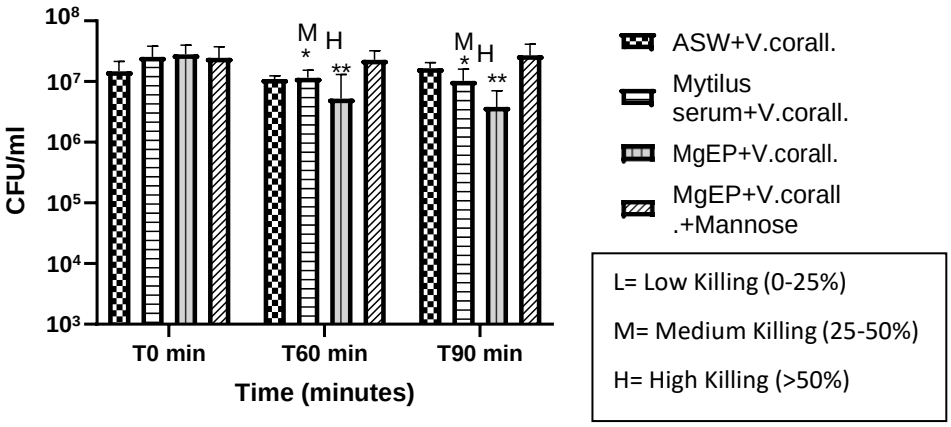

Figure 24. Killing of V. coralliilyticus ATTCC BAA 450 by M. galloprovincialis hemocytes significantly increases in the presence of MgEP after 60 and 90 minutes, and also in the presence of serum after 60 and 90 minutes. No killing was observed in the presence of MgEP and D-Mannose. The killing is shown as decreasing of viable bacteria, expressed as CFU/ml.

Vibrio strains adhesion and sensitivity to killing of *Crassostrea gigas* hemocytes
Experiments were conducted to study adhesion and sensitivity to killing of the pathogens strain for oysters *Vibrio aestuarianus* 01/032 and *Vibrio aestuarianus* 02/041 to *C. gigas* hemocytes. To this end, hemocytes were exposed to bacteria in the presence and in the absence of hemolymph serum and MgEP protein. Bacteria cells were quantified by Real-Time PCR.

V. aestuarianus 01/032

Adhesion: In Figure 25 is shown that, in comparison to the condition with ASW, adhesion of *V. aestaurianus* 01/032 cells to oyster hemocytes monolayers significantly increased in the presence of oyster serum and also in the presence of MgEP protein. Moreover, adhesion of *V. aestuarianus* 01/032 to *M. galloprovincialis* hemocytes didn't increase in the presence of MgEP and D- Mannose.

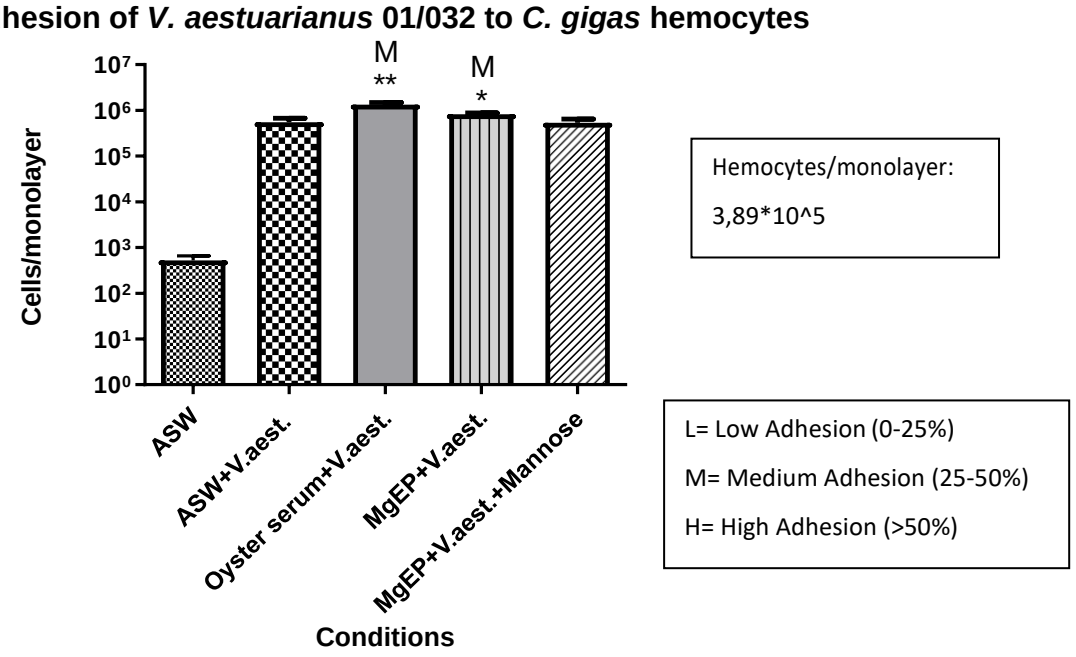

Figure 25. Adhesion of V. aestuarianus 01/032 (expressed as cells per monolayers) to C. gigas hemocytes significantly increases in the presence of oyster serum and MgEP. Adhesion of V. aestuarianus 01/032 to C. gigas hemocytes didn't increase significantly in the presence of MgEP+D- Mannose.

Killing: In Figure 26 is shown that, in comparison to the condition with ASW, killing (expressed as decreasing of CFU/ml in each condition) of *V. aestuarianus* 01/032 cells by oyster hemocytes significantly increased in the presence of mussel serum and in the presence of MgEP after 60 and 90 minutes of incubation. No killing by oyster hemocytes was observed in the presence of oyster serum.

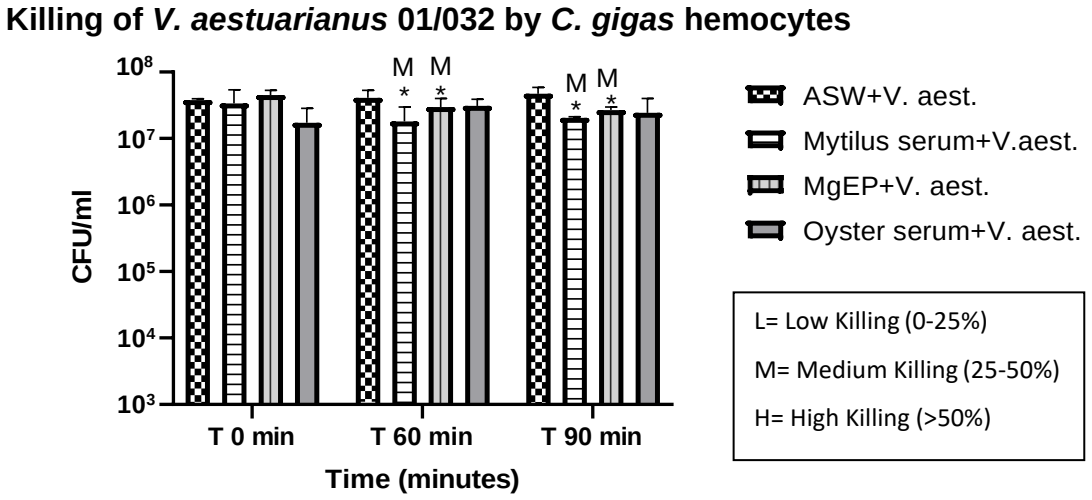

Figure 26. killing of V. aestuarianus 01/032 (expressed as cells per monolayers) by C. gigas hemocytes significantly increases in the presence of mussel serum after 60 and 90 minutes. Significative killing is observed also in the presence of MgEP after 60 and 90 minutes. No killing is observed in the presence of oyster serum. The killing is shown as decreasing of viable bacteria, expressed as CFU/ml.

V. aestuarianus 02/041

Adhesion: In Figure 27 is shown that, in comparison to the condition with ASW, adhesion of *V. aestuarianus* 02/041 cells to *C. gigas* hemocytes monolayers significantly increased in the presence of mussel serum, in the presence of MgEP and also in the presence of oyster serum. Moreover, adhesion of *V. aestuarianus* 02/041 to *C. gigas* hemocytes significantly decreases in the presence of MgEP and D- Mannose in comparison to mussel serum, oyster serum and MgEp conditions.

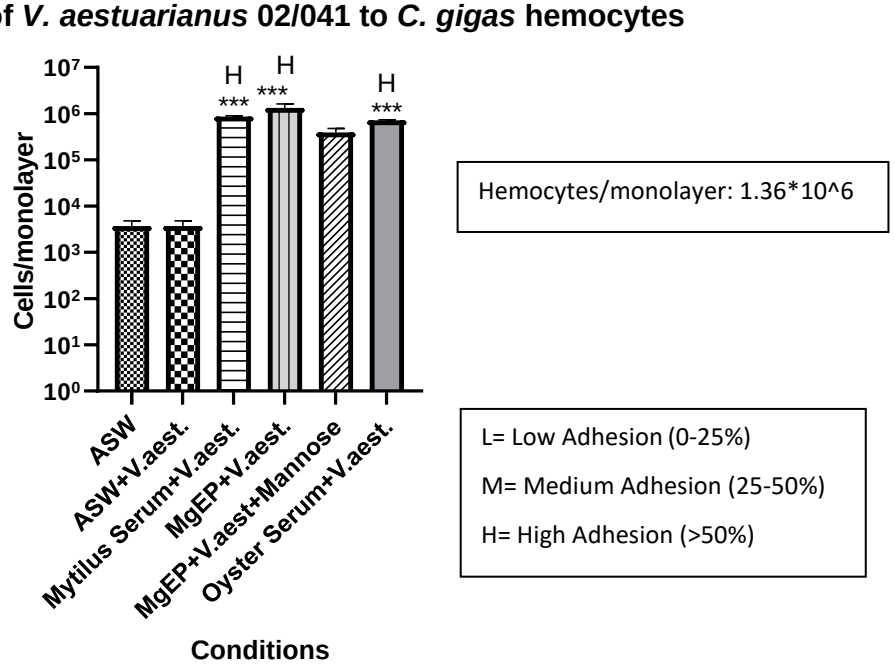

Figure 27. Adhesion of V. aestuarianus 02/041 (expressed as cells per monolayers) to C. gigas hemocytes significantly increases in the presence of mussel serum, in the presence of MgEP, and also in the presence oyster serum Adhesion of V. aestuarianus 02/041 to C. gigas hemocytes significantly decreases in the presence of MgEP and D- Mannose in comparison to mussel serum, oyster serum and MgEp conditions.

Killing: In Figure 28 is shown that, in comparison to the condition with ASW, killing (expressed as decreasing of CFU/ml in each condition) of *V. aestuarianus* 02/041 cells by oyster hemocytes significantly increased in the presence of mussel serum after 60 and 90 minutes. Killing by hemocytes is observed also in the presence of MgEP after 60 and 90 minutes. No killing by oyster hemocytes was observed in the presence of oyster serum and also in the presence of MgEP and D-Mannose. Killing by hemocytes was observed in the presence of MgEP added to oyster serum after 90 minutes.

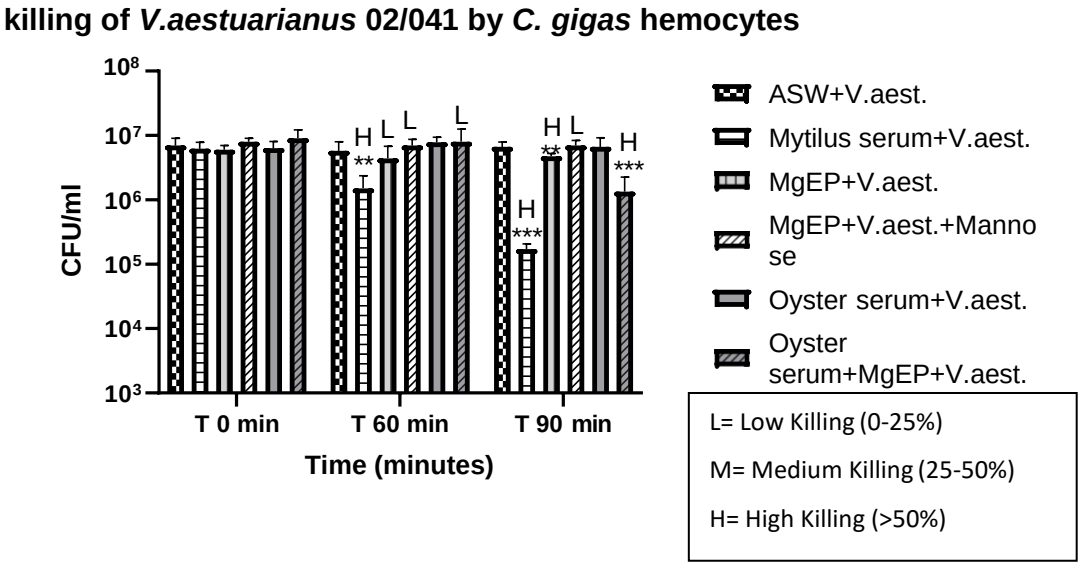

Figure 28. killing of V. aestuarianus 02/041 (expressed as cells per monolayers) by C. gigas hemocytes significantly increases in the presence of mussel serum after 60 and 90 minutes. Significative killing is observed also in the presence of MgEP after 90 minutes. A low killing is observed in the presence of MgEP also after 60 minutes. Significative killing is observed in the presence of oyster serum +MgEP after 90 minutes No killing is observed in the presence of oyster serum and also in the presence of MgEP and D-Mannose. The killing is shown as decreasing of viable bacteria, expressed as CFU/ml.

Determination of LMS in C. gigas haemocytes

Haemocyte monolayers were pre-incubated for 60 min with suspensions of *V. aestuarianus* 02/041 (2–3 × 10^7 bacteria ml−1) in ASW, haemolymph serum obtained from oysters or from mussels and LMS was evaluated by the NRRT assay, as previously described (Figure 29).

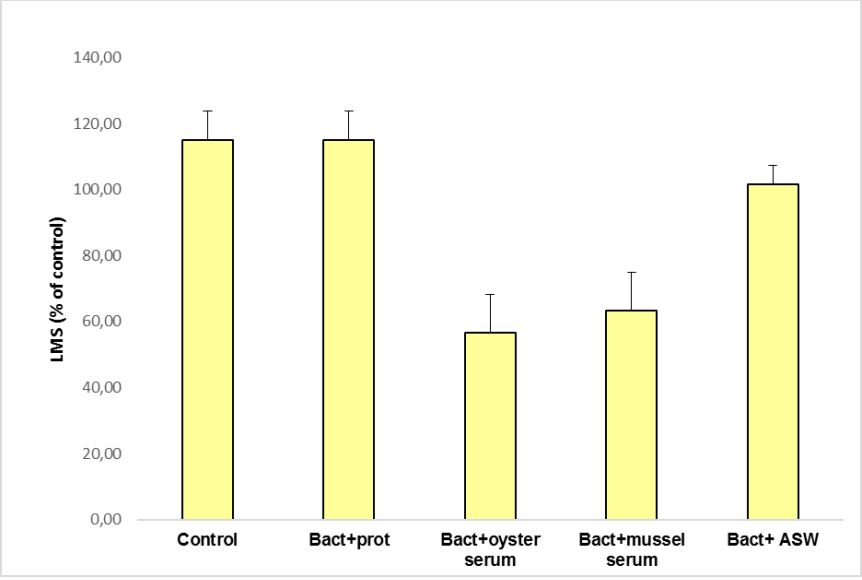

Figure 29. LMS of oyster hemocytes incubated for 60 mins with V. aestuarianus 02/041 (conc. 10^7 CFU/ml) in the presence of MgEP (prot), oyster serum, mussel serum and ASW. Only hemocytes in ASW are used as control. LMS is expressed as % of Lysosomal stability in all the experimental conditions in comparison to the control (100%). LMS in MgEP and bacteria is higher than in the presence of oyster serum and mussel serum too.

In Figure 30 is shown that, in the presence of MgEP, alive bacteria are visible and moving around and inside oyster hemocytes (Figure 30, B). In the condition with mussel serum, no bacteria are visible in the surrounding of hemocytes. Hemocytes are very bad and destabilized already at Time 0, and there is the presence of a large transparent aggragates all around (Figure 30, C). In the condition with oyster serum, there are visible alive bacteria cells moving between and inside hemocytes, moving also within structures like vacuoles (Figure 30, D).

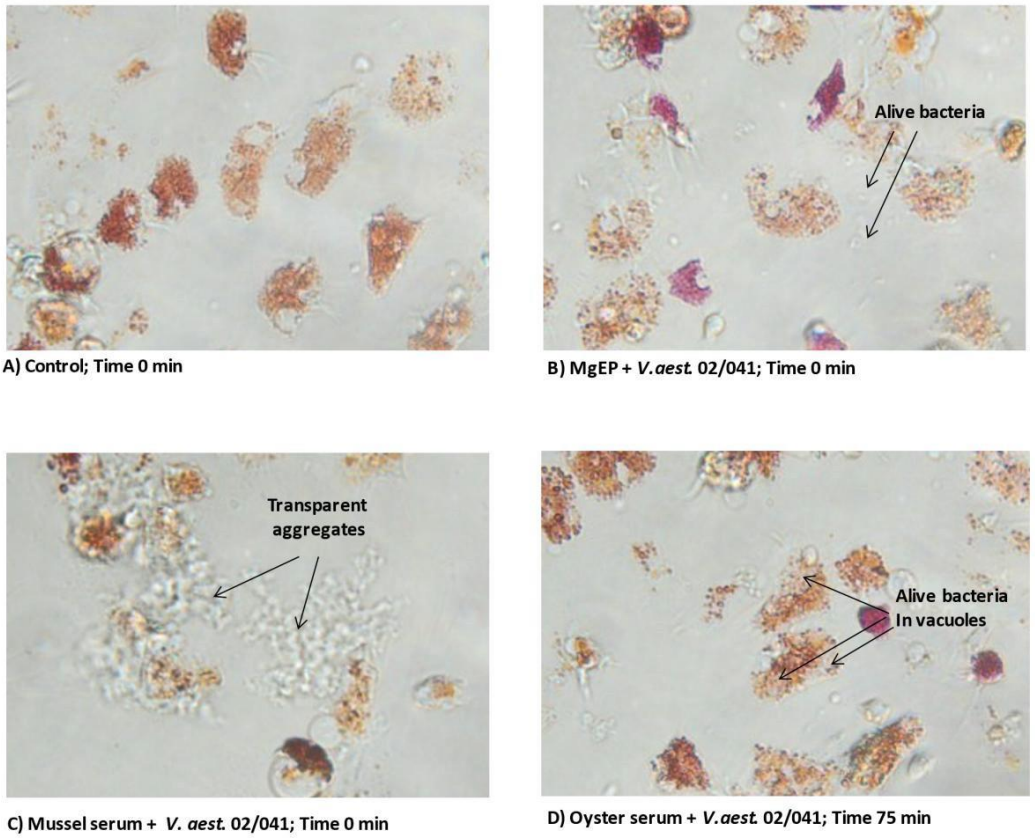

Figure 30. LMS of oyster hemocytes incubated for 60 mins with V. aestuarianus 02/041 (conc. 10^7 CFU/ml) in the presence of MgEP, oyster serum, mussel serum and ASW. A) Hemocytes in ASW at time 0; B) Hemocytes in the presence MgEP and V. aestuarianus 02/041 at time 0; C) Hemocytes in the presence of mussel serum and V. aestuarianus 02/041 at time 0; D) Hemocytes in the presence of oyster serum and V. aestuarianus 02/041 at time 75 mins.

2.1.4 Discussion

In previous studies the results of nano-HPLC-ESI-MS/MS identified the purified protein as the EP precursor EP (*M. edulis*), or putative C1q domain containing protein MgC1q6 (*M. galloprovincialis*). EP represents the major plasma protein in *Mytilus* and has a possible role in multiple biological functions including shell formation, metal ion transportation and detoxification (Zhou *et al*., 2013). Interestingly, EP also shows a conserved domain homologous to MgC1q6, a complement component identified in *M. galloprovincialis* (MgEP) that in vertebrates enhances phagocytosis (Gerdol *et al*., 2011). In bivalves and many other invertebrates lacking adaptive immunity, C1q domain containing proteins are abundant and their involvement as ancient innate immune response proteins has been proposed, although the role of specific members of this highly diverse family in many different processes needs additional study (Gerdol *et al*., 2011). A recent study of *M. galloprovincialis* serum proteome (Oliveri *et al*., 2014) definitively demonstrated that the EP precursor, or putative C1q domain containing protein MgC1q6, represents the most abundant serum protein in mussels, with different bands detected by both one- and two-dimensional gel electrophoresis and MS analysis. The protein has several putative phosphorylation sites; moreover, Western blot analyses performed using a custom polyclonal anti-EP antibody recognized the EP protein at approximately 35 kDa.

The data here presented ascribe to MgEP the additional role of mediating adhesion and killing of invading bacteria carrying D-mannose-sensitive ligands. MgEP may contribute to higher resistance of mussels to certain bacterial pathogens: due to its capability to mediate mannose-sensitive interactions between bacteria and mussel haemocytes, it is expected that MgEP may work as an opsonin not only towards *V. aestuarianus* 01/032 (Pezzati *et al*., 2015), but also other bacteria with adhesins sharing the same D-mannose specificity.

The results of this work showed that MgEP, maybe also in cooperation with other soluble haemolymph fractions of *M. galloprovincialis*, is responsible for promoting mannose-sensitive interactions of *V. aestuarianus* 01/032 and other bivalve infectious agents and, more in general, microorganisms present in aquaculture water, such as *V. coralliilyticus* ATCC BAA 450 and *V. aestuarianus* 02/041 with mussel haemocytes (adhesion and killing), and also added to oyster hemocytes, thus serving as an opsonin, as showed in the following summary tables:

Vibrio (10^7 CFU/well)	Killing by mussel hemocytes in the presence of			Adhesion to hemocytes monolayers in the presence of		
	ASW	Mussel serum	Mussel opsonin (MgEP)	ASW	Mussel serum	Mussel opsonin (MgEP)
V. aestuarianus 01/032	-	+++ MS	+++ MS	+	+++ MS	+++ MS
V. tasmaniensis LGP 32	-	+	++	+	++	++
V. harveyi VH2	-	+++	-	+	+	+
V. coralliilyticus ATCC BAA 450	-	++	+++	+	++	++
V. tapetis CECT 4600	-	++	-	+	++	+++
V. aestuarianus 02/041	-	+	+++ MS	+	+++ MS	+++ MS

Vibrio (10^7 CFU/well)	Killing by oyster hemocytes in the presence of				Adhesion to oyster hemocytes monolayers in the presence of			
	ASW	Oyster serum	Mussel opsonin (MgEP)	Mussel serum	ASW	Oyster serum	Mussel opsonin (MgEP)	Mussel serum
V. aestuarianus 01/032	-	+++	++	++	+	++	++	++
V. aestuarianus 02/041	-	+	+++ MS	+++ MS	+	+++	+++ MS	+++ MS

Legend: - = no killing/no adhesion; + = low killing/low adhesion; ++ = medium killing/medium adhesion; +++ = high killing/high adhesion; MS = Mannose-Sensitive

The experiments here presented showed that in *V. aestuarianus* 01/032, *V. tasmaniensis* LGP 32, *V. coralliilyticus* ATCC BAA 450, *V. tapetis* CECT 4600 and *V. aestuarianus* 02/041 strains the adhesion to and killing by *M. galloprovincialis* hemocytes increased in the presence of mussel serum and MgEP, suggesting a role in bacteria adhesion played by this protein present in mussel serum. Interestingly, not for all these bacteria the adhesion was inhibited by D-mannose, suggesting that interactions different from those observed with *M. galloprovincialis* haemocytes that are based on the specific recognition of this sugar, are involved. Moreover, when oyster haemocytes were incubated with either mussel serum or ASW containing MgEP in place of homologous serum, these cells acquired the capacity to kill *V. aestuarianus* 02/041(Figure 28). This suggests that oyster serum lacks the soluble component mediating mannose-sensitive interactions between the pathogen for oysters *V. aestuarianus* 02/041 bacteria and haemocytes leading to efficient killing.

Overall, available data indicate that species-specific serum components are present in bivalve

serum involved in mediating differential interactions with vibrios, this resulting in different sensitivities to the bactericidal activity of haemolymph.

2.2 Dynamics of the Pacific Oyster microbiota

2.2.1 Introduction

In Europe mass mortality episodes of the *C. gigas* in farming areas were reported at increasing frequency in recent years and are attributed to complex interactions among oysters, microbial pathogens and environmental variables (Pernet *et al*., 2012). In particular, stressful environmental conditions such as warmer seawater temperatures were observed to favour shift of *C. gigas* bacterial communities toward pathogen-dominated communities also promoting colonization by secondary opportunistic pathogens and non-resident microbial species (Lokmer and Wegner, 2015).

Under this perspective, evidence has been provided supporting the view that oyster infections might be seen as infectious disorders caused by the contribution of a larger number of pathogens (e.g. populations or consortia) than previously thought (Lemire *et al*., 2015). The question now is no longer whether microorganisms are involved in the pathogenesis of such diseases, but which specific microbial species or strains are involved.

Although specific microbial pathogens (e.g. OsHV-1 and *V. aestuarianus*) and some virulence factors have been identified to play a role in oyster diseases (Travers *et al*., 2015) there is an emerging view that microbial infections may derive from the contribution of different microbial species/strains that act as a "community of pathogens" rather than a single species/strain as the only etiological agent (Lemire et al., 2015).

To understand this aspect, *C. gigas* samples were selected to study all the pathogenic component of the microbiota, the pathobiota, by using 16S rRNA gene-based analysis of the microbial diversity, based on next-generation sequencing protocols for taxonomic identification of bivalve-associated bacteria (Lokmer and Wegner, 2015; Lokmer *et al*., 2016).

In this study, we want to determine the microbial community associated with *C. gigas* samples collected during recurrent episodes of mortality in different European sites: delta Ebro river (lat 40 ° 29'37.7 " N - long 0 ° 48'24.82 "E, Spain), Dungarvan Bay (lat 52 ° 4'1.35" N - long 7 ° 33'51.74 "W, Ireland), Bay of Brest (lat 48 ° 20'24.94" N - along 4 ° 29'15.39 "W, France). A total of 525 specimens of C. gigas (365 juveniles and 160 adults) were collected in the period between March 2016 and October 2017.

The samples were shipped to the laboratory and the tissues were extracted, to be then frozen and processed for molecular analysis. After DNA extraction from, the samples were screened for main *C. gigas* bacterial pathogens (*V. aestuarianus*) presence by using a real-time PCR specific protocol and producing amplicon libraries using 16SrDNA starting from the DNA extracted from the single samples. The libraries were sequenced using an Ion Torrent (PGM) platform (Thermo Fisher Scientific, MA).

2.2.2 Experimental procedures

Samples collection during mortality episodes in Europe

In the frame of the EU funded H2020 project VIVALDI (Preventing and mitigating farmed bivalve diseases) 525 C. gigas individuals (365 spat and 160 adult) were collected between March 2016 and October 2017 at different European sites: delta Ebro river (lat 40 ° 29'37.7 " N - long 0 ° 48'24.82 "E, Spain), Dungarvan Bay (lat 52 ° 4'1.35" N - long 7 ° 33'51.74 "W, Ireland), Bay of Brest (lat 48 ° 20'24.94" N - along 4 ° 29'15.39 "W, France) (Figure 28).

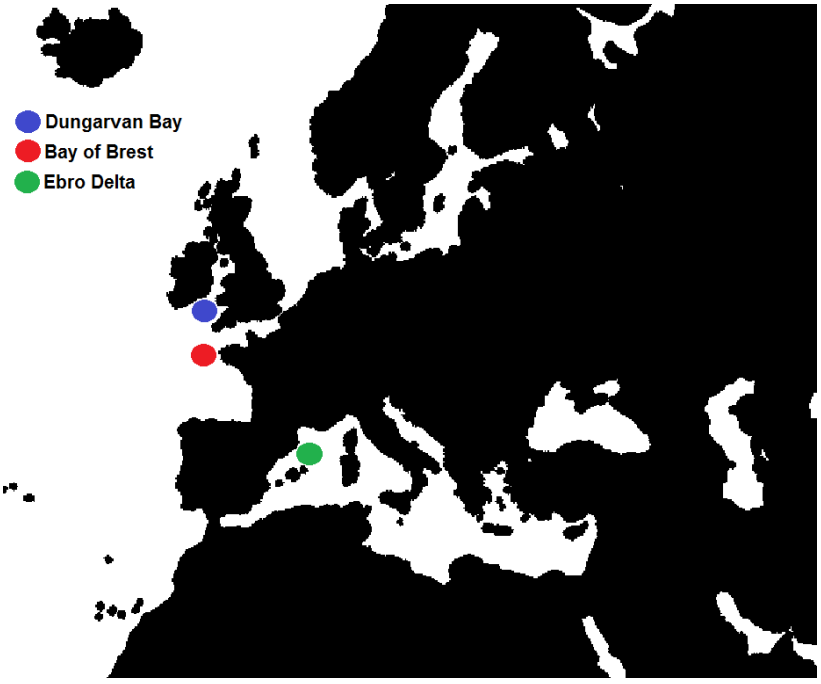

Figure 28. C. gigas aquaculture sampling sites

Immediately after collection, individual oyster samples were transported to the laboratory and prepared for downstream molecular analysis according to EU Council Directive 175/2010. Briefly, bivalve tissues were extracted from single specimen and placed on a 2 ml tube containing beads, and frozen at −20°C until processed.

DNA Extraction and quantification

Samples were placed on 180 µl of ATL buffer and 20 µl of proteinase K to be homogenized, followed by DNA extraction using Blood and Tissue Kit (QIAGEN srl, Milan, Italy), following the instructions for Tissue Protocol. Briefly, homogenized samples, proteinase K and ATL buffer were vortexed and incubated at 56°C for 10 min (until completely lysed). After this step, 200 µl ethanol (96-100%) were added, and the solution pipetted into a DNeasy Mini spin column placed in a 2 ml collection tube, centrifuged at 6.000 x g (8.000 rpm) for 1 min. After discarded flow-through and the collection tube, the spin column was placed in a new 2 ml collection tube and 500 µl of Buffer AW 1 were added. The tube was centrifuged for 1 min at 6.000 x g, the collection tube was discarded and the spin column was placed in a new 2 ml collection tube, 500 µl of Buffer AW 2 were added and centrifuged for 3 min at 20.000 x g (14.000 rpm). The collection tube was discarded and the spin column was transferred in a new 1.5 ml microcentrifuge tube for the elution, by adding 200 µl of Buffer AE to the center of the spin column membrane. After 1 minute of incubation at room temperature and centrifuged for 1 min at 6.000 x g, the amount of extracted DNA was quantified using the Quantifluor double-stranded DNA quantification Kit (Promega Italia, Milan, Italy).

OsHV-1 and Vibrio aestuarianus detection in C. gigas samples by qPCR

Individual oyster samples were preliminary screened for the presence of OsHV-1 and *Vibrio aestuarianus* by real-time PCR. For detection of OsHV-1 real-time PCR was performed using primers HVDP-F and HVDP-R according to Webb *et al*. (2007) (Figure 29).

Target Gene	Primer sequences
HVDP	HVDP-F: ATTGATGATGTGGATAATCTGTG
	HVDP-R: GGTAAATACCATTGGTCTTGTTCC

Figure 29. primers used for detection of OsHV-1 by real-time PCR.

Amplification was performed using a ABI 7300 Thermocycler (Applied Biosystems, CA) in a total volume of 20 µl. The PCR mix included 1 µl of extracted DNA, 10 µl 2× SYBR GREEN dye, 0.50 µl of each diluted primers (final concentration 0.5 µM) and 8 µl of molecular grade water. Plasmid DNA containing cloned viral DNA was used as a positive control. Quantification of OsHV-1 DNA copies was carried out using a standard curve based on 10-fold dilutions of OsHV-1 genomic DNA.

For detection of *V. aestuarianus*, a Taqman real-time PCR protocol with the LightCyler (Roche Diagnostics, Mannheim, Germany) was used. *Vibrio aestuarianus* specific primers and probe were used (Figure 30).

Target Gene	Primer sequences
DNAj	DNA j F: GTATGAAATTTTAACTGACCCACAA
	DNA j R: CAATTTCTTTCGAACAACCAC
	Probe: DNA j FAM- TGGTAGCGCAGACTTCGGCGAC-BHQ2

Figure 30. primers and probe used for detection of V. aestuarianus by real-time PCR.

Each reaction mixture contained 1× LightCycler Taqman master (Roche Diagnostics, Mannheim, Germany) and 1 μM of each primer and 0.1 μM of each probe in a final volume of 20 μl. Five microliters of DNA template (DNA concentration for all samples varied from 10 to 100 ng μl−1) was added to the reaction mixture. Accurately quantified copy number genomic DNA of *V. aestuarianus* 01/32 strains was used as a standard. Positive and negative controls (PCR grade water, Sigma Aldrich S.R.L., Milan) were included in all qPCR assays.

Analysis of bivalve 'microbiota' by 16S rRNA gene-based profiling of the bacterial community

16S rDNA PCR amplicon libraries were generated from genomic DNA extracted from individual bivalve samples using primers amplifying positions 515–802 of the *Escherichia coli* numbering of the 16S rRNA gene that include the V4 hypervariable region. All primers were custom designed to include 16S rRNA complementary regions plus the complementary sequences to the Ion Torrent specific adapters. Two PCR assays were performed. A 1st target enrichment PCR assay with the 16S conserved primers. A 2nd PCR assay, with customized primers and included adapters' complementary regions. The obtained libraries were sequenced using an Ion Torrent (PGM) Platform. (Figure 31).

First PCR	
515f_UNI1+ *Unitail* 1	*CAG GAC CAG GGT ACG GTG* GTG CCA GCM GCC GCG GTA A
Second PCR	
802 R + *Unitail* 2	*CGC AGA GAG GCT CCG TG* T ACN VGG GTA TCT AAT CC
806 R + *Unitail* 2	*CGC AGA GAG GCT CCG TG* G ACT ACH VGG GTW TCT ATT

Figure 31. primers sequences for the 16S rRNA gene-based microbiome profiling

Bioinformatic Analysis

Bioinformatics analysis of NGS data was performed using the Microbial Genomics module (version 1.3) workflow of the CLC Genomics Workbench (version 9.5.1) and other comparable software. After quality trimming based on quality scores and length trimming, reads were clustered at 97% level of similarity into Operational Taxonomical Units (OTUs). Chimera detection and removal were performed. Ribosomal RNA gene reads were classified against the non-redundant version of the SILVA SSU reference taxonomy (release 119; http://www.arb-silva.de). Alpha diversity analysis was then conducted on total OTUs by constructing rarefaction curves calculated by sub-sampling OTUs abundances in the different samples at different depths. Beta diversity analysis was also performed by calculating Bray-Curtis distances between each pair of samples and applying Principal Coordinate Analysis (PCoA) on the distance matrices.

The core microbiota, defined as the microbial taxa belonging to OTUs present in all the samples, was analyzed using the Corbata software (CORe microbiome Analysis Tools, Li *et al*., 2013). A two- parameter model (Ubiquity-Abundance) was applied to quantitatively identify the core taxonomic members of each sample group microbiota considering the different conditions. This software allows the determination of the core members (high abundance and high ubiquity) of a single set of samples, but also allows the comparison of the core microbiota of two different groups of samples. Furthermore, the analysis of the "minor" core can be performed, thus, identifying bacterial groups at a very low abundance but high ubiquity. The AWKS statistic test (Abundance- Weighted Kolmogorov-Smirnov) was used to compared core microbiota profiles among samples.

2.2.3 Results

OsHV-1 and Vibrio aestuarianus detection in C. gigas samples by qPCR

A total of 525 C. gigas samples collected from 2016 to 2017 in three European sites, i.e., Ebro delta river, Dungarvan Bay and Bay of Brest were screened for the presence of OsHV-1 and *V. aestuarianus* using quantitative real-Time PCR, as previously described. *V. aestuarianus* was found associated to adult *C. gigas* mortality observed in the Ebro delta on 13th April 2016 and 31st May 2017 and in Dungarvan Bay on 3rd October 2016 (Figure 32). OsHV-1 DNA was detected in spat *C. gigas* sampled during 12 mortality episodes in the Ebro river delta, Dungarvan Bay and Bay of Brest (Figure 32).

Sampling Date	Code	Age	Origin	Ploidy	Mortality (%)	OshV-1 (Real-Time PCR)	*V. aestaurianus* (Real-Time PCR)
Ebro Delta (Spain)							
13/04/2016	EbDva13apr16/EbH13apr16	Adult	N	D	23% (Up to 50%)	0+/30	22+/30
26/04/2016	EbDoshV26apr16(c3)/EbH26apr16(c4)	Spat	N	D	76% (Up to 90%)	17+/30	0+/30
26/04/2016	EbDoshV26apr16(c5)/EbDva26apr16(c6)/EbH26apr16(c6)	Spat	N	D	46.6% (Up to 80%)	21+/30	4+/30
19_07_2016	EbDoshV19jul16/EbH19jul16	Spat	H	D	3% (light mortality)	1+/30	0+/30
19_07_2016	EbH19jul16(c2)	Spat	N	D	No mortality	0+/30	0+/30
24_11_2016	EbH24nov16/EbDoshV24nov16/EbDva24nov16	Spat	N	D	30% recent mortality	7+/30	1+/30
25_01_2017	EbH25jan17	Spat	H	D	No mortality	0+/30	0+/30
26_01_2017	EbH26jan17	Spat	H	D	No mortality	0+/30	0+/30
05_05_2017	EbDoshV5may17/EbH5may17	Spat	H	T	87.83% mortality	10+/18	0+/18
05_05_2017	EbH5may17(c1)	Spat	H	T	No mortality	0+/30	0+/30
31_05_2017	EbDva31may17/EbH31may17	Spat	H	T	85% mortality	0+/30	9+/30
Dungarvan Bay (Ireland)							
05_07_2016	DrDva7jul16/DrH7jul16	Adult	H	T	20%	0+/30	2+/30
05_07_2016	DrDoshV7jul16SPAT/DrDva7jul16SPAT/DrH7jul16SPAT	Spat	H	T	70%–100%	25+/30	3+/30
03_10_2016	DrDva3oct16/DrH3oct16	Adult	H	T	End of mortality	0+/30	11+/30
03_10_2016	DrDoshV3oct16SPAT/DrDvaV3oct16SPAT/DrH3oct16SPAT	Spat	H	T	End of mortality	12+/30	1+/30
10_01_2017	DrH10jan17	Adult	H	T	No mortality	0+/30	0+/30
Bay of Brest (France)							
10_07_2017	BbDoshV10jul17/BbDva10jul17/BbH10jul17	ad/sp/jv	H	D	Mortality	2+/12	2+/12
05_10_2017	BbDoshV5oct17/BbDva5oct17/BbH5oct17	ad/sp/jv	H	D	No mortality	3+/15	1+/15

Figure 32. Crassostrea gigas samples collected at different European sites and analysed in this study (n + number of samples/total number of analysed samples scoring positive to species-specific qPCR targeting the pathogen V. aestuarianus or OshV-1 in oyster tissues).

Legend: (ad, Adult; sp, Spat; jv, juvenile; N, Nature; H, Hatchery; D, Diploid; T, Triploid)

Microbiota analysis

One hundred one contrasting C. gigas samples were selected in the Ebro river Delta (n = 50), Dungarvan bay (n = 40) and the Bay of Brest (n = 11) formicrobiota analysis based on results from PCR screening analysis. In the experimental design, most interesting sampling periods were chosen (e.g. periods with high mortality or absence of mortality), and for each period, 10 contrasting individual oyster samples (five samples infected byOsHV-1 or *V. aestuarianus* and five noninfected control samples) were selected. Sequencing of the samples by Ion Torrent technology produced more than 14.000.000 amplicon sequence reads spanning the V4 hypervariable region of the bacterial 16S rRNA gene. Barcode and adapters sequences were removed and raw sequences were trimmed to minimize bias associated with PCR amplification of target genes. In particular, reads that contained one or more ambiguous bases, had errors in the barcode or primer sequence, were atypically short (100 bp), and had an average quality score <0.05 were removed from the data set. This process produced 13.143.153 trimmed reads corresponding on average to 146.000 sequence reads per analysed sample. In general, the composition of the bacterial community associated to *C. gigas* was dominated by the classes of *Gamma* and *Alphaproteobacteria* accounting on average for 28% and 15% of the total bacterial diversity followed by *Epsilonproteobacteria* (11%), *Mollicutes* (10%) and *Flavobacteria* (9%) (Figure 33).

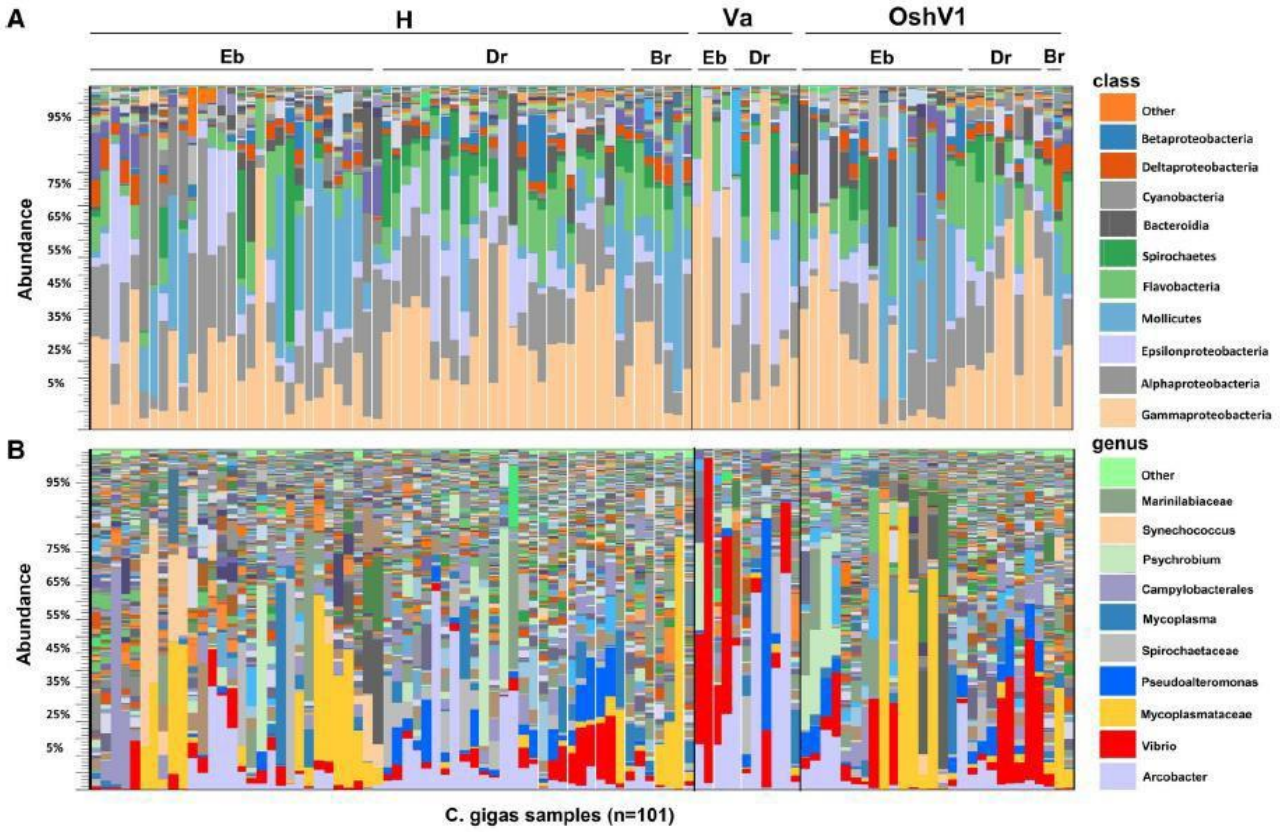

Figure 33. Taxonomic composition at class (A) and genus (B) level of the microbiota of the 101 specimens of C. gigas, grouped according to the health status of the oysters (H, uninfected oysters; Va, oysters infected by Vibrio aestuarianus; OshV1, oysters infected by Ostreid herpesvirus 1) and geographic location (Eb, Ebro delta; Dr, Dungarvan bay; Br, Bay of Brest), as revealed by sequencing analysis of the hypervariable region V4 of the 16S rRNA gene.

Rarefaction curves computed for total operational taxonomical units (OTUs) abundance almost reached a plateau indicating that sequencing effort was good enough to describe the majority of phylotypes in most of the samples. Generally, alpha diversity was lower in adult oysters infected by *V. aestuarianus* whilst it was higher in oyster spat infected by OsHV-1 (Figure 34).

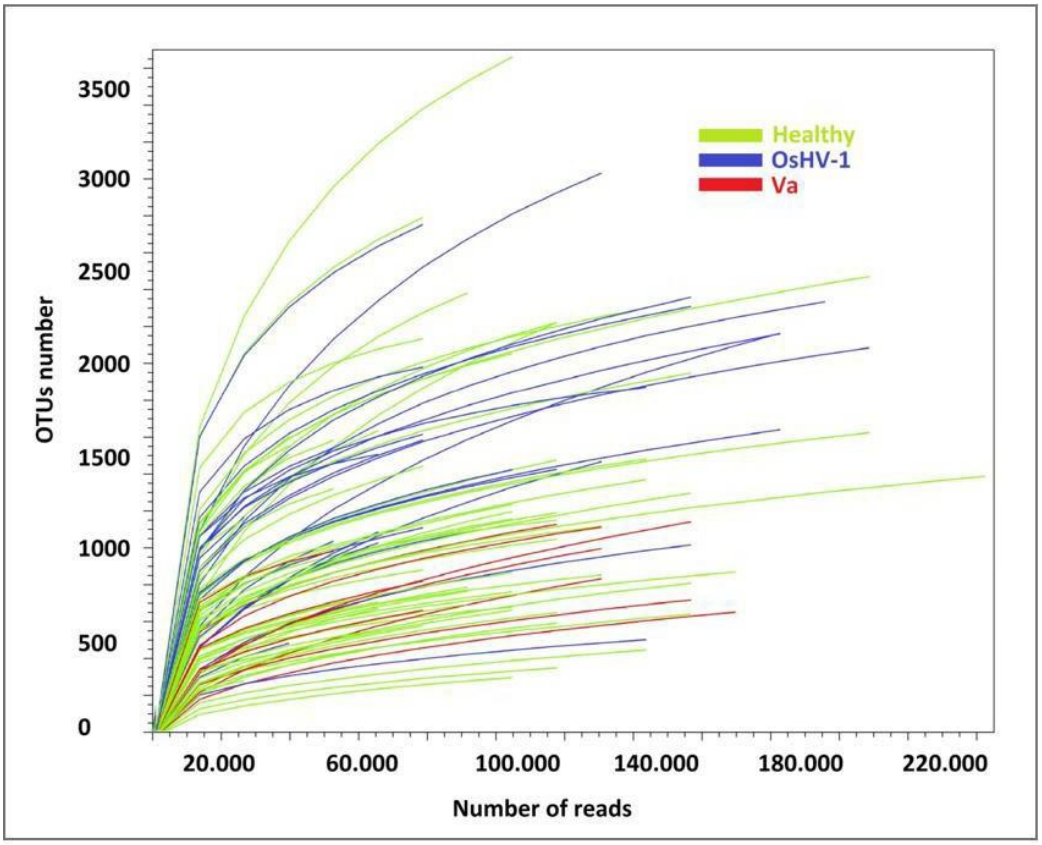

Figure 34. Rarefaction curves built on the abundance of OTU (Alpha-diversity) sequences (H=Healthy oysters; Va = oysters infected with Vibrio aestuarianus; OshV1 = Oysters infected with Ostreid herpesvirus).

Different physiological or environmental conditions including animal health status and age, geographic location and season significantly influenced the composition of the oyster microbiota as showed by beta diversity analysis and PERMANOVA testing ($p < 0.01$) (Figure 35). Analysis of contrasting bivalve samples based on the presence/absence of microbial pathogens showed that a significant shift in the microbiota community was observed in adult oyster infected by *V. aestuarianus* (Figure 35). In particular, an increase in abundance of bacteria belonging to the genus *Vibrio* and *Arcobacter* was observed in *V. aestuarianus*-infected oysters compared to either *V. aestuarianus* non-infected or OsHV-1 infected oysters. In oyster spats infected by OsHV-1 an increase in the *Vibrio* fraction was also observed compared with non-infected oysters.

The analysis of the core microbiota showed that the microbial community of oyster samples is dominated by two main bacterial groups, namely *Vibrio* and an uncultured bacterial group (uncultured-053) (Figure 36). When analysing adult *C. gigas* samples infected with *V. aestuarianus*, core taxa were assigned to *Arcobacter* and *Vibrio* genera. In contrast, core taxa of *V. aestuarianus* non-infected samples were assigned to the uncultured-053 group. When OsHV-1 DNA was detected in spat oysters, the core microbiota included *Vibrio* but also the uncultured-053 group. While Vibrio and Arcobacter were members of the core microbiota in adult oysters, in oyster spats the core group was dominated by Vibrio, uncultured-053, *Haliea* and *Marinicella*. Differences in the core microbiota were also evident across the different geographic locations. In oysters from Dungarvan bay the core groups were *Sulfitobacter*, uncultured-053, *Arcobacter, Pseudoalteromonas*, *Marinicella*, *Vibrio* and *Borrelia*, while in Ebro river Delta the core microbiota was formed only by *Vibrio* and uncultured-053. On the other hand, the core microbiota of the samples from the Bay of Brest was more diverse than that of oysters from other sites, with more than 20 different bacterial groups (*Arcobacter, Vibrio, Mycoplasma, Winogradskyella, Haliea, Sulfitobacter, Polaribacter, Marinicella, Lutimonas, Aquibacter, Roseovarius*, uncultured-104, uncultured-079, uncultured-053, uncultured-015, OM60(NOR5) clade, uncultured bacterium-088, uncultured-072, uncultured-050 and uncultured bacterium-248) probably reflecting the smaller number of samples analysed in this site. Seasonality also affected the composition of the core microbiota, and a transition of specific genera was identified (e.g. *Sulfitobacter* and *Marinicella* from cold seasons to warmer seasons.

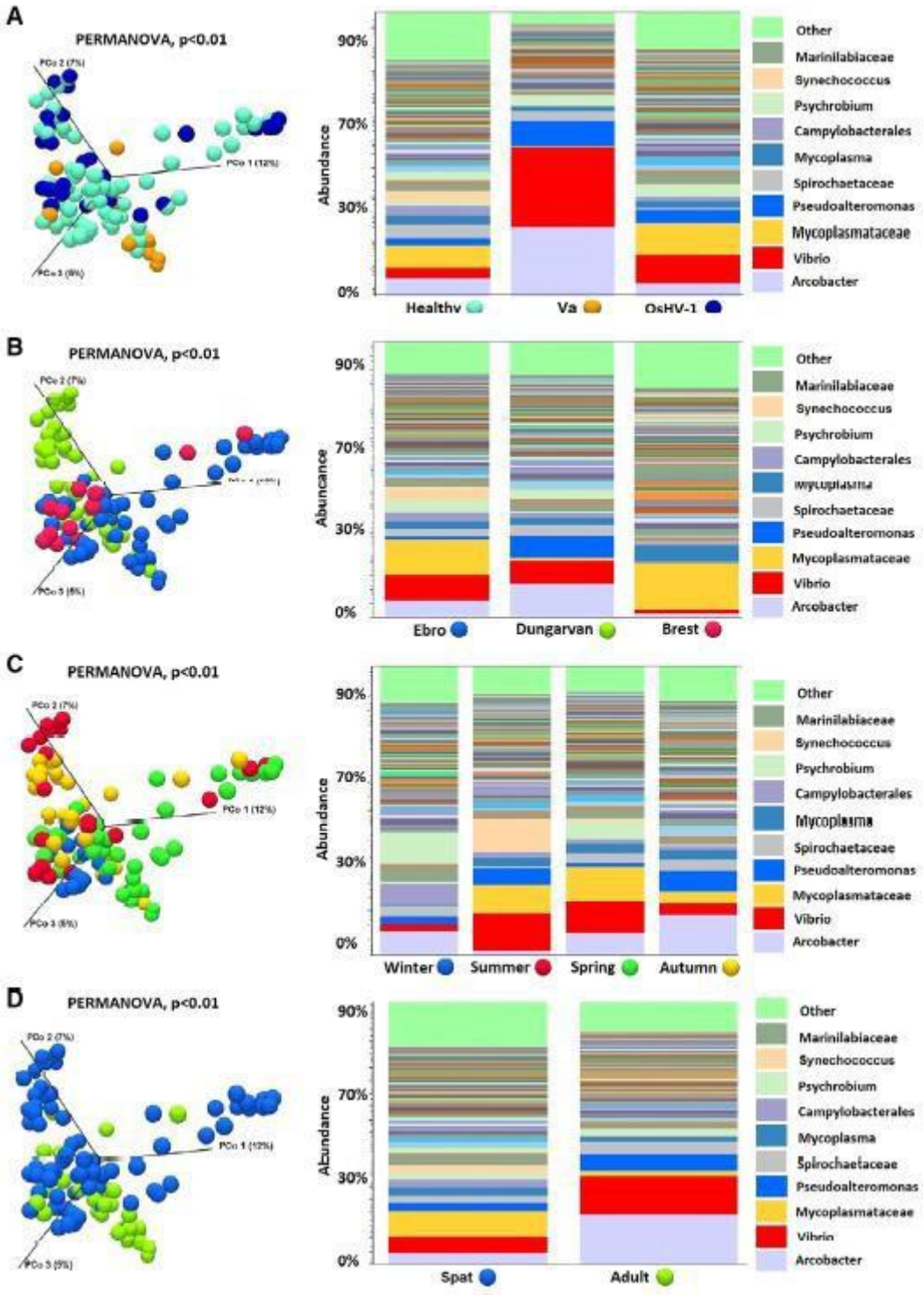

Figure 35. Comparative analysis of C. gigas microbiota (Beta diversity analysis) under different conditions: health status (A), geographic location (B), season (C) and animal age (D) (Va, Vibrio aestuarianus-infected oysters; OshV1, Ostreid herpesvirus 1-infected oysters.

All samples (n=101)	
Genera	*Vibrio* uncultured-053

	No infection	**OshV-1**	***V. aestuarianus***
Genera	uncultured-053	*Vibrio* uncultured-053	*Arcobacter* *Vibrio*

	Ebro	**Brest**	**Dungarvan**
Genera	*Vibrio* uncultured-053	*Arcobacter* *Vibrio* *Mycoplasma* *Winogradskyella* *Haliea* *Sulfitobacter* *Polaribacter* *Marinicella* *Lutimonas* *Aquibacter* *Roseovarius* uncultured-104 uncultured-079 uncultured-053 uncultured-015 OM60(NOR5) clade uncultured bacterium-088 uncultured-072 uncultured-050 uncultured bacterium-248	*Arcobacter* *Vibrio* *Pseudoalteromonas* *Borrelia* *Sulfitobacter* *Marinicella* uncultured-053

	Winter	**Spring**	**Summer**	**Autumn**
Genera	*Arcobacter* *Vibrio* *Sulfitobacter* *Colwellia* *Marinicella* uncultured-053	*Vibrio*	*Vibrio* *Haliea* *Marinicella* *Pseudahrensia* uncultured-104 uncultured-079 uncultured-053 uncultured-017	*Arcobacter* *Vibrio* *Winogradskyella* *Sulfitobacter* *Marinicella* *Lutimonas* uncultured-053 OM60(NOR5) clade

	Juvenile	**Adult**
Genera	Uncultured-053 *Haliea*	*Arcobacter* *Vibrio*

Figure 36. Core microbiota, shared genera in the different conditions at 0.1% of relative abundance and presence in, at least, 90 % of the samples

2.2.4 Discussion

This part of the work investigated for the first time the microbiota associated to farmed *C. gigas* at a European scale and provided new data on its composition and pattern of variability with particular reference to the occurrence of abnormal mortality episodes. In general, the composition of the bacterial community of *C. gigas* was dominated by the classes of *Gamma* and *Alphaproteobacteria* followed by *Epsilonproteobacteria*, *Mollicutes* and *Flavobacteria*. The composition of the microbial community of *C. gigas* was highly variable in relation to health status, geographic location, season and oyster age (Figure 33). Accordingly, many transient and opportunistic microbial taxa appeared to dominate oyster microbiota while core microbial communities were restricted to only a few, most probably resident bacteria, such as *Vibrio* and the uncultured-053 group. This may be linked to the filter feeding behaviour of oysters, which expose the animals to colonization by complex and highly variable microbial communities found in the seawater environment. *Mycoplasmataceae*, *Arcobacter*, *Synechococcus* and *Spirochaetaceae* dominated the microbiota in healthy (non-infected) oysters suggesting these taxa might play a beneficial role in oyster fitness and health status (King *et al*., 2019).

Comparative analysis of healthy versus infected *C. gigas* samples clearly showed that infected oysters displayed signs of community structure disruption and were characterized by a low diversity and proliferation of few bacterial taxa. This was particularly evident for *V. aestuarianus* infected oysters where dominance by bacteria belonging to the genus *Vibrio* and Arcobacter resulted in low microbial diversity compared with healthy oysters. In the case of OsHV-1 infected oyster, loss of Alpha diversity was less clear and mostly linked to proliferation of *Vibrio* and a significant decline of some bacterial taxa such as cyanoprokaryotes (e.g. *Synechococcus*) (Figure 33). Loss of microbiota diversity and proliferation of few OTUs (‘dysbiosis’) has previously been linked with impaired health in oysters (Green and Barnes, 2010; King *et al*., 2019), including *C. gigas* (Garnier *et al*., 2007; Lokmer and Wegner, 2015). It is thus apparent that specific microbial taxa and especially members of the *Vibrio* genus are likely to play a role in affecting oyster health status during disease outbreaks. Nevertheless, whether the condition of ‘dysbiosis’ is a prerequisite for oyster infection or it is a consequence of developing disease it is difficult to discern.

Recently two different studies, de Lorgeril *et al*. (2018) and Lemire *et al.* (2015), showed that the onset of disease in oysters is associated with progressive replacement of diverse benign bacterial colonizers by members of a phylogenetically coherent virulent population. According to these results ‘dysbiosis’ might be seen as a new form of polymicrobial disease, in which a population/consortium of virulent strains but also non-pathogenic strains contribute to oyster mortality (Lemire *et al*., 2015).

3. Conclusions

Due to their filter-feeding habit, bivalves normally accumulate a rich bacterial microbiota. Persistence of entrapped bacteria inside bivalve tissues depends, at least in part, on their capacity to survive the hemolymph bactericidal activity that is exerted by both hemocytes and soluble factors. The Laboratory of Microbiology at DISTAV, which has long been involved in studies on the interactions between bacteria and bivalve hemocytes, recently shown that the adhesion of *Vibrio cholerae* and *Escherichia coli* to the hemocytes of *Mytilus galloprovincialis* and the subsequent killing of the attached and internalized bacteria are mediated from a serum opsonin which has been identified as the precursor of the extrapalleal protein (EP) in *Mytilus edulis* (Canesi *et al*., 2016). The opsonin (named MgEP = *M. galloprovincialis* EP) contains residues of D-mannose and, following the bond with the sensitive mannose adhesin (MS) MSHA (MS HemAgglutinin) present on the surface of bacterial cells, works as a bridge between hemocytes and vibrios and promotes bacterial killing. In this study we showed that MgEP promotes D- mannose sensitive adhesion to and killing by hemocytes of the bivalve pathogens *V. aestuarianus* 01/032, *V. aestuarianus* 02/041, *V. tasmaniensis* LGP32 and *V. coralliilyticus* ATCC BAA 450. This may explain the fact that mussels are more resistant than oysters (which lack the MgEP serum protein) to infection by these bacteria. Accordingly, a significant bacterial killing was observed by oysters hemocytes consequently to the addition of MgEP to oyster serum and oyster hemocytes. This suggests that MgEP exerts an effect on *V. aestuarianus* in cooperation with oyster haemocytes, while oyster serum, which does not contain the opsonin MgEP, does not perform any bactericidal action against these pathogenic strains for oysters.

Overall, the results of our study may represent the starting point to decipher molecular basis for the higher susceptibility to infections by *Vibrio* strains exhibited by mussels in comparison with oysters. These studies are central to better understand molecular basis of bacteria-hemolymph interactions, improve bivalve depuration systems, and prevent diseases affecting bivalve production worldwide.

Infectious agents such as the bacteria *Vibrio aestuarianus* or Ostreid herpesvirus 1 have been repeatedly associated with dramatic disease outbreaks of *Crassostrea gigas* beds in Europe. Beside roles played by these pathogens, microbial infections in *C. gigas* may derive from the contribution of a larger number of microorganisms than previously thought, according to an emerging view supporting the polymicrobial nature of bivalve diseases. In this study, the microbial communities associated with a large number of *C. gigas* samples

collected during recurrent mortality episodes at different European sites were investigated by real-time PCR and 16SrRNA gene based microbial profiling. It was shown that primary infectious agents such as the bacteria *V. aestuarianus* and Ostreid herpesvirus-1 (OsHV-1) dominated the pathobiota community of infected animals during mortality outbreak ascribed to these pathogens together with a previously undetected community of potential pathogenic bacterial species mostly belonging to the genus *Vibrio* and *Arcobacter*.

It is suggested that the biology and ecology of detected microbial species and their consortia should be targeted by future studies aimed to shed light on mechanisms underlying polymicrobial infections in *C. gigas*. More generally, the developed protocol and approach may be of great interest in monitoring oyster disease dynamics as well as in studies investigating infection diseases in other marine organisms and the biology and ecology of marine microbial pathogenic communities.

4. Abbreviations

ASW Artificial Seawater
Composition: NaF 1.9 mg/l; $SrCl2*6H_2O$ 13 mg/l; H_3BO_3 20 mg/l; KBr 67 mg/l; KCl 466 g/l; $CaCl_2*2H2O$ 733 mg/l; Na_2SO_4 2.66 g/l; $MgCl2*6H_2O$ 3.33 g/l; $NaHCO_3$ 133
mg/l; NaCl 27.65 g/l; pH 8

MgEP *Mytilus galloprovincialis* extrapallial protein

CFU Colony Forming Unit

LB Luria Bertani

LMS Lysosomal Membrane Stability

NRRT Neutral Red Retention Time

PBS Phosphate Buffered Saline
Composition: NaCl 8 g/l; KCl 0.2 g/l; $Na_2HPO_4.12H_2O$ 3.62 g/l; $KHPO_4$ 0.24 g/l

Ppt Parts Per Thousands

RT-PCR Real -Time Polymerase Chain Reaction

TCBS Thiosulfate Citrate Bile salts sucrose

Eb Ebro delta

Dr Dungarvan bay

Br Bay of Brest

5. BIBLIOGRAPHY

Alfaro A. C., Nguyen T. V. and Merien F. (2018) The complex interactions of *Ostreid herpesvirus 1*, *Vibrio* bacteria, environment and host factors in mass mortality outbreaks of *Crassostrea gigas*. *Rev Aquacult*. doi:10.1111/raq.12284

Austin B., Austin D., Sutherland R., Thompson F., Swings J. (2005) Pathogenicity of vibrios to rainbow trout (Oncorhynchus mykiss, Walbaum) and *Artemia nauplii*. *Environ Microbiol.* 7(9):1488-95.

Aboubaker, M.H., Sabrié, J., Huet, M., and Koken, M. (2013) Establishment of stable GFP-tagged *Vibrio aestuarianus* strains for the analysis of bacterial infection-dynamics in the Pacific oyster, *Crassostrea gigas*. *Vet Microbiol* 164:392–398.

Balbi, T., Fabbri, R., Cortese, K., Smerilli, A., Ciacci, C., Grande, C., et al. (2013) Interactions between *Mytilus galloprovincialis* hemocytes and the bivalve pathogens *Vibrio aestuarianus* 01/032 and *Vibrio splendidus* LGP32. *Fish Shellfish Immunol* 35: 1906–1915.

Canesi, L., Pruzzo, C., Tarsi, R., and Gallo, G. (2001) Surface interactions between *Escherichia coli* and hemocytes of the Mediterranean mussel *Mytilus galloprovincialis* lam. leading to efficient bacterial clearance. *Appl Environ Microbiol* 67: 464–468.

Canesi, L., Gavioli, M., Pruzzo, C., and Gallo, G. (2002) Bacteriae hemocyte interactions and phagocytosis in marine bivalves. *Microsc Res Tech* 57:469e76.

Canesi L., Grande C., Pezzati E., Balbi T., Vezzulli L., Pruzzo C. (2016) Killing of *Vibrio cholerae* and *Escherichia coli* strains carrying D-mannose-sensitive ligands by Mytilus Hemocytes is promoted by a multifunctional hemolymph serum protein. *Microb Ecol* (2016) 72:759−762. DOI 10.1007/s00248-016-0757-1

Carballal M.J., Lopez C., Azevedo C., Villalba A. (1997) Enzymes involved in defense functions of hemocytes of Mussel *Mytilus galloprovincialis*. Journal of Invertebrate Pathology 70, 96–105 (1997). Article No. In974670

Cash R.A., Music S.I., Libonati J. P., Snyder M., Wenzel R.P., Hornick R.B. Response of Man to Infection with *Vibrio cholerae* (1974). I. Clinical, Serologic, and Bacteriologic Responses to a Known Inoculum *The Journal of Infectious Diseases*, Volume 129, Issue 1, January 1974, Pages 45–52, https://doi.org/10.1093/infdis/129.1.45

Chakraborty S., Nair G.B., and Shinoda S. (1997) Patho-genic vibrios in the natural aquatic environment. *Rev Environ Health* 12: 63–80.

Cheng T.C., Rodrick G.E., Foley D.A., Koehler S.A. (1975). Release of lysozyme from hemolymph cells of Mercenaria mercenaria during phagocytosis. *Journal of Invertebrate Pathology*, https://doi.org/10.1016/0022-2011(75)90076-2.

Ciacci C., Betti M., Canonico B., Citterio B., Roch P. and Canesi L. (2010). Specificity of antivibrio immune response through p38 MAPK and PKC activation in the hemocytes of the mussel *Mytilus galloprovincialis*. *J Invertebr Pathol* 105: 49e55.

Colwell R., Spira W.M. The Ecology of *Vibrio cholerae* (1992). Current Topics in Infectious Disease.

Colwell R., Huq A. Environmental Reservoir of *Vibrio cholerae* The Causative Agent of Cholera (1994). *Annals of the New York Academy of Sciences*. https://doi.org/10.1111/j.1749-6632.1994.tb19852.x

Eiler A., Johansson M., Bertilsson S. Environmental Influences on *Vibrio* Populations in Northern Temperate and Boreal Coastal Waters (Baltic and Skagerrak Seas) (2006). *Microbial Ecology*. DOI: 10.1128/AEM.00917-06.

EFSA Panel on Animal Health and Welfare (AHAW). «Oyster Mortality: Oyster Mortality». EFSA Journal 13, n. 6 (june 2015): 4122. https://doi.org/10.2903/j.efsa.2015.4122.

Elston R.A., Infectious diseases of the Pacific oyster, *Crassostrea gigas. Elsevier.* https://doi.org/10.1016/0959-8030(93)90038-D

FAO 2014, Cultured Aquatic Species Information Programme.

Fao.org

Farmer J.J. & Hickman-Brenner F.W. (2006) The Genera *Vibrio* and *Photobacterium*. In: Dworkin M., Falkow S., Rosenberg E., Schleifer KH., Stackebrandt E. (eds) The Prokaryotes. Springer, New York, NY.

FAOSTAT, 2012. Food and Agriculture Organization of the United Nations, Statistical Yearbook, Rome.

Freyer E.S., Bayne C.J., Host—Parasite Interactions in Molluscs (1996). *Invertebrate Immunology.*

Hine P.M., The inter-relationships of bivalve haemocytes. *Fish and Shellfish Immunology*. https://doi.org/10.1006/fsim.1998.0205

Gay, M., Berthe, F.C., and Le Roux, F. (2004) Screening of *Vibrio* isolates to develop an experimental infection model in the Pacific oyster *Crassostrea gigas*. *Dis Aquat Organ* 59: 49–56.

Garnier M., Labreuche Y., Garcia C., Robert A. and Nicolas J.L. (2007) Evidence for the involvement of pathogenic bacteria in summer mortalities of the Pacific oyster *Crassostrea gigas*. *Microbial Ecology*, 53, 187-196.

Garnier M., Labreuche Y., e Nicolas J.L. (2008) Molecular and Phenotypic Characterization of *Vibrio aestuarianus* Subsp. *Francensis* Subsp. Nov. a Pathogen of the Oyster *Crassostrea gigas*. *Systematic and Applied Microbiology* 31, n. 5 (2008): 358–65.

Gauthier M.J. (2000). Nonculturable microorganisms in the environment (pp 87-112) *Washington D.C.: American Society for Microbiology.*

Gerdol, M., Manfrin, C., De Moro, G., Figueras, A., Novoa, B., Venier, P., and Pallavicini, A. (2011). The C1q domain containing proteins of the Mediterranean mussel *Mytilus galloprovincialis*: a widespread and diverse family of immune-related molecules. *Dev Comp Immunol* 35: 635–643.

Goudenège D., Travers M.A., Lemire A., Haffner P., Labreuche Y., Petton B., Mangenot S., Calteau A., Mazel D., Nicolas J.L., Jacq A. and Le Roux F. (2015). A single regulatory gene is sufficient to alter *Vibrio aestuarianus* pathogenicity in oysters. *Environmental Microbiology*.

Green, T.J., and Barnes, A.C. (2010). Bacterial diversity of the digestive gland of Sydney rock oysters, *Saccostrea glomerata* infected with the paramyxean parasite, *Marteilia sydneyi*. *J Appl Microbiol* 109: 613–622.

http://www.arb-silva.de

Igbinosa O. E., Okoh A. I. (2008) Emerging *Vibrio* species: an unending threat to public health in developing countries. *Research in Microbiology*, Volume 159, Issues 7–8, 2008, Pages 495-506, ISSN 0923-2508.

Keeling S.E., Brosnahan C.L., Williams R., Gias E., Hannah M., Bueno R., McDonald W.L. and Johnston C. (2014) New Zealand juvenile oyster mortality associated with ostreid herpesvirus 1-an opportunistic longitudinal study. *Diseases of Aquatic Organisms*,109, 231-239.

King, W.L., Siboni, N., Williams, N.L.R., Kahlke, T., Nguyen, K.V., Jenkins, C., et al. (2019). Variability in the composition of Pacific oyster microbiomes across oyster families exhibiting different levels of susceptibility to OsHV-1 μvar disease. *Front Microbiol* 10: 473–473.

Labreuche, Y., Soudant, P., Goncalves, M., Lambert, C., and Nicolas, J.L. (2006). Effects of extracellular products from the pathogenic *Vibrio aestuarianus* strain 01/32 on lethality

and cellular immune responses of the oyster Crassostrea gigas. *Dev Comp Immunol* 30: 367e79.

Labreuche, Y., Le Roux, F., Henry, J., Zatylny, C., Huvet, A., Lambert, C., et al. (2010). *Vibrio aestuarianus* zinc metalloprotease causes lethality in the Pacific oyster *Crassostrea gigas* and impairs the host cellular immune defenses. Fish Shellfish Immunol 29: 753–758.

Lemire, A., Goudene, D., Versigny, T., Petton, B., Calteau, A., Labreuche, Y., et al. (2015) Populations, not clones, are the unit of *vibrio* pathogenesis in naturally infected oyster. *ISME* J 9: 1523–1531.

Lipp E.K., Huq A., Colwell R.R. (2002). Effects of global climate on infectious disease: the cholera model. doi: 10.1128/CMR.15.4.757-770.2002 *Clin. Microbiol.* Rev. October 2002 vol. 15 no. 4 757-770 1 October 2002.

Lacoste, A., Jalabert, F., Malham, S., Cueff, A., Gelebart, F., Cordevant, C., et al. (2001) A *Vibrio splendidus* strain is associated with summer mortality of juvenile oysters *Crassostrea gigas* in the Bay of Morlaix (North Brittany, France). *Dis Aquat Organ* 46: 139–145.

Leippe M., Renwrantz L., Release of cytotoxic and agglutinating molecules by Mytilus hemocytes. *Developmental & Comparative Immunology.* https://doi.org/10.1016/0145-305X(88)90006-7.

Leclerc M., Humoral Factors in Marine Invertebrates (1996). *Invertebrate Immunology*.

Li, K., Bihan, M., and Methé, B.A. (2013) Analyses of the stability and core taxonomic memberships of the human microbiome. *PLoS One* 8: e63139.

Lokmer, A., Goedknegt, M.A., Thieltges, D.W., Fiorentino, D., Kuenzel, S., Baines, J.F., et al. (2016). Spatial and temporal dynamics of pacific oyster hemolymph microbiota across multiple scales. *Front Microbiol* 7: 1367.

Lokmer, A., and Wegner, K.M. (2015) Hemolymph microbiome of Pacific oysters in response to temperature, temperature stress and infection. *ISME* J 9: 670–682.

Lorgeril J., Lucasson A., Mitta G., Immune-suppression by OsHV-1 viral infection causes fatal bacteraemia in Pacific oysters (2018). *Nature Communications* volume 9, Article number: 4215.

McGladdery SE., Shellfish diseases (viral, bacterial and fungal) (1999). *Fish diseases and disorders.*

Mitta, G., Vandenbulcke, F., and Roch, P. (2000) Original involvement of antimicrobial peptides in mussel innate immunity. *FEBS* Lett 486: 185e90.

Olafsen J.A., Mikkelsen H.V., Giæver H.M., Hansen G.H. (1993). Indigenous Bacteria in Hemolymph and Tissues of Marine Bivalves at Low Temperatures. *Appl Environ Microbiol*. 1993 Jun; 59(6): 1848–1854.

Oliveri, C., Peric, L., Sforzini, S., Banni, M., Viarengo, A., Cavaletto, M., and Marsano, F. (2014). Biochemical and proteomic characterisation of haemolymph serum reveals the origin of the alkali-labile phosphate (ALP) in mussel (*Mytilus galloprovincialis*). *Comp Biochem Physiol Part D Genomics*.

Oliver J. D., Nilsson L., & Kjelleberg S. (1991). Formation of nonculturable *Vibrio vulnificus* cells and its relationship to the starvation state. *Applied and Environmental Microbiology*, 57(9), 2640–2644.

Paillard, C., Le Roux, F., and Borrego, J.J. (2004). Bacterial disease in marine bivalves, a review of recent studies: trends and evolution. *Aquat Living Resour* 17: 477–498.

Pernet F., Barret J., Le Gall P., Corporeau C., Dégremont L., Lagarde F., Pépin J., Keck N. (2012). Mass mortalities of Pacific oysters *Crassostrea gigas* reflect infectious diseases and vary with farming practices in the Mediterranean Thau lagoon, France. *Aquacult Environ Interact* 2:215-237.

Pezzati E., Canesi L., Damonte G., Salis A., Marsano F., Grande C., Vezzulli L., Pruzzo C. (2015). Susceptibility of *Vibrio aestuarianus* 01/032 to the antibacterial activity of *Mytilus* haemolymph: identification of a serum opsonin involved in mannose-sensitive interactions. *Environ Microbiol*. doi:10.1111/1462-2920.12750.

Pipe R.K., Hydrolytic enzymes associated with the granular haemocytes of the marine mussel *Mytilus edulis* (1990*). The Histochemical Journal.*

Pruzzo, C., Gallo, G., and Canesi, L. (2005) Persistence of vibrios in marine bivalves: the role of interactions with haemolymph components. *Environ Microbiol* 7: 761–772.

Pruzzo C., Vezzulli L. and Colwell R. R. (2008) Global impact of *Vibrio cholerae* interactions with chitin. *Environ Microbiol*, 10: 1400-1410. doi:10.1111/j.1462-2920.2007.01559.x

Rasmussen T., Rasmus Bugge J. and Ole S. (2007). The two chromosomes of *Vibrio cholerae* are initiated at different time points in the cell cycle. *The EMBO Journal* 26, n. 13 (11 luglio 2007): 3124.

Renault, T. (1996). Appearance and spread of diseases among bivalve molluscs in the northern hemisphere in relation to international trade. *Rev Sci Tech* 15: 551–561.

Rees J., Pond K., Kay D., Bartram J., Domingo J.S. (2010). World Health Organization: Safe management of shellfish and harvest waters. *IWA Publishing London, United Kingdom*.

Romero, A., Costa, M.D., Forn-Cuni, G., Balseiro, P., Chamorro, R., Dios, S., *et al*. (2014) Occurrence, seasonality and infectivity of *Vibrio* strains in natural populations of mussels *Mytilus galloprovincialis*. *Dis Aquat Organ* 108:149–163.

Saulnier D., De Decker S., Haffner P., Cobret L., Robert M. and Garcia C. (2010). A Large-Scale Epidemiological Study to Identify Bacteria Pathogenic to Pacific Oyster *Crassostrea gigas* and Correlation Between Virulence and Metalloprotease-like Activity. *Microbial Ecology*, 59, 787-798.

Scarano C., Spanu C., Ziino G., Pedonese F., Dalmasso A., Spanu V., Virdis S. and De Santis E.P.L. (2014). Antibiotic resistance of *Vibrio* species isolated from Sparus aurat areared in Italian mariculture. *New Microbiologica*,37, 329-337.

Schikorski, D., Faury, N., Pépin, J.F., Saulnier, D., Tourbiez, D., and Renault, T. (2011). Experimental ostreid herpesvirus 1 infection of the Pacific oyster *Crassostrea gigas*: kinetics
of virus DNA detection by q-PCR in seawater and in oyster samples. *Virus Res* 155: 28–34.

Segarra, A., Pépin, J.F., Arzul, I., Morga, B., Faury, N., and Renault, T. (2010). Detection and description of a particular ostreid herpesvirus 1 genotype associated with massive mortality outbreaks of Pacific oysters, *Crassostrea gigas*, in France in 2008. *Virus Res* 153: 92–99.

Sindermann C.J., Principal Diseases of Marine and Shellfish (1990).

Singleton F.L., Attwell R., Jang S., Colwell R.R., Effects of Temperature and Salinity on *Vibrio cholerae* Growth (1982). *Applied and Environmental Microbiology*. 0099-2240/82/111047-12$02.00/0.

Sminia T., van der Knaap W.P.W., Edelenbosch P., The role of serum factors in phagocytosis of foreign particles by blood cells of the freshwater snail *Lymnaea stagnalis* (1979). *Developmental & Comparative Immunology*. https://doi.org/10.1016/S0145-305X(79)80004-X

Tantillo G., Fontanarosa M., Di Pinto A. and Musti M. (2004). Updated perspectives on emerging vibrios associated with human infections. *Letters in Applied Microbiology*, 39: 117-126. doi:10.1111/j.1472-765X.2004.01568.x

Thompson F.L., Tetsuya L., Swings J., Biodiversity of *Vibrios* (2004). *Microbiology and Molecular Biology Reviewes.* DOI: 10.1128/MMBR.68.3.403-431.2004

Tison D.L. and Seidler R.J. (1983). *Vibrio-Aestuarianus* – a New Species from Estuarine Waters and Shellfish. *International Journal of Systematic Bacteriology*, 33, 699-702.

Travers M.A., Boettcher Miller K., Roque A., Friedman C.S. (2015). Bacterial diseases in mirane bivalves. J Invertebr Pathol. 2015 Oct; 131:11-31. doi: 10.1016/j.jip.2015.07.010

Tunkijjanukij L., Sialic acid-binding lectin with antibacterial activity from the horse mussel: further characterization and immunolocalization (1998). *Developmental & Comparative Immunology*. https://doi.org/10.1016/S0145-305X(98)00017-2

Vezzulli, L., Pezzati, E., Stauder, M., Stagnaro, L., Venier, P., and Pruzzo, C. (2014). Aquatic ecology of the oyster pathogens *Vibrio splendidus* and *Vibrio aestuarianus*. Environ Microbiol. doi:10.1111/1462-2920.12484.

Waechter, M., Le Roux, F., Nicolas, J.L., Marissal, E., and Berthe, F. (2002). Characterization of pathogenic bacteria of the cupped oyster *Crassostrea gigas*. *C R BIOL* 325: 231–238.

Wendling, C.C., Batista, F.M., and Wegner, K.M. (2014). Persistence, seasonal dynamics and pathogenic potential of *Vibrio* communities from pacific oyster hemolymph. *PLoS ONE* 9: e94256. doi:10.1371/journal.pone.0094256.

Zhang X.J., Qin G.M., Bing X.W., Yan B.L. and Liang L.G. (2011). Molecular and phenotypic characterization of *Vibrio aestuarianus*, a pathogen of the cultured tongue sole, *Cynoglossus semilaevis* Gunther. *Journal of Fish Diseases*,34, 57.

Zampini, M., Canesi, L., Betti, M., Ciacci, C., Tarsi, R., Gallo, G., and Pruzzo, C. (2003). A role for the mannose-sensitive hemagglutinin (MSHA) in promoting the interactions between *Vibrio cholerae* El Tor and mussel hemolymph. *Appl Environ Microbiol* 69: 5711–5715.

Zhou, H., Hanneman, A.J., Chasteen, N.D., and Reinhold, V.N. (2013). Anomalous N-glycan structures with an internal fucose branched to GlcA and GlcN residues isolated from a mollusk shell-forming fluid. *J Proteome Res* 12: 4547– 4555.

6. ACKNOWLEDGEMENTS

Upon completion of this path, I would like to thank my Supervisor, Professor Luigi Vezzulli, and Professor Carla Pruzzo for their great availability and for having been able to work with them in the DISTAV Microbiology Laboratory, an experience that has enriched me both from the point of view of both professionally and personally. Thanks also to Professor Laura Canesi and the whole physiology group for the invaluable help provided during the activity of these years.

I would also like to thank Professor Firpo, the Professor Staff and the Technical staff of DISTAV for their availability and collaboration during the PhD activity.

I would like to thank all my family, my father, my mother, my brother Manuele and my uncles for their support, their presence and their love.

A thought to my beloved grandparents Ines, Francesco, Anna and Rino, who, although unfortunately not present to attend this important stage, have been fundamental in my life with their presence and their affection, and I will always thank them, dedicating and sharing also with them happy moments and satisfactions like this one.

A special thanks to my loved Elisa, who has supported me (and has endured) for over 8 years, always next to me, and who has supported me a lot to complete this path.

A heartfelt thanks also to my fellow PhD students and friends I met during this beautiful journey, with whom I not only shared many good moments but I also learned a lot: Francesca, Caterina, Aide, Chiara, Giovanni, Andrea, Manon, Teresa, Sirio, Khalil and Peter.

Published articles:

environmental microbiology reports

Environmental Microbiology Reports (2018) **10**(4), 458–464 doi:10.1111/1758-2229.12665

ddPCR applied on archived Continuous Plankton Recorder samples reveals long-term occurrence of class 1 integrons and a sulphonamide resistance gene in marine plankton communities

Andrea Di Cesare,[1†*] Sara Petrin,[2†] Diego Fontaneto,[3] Carmen Losasso,[2] Ester M. Eckert,[3] Giovanni Tassistro,[1] Alessio Borello,[1] Antonia Ricci,[2] William H. Wilson,[4] Carla Pruzzo[1] and Luigi Vezzulli[1]

[1]*Department of Earth, Environmental and Life Sciences (DISTAV), University of Genoa, Genoa, Italy.*

[2]*O.U. Microbial Ecology, Department of Food Safety, Istituto Zooprofilattico Sperimentale delle Venezie, Legnaro, Italy.*

[3]*Microbial Ecology Group (MEG), National Research Council - Institute of Ecosystem Study (CNR-ISE), Verbania, Italy.*

[4]*CPR Survey, Marine Biological Association, The Laboratory, Citadel Hill, Plymouth, UK.*

Summary

Antibiotic resistance is a rising threat for human health. Although in clinical settings and terrestrial environments the rise of antibiotic resistant bacteria is well documented, their dissemination and spread in the marine environment, covering almost two-thirds of the Earth's surface, is still poorly understood. In this study, the presence and abundance of sulphonamide resistance gene (*sul*2) and class 1 integron-integrase gene (*intI*1), used as markers for the occurrence and spread of antibiotic resistance genes since the beginning of the antibiotic era, were investigated. Twenty-nine archived formalin-fixed samples, collected by the Continuous Plankton Recorder (CPR) survey in the Atlantic Ocean and North Sea from 1970 to 2011, were analysed using Droplet Digital PCR (ddPCR) applied for the first time on CPR samples. The two marker genes were present in a large fraction of the samples (48% for *sul*2 and 76% for *intI*1). In contrast, results from Real-Time PCR performed on the same samples greatly underestimate their occurrence (21% for *sul*2 and 52% for *intI*1). Overall, besides providing successful use of ddPCR for the molecular analysis of CPR samples, this study reveals long-term occurrence and spread of *sul*2 gene and class 1 integrons in the plankton-associated bacterial communities in the ocean.

Received 14 March, 2018; accepted 27 May, 2018. *For correspondence. E-mail andrea.di.cesare@unige.it; Tel. (+39) 010 3538135; Fax (+39) 010 3538267. †These authors contributed equally to this work.

Introduction

Antibiotic resistance is a global concern for human health (Marti *et al*., 2014). The massive use and misuse of antibiotics in human care settings and animal farming led to the release of high amounts of antibiotics in aquatic environments, causing the selection and spread of antibiotic resistant bacteria (Kümmerer, 2009). Antibiotic resistance genes (ARGs) have been found to be constitutively present within aquatic microbial communities, especially in coastal areas subjected to strong anthropogenic influence such as urban areas and aquaculture sites (Taylor *et al*., 2011; Di Cesare *et al*., 2012; 2015; Czekalski *et al*., 2015; Zhu *et al*., 2017). Antibiotic resistant bacteria (ARB) can be found both as free-living cells and associated with floating particles and plankton (Eckert *et al*., 2016; 2018); the latter was recently proposed as an important ecological driver for the evolution and spread of ARB in the aquatic ecosystem (Taylor *et al*., 2011). Zooplankton species may host abundant bacterial communities: copepods might even be regarded as microbial hot spots in the ocean (Tang, 2005). Eckert and colleagues (2016) hypothesized *Daphnia obtusa* as a refuge for ARB, supporting the idea that bacteria coming from wastewater treatment plants (WWTPs) could better survive when attached to the exoskeleton or gut of aquatic crustaceans (Hall-Stoodley *et al*., 2004). In addition, zooplankton species, with their diel circulation, are also responsible for vertical mobilization and consequent relocation of associated bacteria, which may be pathogenic (Grossart *et al*., 2010) and even antibiotic resistant. Similar to zooplankton, different cyanobacteria genera in the phytoplankton harbour their own microbial communities (Zhu *et al*., 2016; Callieri *et al*., 2017).

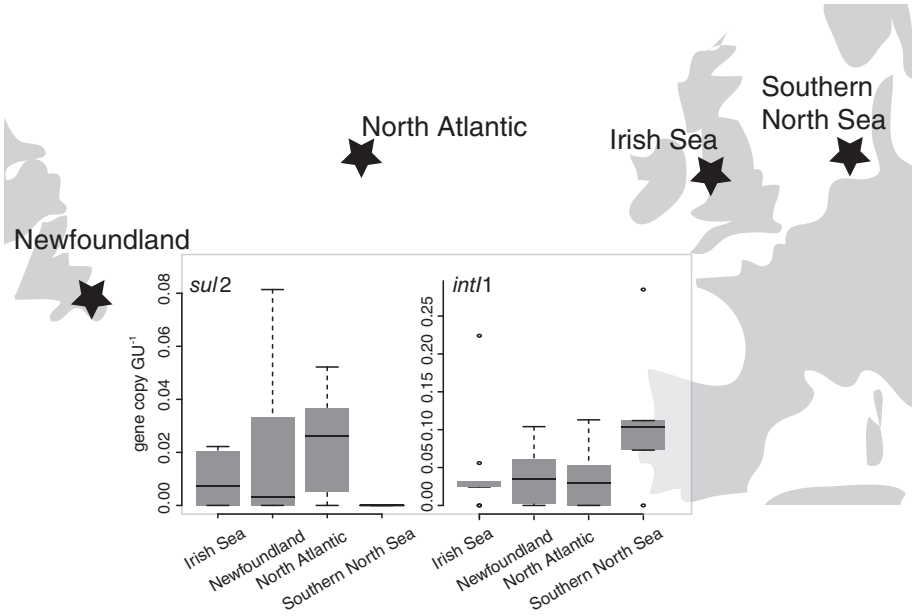

Fig. 1. Simplified map of the sampling area with the Atlantic Ocean in the centre. Sampling stations are indicated by a black star symbol. Boxplots represent the total gene copies GU^{-1} for *sul*2 and *intI*1 as measured in all the samples taken at a specific station by ddPCR. The black line in the box represents the median (2^{nd} quartile), the box edges mark the 1^{st} and 3^{rd} quartiles. Whiskers extend to the highest and lowest values in the ± 1.5 interquartile range from the box. Outliers, defined as values outside the range, are indicated as circles.

With the aim to investigate, for the first time, the long-term occurrence and spread of antibiotic resistance in the marine plankton community, we analysed by Droplet Digital PCR (ddPCR) the presence and abundance of *sul*2 and class 1 integron-integrase gene (*intI*1) in 29 archived formalin-fixed samples collected by the Continuous Plankton Recorder (CPR) survey in the Atlantic Ocean and North Sea from 1970 to 2011 (Fig. 1) (Vezzulli *et al*., 2016). The CPR is a high-speed plankton sampler designed to be towed from ships over long distances and the CPR archive, operating since 1931, is one of the longest and geographically most extensive collections of marine biological samples in the world (Reid *et al*., 2003). Therefore, archived CPR samples offer a unique opportunity to retrospectively investigate the marine plankton community over a multidecadal timescale.

Sulphonamides (SUL) are among the oldest used antibiotics, first introduced into medical practice in 1932 (Huovinen *et al*., 1995). They were extensively employed in human medicine until the 1970s and are nowadays only of limited use in clinic; however, they remain largely administered in veterinary medicine (summarized in Di Cesare *et al*., 2015). One of the plasmid SUL resistance gene, *sul*2, is widely distributed and permanently present within the aquatic microbial community (Czekalski *et al*., 2012; Di Cesare *et al*., 2015) and was suggested to be a good indicator of anthropogenic pollution (Gao *et al*., 2012; Pruden *et al*., 2012; Czekalski *et al*., 2014). Considering the early introduction of SUL antibiotic and the fact that a resistance gene can arise in clinical settings within few months or years from the first use of the antibiotic (Walsh, 2000), *sul*2 gene was selected as a suitable marker for ARGs circulating from the beginning of the antibiotic era.

In addition, class 1 integrons were selected as markers for the spread of ARGs in the marine environment (Stalder *et al*., 2014). Class 1 integrons are genetic capture elements often associated to ARGs, that play a recognized role in ARGs spread among the microbial communities (Gillings, 2014). Accordingly, *sul*2 has been found strongly associated to class 1 integrons (Di Cesare *et al*., 2016). It is worth noting that class 1 integrons are common in environmental bacteria including several marine bacterial species (e.g., all *Vibrio* species) (Gillings, 2014), and they were also recently proposed as proxies of anthropogenic pollution in aquatic ecosystems (Gillings *et al*., 2015).

In this study, *sul*2 and *intI*1 genes were investigated in historical CPR samples as markers for the occurrence and spread of antibiotic resistance genes in the plankton associated bacterial community of the ocean. The correlation between presence and abundances of the tested genes, biotic (i.e., copepods, phytoplankton and *Vibrio* spp., this latter used as proxy of abundance for indigenous human pathogenic bacteria), and abiotic (i.e., sea surface temperature [SST]) factors was also tested.

Results and discussion

In recent studies, molecular analyses applied on CPR samples have been successfully employed to investigate

the plankton associated microbial community in the North Sea and North Atlantic over the past half century (Vezzulli *et al*., 2012; 2016). The performance of molecular quantification methods such as quantitative Real-Time PCR (qPCR) applied on CPR samples could however be problematic because of the low quality of extracted DNA (largely dependent upon sample age and storage in formalin, which might precludes the detection and quantification of low-abundance molecular targets) (Vezzulli *et al*., 2012). To overcome this problem, ddPCR was applied for the first time on CPR samples to detect and quantify *sul*2 and *intI*1 genes. ddPCR is a relatively new PCR technology which improves classical PCR and qPCR, giving the possibility to quantify a target sequence of DNA in an absolute way without external references and with a proven resistance to the variability of PCR efficiency (Hindson *et al*., 2013). In recent years, it has been used in environmental microbiology for different purposes, from the quantification of faecal indicator bacteria in water (Wang *et al*., 2016), to the quantification of ARGs in soil, manure, or urban waste (Cavé *et al*., 2016).

Results from the analyses were surprising as 14 out of 29 analysed samples collected in different marine areas from 1970 to 2011 scored positive for *sul*2 gene. Its concentration ranged between 3.22×10^{-3} and 8.14×10^{-2} copies genomic unit^{-1} (GU, previously quantified by qPCR and expressed as the ratio between 16SrDNA gene copy number in tested samples and average 16SrDNA copy number in Proteobacteria, Vezzulli *et al*., 2016) (Fig. 2). The *intI*1 marker was also found by ddPCR analysis in 22 out of 29 samples, with a concentration ranging between 3.22×10^{-3} and 2.85×10^{-1} copies GU^{-1} (Fig. 2). Interestingly, both genes were found in aged CPR samples, the oldest of which date back to August 1970. In contrast, results from qPCR performed on the same samples greatly underestimate the occurrence of *sul*2 and *intI*1 genes (6 positive samples for *sul*2 and 15 for *intI*1), whose abundances were below the limits of quantification (LOQ, Supporting Information Table S1). This is related to the higher sensitivity of ddPCR compared with qPCR protocols, as shown by sensitivity assays (Supporting Information Fig. S1). The measured *sul*2 copies GU^{-1} did not vary significantly over time (Linear Model: $F_{6,10} = 0.5$, $p = 0.760$, Supporting Information Table S1, Supporting Information Text S1), while the relative abundance of *intI*1 was shown to be significantly different between quinquennia ($F_{6,10} = 7.7$, $p = 0.003$), with 1990–1994 being higher than 2000–2005 (Tukey: $p = 0.011$) (Supporting Information Table S2). Previous studies based on the analysis of the abundances of ARGs from long-term series of soil and sediment samples showed, with some exceptions, a general increase in abundance of ARGs over time (Knapp *et al*., 2010; Madueno *et al*., 2018). Although care must be taken due to the limited sampling size, such a trend was not observed in the present study (Supporting Information Text S2). As a speculation, this might be related to the different nature of the environmental matrices analysed: soils and sediments are static matrices, accumulating ARGs over long period of time, while zoo- and phyto-plankton are motile organisms, more directly influenced by water quality conditions (e.g., improved water quality due to improved wastewater treatment practices over time may have had a detectable influence on ARGs presence in the pelagic and planktonic communities).

Fig. 2. Temporal changes for *sul*2 (diamond) and *intI*1 (circle) gene copies GU^{-1} as measured in the North Atlantic, Irish Sea, Sothern North Sea and Newfoundland sampling stations by ddPCR. Note that the span of the X- and Y-axis differ for each of the plots.

The abundance of *sul*2 gene was also not significantly different between geographic areas ($F_{3,10} = 2.2$, $p = 0.150$, Fig. 1, Supporting Information Table S2). In contrast, the abundance of *intI*1gene was significantly higher in the Southern North Sea than in the other

sampling sites (Tukey tests with p values between 0.007 and 0.011, Fig. 1, Supporting Information Table S3). This might be related to the high level of anthropogenic pollution in the area (Gillings *et al*., 2015). Indeed, several rivers, for example, Scheldt, Meuse, Rhine, Ems, Weser, Elbe and Thames, receive high amount of nutrients, heavy metals, and organic compounds when crossing different towns of Western Europe (Moulder and International Association on Water Pollution Research and Control, 1986).

*intI*1 and *sul*2 abundances did not correlate with any of the measured environmental variables, that is, SST, zoo- and phyto-plankton abundances, and *Vibrio* spp. concentrations. This suggests that they are not likely to play a major role in determining long-term occurrence of these genes in the investigated areas (Supporting Information Table S4). Anthropogenic influence (e.g., ARGs discharge through human pollution) and/or environmental factors other than those investigated in this study likely play a more significant role in this framework (Di Cesare *et al*., 2015).

Furthermore, co-occurrence between *intI*1 and *sul*2 genes in the analysed samples was not observed (Pearson's $r = 0.07$, $p = 0.734$), despite it recently being reported for freshwater WWTPs microbial communities (Di Cesare *et al*., 2016). These findings suggest that different factors drive the dynamics of these two genes within the ocean microbial community.

Taken together, these results support the effective use of ddPCR for the analysis of CPR samples, which also allows for the quantitative analysis of target genes that are otherwise not quantifiable by qPCR. In addition, ddPCR applied on historical CPR samples revealed long-term occurrence and spread of *sul*2 gene and class 1 integrons carrying bacteria in the ocean. Zoo- and phyto-plankton are relevant components of the aquatic food web, and they could influence the dynamics of ARGs carrying bacteria within the whole microbial community of the aquatic system.

Experimental procedures

Selection of CPR samples

CPR samples retain zooplankton and phytoplankton (Vezzulli *et al*., 2012). We selected 29 CPR samples coming from different locations: 6 from the Southern North Sea, 10 from the Irish Sea, 7 from Newfoundland (coastal sites) and 6 from the North Atlantic (pelagic site) (Fig. 1) collected in August from 1970 to 2011. SST, phytoplankton (expressed as Phytoplankton Colour Index [PCI], an index of total phytoplankton biomass) and the total number of copepods per CPR sample (a detailed description of how CPR plankton data are generated is provided by Richardson *et al*., 2006) were previously measured for 28 out of 29 samples (Supporting Information Table S1) (Vezzulli *et al*., 2016). The sample with which we could not recover such data has been excluded from the statistical analyses. DNA was previously extracted and analysed for the abundance of the total bacteria (using the primers, 967F 5′-CAACGCGAAGAACCTTACC-3′ and 1046R 5′-CGACAGCCATGCANCACCT-3′) (Sogin *et al*., 2006) expressed as GU and the abundance of *Vibrio* spp. expressed as *Vibrio* index (VAI) by qPCR (Supporting Information Table S1) (Vezzulli *et al*., 2016).

qPCR and ddPCR analyses

All the DNA samples were tenfold diluted and analysed in duplicate for *sul*2 and *intI*1 gene abundances by both qPCR and ddPCR. The sequences of primers used to amplify the targeted genes in qPCR and ddPCR were sul2F (5′-TCCGGTGGAGGCCGGTATCTGG-3′) and sul2R (5′-CGGGAATGCCATCTGCCTTGAG-3′) for *sul*2 gene (Pei *et al*., 2006) and intI1LC5 (5′-GATCGGTCGAATGCGTGT-3′) and intI1LC1 (5′-GCCTTGATGTTACCCGAGAG-3′) for *intI*1gene (Barraud *et al*., 2010). The qPCR assays were carried out in 20 μl:5 μl of DNA, 0.5 μM of each primer, 10 μl of SsoAdvanced universal SYBR Green Supermix (Bio-Rad), and filtered and autoclaved MilliQ water (Millipore) to the final volume, using a CFX96 Real-Time System (Bio-Rad). The qPCR program was 95°C for 2 min, 35 cycles of 95°C for 15 s, 60°C for 30 s and 72°C for 15 s. Melt curve analysis was performed from 60°C to 95°C with increments of 0.5°C/5 s. Standard curves were carried out as described in Di Cesare *et al*. (2013). The specificity of reaction was verified by melting profile analysis on Bio-Rad CFX Manager IDE v2.2 software (Bio-Rad) and by electrophoresis run (1% agarose gel, 80 V, 40 min) of positive samples. The efficiencies of reaction were 94% and 100% for *sul*2 and *intI*1 genes, respectively, with R^2 values always >0.99. The LOQ were determined according to Bustin *et al*., (2009) and were 9 and 3 copy μl^{-1} for *sul*2 and for *intI*1 genes respectively. The inhibition test of qPCR was carried out as described in Di Cesare *et al*. (2013) and was shown to be always less than 1.5 threshold cycle. The ddPCR assays were performed on QX200 Droplet Digital PCR System (Bio-Rad). The reaction mix was prepared assembling 11 μl of 2× QX200 ddPCR EvaGreen Supermix with specific forward and reverse primers (final concentration 150 nM), 5 μl of DNA and nuclease free grade water to a final volume of 22 μl for each sample. Aliquots of 20 μl for each reaction were thoroughly mixed, centrifuged and loaded into a sample well of a DG8 Cartridge for QX200 Droplet Generator (Bio-Rad) followed by 70 μl of QX200 Droplet Generation Oil as per manufacturer's

instructions. Droplets were carefully transferred into a clean 96-well plate for the amplification step on a Bio-Rad C1000 Touch Thermal Cycler. Amplification conditions were optimized for both the target genes using a gradient of annealing temperatures (from 56.2°C to 61°C for both *sul*2 and *intI*1 genes), testing standards used in qPCR. The final program, according to manufacturer's instructions, was 5 min at 95°C for enzyme activation, followed by 40 cycles of a two-step denaturation (95°C for 30 s) and annealing/extension (60.2°C for 1 min for both genes) with a reduced ramp rate of 2°C s^{-1}. Signal was stabilized with subsequent steps at 4°C for 5 min and 90°C for 5 min, followed by holding at 4°C. The plates were then transferred in the QX200Droplet Reader (Bio-Rad) to analyse the fluorescence signal and to acquire concentration data. Two no template controls (NTC) and two positive controls (standards from qPCR) were included together with samples in each run. Only reactions with more than 10 000 droplets were analysed (droplets were $1.54 \times 10^4 \pm 1.87 \times 10^3$ for *sul*2 and $1.64 \times 10^4 \pm 1.60 \times 10^3$ for *intI*1). Thresholds to discriminate between positive and negative droplets were manually set up and only samples with ≥ 3 positive droplets were considered as positive. An example of result output is given in Supporting Information Fig. S2. Quantification data were analysed by QuantaSoft Analysis Pro software v1.0.596 (Bio-Rad, California) and expressed as gene copy μl^{-1}. In order to evaluate the sensitivity of ddPCR protocols the standard curves were carried out as above and the LOQ were 2.1×10^{-1} and 2.3×10^{-1} for *sul*2 and *intI*1 genes respectively. The inhibition test was performed as for qPCR and no inhibition was observed. Finally, concentrations of the tested genes were expressed in a relative manner as gene copy GU^{-1}.

Statistical analysis

The first question to be addressed was whether abundances of *sul*2 and *intI*1 GU^{-1} were different between different stations and different time periods. Four stations and seven quinquennia (from 1970–1974 to 2010–2014) were considered to address the first question. Because of the scarce temporal resolution of the data set, with 29 samples from four areas across more than 40 years, single years could not be used, but time periods were identified in groups of 5 years. Analysis of variance as linear model (LM) was used to test the effect of differences between stations and quinquennia and of the interaction between stations and quinquennia. In case of significant differences, Tukey Honestly Significant Difference (HSD) test was used to identify which stations or quinquennia were different from the others. Given the inherent potential bias introduced by grouping years in quinquennia, with some stations having a wider temporal span than others, we provide additional support on temporal trends by directly performing Mann–Kendall trend tests for each station independently (Supporting Information Text S1).

Then, after assessing whether spatial (stations) and temporal (quinquennia) patterns were present, the drivers of such differences were inferred from four environmental variables. The statistical models asked whether SST, phytoplankton, copepods and VAI could influence the relative abundances of *sul*2 and *intI*1 genes. Linear models were used with the four environmental variables and no interactions as explanatory variables. Given the potential pseudoreplication problems of variables being inherently more similar between samples within the same station or the same quinquennium, linear mixed effect models (LMEMs) were used by including as random effects the stations, which came out as significant in several analyses. Before assessing the effect of environmental variables, the correlation between them was tested using Pearson multiple correlation tests. Also, a multivariate analysis of variance (MANOVA) was used to assess whether the environmental variables were influenced by the spatial (four stations) and temporal (seven quinquennia) groups, mirroring the same structure of the analyses performed for *sul*2 and *intI*1 genes (Supporting Information Text S2). All analyses were performed in R 3.3.3 (R Core Team, 2017). Model fit for linear models was visually checked by assessing normal distribution of model residuals, absence of deviations in QQ-plots, and small values of Cook's distances (Crawley, 2013). For the analyses including random effects, we used linear mixed effect models (LMEMs) with R package nlme v 3.1–131 (Pinheiro *et al*., 2017). Mann–Kendall trend tests were performed with R package trends v1.0.1 (Pohlert, 2017).

Acknowledgements

We wish to thank all past and present members and supporters of the CPR Survey, whose efforts have enabled the establishment and long-term maintenance of the CPR data set and the archived samples used in this study. We are particularly indebted to Prof. Philip Chris Reid, Prof. Martin Edwards and Dr. Robert Camp (Sir Alister Hardy Foundation for Ocean Science, Plymouth, UK) for helpful assistance and advice in the selection and analysis of CPR samples. We thank Peter Smith for the critical comments on the style of the manuscript. We also thank three anonymous reviewers for their suggestions improving the earlier draft of the manuscript.

This work was supported by the HORIZON2020 project 'Preventing and mitigating farmed bivalve disease-VIVALDI (grant number 678589)'.

References

Barraud, O., Baclet, M.C., Denis, F., and Ploy, M.C. (2010) Quantitative multiplex real-time PCR for detecting class

1, 2 and 3 integrons *J Antimicrob Chemother* **65**: 1642–1645.

Bustin, S.A., Benes, V., Garson, J.A., Hellemans, J., Huggett, J., Kubista, M., *et al*. (2009) The MIQE guidelines: minimum information for publication of quantitative real-time PCR experiments. *Clin Chem* **55**: 611–622.

Callieri, C., Amalfitano, S., Corno, G., Di Cesare, A., Bertoni, R., and Eckert, E.M. (2017) The microbiome associated with two *Synechococcus* ribotypes at different levels of ecological interaction *J Phycol* **53**: 1151–1158.

Cavé, L., Brothier, E., Abrouk, D., Bouda, P.S., Hien, E., and Nazaret, S. (2016) Efficiency and sensitivity of the digital droplet PCR for the quantification of antibiotic resistance genes in soils and organic residues *Appl Microbiol Biotechnol* **100**: 10597–10608.

Crawley, M.J. (2013) *The R Book Second Edition*. Chichester, West Sussex, United Kingdom: Wiley.

Czekalski, N., Berthold, T., Caucci, S., Egli, A., and Bürgmann, H. (2012) Increased levels of multiresistant bacteria and resistance genes after wastewater treatment and their dissemination into Lake Geneva, Switzerland *Frontiers in Microbiology* **3**: 106.

Czekalski, N., Gascón Díez, E., and Bürgmann, H. (2014) Wastewater as a point source of antibiotic-resistance genes in the sediment of a freshwater lake *ISME J* **8**: 1381–1390.

Czekalski, N., Sigdel, R., Birtel, J., Matthews, B., and Bürgmann, H. (2015) Does human activity impact the natural antibiotic resistance background? Abundance of antibiotic resistance genes in 21 Swiss lakes *Environ Int* **81**: 45–55.

Di Cesare, A., Vignaroli, C., Luna, G.M., Pasquaroli, S., and Biavasco, F. (2012) Antibiotic-resistant enterococci in seawater and sediments from a coastal fish farm *Microb Drug Resist* **18**: 502–509.

Di Cesare, A., Luna, G.M., Vignaroli, C., Pasquaroli, S., Tota, S., Paroncini, P., and Biavasco, F. (2013) Aquaculture can promote the presence and spread of antibiotic-resistant enterococci in marine sediments *PLoS ONE* **8**: e62838.

Di Cesare, A., Eckert, E.M., Teruggi, A., Fontaneto, D., Bertoni, R., Callieri, C., and Corno, G. (2015) Constitutive presence of antibiotic resistance genes within the bacterial community of a large subalpine lake *Mol Ecol* **24**: 3888–3900.

Di Cesare, A., Eckert, E.M., D'Urso, S., Bertoni, R., Gillan, D.C., Wattiez, R., and Corno, G. (2016) Co-occurrence of integrase 1, antibiotic and heavy metal resistance genes in municipal wastewater treatment plants *Water Res* **94**: 208–214.

Eckert, E.M., Di Cesare, A., Stenzel, B., Fontaneto, D., and Corno, G. (2016) Daphnia as a refuge for an antibiotic resistance gene in an experimental freshwater community *Sci Total Environ* **571**: 77–81.

Eckert, E.M., Di Cesare, A., Kettner, M.T., Arias-Andres, M., Fontaneto, D., Grossart, H.-P., and Corno, G. (2018) Microplastics increase impact of treated wastewater on freshwater microbial community *Environ Pollut* **234**: 495–502.

Gao, P., Mao, D., Luo, Y., Wang, L., Xu, B., and Xu, L. (2012) Occurrence of sulfonamide and tetracycline-resistant bacteria and resistance genes in aquaculture environment *Water Res* **46**: 2355–2364.

Gillings, M.R. (2014) Integrons: past, present, and future *Microbiol Mol Biol Rev* **78**: 257–277.

Gillings, M.R., Gaze, W.H., Pruden, A., Smalla, K., Tiedje, J. M., and Zhu, Y.-G. (2015) Using the class 1 integron-integrase gene as a proxy for anthropogenic pollution *ISME J* **9**: 1269–1279.

Grossart, H.-P., Dziallas, C., Leunert, F., and Tang, K.W. (2010) Bacteria dispersal by hitchhiking on zooplankton *Proc Natl Acad Sci U S A* **107**: 11959–11964.

Hall-Stoodley, L., Costerton, J.W., and Stoodley, P. (2004) Bacterial biofilms: from the natural environment to infectious diseases *Nat Rev Microbiol* **2**: 95–108.

Hindson, C.M., Chevillet, J.R., Briggs, H.A., Gallichotte, E. N., Ruf, I.K., Hindson, B.J., *et al*. (2013) Absolute quantification by droplet digital PCR versus analog real-time PCR. *Nat Methods* **10**: 1003–1005.

Huovinen, P., Sundström, L., Swedberg, G., and Sköld, O. (1995) Trimethoprim and sulfonamide resistance *Antimicrob Agents Chemother* **39**: 279–289.

Knapp, C.W., Dolfing, J., Ehlert, P.A.I., and Graham, D.W. (2010) Evidence of increasing antibiotic resistance gene abundances in archived soils since 1940. *Environ Sci Technol* **44**: 580–587.

Kümmerer, K. (2009) Antibiotics in the aquatic environment – a review – part II *Chemosphere* **75**: 435–441.

Madueño, L., Paul, C., Junier, T., Bayrychenko, Z., Filippidou, S., Beck, K., Greub, G., Bürgmann, H., and Junier, P. (2018) A historical legacy of antibiotic utilization on bacterial seed banks in sediments. *PeerJ* **6**: e4197.

Marti, E., Variatza, E., and Balcazar, J.L. (2014) The role of aquatic ecosystems as reservoirs of antibiotic resistance. *Trends Microbiol* **22**: 36–41.

Moulder, D.S., and International Association on Water Pollution Research and Control. (1986) Estuarine and coastal pollution: detection, research and control. In: proceedings of the IAWPRC NERC specialised conference held at Plymouth, UK, 16–19 July 1985. Pergamon Press: Oxford.

Pei, R., Kim, S.-C., Carlson, K.H., and Pruden, A. (2006) Effect of river landscape on the sediment concentrations of antibiotics and corresponding antibiotic resistance genes (ARG) *Water Res* **40**: 2427–2435.

Pinheiro, J., Bates, D., DebRoy, S., Sarkar, D., and R Core Team. (2017) nlme: Linear and Nonlinear Mixed Effects Models_. R package version 3.1–131, https://CRAN.R-project.org/package=nlme.

Pohlert, T. (2017). Trend: Non-Parametric Trend Tests and Change-Point Detection [R package version 1.0.1]. https://CRAN.R-project.org/package=trend

Pruden, A., Arabi, M., and Storteboom, H.N. (2012) Correlation between upstream human activities and riverine antibiotic resistance genes *Environ Sci Technol* **46**: 11541–11549.

Reid, P.C., Colebrook, J.M., Matthews, J.B.L., and Aiken, J. (2003) The continuous plankton recorder: concepts and history, from plankton indicator to undulating recorders *Prog Oceanogr* **58**: 117–173.

Richardson, A.J., Walne, A.W., John, A.W.G., Jonas, T.D., Lindley, J.A., Sims, D.W., *et al*. (2006) Using continuous plankton recorder data *Prog Oceanogr* **68**: 27–74.

Sogin, M.L., Morrison, H.G., Huber, J.A., Welch, D.M., Huse, S.M., Neal, P.R., *et al*. (2006) Microbial diversity in the deep sea and the underexplored "rare biosphere." *Proc Natl Acad Sci US A* **103**: 12115–12120.

Stalder, T., Barraud, O., Jové, T., Casellas, M., Gaschet, M., Dagot, C., and Ploy, M.-C. (2014) Quantitative and qualitative impact of hospital effluent on dissemination of the integron pool *ISME J* **8**: 768–777.

Tang, K. (2005) Copepods as microbial hotspots in the ocean: effects of host feeding activities on attached bacteria *Aquat Microb Ecol* **38**: 31–40.

Taylor, N.G.H., Verner-Jeffreys, D.W., and Baker-Austin, C. (2011) Aquatic systems: maintaining, mixing and mobilising antimicrobial resistance? *Trends Ecol Evol* **26**: 278–284.

Vezzulli, L., Brettar, I., Pezzati, E., Reid, P.C., Colwell, R.R., Höfle, M.G., and Pruzzo, C. (2012) Long-term effects of ocean warming on the prokaryotic community: evidence from the vibrios *ISME J* **6**: 21–30.

Vezzulli, L., Grande, C., Reid, P.C., Hélaouët, P., Edwards, M., Höfle, M.G., *et al*. (2016) Climate influence on *Vibrio* and associated human diseases during the past half-century in the coastal North Atlantic. *Proc Natl Acad Sci U S A* **113**: E5062–E5071,

Walsh, C. (2000) Molecular mechanisms that confer antibacterial drug resistance *Nature* **406**: 775–781.

Wang, D., Yamahara, K.M., Cao, Y., and Boehm, A.B. (2016) Absolute quantification of Enterococcal 23S rRNA gene using digital PCR *Environ Sci Technol* **50**: 3399–3408.

Zhu, L., Zancarini, A., Louati, I., De Cesare, S., Duval, C., Tambosco, K., *et al*. (2016) Bacterial communities associated with four cyanobacterial genera display structural and functional differences: evidence from an experimental approach *Front Microbiol* **7**: 1662.

Zhu, Y.-G., Zhao, Y., Li, B., Huang, C.-L., Zhang, S.-Y., Yu, S., *et al*. (2017) Continental-scale pollution of estuaries with antibiotic resistance genes. *Nat Microbiol* **2**: 16270.

Supporting Information

Additional Supporting Information may be found in the online version of this article at the publisher's web-site:

Appendix S1: Supporting information.

environmental microbiology

Environmental Microbiology (2019) **21**(12), 4548–4562 doi:10.1111/1462-2920.14750

Dynamics of the Pacific oyster pathobiota during mortality episodes in Europe assessed by 16S rRNA gene profiling and a new target enrichment next-generation sequencing strategy

Aide Lasa,[1,2] **Andrea di Cesare**,[3] **Giovanni Tassistro**,[1] **Alessio Borello**,[1] **Stefano Gualdi**,[4] **Dolors Furones**,[5] **Noelia Carrasco**,[5] **Deborah Cheslett**,[6] **Amanda Brechon**,[6] **Christine Paillard**,[7] **Adeline Bidault**,[7] **Fabrice Pernet**,[8] **Laura Canesi**,[1] **Paolo Edomi**,[9] **Alberto Pallavicini**,[9] **Carla Pruzzo**[1] **and Luigi Vezzulli**[1*]

[1]*Department of Earth, Environmental and Life Sciences (DISTAV), University of Genoa, Genoa, Italy.*

[2]*Department of Microbiology and Parasitology, Universidade de Santiago de Compostela, Santiago de Compostela, Spain.*

[3]*National Research Council-Water Research Institute (CNR-IRSA), Largo Tonolli 50, 28822 Verbania, Italy.*

[4]*Department of Plant and Microbial Biology, University of Zürich, Zürich, Switzerland.*

[5]*IRTA, Sant Carles e la Ràpita, Tarragona, Spain.*

[6]*Fish Health Unit, The Marine Institute, Rinville Oranmore, Galway, Ireland.*

[7]*Laboratoire des sciences de l'Environnement Marin, Institut Universitaire Européen de la M, Université de Bretagne Occidentale – UMR6539 CNRS/UBO/IRD/Ifremer, Plouzané, France.*

[8]*Ifremer, Physiologie Fonctionnelle des Organismes Marins, UMR 6539 LEMAR (CNRS/Ifremer/IRD/UBO) Technopole Iroise, CS 10070, 29280, Plouzane, France.*

[9]*Department of Life Sciences, University of Trieste, Trieste, Italy.*

Summary

Infectious agents such as the bacteria *Vibrio aestuarianus* or *Ostreid herpesvirus 1* have been repeatedly associated with dramatic disease outbreaks of *Crassostrea gigas* beds in Europe. Beside roles played by these pathogens, microbial infections in *C. gigas* may derive from the contribution of a larger number of microorganisms than previously thought, according to an emerging view supporting the polymicrobial nature of bivalve diseases. In this study, the microbial communities associated with a large number of *C. gigas* samples collected during recurrent mortality episodes at different European sites were investigated by real-time PCR and 16SrRNA gene-based microbial profiling. A new target enrichment next-generation sequencing protocol for selective capturing of 884 phylogenetic and virulence markers of the potential microbial pathogenic community in oyster tissue was developed allowing high taxonomic resolution analysis of the bivalve pathobiota. Comparative analysis of contrasting *C. gigas* samples conducted using these methods revealed that oyster experiencing mortality outbreaks displayed signs of microbiota disruption associated with the presence of previously undetected potential pathogenic microbial species mostly belonging to genus *Vibrio* and *Arcobacter*. The role of these species and their consortia should be targeted by future studies aiming to shed light on mechanisms underlying polymicrobial infections in *C. gigas*.

Introduction

Recent advances in DNA sequencing technology is enabling new quantitative insights into the microbial community diversity associated with human and animal tissues (Yatsunenko *et al*., 2012; Yarza *et al*., 2014). It is now recognized that host-associated microbial communities (also named the microbiota) (Lederberg and McCray, 2001) are playing an important role in animal health by providing prominent services ranging from nutrient processing to protection from diseases. Marine bivalves host high microbial abundance and diversity and alteration of the microbiota due to stressful conditions and/or environmental changes was previously linked with a condition of a compromised health status and susceptibility to diseases (Lokmer and Wegner, 2015).

Diseases affecting the Pacific oyster (*Crassostrea gigas*) have been rising over the past decades, representing a

Received 29 May, 2019; revised 12 July, 2019; accepted 14 July, 2019. *For correspondence. E-mail luigi.vezzulli@unige.it; Tel. +39-01035338018.

significant threat for commercial exploitation of both farmed and natural stocks (Alfaro *et al*., 2018). In Europe, mass mortality episodes of *C*. *gigas* in farming areas are attributed to complex interactions among oysters, microbial pathogens and environmental variables (Pernet *et al*., 2012). In particular, stressful environmental conditions, such as warmer seawater temperatures, were observed to favour a shift in *C*. *gigas* bacterial communities toward pathogen-dominated communities also promoting colonization by secondary opportunistic pathogens and non-resident microbial species (Lemire *et al*., 2015; Lokmer and Wegner, 2015).

Mortality of *C*. *gigas* spat and juvenile is mainly associated with infection by the herpes-like virus Oyster Herpesvirus type 1 (OsHV-1) usually when water temperature reaches 16°C (Segarra *et al*., 2010). Infected oysters show a reduction in feeding and swimming activities and mortality can reach 100% in a few days. In contrast, mortality of adult oysters in Europe has been mainly reported in association with the detection of the bacterium *Vibrio aestuarianus* (Travers *et al*., 2015). In this case, infection seems to last for a long period, reaching a cumulative mortality rate up to ~30% at the end of the farming cycle.

Although these pathogens have been identified to play a role in oyster diseases, there is an emerging view that microbial infections, in marine bivalves, may derive from the contribution of different microbial species/strains that act as a 'community of pathogens' (hereafter referred to as the 'pathobiota') rather than a single species/strain as the only etiological agent (Lemire *et al*., 2015; de Lorgeril *et al*., 2018). Under this perspective evidence has been provided supporting the view that oyster infections might be seen as infectious disorders caused by the contribution of a larger number of pathogens (e.g. populations or consortia) than previously thought (Lemire *et al*., 2015). The question now is no longer whether microorganisms are involved in the pathogenesis of such diseases, but which specific microbial species or strains are involved.

Although addressing this issue will be of great value in improving the general understanding of bivalve diseases and to drive future studies to unravel their mechanisms, answering the above question is not straightforward.

In fact, accurate phylogenetic analysis of the bivalve microbiota, including the potential pathogenic community, has been historically hampered by methodological constrains, such as the use of traditional culture-dependent protocols, as a large fraction of the bivalve-associated microbial community (e.g. unculturable bacteria) may go undetected using these methods (Garnier *et al*., 2007). More recently, 16S rRNA gene-based analysis of the microbial diversity, based on next-generation sequencing protocols, was employed for taxonomic identification of bivalve-associated bacteria (Lokmer and Wegner, 2015; Lokmer *et al*., 2016). However, although this approach allows us to overcome the cultivation bias, 16S rRNA profiling could not be successfully applied for high taxonomic resolution analysis of the microbial community (e.g. taxonomic resolution to the level of species or strains) due to the lack of phylogenetic value of the 16S rRNA gene for many bacterial groups (Rajendhran and Gunasekaran, 2011). This is particularly true for bacteria belonging to the *Vibrio* genus that are thought to play a primary role in oyster infections and mortality outbreak (Vezzulli *et al*., 2015). The same holds true for shotgun metagenomic techniques due to difficulties in separation of host DNA from microbial DNA resulting in non-optimal detection and taxonomic resolution of microbial species. Thus, investigating polymicrobial nature of OsHV-1 disease and the unknown nature of V. aestuarianus infection affecting *C*. *gigas* deserve new tools.

The aim of this study was to overcome these constrains and be able to provide new insights into the high-level (species) taxonomic composition of the oyster pathobiota in *C*. *gigas* samples collected during mortality outbreaks in Europe. To this end, a new target enrichment next-generation sequencing approach was developed and applied to target 884 phylogenetic and virulence markers of the potential pathogen community associated to bivalve tissues. 16S rRNA gene profiling of the microbial community was also conducted on a large number of contrasting (e.g. infected vs not infected) *C*. *gigas* samples to support the 'pathobiota' analysis and to extensively investigate the patterns and dynamics of oyster microbiota during mortality events.

Results

OsHV-1 and V. aestuarianus *detection in* C. gigas *samples*

A total of 525 *C*. *gigas* samples collected from 2016 to 2017 in three European sites, i.e., Ebro delta, Dungarvan Bay and Bay of Brest (Supplementary Material and Methods, Fig. S1, Table S1) were screened for the presence of OsHV-1 and *V*. *aestuarianus* using quantitative real-Time PCR (Table 1). In general, samples collected during oyster mortality episodes tested positive for at least one of the two pathogens suggesting a strong link between presence of these microorganisms in the oyster tissues and development of disease (Labreuche *et al*., 2010; Segarra *et al*., 2010). In particular, *V*. *aestuarianus* was found associated to adult *C*. *gigas* mortality observed in the Ebro delta on 13th April 2016 and 31st May 2017 and in Dungarvan Bay on 3rd October 2016 (Table 1). OsHV-1 DNA was detected in spat *C*. *gigas* sampled during 12 mortality episodes in the Ebro delta, Dungarvan Bay and Bay of Brest (Table 1).

Table 1. *Crassostrea gigas* samples collected at different European sites and analysed in this study (*n* + number of samples/total number of analysed samples scoring positive to species-specific qPCR targeting the pathogen *V. aestuarianus* or OshV-1 in oyster tissues).

Sampling date	Code	Age	Origin	Ploidy	Mortality (%)	OshV-1 (Real-time PCR)	*V. aestuarianus* (Real-time PCR)
Ebro Delta (Spain)							
13_04_2016	EbDva13apr16/EbH13apr16	Adult	Nature	Diploid	23% (Up to 50%)	0+/30	22+/30
26_04_2016	EbDoshV26apr16(c3)/EbH26apr16(c4)	Spat	Nature	Diploid	76% (Up to 90%)	17+/30	0+/30
26_04_2016	EbDoshV26apr16(c5)/EbDva26apr16(c6)/EbH26apr16(c6)	Spat	Nature	Diploid	46.6% (Up to 80%)	21+/30	4+/30
19_07_2016	EbDoshV19jul16/EbH19jul16	Spat	Hatchery	Diploid	3% (light mortality)	1+/30	0+/30
19_07_2016	EbH19jul16(c2)	Spat	Nature	Diploid	No mortality	0+/30	0+/30
24_11_2016	EbH24nov16/EbDoshV24nov16/EbDva24nov16	Spat	Nature	Diploid	30% recent mortality	7+/30	1+/30
25_01_2017	EbH25jan17	Spat	Hatchery	Diploid	No mortality	0+/30	0+/30
26_01_2017	EbH26jan17	Spat	Hatchery	Diploid	No mortality	0+/30	0+/30
05_05_2017	EbDoshV5may17/EbH5may17	Spat	Hatchery	Triploid	87.83% mortality	10+/18	0+/18
05_05_2017	EbH5may17(c1)	Spat	Hatchery	Triploid	No mortality	0+/30	0+/30
31_05_2017	EbDva31may17/EbH31may17	Spat	Hatchery	Triploid	85% mortality	0+/30	9+/30
Dungarvan Bay (Ireland)							
05_07_2016	DrDva7jul16/DrH7jul16	Adult	Hatchery	Triploid	20%	0+/30	2+/30
05_07_2016	DrDoshV7jul16SPAT/DrDva7jul16SPAT/DrH7jul16SPAT	Spat	Hatchery	Triploid	70%–100%	25+/30	3+/30
03_10_2016	DrDva3oct16/DrH3oct16	Adult	Hatchery	Triploid	End of mortality	0+/30	11+/30
03_10_2016	DrDoshV3oct16SPAT/DrDvaV3oct16SPAT/DrH3oct16SPAT	Spat	Hatchery	Triploid	End of mortality	12+/30	1+/30
10_01_2017	DrH10jan17	Adult	Hatchery	Triploid	No mortality	0+/30	0+/30
10_01_2017	DrH10jan17SPAT	Spat	Hatchery	Triploid	No mortality	0+/30	0+/30
Bay of Brest (France)							
10_07_2017	BbDoshV10jul17/BbDva10jul17/BbH10jul17	ad/sp/jv	Hatchery	Diploid	Mortality	2+/12	2+/12
05_10_2017	BbDoshV5oct17/ BbDva5oct17/BbH5oct17	ad/sp/jv	Hatchery	Diploid	No mortality	3+/15	1+/15

Code legend = [Eb, Ebro delta; Dr, Dungarvan bay; Bb, Bay of Brest]/[D, Infected; H, Not Infected]/[va, *Vibrio aestuarianus*; oshV, *Ostreid herpesvirus* 1]/[collection date].

Microbiota analysis

One hundred one contrasting *C. gigas* samples were selected in the Ebro Delta (n = 50), Dungarvan bay (n = 40) and the Bay of Brest (n = 11) for microbiota analysis based on results from PCR screening analysis. In the experimental design, most interesting sampling periods were chosen (e.g. periods with high mortality or absence of mortality), and for each period, 10 contrasting individual oyster samples (five samples infected by OsHV-1 or *V. aestuarianus* and five non-infected control samples) were selected. Sequencing of the samples by Ion Torrent technology produced more than 14.000.000 amplicon sequence reads spanning the V4 hypervariable region of the bacterial 16S rRNA gene. Barcode and adapters sequences were removed and raw sequences were trimmed to minimize bias associated with PCR amplification of target genes. In particular, reads that contained one or more ambiguous bases, had errors in the barcode or primer sequence, were atypically short (100 bp), and had an average quality score <0.05 were removed from the data set. This process produced 13.143.153 trimmed reads corresponding on average to 146.000 sequence reads per analysed sample.

In general, the composition of the bacterial community associated to *C. gigas* was dominated by the classes of *Gamma* and *Alphaproteobacteria* accounting on average for 28% and 15% of the total bacterial diversity followed by *Epsilonproteobacteria* (11%), *Mollicutes* (10%) and *Flavobacteria* (9%) (Fig. 1). Rarefaction curves computed for total operational taxonomical units (OTUs) abundance almost reached a plateau indicating that sequencing effort was good enough to describe the majority of phylotypes in most of the samples (Fig. S2). Generally, alpha diversity was lower in adult oysters infected by *V. aestuarianus* whilst it was higher in oyster spat infected by OsHV-1 (Fig. S2). Different physiological or environmental conditions including animal health status and age, geographic location and season significantly influenced the composition of the oyster microbiota as showed by beta diversity analysis and PERMANOVA testing (p < 0.01) (Fig. 2). Analysis of contrasting bivalve samples based on the presence/absence of microbial pathogens showed that a significant shift in the microbiota community was observed in adult oyster infected by *V. aestuarianus* (Fig. 2). In particular, an increase in abundance of bacteria belonging to the genus *Vibrio* and *Arcobacter* was observed in

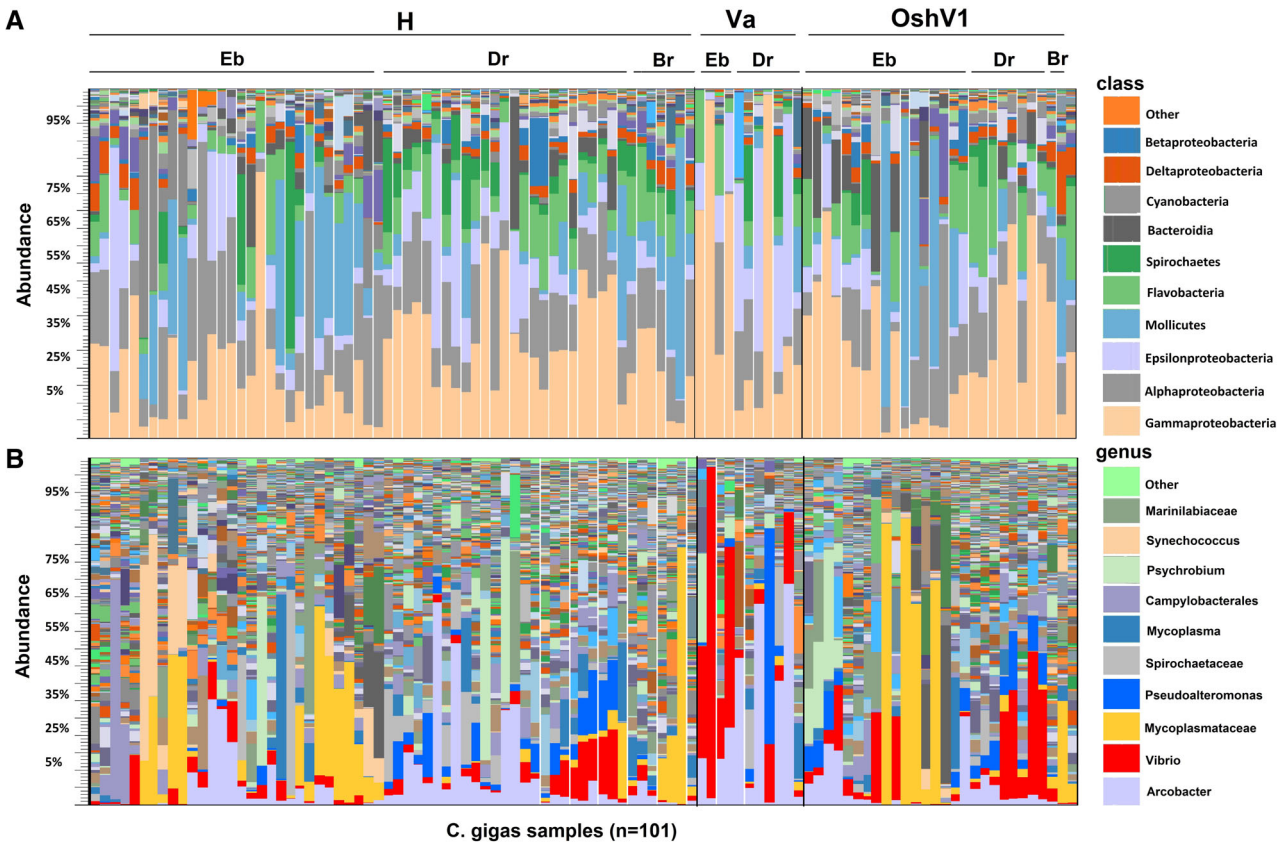

Fig. 1. Taxonomical composition at the class (A) and genus (B) level of 101 *C. gigas* microbiota grouped by oyster health status (H, not infected oysters; Va, *Vibrio aestuarianus*-infected oysters; OshV1, Ostreid herpesvirus 1-infected oysters) and geographic locations (Eb, Ebro delta; Dr, Dungarvan bay; Br, Bay of Brest), as revealed by sequencing of the V4 hypervariable region of the 16S rRNA gene. [Color figure can be viewed at wileyonlinelibrary.com]

V. aestuarianus-infected oysters compared to either *V. aestuarianus* non-infected or OsHV-1 infected oysters. In oyster spats infected by OsHV-1 an increase in the *Vibrio* fraction was also observed compared with non-infected oysters.

The analysis of the core microbiota showed that the microbial community of oyster samples is dominated by two main bacterial groups, namely *Vibrio* and an uncultured bacterial group (uncultured-053) (Supplementary Material and Methods, Table S2). When analysing adult *C. gigas* samples infected with *V. aestuarianus*, core taxa were assigned to *Arcobacter* and *Vibrio* genera. In contrast, core taxa of *V. aestuarianus* non-infected samples were assigned to the uncultured-053 group. When OsHV-1 DNA was detected in spat oysters, the core microbiota included *Vibrio* but also the uncultured-053 group. Interestingly, the

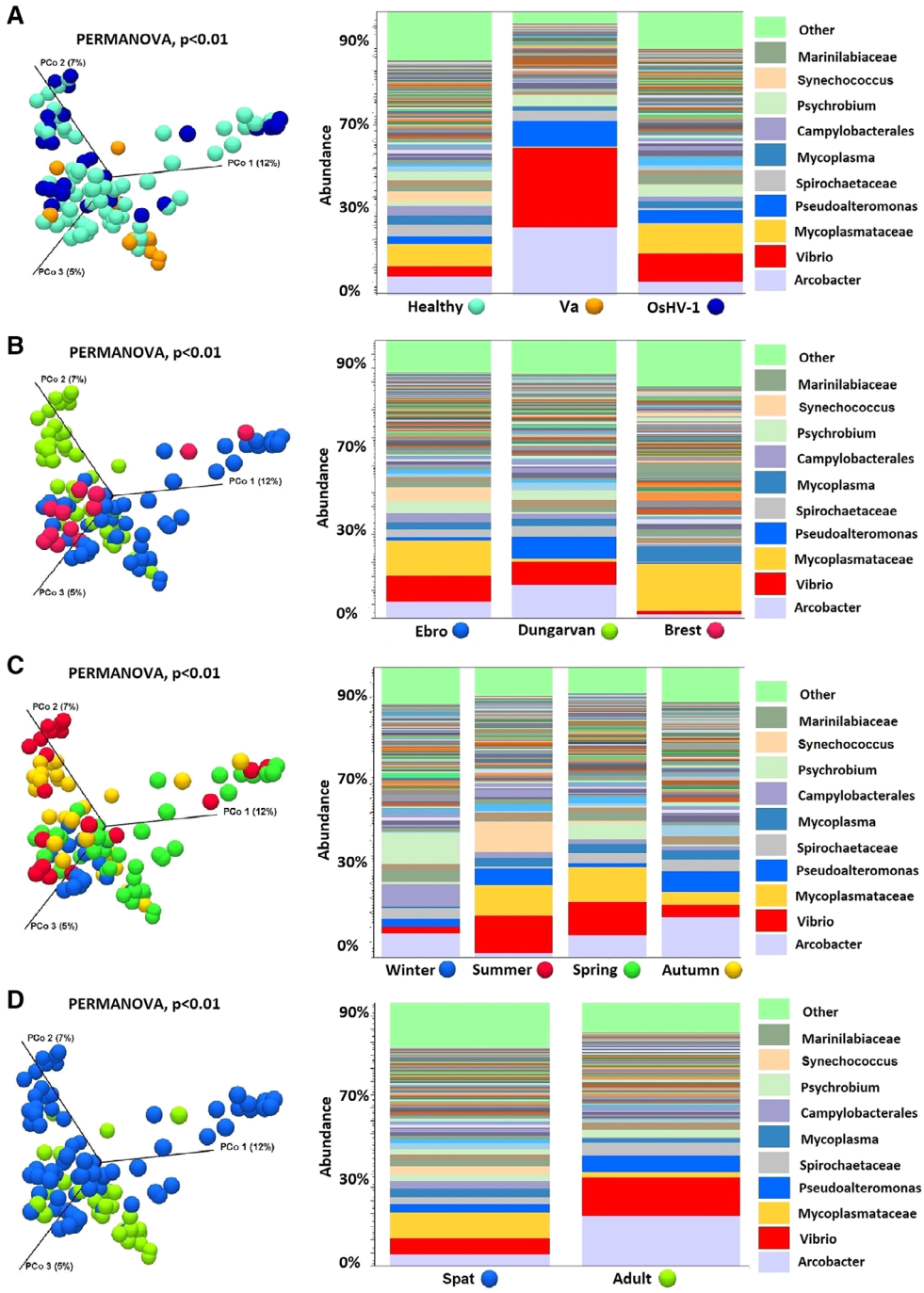

Fig. 2. Comparative analysis of *C. gigas* microbiota (Beta diversity analysis) under different conditions: health status (A), geographic location (B), season (C) and animal age (D) (Va, *Vibrio aestuarianus*-infected oysters; OshV1, Ostreid herpesvirus 1-infected oysters). [Color figure can be viewed at wileyonlinelibrary.com]

Table 2. Phylogenetic and virulence markers targeted by the target enrichment NGS protocol to study the potential microbial pathogenic community (pathobiota) in *C. gigas* tissues (Rosenberg *et al*., 2007; Travers *et al*., 2015).

Target	Taxonomy	Main host	Marker gene	No. of allelic variants	Length (nt)
Vibrio spp.	*Vibrio* spp.	Human, Animal	*gyrB*	243	400
	Vibrio spp.	Human, Animal	*recA*	204	400
	Vibrio spp.	Human, Animal	*atpA*	133	400
	Vibrio spp.	Human, Animal	*dnaJ*	56	400
	Vibrio spp.	Human, Animal	*pyrH*	113	400
	V. tasmaniensis	*Crassostrea gigas*	LGP32 probes	10	400
	V. cholerae O1 El Tor	Human	*ctxA*	1	777
	V. cholerae O1 El Tor	Human	*ctxB*	1	375
	V. cholerae O139	Human	*ctxA-B*	1	938
	V. cholerae O1 el Tor	Human	*tcpA*	1	675
	V. cholerae O1 classical	Human	*tcpA*	1	675
	V. cholerae O1 el Tor	Human	*rstR*	1	339
	V. cholerae O1 classical	Human	*rstR*	1	336
	V. cholerae O139	Human	*wbf*	1	449
	V. cholerae O1 el Tor	Human	*gbpA*	1	400
	V. parahaemolyticus	Human	*toxR*	1	552
	V. parahaemolyticus	Human	*tdh*, *trh*	3	570
	V. vulnificus	Human	*vvhA*	1	1416
	V. vulnificus	Human	*rtxA1*	1	400
	V. tasmaniensis	*Crassostrea gigas*	*vsm* (LGP32 strain)	1	1824
	V. tasmaniensis	*Crassostrea gigas*	*ompU* (LGP32 strain)	1	400
	V. aestuarianus	*Crassostrea gigas*	*vam*	1	1836
	V. tapetis	*Ruditapes philippinarum*	*djlA*	1	1826
	V. coralliilyticus	*Paramuricea clavata*	*vcpA*	15	1824
	V. harveyi	Stony corals	*vhhA*	1	1260
	V. crassostreae	*Crassostrea gigas*	*R-5.7*	1	2397
	V. tubiashii	*Crassostrea gigas*	Metalloprotease	1	1821
	Vibrio spp.	Human, Animal	*MSHA*	12	400
Arcobacter spp.	*Arcobacter* spp.	Human	*gyrB*	27	400
Nocardia crassostrea	*Nocardia crassostrea*	*Crassostrea gigas*, *Ostrea edulis*	*rpoB*, *hsp65*, *gyrB*	3	400
Marteilia refringens	*Marteilia refringens*	*Ostrea edulis*, *Mytilus edulis*, *M. galloprovincialis*	ITS1O, ITS1M, probe	3	400
Bonamia ostreae	*Bonamia ostreae*	*Ostrea edulis*	5.8S-ITS rDNA, *hsp90*, *act1*	3	400
OsHV-1	Ostreid herpesvirus 1	*Crassostrea gigas*	C2/C6 (2), IA1-IA2, orf4, Hyp. Protein, RING finger protein gene	7	400
			ORF100	1	198
			C9-C10	1	197
			B3-B4	1	207
Enterococcus spp.	*E. faecalis*, *E. faecium*, *E. avium*, *E. gallinarum*, *E. casseliflavus*, *E. durans*, *E. raffinosus*, *E. mundtii*	Human	*atpA*	8	400
Roseovarius crassostrea	*Roseovarius crassostrea*	*Crassostrea virginica*	*dnaJ*, *pyrH*	6	400
Escherichia coli	*Escherichia coli*	Human	*dnaJ*, *pyrH*, *atpA*, *gyrB*	4	400
Aspergillus sydowii	*Aspergillus sydowii*	*Gorgonia ventalina*, Human	TUB2, *trpC*, ITS, calmodulin gene	4	400
Aurantimonas coralicida	*Aurantimonas coralicida*	Corals	*atpD*, *gyrB*, *recA*, *rpoB*	4	400
Serratia marcescens	*Serratia marcescens*	*Acropora palmata*	*gyrB*, *recA*, *dnaJ*	3	400
Pseudoalteromonas sp.	*Pseudoalteromonas* sp.	*Rhopaloeides odorabile*	*gyrB*	1	400
			Total	884	29,292

core microbiota of oyster spats and adult was clearly different. While *Vibrio* and *Arcobacter* were members of the core microbiota in adult oysters, in oyster spats the core group was dominated by *Vibrio*, uncultured-053, *Haliea* and *Marinicella*. Differences in the core microbiota were also evident across the different geographic locations. In oysters from Dungarvan bay the core groups were *Sulfitobacter*, uncultured-053, *Arcobacter*, *Pseudoalteromonas*, *Marinicella*, *Vibrio* and *Borrelia*, while in Ebro Delta the core microbiota was formed only by *Vibrio* and uncultured-053. On the other hand, the core microbiota of the samples from the Bay of Brest was more diverse than that of oysters from other sites, with more than 20 different bacterial groups (*Arcobacter*, *Vibrio*, *Mycoplasma*, *Winogradskyella*, *Haliea*, *Sulfitobacter*, *Polaribacter*, *Marinicella*, *Lutimonas*, *Aquibacter*, *Roseovarius*,

uncultured-104, uncultured-079, uncultured-053, uncultured-015, OM60(NOR5) clade, uncultured bacterium-088, uncultured-072, uncultured-050 and uncultured bacterium-248) probably reflecting the smaller number of samples analysed in this site. Seasonality also affected the composition of the core microbiota, and a transition of specific genera was identified (e.g. *Sulfitobacter* and *Marinicella* from cold seasons to warmer seasons) (Supplementary Material and Methods, Table S2).

Pathobiota analysis

A target enrichment next-generation sequencing protocol was for the first time applied for high taxonomic resolution analysis of the bivalve pathobiota on a total of 12 selected contrasting *C. gigas* samples collected during mortality episodes (e.g. *C. gigas* samples infected and non-infected by *V. aestuarianus* or OsHV-1) and in the absence of mortality. A mock community sample (positive control) and a nuclease-free water sample (negative control) were also included in the analysis (see methods section for details). To run the protocol, a 'pathobiota' sequence database containing 884 phylogenetic and virulence markers of the bivalve microbial pathogen community was built and used to produce a total of 12.114 biotinylated RNA baits for selective capturing of target DNA via hybridization as described in the methods section (Table 2). Sequencing of enriched DNA libraries

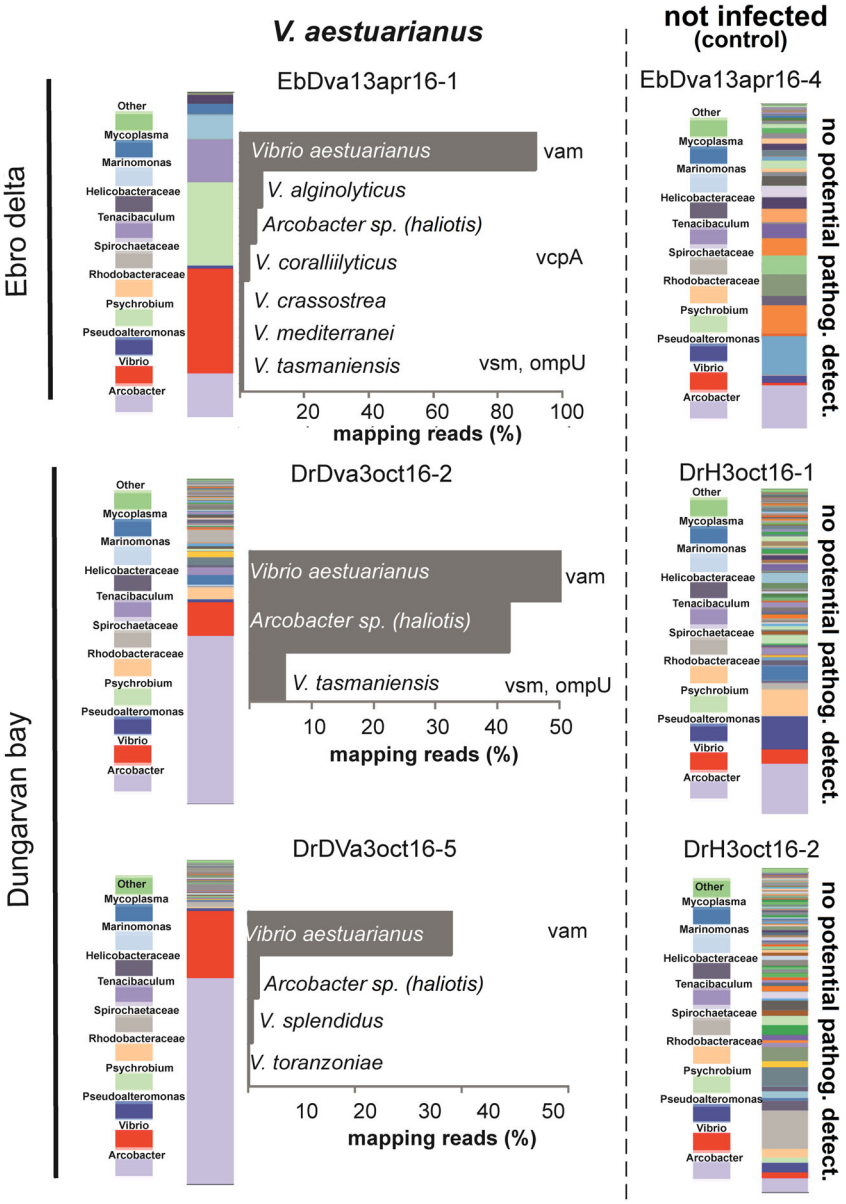

Fig. 3. Results from target enrichment NGS analysis investigating *C. gigas* pathobiota in contrasting samples infected or not infected (control) by the bacteria *V. aestuarianus*. Relative abundance is calculated from the number of reads specifically mapping on target sequences and expressed as percentage (see main text for details on mapping parameters settings). Presence of virulence genes is also shown. [Color figure can be viewed at wileyonlinelibrary.com]

produced a total of 67.614.544 sequence reads corresponding to about 5.634.545 reads for each sample. On average, less than 5% of the reads mapped against reference sequences from the pathobiota database and were used to produce consensus sequences for pathobiota taxonomic classification with the NCBI BLAST function.

Results of the target enrichment protocol allowed the detection and relative quantification of members of the bivalve pathogen community (pathobiota) associated to oyster tissues with a taxonomic resolution up to the species level. Generally, although the oyster pathobiota was composed of different species in all samples a dominance of primary pathogens such as *V. aestuarianus* and OsHV-1 was observed in *C. gigas* samples collected during mortality episodes linked to these pathogens (Figs 3 and 4).

In particular, adult *C. gigas* samples collected during mortality episodes linked to *Vibrio aestuarianus* outbreaks in Ebro Delta and Dungarvan bay (e.g. samples EbDva13apr16-1, DrDva3oct16-2, DrDva3oct16-5) showed a large proportion of reads specifically mapping on *V. aestuarianus* phylogenetic (e.g. *gyrB*, *recA*, *atpA*, *dnaJ* and *pyrH*) and virulence (e.g. *vam)* marker sequences accounting on average for more than 40% of total read sequences. Accordingly, consensus sequences obtained from read mapping were unequivocally assigned to the species *V. aestuarianus* by BLAST sequence analysis (Fig. 3). In addition, a significant fraction of reads common to all *V. aestuarianus* infected samples were specifically mapping on *Arcobacter haliotis* marker sequences (*gyrB*). Albeit at lower relative abundance other species identified in these samples included *V. alginolyticus*, *V. coralliilyticus*, *V. crassostreae*, *V. mediterranei*, *V. toranzoniae*, *V. splendidus* and *V. tasmaniensis* (Fig. 3). Virulence genes such as metalloproteases (*V. splendidus vsm*, *V. coralliilyticus vcpA*) and *ompU* of *V. tasmaniensis* were also detected (Fig. 3).

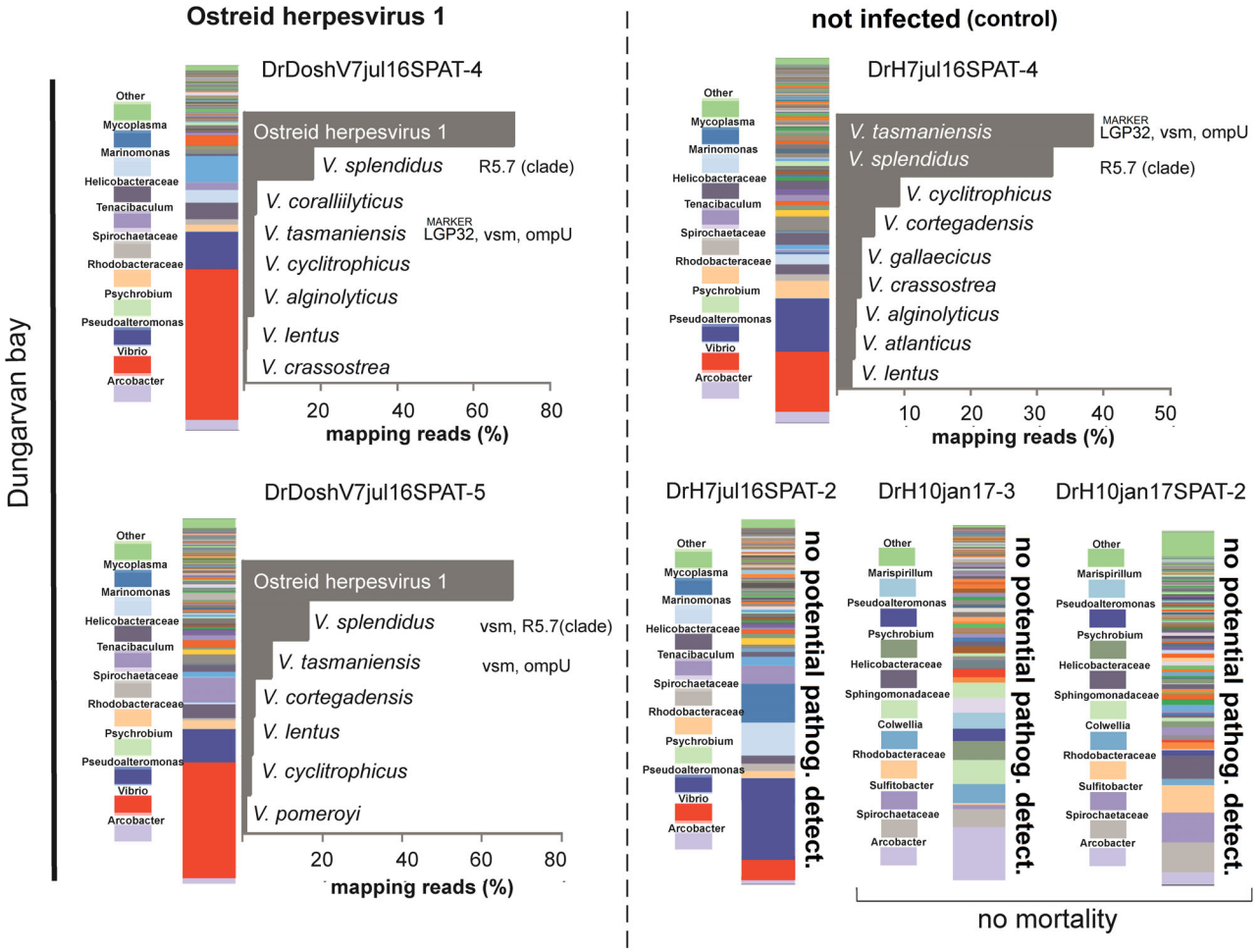

Fig. 4. Results from target enrichment NGS analysis investigating *C. gigas* pathobiota in contrasting samples infected or not infected (control) by Ostreid herpesvirus 1 (OshV1). Samples DrH10jan17-3 and DrH10jan17-SPAT2 were collected during period of no mortality. Relative abundance is calculated from the number of reads specifically mapping on target sequences and expressed as percentage (see main text for details on mapping parameters settings). Presence of virulence genes is also shown. [Color figure can be viewed at wileyonlinelibrary.com]

Similarly, *C. gigas* samples collected during mortality episodes of spat oysters linked to an OsHV-1 outbreak in Dungarvan bay (e.g. samples DrDoshV7jul16SPAT-4, DrDoshV7jul16SPAT-5) showed a large number of reads (on average more than 60% of the total read sequences) specifically mapping on OsHV-1 marker sequences (e.g. C2/C6 (2), IA1-IA2, orf4, Hyp. Protein, RING finger protein gene, ORF100, C9-C10, B3-B4). An additional fraction of reads found in these samples pointed to the presence of bacterial species belonging to the Splendidus clade including *V. splendidus*, *V. tasmaniensis*, *V. cyclitrophicus* and *V. lentus*. Other bacterial species found in OsHV-1 infected oyster included *V. coralliilyticus*, *V. alginolyitucs*, *V. crassostreae*, *V. cortegadensis* and *V. pomeroyi* (Fig. 4). Virulence genes (e.g. *V. tasmaniensis vsm* and *ompU*) and the genetic element R5.7 were also found (Fig. 4).

Generally, no reads were observed to map on reference sequences above defined thresholds in control samples, suggesting that target bacterial concentrations were either absent or below the limit of detection in these samples (Figs 3 and 4). An exception to this was observed for sample DrH7jul16SPAT-4 collected in Dungarvan Bay during an OsHV-1 outbreak in July 2016 where a diversified pathobiota community dominated by members of the Splendidus clade such as *V. splendidus* and *V. tasmaniensis* was found (Fig. 4). Virulence genes (e.g. *vsm* and *ompU*) and the genetic element R5.7 were detected in this sample as well as a number of other *Vibrio* species including *V. cyclitrophicus*, *V. cortegadensis*, *V. gallaecicus*, *V. crassostreae*, *V. alginolyticus*, *V. atlanticus* and *V. lentus* (Fig. 4). In contrast, no target sequences were detected in samples DrH10jan17SPAT-2 and DrH10jan17-3 collected in Dungarvan bay in winter in the absence of significant mortality.

All species included in the mock community sample were correctly identified by the target enrichment protocol developed in this study (Supplementary Material and Methods, Fig. S3), whilst no sequences were obtained from analysis of the negative control ruling out laboratory contamination.

Discussion

Microbiota composition of healthy C. gigas *oysters in European farming sites*

The composition of *C. gigas* microbiota in this study was dominated by the classes of *Gamma* and *Alphaproteobacteria* and was highly variable in relation to health status, geographic location, season and oyster age (Fig. 2). Accordingly, many transient and opportunistic microbial taxa appeared to dominate oyster microbiota while core microbial communities were restricted to only a few, most probably resident bacteria, such as *Vibrio* and the uncultured-053 group. This may be linked to the filter feeding behaviour of oysters, which expose the animals to colonization by complex and highly variable microbial communities found in the seawater environment. *Mycoplasmataceae*, *Arcobacter*, *Synechococcus* and *Spirochaetaceae* dominated the microbiota in healthy (non-infected) oysters suggesting these taxa might play a beneficial role in oyster fitness and health status (King *et al*., 2019). Interestingly, *Arcobacter* and *Mycoplasmataceae* were found to represent an abundant fraction of the microbiota in the Eastern oyster (*Crassostrea virginica*) and Chilean oyster (*Tiostrea chilensis*) respectively, although their role within the host is still largely unknown (Romero *et al*., 2002; King *et al*., 2012). Similarly, *Synechococcus* was observed in the cytosol of the digestive gland, connective tissue, mantle, and gonad of *C. gigas* and a host-endobiont relationship between *C. gigas* and *Synechococcus* cells was recently suggested (Avila-Poveda *et al*., 2014). In addition, since cyanoprokaryotes are particularly abundant in the digestive gland (Avila-Poveda *et al*., 2014) and colonize the oyster microbiota especially in the summer period when seawater concentrations of these bacteria are higher (Fig. 1), it can be speculated that their accumulation in oyster tissues may directly derive from the natural environment. Host-associated spirochetes have been found mainly in the digestive tract of eukaryotes including molluscs (Romero and Espejo, 2001; Duperron *et al*., 2007) but again little is known on their association and role with their *C. gigas* hosts.

Changes in the microbiota community structure associated to C. gigas *infections during mass mortality episodes in Europe*

Comparative analysis of healthy versus infected *C. gigas* samples clearly showed that infected oysters displayed signs of community structure disruption and were characterized by a low diversity and proliferation of few bacterial taxa. This was particularly evident for *V. aestuarianus*-infected oysters where dominance by bacteria belonging to the genus *Vibrio* and *Arcobacter* resulted in low microbial diversity compared with healthy oysters. In the case of OsHV-1 infected oyster, loss of Alpha diversity was less clear and mostly linked to proliferation of *Vibrio* and a significant decline of some bacterial taxa such as cyanoprokaryotes (e.g. *Synechococcus*) (Fig. 1). Loss of microbiota diversity and proliferation of few OTUs ('dysbiosis') has previously been linked with impaired health in oysters (Green and Barnes, 2010; King *et al*., 2019), including *C. gigas* (Garnier *et al*., 2007; Lokmer and Wegner, 2015). It is thus apparent that specific microbial taxa and especially members of the *Vibrio* genus are likely to play a role in affecting oyster health status during disease outbreaks. Nevertheless, whether

the condition of 'dysbiosis' is a prerequisite for oyster infection or it is a consequence of developing disease it is difficult to discern.

Recently an elegant study carried out by de Lorgeril *et al*. (2018) using experimental inoculations reproducing the natural route of infection in contrasting (susceptible vs. resistant) oyster families showed that the disease is caused by multiple infection with an initial and necessary step of infection of oyster haemocytes by the Ostreid herpesvirus OsHV-1 μVar and subsequent bacteraemia by opportunistic bacteria. Accordingly, Lemire *et al*. (2015) showed that the onset of disease in oysters is associated with progressive replacement of diverse benign bacterial colonizers by members of a phylogenetically coherent virulent population. According to these results 'dysbiosis' might be seen as a new form of polymicrobial disease, in which a population/consortium of virulent strains but also non-pathogenic strains contribute to oyster mortality (Lemire *et al*., 2015).

Potential pathogenic microbial communities (pathobiota) of C. gigas *assessed through a new target enrichment next-generation sequencing approach*

A larger number of microbial pathogens than previously thought might be involved in the establishment of oyster infection and development of diseases. Nevertheless, current knowledge in this field is restricted to culturable microorganisms (Lemire *et al*., 2015) most probably providing an incomplete view of the microbial communities potentially structuring the oyster pathobiota. Culture independent techniques such as 16S rRNA profiling or shotgun metagenomics widely employed in microbiome studies would also not be of great help to this purpose as they lack phylogenetic resolution (e.g. 16S rRNA gene-based analysis) and/or might be hampered by large amounts of host DNA (Nhung *et al*., 2007; Forbes *et al*., 2017). For instance, *C. gigas* haemolymph is composed of approximately 10^6 bacterial cells ml^{-1} (average bacterial genome size = 5×10^6 bp) and typically in the order of 2×10^6 haemocytes cells ml^{-1} (genome size = 8.2×10^8 bp) resulting in a genomic content (calculated as the sum of bacterial plus host genomic DNA) of up to 1.6×10^{15} bp ml^{-1} of haemolymph (Hedgecock *et al*., 2005; Vezzulli *et al*., 2015). Considering that high-performance sequencing technologies (e.g. NovaSeq 6000 System) might provide output up to 3×10^{12} bp per single run (2×10^{10} reads with 150 bp average read length), it can be theoretically calculated that shotgun metagenomic approaches might provide very low coverage (<0.002×) of metagenomic DNA derived from oyster tissues. In other words, in order to detect target genetic traits such as the bacteria phylogenetic or virulence markers investigated in this study with shotgun metagenomics, we might require them to be present at a concentration of at least 10^3 (i.e. at least 2× coverage of the target region) in the analysed samples. Such concentrations probably need to be higher considering analysis bias such as non-optimal sequencing performance, and the fact that whole tissue homogenate might show a greater genomic content than the one estimated above for theoretical calculations in oyster haemolymph.

To overcome these constrains, a new target enrichment next-generation sequencing approach was developed and successfully applied to explore the Pacific Oyster pathobiota during mortality episodes in Europe. The protocol is based on the use of biotinylated RNA baits (on average >100-mer) for selective capturing of 884 phylogenetic and virulence markers targeting the *Vibrio* community and other potential pathogenic microorganisms in oyster tissues via hybridization (Table 2). This approach is estimated to increase target DNA coverage by about three orders of magnitude compared with current approaches such as shotgun metagenomics (Vezzulli *et al*., 2017).

Generally, although the pathobiota community was composed of different microbial species in infected *C. gigas* samples a dominance of primary pathogens such as *V. aestuarianus* and OsHV-1 was apparent (Figs 3 and 4). *Crassostrea gigas* samples infected by *V. aestuarianus* collected during infection outbreaks ascribed to this pathogen, showed the presence, albeit at lower relative abundance, of other potential pathogenic vibrios species including *V. coralliilyticus*, *V. splendidus*, *V. crassostreae*, *V. tasmaniensis* and their associated virulence genes (*vsm*, *vcpA* and *ompU*) (Fig. 3). These are likely opportunistic bacteria known to take advantage of a compromised host health status linked to infection and/or occurrence of stressful events (e.g. temperature stress) (Vezzulli *et al*., 2010). Accordingly, seawater temperature greater than 15°C is known to promote *Vibrio* replication in coastal marine waters, a condition commonly found during periods of mortality (e.g. summer) (Vezzulli et al., 2003; Stauder *et al*., 2010).

Interestingly, an *Arcobacter* sp. strain phylogenetically related to the species *Arcobacter haliotis* was consistently found in *V. aestuarianus*-infected *C. gigas* samples collected both in the Ebro delta and Dungarvan bay. *Arcobacter* spp. strains have been previously found in association with the oyster haemolymph and proposed to represent specific symbionts of *C. gigas* (Lokmer and Wegner, 2015). Nevertheless, bacteria belonging to this genus were also observed in high abundance in moribund oysters, suggesting they might also turn into opportunistic pathogens at high density (Lokmer and Wegner, 2015). In this study, *Arcobacter* spp. represent an important fraction of the oyster microbiota whose relative abundance significantly increased in concomitance with V. aestuarianus infection. The species *Arcobacter haliotis* was isolated from the gut of an abalone of the

species *Haliotis gigantea* collected in Japan (Tanaka *et al*., 2017), however, taxonomy of the *Arcobacter* sp. strain found in this study and its potential role as an opportunistic pathogen for *C. gigas* deserve further investigations (Pérez-Cataluña *et al*., 2018).

The pathobiota community in OsHV-1 infected oysters was also composed of a variety of potentially pathogenic *Vibrio* species most of which belong to the Splendidus super-clade, e.g., *V. splendidus*, *V. tasmaniensis* (including the LGP32 pathogenic strain), *V. cyclitrophicus*, *V. lentus*, *V. pomeroyi* (Fig. 4) and other *Vibrio* species including *V. coralliilyticus*, *V. alginolyticus* and *V. cortegadensis*. Such observations add to previous findings from culture-based studies investigating *Vibrio* microbiota in naturally infected specific-pathogen-free oysters by direct culturing on selective media (Lemire *et al*., 2015). Bacterial members of the Splendidus clade colonizing oyster tissues were found to belong to a phylogenetically coherent virulent population that may share virulence factors needed for oyster infection (Lemire *et al*., 2015). Accordingly, population-specific genomic regions such as the R5.7 genetic element that was shown to play a role in oyster infection was detected in the microbiota of OsHV-1-infected oysters in this study. Other major virulence genes such as those encoding for *V. splendidus* and *V. tasmaniensis* metalloproteases (*vsm*) and outer membrane proteins (*ompU*) were also present.

In contrast to the above findings, analysis of healthy (non-infected) oysters by target enrichment protocols failed to detect potential pathogenic species and their associated virulence genes in the majority of the samples. This result contrasts with the fact that members of the potential pathogenic microbial community such as genus *Vibrio* and *Arcobacter* were commonly found in control samples by 16S rRNA profiling analysis. Such a discrepancy could be linked to the low abundance of these bacterial groups in control samples compared to infected samples such that their presence might simply go undetected by target enrichment analysis. An exception is represented by sample DrH7jul16SPAT-4 collected in Dungarvan Bay during an OsHV-1 outbreak in July 2016. Even though this sample was not infected by OsHV-1, it showed a diversified pathobiota community similar to the one observed in OsHV-1-infected oysters (Fig. 4). Members of the Splendidus clade including the oyster pathogen *Vibrio tasmaniensis* LGP32 strain dominated such communities; virulence genes (e.g. *vsm* and *ompU*) and the genetic element R5.7 were also present. It should be mentioned that not all *V. tasmaniensis* and *V. splendidus* are pathogenic. Considering that this oyster did, however, belong to the same cohort of oysters that were infected, it can be speculated that such results might reflect some early stage of infection before OsHV-1 DNA reached a threshold above which it can be detected.

Conclusions

Diseases of the Pacific oyster (*C. gigas*) associated with microbial infections have been rising over the past decades, representing a significant threat for the aquaculture production of the Pacific oysters in Europe. Stress-induced changes in the composition of the oyster microbiota linked to compromised immune functions are thought to be responsible for disease development by replacement of benign microbial colonizers by consortia of different pathogens (pathobiota). In this study, the composition of the oyster pathobiota associated to two diseases (e.g. OsHV-1 and *V. aestuarianus* infections) affecting the Pacific oysters at different life stages was for the first time assessed by employing 16S rRNA gene profiling and a new target enrichment next-generation sequencing approach able to detect and relatively quantify potential pathogenic species including not culturable bacteria in oyster tissues. It was shown that primary infectious agents such as the bacteria *V. aestuarianus* and *Ostreid herpesvirus-1* (OsHV-1) dominated the pathobiota community of infected animals during mortality outbreak ascribed to these pathogens together with a previously undetected community of potential pathogenic bacterial species mostly belonging to the genus *Vibrio* and *Arcobacter*.

Our results provide, for the first time, full insight into the species/strain composition of the potential pathogenic microbial community associated to oyster tissues during mortality episodes. It is suggested that the biology and ecology of detected microbial species and their consortia should be targeted by future studies aimed to shed light on mechanisms underlying polymicrobial infections in *C. gigas*. More generally, the developed protocol and approach may be of great interest in monitoring oyster disease dynamics as well as in studies investigating infection diseases in other marine organisms and the biology and ecology of marine microbial pathogenic communities.

Experimental procedures

Crassostrea gigas *samples collection during mortality episodes in Europe*

In the frame of the EU funded H2020 project VIVALDI (Preventing and mitigating farmed bivalve diseases) 525 *C. gigas* individuals (365 spat and 160 adult) were collected between March 2016 and October 2017 at different European sites (Ebro delta, lat 40°29′37.7″N – long 0°48′24.82″E, Spain; Dungarvan Bay, lat 52°4′1.35″N – long 7°33′51.74″W, Ireland; Bay of Brest, lat 48°20′24.94″N – long 4°29′15.39″W, France) experiencing mass mortality episodes (Table 1, Supplementary Material and Methods, Fig. S1). Immediately after collection, individual oyster samples were transported to the laboratory and prepared for downstream molecular analysis according to EU Council

Directive 175/2010. Briefly, bivalve tissues were extracted from single specimen and placed on a 2 ml tube containing beads, and frozen at −20°C until processed. Samples were placed on 180 μl of ATL buffer and 20 μl of proteinase K to be homogenized, followed by DNA extraction using Blood and Tissue Kit (QIAGEN srl, Milan, Italy), following the instructions for Tissue Protocol. The amount of extracted DNA was quantified using the Quantifluor double-stranded DNA quantification kit (Promega Italia, Milan, Italy).

OsHV-1 and Vibrio aestuarianus *detection in* C. gigas *samples by qPCR*

Individual oyster samples were preliminary screened for the presence of OsHV-1 and *Vibrio aestuarianus* by real-time PCR as previously described (Webb *et al*., 2007; IFREMER, 2013). Briefly, for detection of OsHV-1 real-time PCR was performed using primers HVDP-F ATTGATGATGTGGATAATCTGTG and HVDP-R GGTAAATACCATTGGTCTTGTTCC according to Webb *et al*. (2007). Amplification was performed using a ABI 7300 Thermocycler (Applied Biosystems, CA) in a total volume of 20 μl. The PCR mix included 1 μl of extracted DNA, 10 μl 2× SYBR GREEN dye, 0.50 μl of each diluted primers (final concentration 0.5 μM) and 8 μl of molecular grade water. Plasmid DNA containing cloned viral DNA was used as a positive control. Quantification of OsHV-1 DNA copies was carried out using a standard curve based on 10-fold dilutions of OsHV-1 genomic DNA.

For detection of *V. aestuarianus*, a Taqman real-time PCR protocol with the LightCyler (Roche Diagnostics, Mannheim, Germany) was used. *Vibrio aestuarianus* specific primers and probe (DNAj F GTATGAAATTTTAAC TGACCCACAA; DNAj R CAATTTCTTTCGAACAACCAC; DNAj probe FAM– TGGTAGCGCAGACTTCGGCGAC –BHQ2) (IFREMER, 2013) were used in the assays. Each reaction mixture contained 1× LightCycler Taqman master (Roche Diagnostics, Mannheim, Germany) and 1 μM of each primer and 0.1 μM of each probe in a final volume of 20 μl. Five microliters of DNA template (DNA concentration for all samples varied from 10 to 100 ng μl^{-1}) was added to the reaction mixture. Accurately quantified copy number genomic DNA of *V. aestuarianus* 01/32 strains was used as a standard. Positive and negative controls (PCR grade water, Sigma Aldrich S.R.L., Milan) were included in all qPCR assays. Presence/absence of the targeted pathogens in the analysed samples is presented in this study.

Analysis of bivalve 'microbiota' by 16S rRNA gene-based profiling of the bacterial community

16S rDNA PCR amplicon libraries were generated from genomic DNA extracted from individual bivalve samples using primers amplifying positions 515–802 of the *Escherichia coli* numbering of the 16S rRNA gene that include the V4 hypervariable region. All primers were custom designed to include 16S rRNA complementary regions plus the complementary sequences to the Ion Torrent specific adapters. Two PCR assays were performed. A first target enrichment PCR assay with the 16S conserved primers (Supplementary Material and Methods, Table S1). A second PCR assay, with customized primers including adapters' complementary regions (Supplementary Material and Methods, Table S1). The obtained libraries were sequenced using an Ion Torrent (PGM) Platform (Thermo Fisher Scientific, MA).

Bioinformatic analysis of NGS data was performed using the Microbial Genomics module (version 1.3) workflow of the CLC Genomics workbench (version 9.5.1) and other comparable software. After quality trimming based on quality scores and length trimming, reads were clustered at 97% level of similarity into OTUs. Chimera detection and removal was performed. Ribosomal RNA gene reads were classified against the non-redundant version of the SILVA SSU reference taxonomy (release 123; http://www.arb-silva.de). Only reads occurring at least five times in the trimmed data set were assigned to bacterial taxa and included in the results.

Alpha diversity analysis was then conducted on total OTUs by constructing rarefaction curves calculated by sub-sampling OTUs abundances in the different samples at different depths. Beta diversity analysis was also performed by calculating Bray–Curtis distances between each pair of samples and applying Principal Coordinate Analysis on the distance matrices.

The core microbiota, defined as the microbial taxa belonging to OTUs present in all the samples, was analysed using the Corbata software (CORe microbiome Analysis Tools) (Li *et al*., 2013). A two-parameter model (Ubiquity-Abundance) was applied to quantitatively identify the core taxonomic members of each sample group microbiota considering the different conditions. Sequence reads data were archived at NCBI sequence read archive (SRA) with Accession Number PRJNA542081.

Target enrichment next-generation sequencing protocol for the analysis of the bivalve Pathobiota

A target enrichment next-generation sequencing protocol for the analysis of bivalve 'pathobiota' was applied following the approach previously developed for the target sequencing of *Vibrio cholerae* DNA in complex environmental samples (Vezzulli *et al*., 2017). To this aim, 884 *Vibrio* phylogenetic and virulence markers, as well as other bivalve and marine invertebrates microbial pathogen markers (Rosenberg *et al*., 2007; Travers *et al*., 2015) with average length of 400 nt, were identified and used to produce 100-mer biotinylated RNA baits for

selective capturing of target DNA markers via hybridization (Table 2). Five hundred nanogram of total RNA baits was produced using the MYcroarray target enrichment proprietary technology (MYcroarray, Ann Arbor, MI) and used for a capture (it is estimated that a single capture is capable of enriching single-copy nuclear loci, i.e., >99.5% of the capture target region) (Vezzulli *et al*., 2017).

Genomic DNA extracted from individual bivalve samples was sized on an Agilent Bioanalyzer and enzymatically fragmented using the KAPA Frag Kit (Roche Diagnostics, Mannheim, Germany) protocol to an average size of about 600 bp. The fragmented DNA was used for the production of an indexed library for next-generation sequencing on the Illumina platform (Illumina) using the KAPA HyperPlus Kit for Illumina (Roche Diagnostics). About 200 ng of the produced library was used for target DNA capturing using the MYbaits protocol (MYcroarray, Ann Arbor, MI) following the manufacturers instructions. Briefly, the genomic DNA library was heat-denatured and hybridized to the RNA baits in stringent conditions. Hybridization was carried out at 65°C for 36H (capturing of target DNA with 5%–10% sequence divergence is expected at this conditions enabling full covering of marker allelic variants including unknown variants). After hybridization, the biotinylated baits hybridized to captured material were pulled out of the solution with streptavidin-coated magnetic beads and the captured genomic DNA was released by chemical degradation of the RNA baits. Enriched libraries were amplified prior to sequencing.

All samples libraries were then pooled and sequenced on a MiSeq Illumina™ platform (V3 flow cell, 600 cycles, 25 M reads 250 bp pair ends). After quality trimming, sequence reads were mapped against reference sequences of phylogenetic and virulence markers used to produce the baits using the CLC mapping tool set with length fraction of 0.5 and similarity fraction of 0.95. Consensus sequences were produced from outputs with a minimum of 10 reads mapping on the reference sequences and blasted against the nucleotide collection (nr) database of NCBI for classification.

In addition to bivalve samples, DNA extracted from a mock community sample (positive control) composed of equal amount of genomic DNA from *Vibrio cholerae* O139 5424, *Vibrio tasmaniensis* LGP32, *Vibrio alginolyticus*, *Vibrio cholerae* non O1/O139, *Vibrio mimicus* CP192, *Vibrio cholerae* O1 CD81 classical, *Vibrio aestuarianus* 01/032,*Vibrio cholerae* N16961^T El Tor, *Vibrio coralliilyticus* ATCC BAA 450, *Vibrio tapetis* CECT 4600^T, *Vibrio vulnificus* ATCC 275262, *Vibrio parahaemolyticus* 54496, *Escherichia coli* ATCC 2922, *Serratia marcescens*, *Enterococcus faecalis* ATCC 29212 and a nuclease-free water sample (negative control) was also analysed and sequenced following the same protocol.

To avoid laboratory contamination of treated samples all the analyses including DNA extraction, DNA amplification and NGS library preparations were carried out in a separate laboratory (non-aquatic/non-microbiological laboratory) using a dedicated set of pipettes, reagents and consumables (Vezzulli *et al*., 2017). Sequence reads data were archived at NCBI SRA with accession: PRJNA542081.

Acknowledgements

This project has received funding from the European Union's Horizon 2020 research and innovation programme under the EU project H2020 VIVALDI Grant No. 678589. We thank all the producers and people helping with sampling collection at the farming sites. We also thank the Ifremer ECOSCOPA network for producing and maintaining the oysters in the Bay of Brest.

Conflict of Interest

The authors declare that they have no conflict of interests related to this work.

Data Availability Statement

Sequence files and metadata for all samples and the mock community (positive control) used in this study have been deposited at NCBI SRA with accession: PRJNA542081. Additional data (Supplementary Material and Methods) including map of sampling areas, sequencing results from mock community analysis, primers used for 16S rRNA sequencing have all been included as additional supplementary files. 100-merBaits sequences developed and used in the target enrichment protocol have also been included in supplementary material.

References

Alfaro, A.C., Nguyen, T.V., and Merien, F. (2018) The complex interactions of Ostreid herpesvirus 1, *Vibrio* bacteria, environment and host factors in mass mortality outbreaks of *Crassostrea gigas*. *Rev Aquacult* 1–21. https://doi.org/10.1111/raq.12284.

Avila-Poveda, O.H., Torres-Ariño, A., Girón-Cruz, D.A., and Cuevas-Aguirre, A. (2014) Evidence for accumulation of *Synechococcus elongatus* (Cyanobacteria: Cyanophyceae) in the tissues of the oyster *Crassostrea gigas* (Mollusca: Bivalvia). *Tissue Cell* **46**: 379–387.

de Lorgeril, J., Lucasson, A., Petton, B., Toulza, E., Montagnani, C., Clerissi, C., *et al*. (2018) Immune-suppression by OsHV-1 viral infection causes fatal bacteraemia in Pacific oysters. *Nat Commun* **9**: 4215.

Duperron, S., Fiala-Médioni, A., Caprais, J.C., Olu, K., and Sibuet, M. (2007) Evidence for chemoautotrophic symbiosis in a Mediterranean cold seep clam (Bivalvia: Lucinidae): comparative sequence analysis of bacterial 16S rRNA, APS reductase and RubisCO genes. *FEMS Microbiol Ecol* **59**: 64–70.

Forbes, J.D., Knox, N.C., Ronholm, J., Pagotto, F., and Reimer, A. (2017) Metagenomics: the next culture-independent game changer. *Front Microbiol* **8**: 1069.

Garnier, M., Labreuche, Y., Garcia, C., Robert, M., and Nicolas, J.L. (2007) Evidence for the involvement of pathogenic bacteria in summer mortalities of the Pacific oyster *Crassostrea gigas*. *Microb Ecol* **53**: 187–196.

Green, T.J., and Barnes, A.C. (2010) Bacterial diversity of the digestive gland of Sydney rock oysters, *Saccostrea glomerata* infected with the paramyxean parasite, *Marteilia sydneyi*. *J Appl Microbiol* **109**: 613–622.

Hedgecock, D., Gaffney, P.M., Goulletquer, P., Guo, X., Reece, K., and Warr, G.W. (2005) The case for sequencing the pacific oyster genome. *J Shellfish Res* **24**: 429–441.

IFREMER report (2013) Vibrio splendidus et V. aestuarianus detection by Real Time Polymerase Chain Reaction European Union Reference Laboratory for Molluscs Diseases. Edition n 1, Laboratoire de Génétique et Pathologie des Mollusques Marins, Av. de Mus de Loup, 17390 La Tremblade France. URL https://www.eurl-mollusc.eu/content/download/72924/file/Vsplendidus&aestuarianus _RealTimePCR.pdf.

King, G.M., Judd, C., Kuske, C.R., and Smith, C. (2012) Analysis of stomach and gut microbiomes of the eastern oyster (*Crassostrea virginica*) from coastal Louisiana, USA. *PLoS One* **7**: e51475.

King, W.L., Siboni, N., Williams, N.L.R., Kahlke, T., Nguyen, K.V., Jenkins, C., *et al*. (2019) Variability in the composition of Pacific oyster microbiomes across oyster families exhibiting different levels of susceptibility to OsHV-1 μvar disease. *Front Microbiol* **10**: 473–473.

Labreuche, Y., Le Roux, F., Henry, J., Zatylny, C., Huvet, A., Lambert, C., *et al*. (2010) *Vibrio aestuarianus* zinc metalloprotease causes lethality in the Pacific oyster *Crassostrea gigas* and impairs the host cellular immune defenses. *Fish Shellfish Immunol* **29**: 753–758.

Lederberg, J., and McCray, A.T. (2001) 'Ome sweet 'Omics – a genealogical treasury of words. *Scientist* **15**: 8.

Lemire, A., Goudene, D., Versigny, T., Petton, B., Calteau, A., Labreuche, Y., *et al*. (2015) Populations, not clones, are the unit of vibrio pathogenesis in naturally infected oyster. *ISME J* **9**: 1523–1531.

Li, K., Bihan, M., and Methé, B.A. (2013) Analyses of the stability and core taxonomic memberships of the human microbiome. *PLoS One* **8**: e63139.

Lokmer, A., Goedknegt, M.A., Thieltges, D.W., Fiorentino, D., Kuenzel, S., Baines, J.F., *et al*. (2016) Spatial and temporal dynamics of pacific oyster hemolymph microbiota across multiple scales. *Front Microbiol* **7**: 1367.

Lokmer, A., and Wegner, K.M. (2015) Hemolymph microbiome of Pacific oysters in response to temperature, temperature stress and infection. *ISME J* **9**: 670–682.

Nhung, P.H., Shah, M.M., Ohkusu, K., Noda, M., Hata, H., Sun, X.S., *et al*. (2007) The dnaJ gene as a novel phylogenetic marker for identification of *Vibrio* species. *Syst Appl Microbiol* **30**: 309–315.

Pérez-Cataluña, A., Salas-Massó, N., Diéguez, A.L., Balboa, S., Lema, A., Romalde, J.L., *et al*. (2018) Revisiting the taxonomy of the genus Arcobacter: getting order from the chaos. *Front Microbiol* **9**: 2077.

Pernet, F., Barret, J., Le Gall, P., Corporeau, C., Dégremont, L., Lagarde, F., *et al*. (2012) Mass mortalities of Pacific oysters *Crassostrea gigas* reflect infectious diseases and vary with farming practices in the Mediterranean Thau lagoon, France. *Aquacult Env Interact* **2**: 215–237.

Rajendhran, J., and Gunasekaran, P. (2011) Microbial phylogeny and diversity: small subunit ribosomal RNA sequence analysis and beyond. *Microbiol Res* **166**: 99–110.

Romero, J., and Espejo, R. (2001) The prevalence of non-cultivable bacteria in oysters (*Tiostrea chilensis*, Philippi, 1845). *J. Shellfish Res* **20**: 1235–1240.

Romero, J., Garcia-Varela, M., Laclette, J.P., and Espejo, R. T. (2002) Bacterial 16S rRNA gene analysis revealed that bacteria related to *Arcobacter* spp. constitute an abundant and common component of the oyster microbiota (*Tiostrea chilensis*). *Microb Ecol* **44**: 365–371.

Rosenberg, E., Koren, O., Reshef, L., Efrony, R., and Zilber-Rosenberg, I. (2007) The role of microorganisms in coral health, disease and evolution. *Nat Rev Microbiol* **5**: 355–362.

Segarra, A., Pepin, J.F., Arzul, I., Morga, B., Faury, N., and Renault, T. (2010) Detection and description of a particular Ostreid herpesvirus 1 genotype associated with massive mortality outbreaks of Pacific oysters, *Crassostrea gigas*, in France in 2008. *Virus Res* **153**: 92–99.

Stauder, M., Vezzulli, L., Pezzati, E., Repetto, B., and Pruzzo, C. (2010) Temperature affects *Vibrio cholerae* O1 El Tor persistence in the aquatic environment via an enhanced expression of GbpA and MSHA adhesins. *Env Microbiol Rep* **2**: 140–144.

Tanaka, R., Cleenwerck, I., Mizutani, Y., Iehata, S., Bossier, P., and Vandamme, P. (2017) *Arcobacter haliotis* sp. nov., isolated from abalone species *Haliotis gigantea*. *Int J Syst Evol Microbiol* **67**: 3050–3056.

Travers, M.A., Boettcher, M.K., Roque, A., and Friedman, C.S. (2015) Bacterial diseases in marine bivalves. *J Invertebr Pathol* **131**: 11–31.

Vezzulli, L., Marrale, D., Moreno, M., and Fabiano, M. (2003) Sediment organic matter and meiofauna communityresponse to long-term fish-farm impact in the Ligurian Sea (Western Mediterranean). *Chem Ecol* **19**(6):431–440.

Vezzulli, L., Previati, M., Pruzzo, C., Marchese, A., Bourne, D.G., Cerrano, C., and The VibrioSea Consortium. (2010) *Vibrio* infections triggering mass mortality events in a warming Mediterranean Sea. *Environ Microbiol* **12**: 2007–2019.

Vezzulli, L., Pezzati, E., Stauder, M., Stagnaro, L., Venier, P., and Pruzzo, C. (2015) Aquatic ecology of the oyster pathogens *Vibrio splendidus* and *Vibrio aestuarianus*. *Environ Microbiol* **17**: 1065–1080.

Vezzulli, L., Grande, C., Tassistro, G., Brettar, I., Höfle, M.G., Pereira, R.P.A., *et al*. (2017) Whole-genome enrichment provides deep insights into *Vibrio cholerae* metagenome from an African river. *Microb Ecol* **73**: 734–738.

Webb, S.C., Fidler, A., and Renault, T. (2007) Primers for PCR-based detection of ostreid herpes virus-1 (OsHV-1): application in a survey of New Zealand mollusks. *Aquaculture* **272**: 126–139.

Yarza, P., Yilmaz, P., Pruesse, E., Glockner, F.O., Ludwig, W., Schleifer, K.H., *et al*. (2014) Uniting the classification of

cultured and uncultured bacteria and archaea using 16S rRNA gene sequences. *Nat Rev Microbiol* **12**: 635–645.
Yatsunenko, T., Rey, F.E., Manary, M.J., Trehan, I., Dominguez-Bello, M.G., Contreras, M., *et al*. (2012) Human gut microbiome viewed across age and geography. *Nature* **486**: 222–227.

Supporting Information

Additional Supporting Information may be found in the online version of this article at the publisher's web-site:

Figure S1. Geographic areas and shellfish farms investigated in this study.
Figure S2. Rarefaction curves computed for total OTUs abundance (Alpha diversity analysis) (Va = *Vibrio aestuarianus* infected oysters; OshV1 = Ostreid herpesvirus 1 infected oysters).
Figure S3. Results from target enrichment NGS analysis targeting *C. gigas* pathobiota on a mock community sample (positive control) composed of equal amount of genomic DNA from *Vibrio cholerae* O139 5424, *Vibrio tasmaniensis* LGP32, *Vibrio alginolyticus*, *Vibrio cholerae* non O1/O139, *Vibrio mimicus* CP192, *Vibrio cholerae* O1 CD81 classical, *Vibrio aestuarianus* 01/032,V*ibrio cholerae* N16961^T El Tor, *Vibrio coralliilyticus* ATCC BAA 450, *Vibrio tapetis* CECT 4600^T, *Vibrio vulnificus* ATCC 275262, *Vibrio parahaemolyticus* 54,496, *Escherichia coli* ATCC 2922, *Serratia marcescens*, *Enterococcus faecalis* ATCC 29212). Relative abundance is calculated from the number of reads specifically mapping on target sequences and expressed as percentage (see main text for details on mapping parameters settings).
Table S1. primers, adapter and barcode sequences used in this study.
Table S2. Core microbiota, shared genera in the different conditions at 0.1% of relative abundance and presence in, at least, 90% of the samples.
Appendix S1: Supplementary File.

Fish and Shellfish Immunology 84 (2019) 352–360

Contents lists available at ScienceDirect

Fish and Shellfish Immunology

journal homepage: www.elsevier.com/locate/fsi

Full length article

Responses of *Mytilus galloprovincialis* to challenge with the emerging marine pathogen *Vibrio coralliilyticus*

Teresa Balbi[a,*], Manon Auguste[a], Katia Cortese[b], Michele Montagna[a], Alessio Borello[a], Carla Pruzzo[a], Luigi Vezzulli[a], Laura Canesi[a]

[a] Dept. of Earth, Environment and Life Sciences (DISTAV), University of Genoa, Italy
[b] Dept. of Experimental Medicine (DIMES), University of Genoa, Italy

ARTICLE INFO

Keywords:
Bivalves
Pathogenic vibrios
Vibrio coralliilyticus
Mediterranean mussels
Hemocytes
Immune response
Embryos

ABSTRACT

Vibrio coralliilyticus has emerged as a coral pathogen of concern throughout the Indo-Pacific reef. The interest towards understanding its ecology and pathogenic potential has increased since *V. coralliilyticus* was shown to be strongly virulent also for other species; in particular, it represents a serious threat for bivalve aquaculture, being one of the most important emerging pathogen responsible for oyster larval mortalities worldwide. *V. coralliilyticus* has a tightly regulated temperature-dependent virulence and it has been related to mass mortalities events of benthic invertebrates also in the temperate northwestern Mediterranean Sea. However, no data are available on the effects of *V. coralliilyticus* in the mussel *Mytilus galloprovincialis*, the most abundant aquacultured species in this area. In this work, responses of *M. galloprovincialis* to challenge with *V. coralliilyticus* (ATCC BAA-450) were investigated. In vitro, short term responses of mussel hemocytes were evaluated in terms of lysosomal membrane stability, bactericidal activity, lysozyme release, ROS and NO production, and ultrastructural changes, evaluated by TEM. In vivo, hemolymph parameters were measured in mussels challenged with *V. coralliilyticus* at 24h p.i. Moreover, the effects of *V. coralliilyticus* on mussel early embryo development (at 48 hpf) were evaluated. The results show that both in vitro and in vivo, mussels were unable to activate immune response towards *V. coralliilyticus*, and that challenge mainly induced lysosomal stress in the hemocytes. Moreover, *V. coralliilyticus* showed a strong and concentration-dependent embryotoxicity. Overall, the results indicate that, although *M. galloprovincialis* is considered a resistant species to vibrio infections, the emerging pathogen *V. coralliilyticus* can represent a potential threat to mussel aquaculture.

1. Introduction

Marine bivalves, due to their filter-feeding habit, accumulate large numbers of bacteria from the harvesting waters. Bivalves possess both cellular and humoral defence mechanisms that co-operate to kill and eliminate infecting bacteria [1,2]. However, some bacteria can be pathogenic to the bivalve host, in particular those belonging to the genus *Vibrio*. Pathogenic vibrios can mainly affect larval stages of cultured bivalves, and are also involved in diseases of juveniles and adults [3–5]. The *Vibrio* species with importance for bivalve hatcheries due to the known pathogenicity for larvae and spat have been recently summarized [6]. These include species from the *Anguillarum*, *Coralliilyticus*, *Harveyi*, *Orientalis*, *Pectenicida* and *Splendidus* clades.

Vibrio coralliilyticus has emerged as a coral pathogen of concern throughout the Indo-Pacific reef [7,8]. The interest towards understanding its ecology and pathogenic potential has increased since *V. coralliilyticus* was shown to be strongly virulent also for other species, such as unicellular algae [9,10], flies [10,11], rainbow trout (*Oncorhynchus mykiss*) and larval brine shrimp (*Artemia* spp.) [12]. Moreover, *V. coralliilyticus* represents a serious threat for bivalve aquaculture, being one of the most important emerging pathogen responsible for oyster larval mortalities worldwide [13–15]. *V. coralliilyticus* has been also associated with outbreaks of vibriosis in several other bivalve species, such as hard clam (*Mercenaria mercenaria*), New Zealand green-lipped mussel (*Perna canaliculus*), Atlantic bay scallop (*Argopecten irradians*) and naval shipworm (*Teredo navalis*) [13,15]. In the purple gorgonian *Paramuricea clavata* of the temperate north-western Mediterranean Sea, experimental infections with *V. coralliilyticus* showed a tightly regulated temperature-dependent virulence, in a range of temperatures consistent with those observed during the occurrence of mortality episodes in the field [16]. However, no information is available of the effects of *V. coralliilyticus* in the Mediterranean mussel

* Corresponding author. Dept. of Earth, Environment and Life Sciences (DISTAV), University of Genoa, Corso Europa, 26 16132, Genoa, Italy.
E-mail address: Teresa.Balbi@unige.it (T. Balbi).

https://doi.org/10.1016/j.fsi.2018.10.011
Received 21 June 2018; Received in revised form 2 October 2018; Accepted 5 October 2018
Available online 06 October 2018
1050-4648/

Mytilus galloprovincialis, which represents the most abundant aquacultured species in this area.

Although *Mytilus* spp., including *M. galloprovincialis*, is particularly resistant to bacterial infections, it shows a remarkable specificity of the immune response towards different *Vibrio* spp. and strains, as demonstrated both *in vitro* and *in vivo* studies in adults [2,17,18]. In contrast, little information is available on the possible vibrio pathogens affecting *Mytilus* embryo development [19].

In this work, data are presented on immune responses of *M. galloprovincialis* to challenge with the emerging marine pathogen *V. coralliilyticus*. *In vitro*, short term responses of mussel hemocytes to *V. coralliilyticus* were evaluated in terms of lysosomal membrane stability (LMS), bactericidal activity, extracellular lysozyme release, Reactive Oxygen Species (ROS) and Nitric oxide (NO) production. The effects on hemocyte morphology were also investigated by Transmission Electron Microscopy (TEM). *In vivo*, hemocyte LMS, ROS production and serum lysozyme activity were measured in mussels challenged with *V. coralliilyticus* at 24 h post-injection. Moreover, the effects of *V. coralliilyticus* on mussel early embryo development (at 48 h post fertilization-hpf) were evaluated.

2. Methods

2.1. Mussels and bacteria

Mussels (*Mytilus galloprovincialis* Lamarck, 1819), 4–5 cm long, were purchased from an aquaculture farm (Arborea-OR, Italy) in October 2017 and kept for 1 day in static tanks containing aerated artificial sea water (ASW), salinity 36 ppt (1 L/mussel) at 18 °C. Hemolymph was extracted from the posterior adductor muscle using a sterile 1 mL syringe with an 18 G1/2″ needle. With the needle removed, hemolymph was filtered through a sterile gauze and pooled in 50 mL Falcon tubes at 18 °C. Hemolymph serum was obtained by centrifugation of whole hemolymph at 100 × *g* for 10 min, and the supernatant was sterilized through a 0.22 μm-pore filter.

V. coralliilyticus ATCC BAA-450 and *V. coralliilyticus* TAV24 (isolated from diseased *Paramuricea clavata* colonies [16]) were cultured in Zobell Marine Broth 2216 (Difco Laboratories) at 20 °C under static conditions; after overnight growth, cells were harvested by centrifugation (4500 × *g*, 10 min), washed three times with artificial seawater (ASW), and resuspended to obtain a concentration of about 10^8 CFU/mL (determined spectrophotometrically as an $Abs_{600} = 1$). Thiosulfate Citrate Bile Salts Sucrose (TCBS) Agar (Conda Lab, Spain) was used throughout the experiments.

2.2. In vitro challenge of Mytilus hemocytes with V. coralliilyticus

Hemocyte monolayers were prepared as previously described [18,20] and incubated at 18 °C with suspensions of *V. coralliilyticus* suitably diluted in hemolymph serum at different concentrations (5×10^5, 5×10^6, 5×10^7 CFU/mL), for different periods of times, depending on the endpoint measured. Untreated hemocyte samples in serum were run in parallel.

2.2.1. Determination of lysosomal membrane stability

Lysosomal membrane stability-LMS in hemocyte monolayers was evaluated by the Neutral Red Retention Time (NRRT) assay as previously described [17,18,20]. Hemocyte monolayers on glass slides were pre-incubated for 30 min with different concentrations of *V. coralliilyticus*. Hemocyte monolayers were washed out and incubated with 20 μL of a neutral red (NR) (Sigma-Aldrich, Milan, Italy) solution (final concentration 40 μg/mL from a stock solution of NR 20 mg/mL DMSO-dimethylsulfoxide). After 15 min, excess of dye was washed out, 20 μL of ASW was added, and slides were sealed with a coverslip. Every 15 min, slides were examined under optical microscope and the percentage of cells showing loss of dye from lysosomes in each field was evaluated. For each time point, 10 fields were randomly observed, each containing 8–10 cells. The endpoint of the assay was defined as the time at which 50% of the cells showed sign of lysosomal leaking, i.e. the cytosol becoming red and the cells rounded. All incubations were carried out at 18 °C.

For comparison, LMS was evaluated using the Mediterranean strain *V. coralliilyticus* TAV24 [16] in the same experimental conditions as described above.

2.2.2. Bactericidal activity

Bactericidal activity was evaluated as previously described [20,21]. Hemocyte monolayers were incubated with different concentrations of *V. coralliilyticus* at 18 °C, for different periods of time. Immediately after the inoculum (T = 0) and after 60 and 90 min of incubation, supernatants were collected and hemocytes were lysed by adding filter sterilized ASW supplemented with 0.05% Triton x-100 and by 10 s agitation. Supernatants and lysates were pooled and tenfold serial diluted in ASW. Aliquots (100 μL) of the diluted samples were plated onto TCBS Agar. After overnight incubation at 20 °C, the number of colony-forming units (CFU) per hemocyte monolayer (representing live, culturable bacteria) was determined. Percentages of killing were determined in comparison to values obtained at zero time. The number of CFU in control hemocytes never exceeded 0.1% of those enumerated in experimental samples.

2.2.3. Lysozyme release, ROS and NO production

For these endpoints, hemocytes were incubated with suspensions of *V. coralliilyticus* in serum at 5×10^6 CFU/mL. Lysosomal enzyme release by mussel hemocytes was evaluated by measuring lysozyme activity in the extracellular medium as previously described [20]. Lysozyme activity in aliquots of serum of control hemocytes and hemocytes incubated *V. coralliilyticus* for different periods of time (from 5 to 30 min), was determined spectrophotometrically at 450 nm using a suspension of *Micrococcus lysodeikticus* (15 mg/100 mL in 66 mM phosphate buffer, pH 6.4). Hen eggwhite (HEW) lysozyme was used as a concentration reference and lysozyme activity was expressed as HEW lysozyme equivalents (U mg protein^{-1} mL^{-1}). Protein content was determined according to the bicinchoninic acid (BCA) method using bovine serum albumin (BSA) as a standard. Data are expressed as percentage of control values.

Extracellular generation of reactive oxygen species (ROS) was measured by the reduction of cytochrome c as previously described [18]. Aliquots of hemocyte suspension were incubated for 30 min with cytochrome c solution (75 mM ferricytochrome c in TBS), with or without *V. coralliilyticus*. Cytochrome c in TBS was used as a blank. Samples were read at 550 nm and the results expressed as changes in OD per mg protein.

Nitric oxide (NO) production was evaluated as described previously [18] by the Griess reaction, which quantifies the nitrite (NO_2^-) content of supernatants. Aliquots of hemocyte suspensions were incubated at 18 °C with or without bacterial suspension of *V. coralliilyticus* for 2 h. After the incubation, samples were frozen and stored at −80 °C until analysis. Before analysis, samples were thawed and centrifuged (12000 × *g* for 30 min at 4 °C). Aliquots of supernatants were incubated for 10 min in the dark with 1% (w/v) sulphanilamide in 5% H_3PO_4 and 0.1% (w/v) N-(1-naphthyl)-ethylenediamine dihydrochloride. Samples were read at 540 nm, and the molar concentration of NO_2^- in the sample was calculated from standard curves generated using known concentrations of sodium nitrite. Data are expressed as nitrite accumulation per protein content, determined according to the bicinchoninic acid (BCA) method using bovine serum albumin (BSA) as a standard.

2.2.4. Transmission electron microscopy

TEM of mussel hemocytes was carried out as previously described [20]. Hemocyte monolayers were seeded on glass chamber slides for

20 min at 18 °C (Lab-Tek, Nunc, 177380), and incubated with *V. coralliilyticus* (5×10^6 CFU/mL in hemolymph serum) for 5, 15 and 30 min. Samples were washed out with 0.1 M cacodylate buffer in ASW and fixed in 0.1 M cacodylate buffer in ASW containing 2.5% glutaraldehyde in ASW, for 1 h at room temperature. The cells were postfixed in 1% osmium tetroxide in ASW for 10 min and 1% uranyl acetate in ASW for 1 h. Subsequently, samples were dehydrated through a graded ethanol series and embedded in epoxy resin (Poly-Bed; Polysciences, Inc., Warrington, PA) overnight at 60 °C. About 50 cells per sample were observed by F20 Tecnai electron microscope (Philips, Eindhoven, The Netherlands), and representative images were taken with an Eagle CCD camera and iTEM software and processed with Adobe Photoshop CS2.3.2.

2.3. In vivo challenge of adult mussels with V. coralliilyticus

Mussels were kept for 24 h in static tanks containing aereated artificial sea water (1 L/mussel) at 18 °C. Mussels were *in vivo* challenged by injection of live *V. coralliilyticus* into the posterior adductor muscle, as previously described [20], with 50 µL of a bacterial suspension containing 1×10^8 CFU/mL in phosphate buffered solution isotonic to hemolymph (PBS−NaCl: 2 mM KH_2HPO_4, 10 mM Na_2HPO_4, 3 mM KCl, 600 mM NaCl in distilled water, pH 7.4), in order to obtain a nominal concentration of 5×10^6 CFU/mussel). Control mussels were injected with PBS−NaCl. After challenge, mussels were returned to sea water. At 24 h post injection (p.i.), hemolymph was collected from the posterior adductor muscle of 4 pools of 4 mussels each. No mortality was observed during the experiments.

At 24 h p.i. in hemolymph samples from control and vibrio-injected mussels, hemocyte LMS and ROS production, soluble lysozyme activity, as well as bacterial counts, evaluated as number of CFU/mL of whole hemolymph, were determined as described above.

2.4. Effects of V. coralliilyticus on embryo development

Sexually mature mussels (*M. galloprovincialis* Lamarck, 1819), purchased from an aquaculture farm in the Ligurian Sea (La Spezia, Italy) between November and March, were transferred to the laboratory and acclimatized in static tanks containing aerated artificial sea water [22], pH 7.9–8.1, 36 ppt salinity (1 L/animal), at 18 ± 1 °C. Mussels were utilized within 2 days for gamete collection. Mussels were kept in tanks until they began to spontaneously spawn. Then each individual was immediately placed in single 250 mL beakers containing 200 mL of aerated ASW until complete gamete emission. After spawning, mussels were removed from beakers and sperms and eggs were sieved through 50 µm and 100 µm meshes, respectively, to remove impurities. Egg quality (shape, size) and sperm motility were checked using an inverted microscope. For each experiment, eggs and sperm from two individuals were selected and counted to give a single pairing. Eggs were fertilized with an egg:sperm ratio 1:10 in polystyrene 96-microwell plates (Costar, Corning Incorporate, NY, USA). After 30 min fertilization success (n. fertilized eggs/n. total eggs x 100) was verified by microscopical observation (> 85%).

The 48-h embryotoxicity assay [22] was carried out in 96-microwell plates as described by Fabbri et al. [23]. Aliquots of 20 µL of suspensions of *V. coralliilyticus* (obtained from a 10^7 CFU/mL stock suspension), suitably diluted in ASW, were added to fertilized eggs in each microwell to reach the nominal final concentrations (10^1, 10^2, 10^3, 10^4, 10^5, 10^6 CFU/mL) in a 200 µL volume. At each dilution step, all suspensions were immediately vortexed prior to use. Microplates were gently stirred for 1 min, and then incubated at 18 ± 1 °C for 48 h, with a 16 h:8 h light:dark photoperiod. All the following procedures were carried out following ASTM [22]. At the end of the incubation time, samples were fixed with buffered formalin (4%). All larvae in each well were examined by optical and/or phase contrast microscopy using an inverted Olympus IX53 microscope (Olympus, Milano, Italy) at 40X, equipped with a CCD UC30 camera and a digital image acquisition software (cellSens Entry). Observations were carried out by an operator blind to the experimental conditions. A larva was considered normal when the shell was D-shaped (straight hinge) and the mantle did not protrude out of the shell, and malformed if had not reached the stage typical for 48 hpf (trocophore or earlier stages) or when some developmental defects were observed (concave, malformed or damaged shell, protruding mantle). The acceptability of test results was based on controls for a percentage of normal D-shell stage larvae > 75% [22]. Moreover, in each sample the percentage of malformed D-veligers, immature veligers, and trocophorae was evaluated.

2.5. Data analysis

Data from hemocyte and hemolymph parameters are the mean ± SD of at least 4 independent experiments with each assay performed in triplicate. Statistical analyses were performed by Mann-Whitney *U* test using the GraphPad Instat software.

Embriotoxicity test data, representing the mean ± SD of 4 independent experiments, carried out in 6 replicate samples in 96-microwell plates, were analyzed by ANOVA plus Tukey's post test. The EC_{50} was defined as the concentration causing 50% reduction in the embryogenesis success, and their 95% confidence intervals (CI) were calculated by PRISM 5 software (GraphPad Prism 5 software package, GraphPad Inc.).

3. Results

3.1. Effects of in vitro challenge with V. coralliilyticus on hemocyte functional parameters

As shown in Fig. 1A, incubation with *V. coralliilyticus* ATCC BAA-450 for 30 min induced a dose-dependent decrease in hemocyte LMS, evaluated by the NRRT assay, with respect to controls. The lowest concentration tested (5×10^5 CFU/mL) was ineffective, while a moderate decrease was observed at 5×10^6 CFU/mL (−25%; $p < 0.05$). At the highest concentration (5×10^7 CFU/mL) lysosomal membranes were completely destabilized (−98%; $p < 0.01$). Interestingly, similar results were obtained with the Mediterranean strain *V. coralliilyticus* TAV24 (Fig. 1A).

The capacity of mussel hemocytes to kill *V. coralliilyticus* ATCC BAA-450 was investigated using a bactericidal assay that evaluates the number of live, culturable bacteria at different times of incubation (Fig. 1B). Hemocytes were incubated with *V. coralliilyticus*, at the same concentrations utilized in the LMS assay, and the results are reported as % of killed bacteria with respect to the inoculum. The results clearly show a dose-dependent bactericidal activity towards *V. coralliilyticus*. At 5×10^5 CFU/mL, *V. coralliilyticus* was efficiently killed by mussel hemocytes (from 40% at 60 min to 65% at 90 min; $p < 0.05$). A lower percentage of killing was observed at the concentration of 5×10^6 CFU/mL (20% at both 60 and 90 min; $p < 0.05$). At the highest concentration tested (5×10^7 CFU/mL) no significant bactericidal activity was recorded (less than 10% at 90 min).

On the basis of these results, subsequent experiments to evaluate other immune parameters were carried out using a concentration of bacteria of 5×10^6 CFU/mL, and the results are reported in Fig. 2. Immediately after addition of ATCC BAA-450 bacteria, a significant increase in extracellular lysozyme activity was observed with respect to controls (+37%, $p < 0.05$). No differences were measured at subsequent times of incubation. *V. coralliilyticus* ATCC BAA-450 did not affect extracellular ROS production (B) or nitrite accumulation (C) after 30 min and 2 h, respectively.

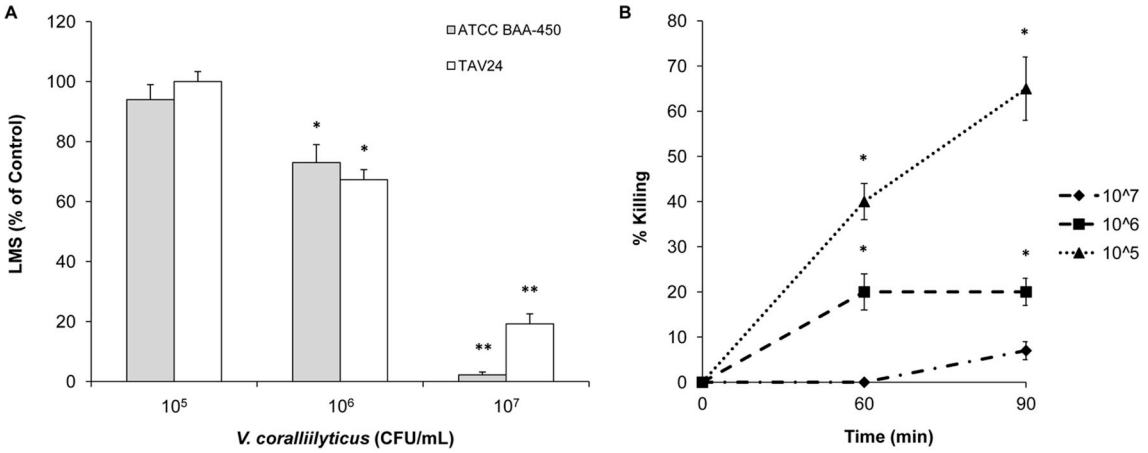

Fig. 1. *In vitro* effects of *V. coralliilyticus* on lysosomal membrane stability-LMS and bactericidal activity.
A) Hemocyte monolayers were treated with different concentrations (5×10^5, 5×10^6, 5×10^7 CFU/mL) of *V. coralliilyticus* ATCC BAA-450 or *V. coralliilyticus* TAV24 for 30 min and LMS was evaluated as described in Methods. Data, expressed as percent values with respect to controls and representing the mean ± SD of 4 experiments in triplicate, were analyzed by Mann-Whitney *U* test (* = $p < 0.05$; ** = $p < 0.01$). B) Hemocytes were incubated for different periods of time (60–90 min) with *V. coralliilyticus* ATCC BAA-450, at the same concentrations utilized in the LMS assay, and the number of viable, cultivable bacteria (CFU) per monolayer was evaluated. Percentages of killing were determined in comparison to values obtained at zero time. Data are the mean ± SD of at least 4 experiments performed in triplicate and statistical analyses were perfomed by Mann-Whitney *U* test (* = $p < 0.05$).

3.2. Effects of in vitro challenge with V. coralliilyticus on hemocyte ultrastructure

The effects of challenge with *V. coralliilyticus* ATCC BAA-450 (5×10^6 CFU/mL) on the morphology of mussel hemocytes were observed by TEM at different times of incubation (5, 15 and 30 min) and representative images are reported in Fig. 3. Fig. 3A shows *V. coralliilyticus* ATCC BAA-450 before the addition to the hemocytes. A control hemocyte is shown in Fig. 3B; as previously reported [18,20], in hemocyte monolayers control cells are mainly represented by granulocytes, whose cytoplasm is filled by small intracellular granules of different electron densities.

V. coralliilyticus induced morphological changes in the hemocytes at the plasma membrane and cytoplasmic level as soon as 5 min from addition. Some cells formed irregular pseudopodial extensions (Fig. 3C) (P), while others showed a more flattened shape, with the cell membrane lining portions of empty cytoplasm (Fig. 3D) (arrowhead). Different ultrastructural changes were more evident at 15 min post-infection. In addition to the formation of long pseudopodia, *V. coralliilyticus* mainly affected the intracellular vacuolar system, as shown by the appearance of enlarged vacuoles of heterogeneous content (HV), empty vacuoles (EV), or vacuoles containing granular material (GV) (Fig. 3E and F). At 30 min (Fig. 3G and H), large electron dense vacuoles of heterogeneous content (HV) were observed, suggesting lysosomal fusion events, together with empty vacuoles and irregular plasma membrane surfaces (arrowheads).

3.3. Effects of in vivo challenge with V. coralliilyticus on hemolymph parameters

Mussels were injected with *V. coralliilyticus* ATCC BAA-450 in order to reach a nominal concentration of 5×10^6 CFU/mL of hemolymph. Samples were collected after 24 h p.i. and hemocyte LMS, serum lysozyme activity and ROS production were evaluated, as well as bacterial cell counts in whole hemolymph samples. The results show that *in vivo* challenge with *V. coralliilyticus* lead to a moderate but significant decrease in LMS at 24 h p.i. (−23%; $p < 0.05$) (Fig. 4A), comparable to that observed in *in vitro* experiments. No increases in serum lysozyme activity (Fig. 4B) and hemocyte ROS production (Fig. 4C) were observed; interestingly, the basal levels of ROS were even reduced with respect to controls (−24%, $p < 0.05$). Finally, in *V. coralliilyticus*-injected mussels, *Vibrio* counts were significantly higher (about 7-folds; $p < 0.01$) in hemolymph collected at 24 h p.i., compared to those in hemolymph collected immediately after infection (T = 0) (Fig. 4D).

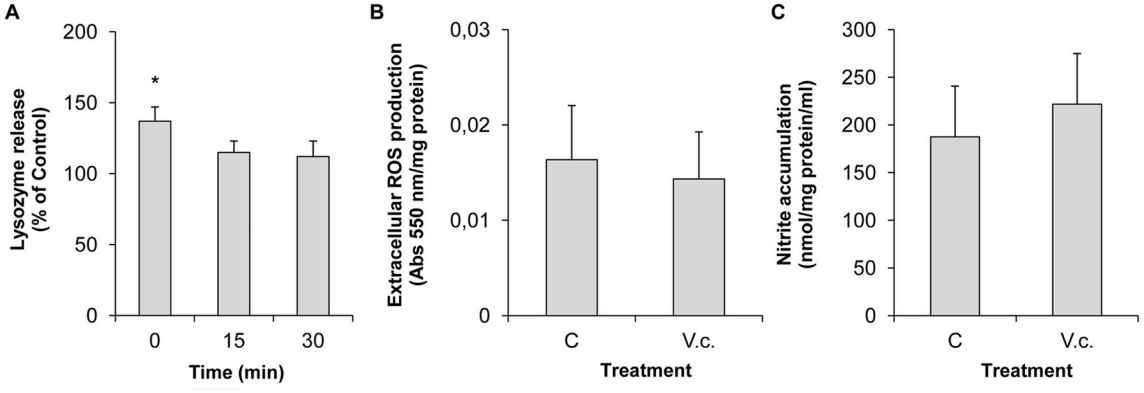

Fig. 2. *In vitro* effects of *V. coralliilyticus* on functional parameters of *Mytilus* hemocytes. Lysosomal enzyme release.
(A), extracellular ROS production (B) and NO accumulation (C) were evaluated after incubation with *V. coralliilyticus* (*V.c.*) at 5×10^6 CFU/mL in hemolymph serum. Data are the mean ± SD of at least 4 experiments performed in triplicate. Statistical analyses were performed by Mann-Whitney *U* test (* = $p < 0.05$).

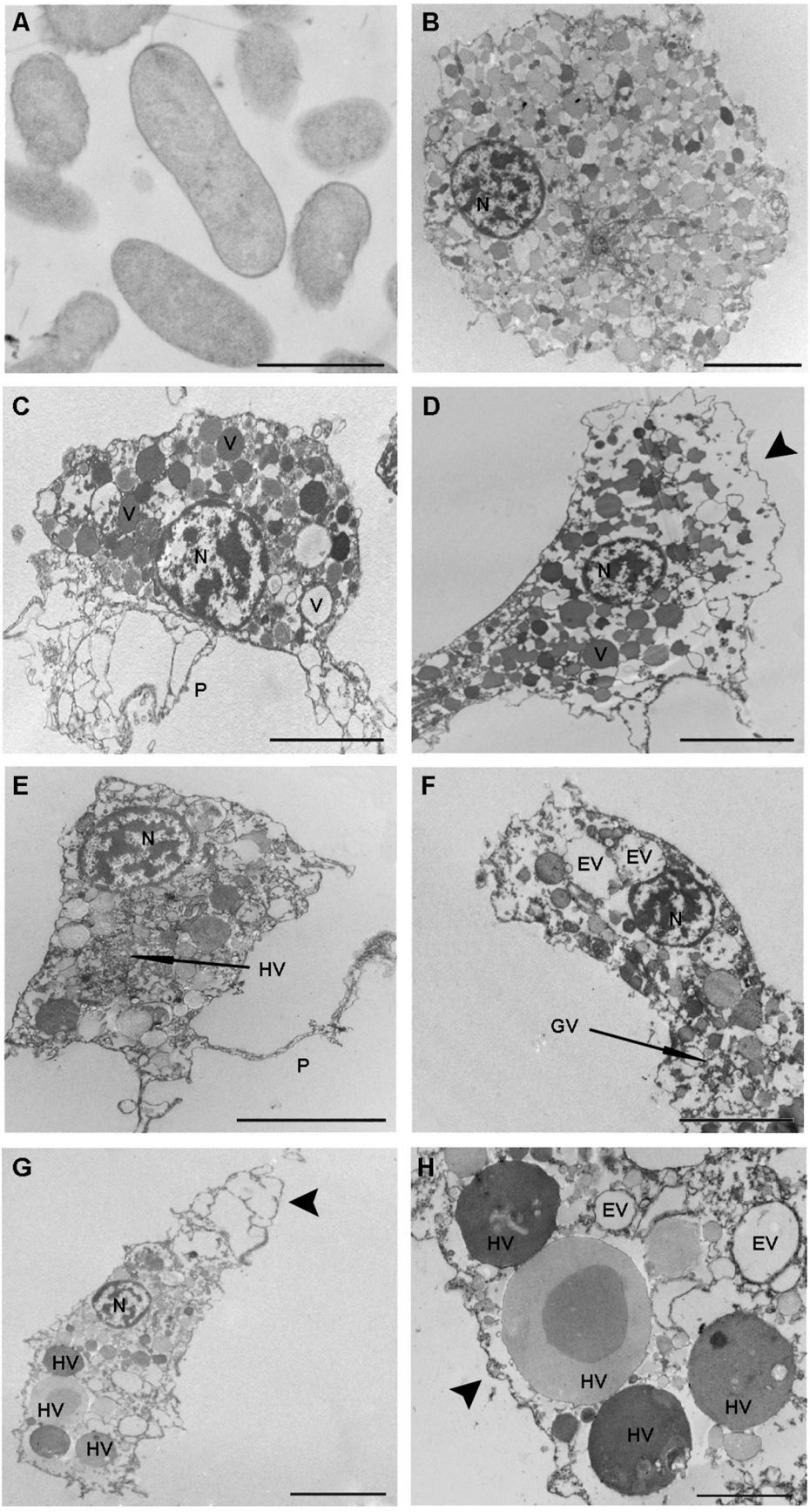

(caption on next page)

Fig. 3. Early *in vitro* effects of *V. coralliilyticus* on the ultrastructure of mussel hemocytes evaluated by TEM.
Representative images of A) *V. coralliilyticus* before addition to the hemocytes; B) Control hemocyte; C-H), hemocytes incubated with *V. coralliilyticus* (5×10^6 CFU/mL) for 5 min (C–D), 15 min (E–F) and 30 min (G–H).
Nuclei (N), pseudopodial extensions (P), vacuoles (V), vesicles with heterogeneous content (HV), vesicles with granular material (GV), empty vesicles (EV), irregular plasma membrane surfaces (arrowheads).
Scale bars: A) 1 μm; B-G) 5 μm; H) 2.5 μm.

3.4. Effects of V. coralliilyticus on embryo development

Fertilized eggs were exposed to different concentrations (from 10^1 to 10^6 CFU/mL) of *V. coralliilyticus* ATCC BAA-450 in 96-microwell plates, and the percentage of normal D-larvae was evaluated after 48 hpf. The results, reported in Fig. 5, show that *V. coralliilyticus* significantly affected normal larval development, with an EC_{50} value of 5.045×10^3 CFU/mL (4.599–5.492, 95% CI) (Fig. 5A). The percentage of normal D-larvae was significantly reduced from the lowest concentration tested (from −30% vs controls at 10 CFU/mL) and a dose-dependent effect was observed at increasing concentrations, up to a complete impairment of normal D-larvae development at 10^6 CFU/mL (−92.8%) ($p < 0.01$).

When the type of effect caused by bacterial challenge was evaluated (Fig. 5B) *V. coralliilyticus* induced a progressive increase in the percentage of malformed embryos. At the highest concentration tested (10^6 CFU/mL), the presence of trocophorae/immature D-veligers was also observed, indicating developmental arrest. In Fig. 5C representative images of control embryos and embryos exposed to different concentrations of *V. coralliilyticus* are reported. From the lowest bacterial concentration tested, malformed D-larvae larvae showed irregular shell margins and hinge line and non symmetric valvae. These types of malformation were independent on the bacterial concentration; moreover, at the highest concentration tested, some larvae did not reach the characteristic D-shape.

4. Discussion

The present work represents the first investigation on the responses of *M. galloprovincialis* to challenge with the emerging marine pathogen *V. coralliilyticus*. To this aim, the reference ATCC BAA-450 strain isolated from bleached corals near Zanzibar [7], was utilized.

In vitro experiments were carried out in the presence of hemolymph serum, in order to simulate the *in vivo* conditions, taking into account also the possible role of soluble hemolymph components, and functional responses of *M. galloprovincialis* hemocytes were evaluated. The results show that *V. coralliilyticus* induced a dose-dependent decrease in hemocyte lysosomal membrane stability that was paralleled by a decrease in the bactericidal activity of whole hemolymph. In particular, at the highest concentration tested (5×10^7 CFU/mL) *V. coralliilyticus* was cytotoxic, and no bacterial killing was observed. Moreover, at lower concentrations (5×10^6 CFU/mL), no activation of immune parameters was observed in response to *V. coralliilyticus,* except for an extremely rapid extracellular lysozyme release. In these conditions, TEM analysis of hemocytes showed rapid cell damage followed by lysosomal fusion events. No vibrio internalization was observed, indicating no intracellular degradation of bacteria. These results were confirmed *in vivo*, in hemolymph from mussels injected with *V. coralliilyticus* (5×10^6 CFU/mL) and sampled after 24 h p.i. In these conditions, *V. coralliilyticus* induced a significant decrease in hemocyte LMS, but did not result in activation of immune parameters; in addition, vibrio challenge even reduced basal ROS production. Accordingly, the results indicate that *V. coralliilyticus* can grow within mussel hemolymph, as shown by the large increase in *Vibrio* counts registered in whole

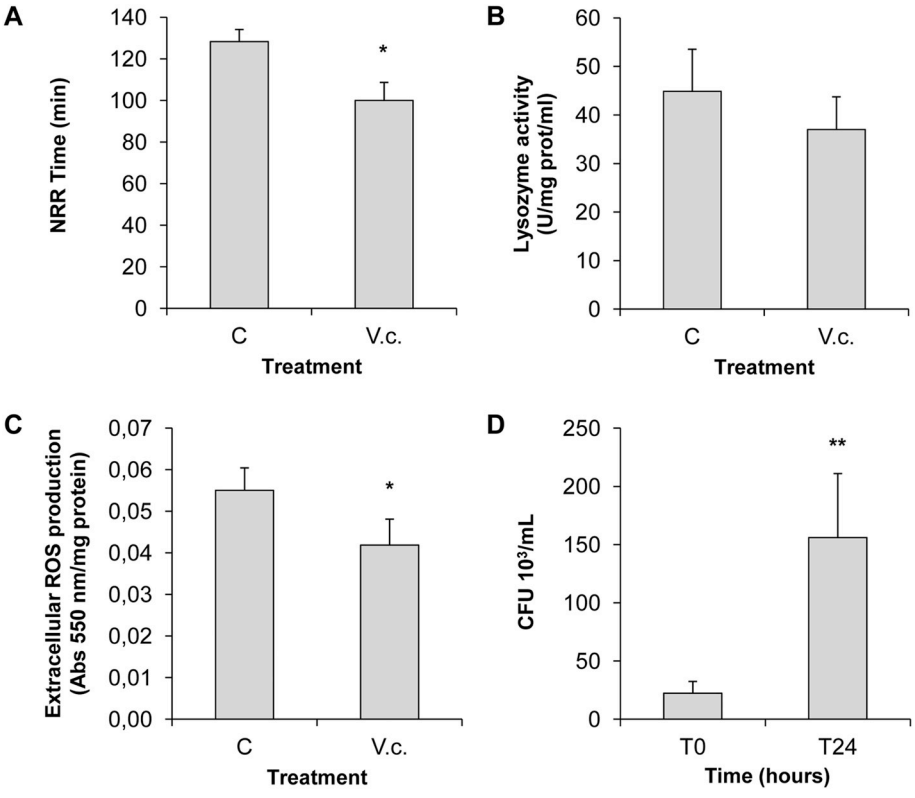

Fig. 4. *In vivo* effects of *V. coralliilyticus* on hemolymph parameters of *Mytilus* hemocytes. Hemocyte lysosomal membrane stability-LMS. (A), serum lysozyme activity (B), ROS production (C) and bacterial cell counts (D) were evaluated in hemolymph sampled from mussels challenged with *V. coralliilyticus* (*V.c.*) at 24 h p.i. Data are the mean ± SD of at least 4 experiments performed in triplicate. Statistical analyses were performed by Mann-Whitney *U* test (* = $p < 0.05$; ** = $p < 0.01$).

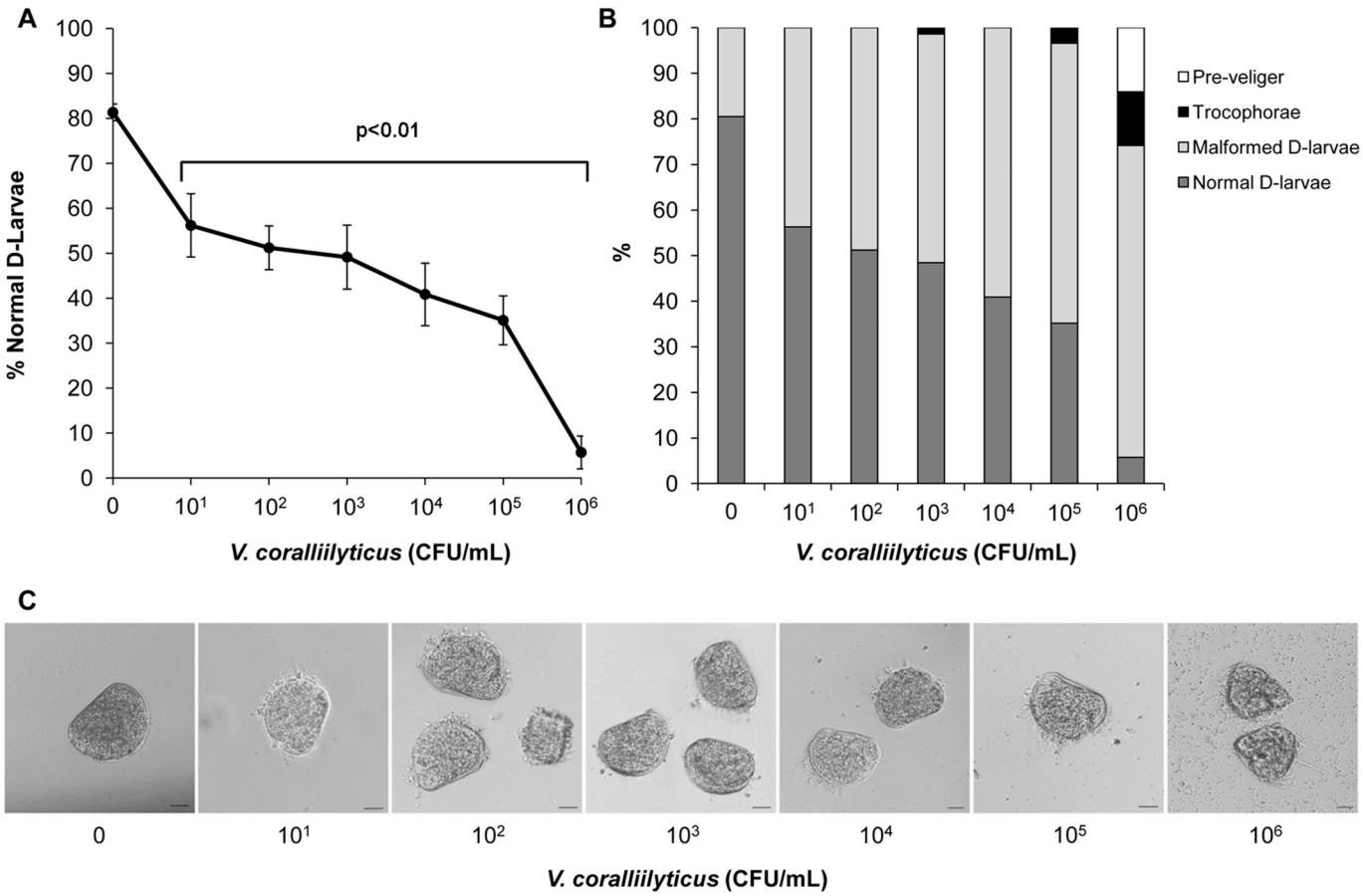

Fig. 5. Effects of different concentrations of *V. coralliilyticus* on *M. galloprovincialis* normal larval development in the 48 h embriotoxicity assay.
A) Percentage of normal D-shaped larvae with respect to controls. B) Percentage of normal D-veliger (dark grey), malformed D-veliger (light grey), pre-veligers (white) and trocophorae (black) in each experimental condition. Data, representing the mean ± SD of 4 experiments carried out in 96-multiwell plates (6 replicate wells for each sample), were analyzed by ANOVA plus Tukey's post test ($p < 0.01$). C) Representative images of control embryos and embryos exposed to different concentrations of *V. coralliilyticus*, showing progressive shell malformations, including asymmetric valvae, irregular hinges, externalized velum and, at the highest concentration of bacteria, immature embryos. Bacteria swarming around larvae can be observed at increasing concentrations.

hemolymph samples at 24 h p.i.

In Table 1, the results of the present work are compared with those previously obtained both *in vitro* and *in vivo* with other vibrios (*V. splendidus* LGP32, *V. aestuarianus* 01/032, *V. tapetis* LP2) in similar experimental conditions [18,20]. Overall, although hemocyte responses to *in vitro* challenge with *V. coralliilyticus* appear generally comparable with those of other potential pathogenic vibrios (Table 1, upper panel), differences in individual responses were observed towards different vibrios. In particular, the overall bactericidal activity towards *V. coralliilyticus* was apparently due to extracellular killing (this work) and lower than that observed with *V. aestuarianus,* that was actively degraded within the lysosomal system [18], whereas no bactericidal activity was observed towards *V. splendidus* and *V. tapetis*. Moreover, only *V. tapetis* induced autophagic processes, indicating a protective mechanisms towards damaged cell components [18]. These differences were reflected by *in vivo* data (Table 1, lower panel) showing that mussels were unable to mount an efficient immune response towards *V. coralliilyticus,* this resulting in bacterial growth within the hemolymph. In this respect, the effects of *V. coralliilyticus* were similar to those of the bivalve pathogen *V. splendidus,* and distinct from those of *V. aestuarianus*.

V. coralliilyticus also affected early embryo development. Challenge with *V. coralliilyticus* generally resulted in embryo malformations in a wide concentration range and developmental delay at the highest concentration tested. In all experimental conditions, erratic closing of the valves, velum detachment, and bacterial swarming around the embryos were observed, which are clear signs of disease in the larvae [4,24,25]. In both Eastern and Pacific oyster larvae, challenge with *V. coralliilyticus* ATCC BAA-450 for 6 days resulted in mortalities with LD_{50} of 2.1 and 4×10^4 CFU/mL, respectively [15]. In *C. gigas*, *V. coralliilyticus* also induced a wide range of physiological, enzymatic, biochemical and molecular changes [14]. However, oyster data were obtained in 1–2 weeks old larvae. The results here reported show that *V. coralliilyticus* affects development of mussel embryos at 48 h post fertilization, with significant effect from concentrations as low as 10 CFU/mL. These represent the first data on the effects of *V. coralliilyticus* on early developmental stages of bivalves. In *M. galloprovincialis*, immune capacities arise during mussel development as early as the trocophorae stage (24 hpf). At this developmental stage, gene expression has contributions of maternal origin, but stimulation induces the expression of immune-related genes [26]. However, the present results underline how mussel early embryos are particularly sensitive to *V. coralliilyticus*, and indicate that they are unable to mount a defence response towards this pathogen.

V. coralliilyticus possess several virulence mechanisms, including powerful extracellular enzymes that have been linked to direct lysis of coral tissue [8]. Several authors demonstrated that the virulence of some strains is associated with the production of toxins, mainly extracellular metalloprotease (VtpA) and hemolysin (VthA) [27–30]. Furthermore, coral diseases not only depend on the presence of *Vibrio* pathogens and their virulence level, but are also the result of complex interactions between the expression of different bacterial virulence

Table 1
Summary of *in vitro* and *in vivo* data on immune responses of *M. galloprovincialis* to challenge with different vibrios.

In vitro	*V. coralliilyticus* ATCC BAA-450[a]	*V. splendidus* LGP32[b]	*V. aestuarianus* 01/032[b]	*V. tapetis* LP2[c]
CFU/mL	5×10^6	10^7	10^7	10^7
LMS	↓	↓	≈	↓
Bactericidal activity	↑	≈	↑↑	≈
Lysozyme activity	↑	↑	↑	≈
ROS production	≈	nd	nd	↓
NO production	≈	nd	nd	≈

In vivo	*V. coralliilyticus* ATCC BAA-450[a]	*V. splendidus* LGP32[b]	*V. aestuarianus* 01/032[b]
CFU/mL	5×10^6	10^7	10^7
LMS	↓	↓	↓
Bactericidal activity	≈	≈	↑
Lysozyme activity	≈	↑	↑
ROS production	↓	nd	nd
NO production	nd	nd	nd

"nd" = not determined; "≈" = no differences compared to control.
[a] This work.
[b] Balbi et al., 2013 [20].
[c] Balbi et al., 2018 [18].

factors and an increase of seawater temperature or other environmental stresses, as well as the physiological and immune status of the coral host [31].

Vibrio species are strongly thermodependent. In particular, for the reference strain of *V. coralliilyticus* ATCC BAA-450 a direct temperature regulation of multiple virulence mechanisms has been demonstrated at 27 °C [32]. *V. coralliilyticus* is able to invade and to lyse the tissue of the coral *Pocillopora damicornis*, one of the most affected organisms, at temperatures higher than 27 °C, while in a temperature range between 24 °C and 26 °C it kills the symbiotic algae of the coral [9]. At temperature below 24 °C is totally avirulent [9,33]. In the present work, all experiments were carried out at the constant temperature of 18 °C, in order to ensure the health and immune status of the mussels. However, even in these conditions, both adult and embryos of *M. galloprovincialis* are apparently unable to mount an efficient immune response towards *V. coralliilyticus*. This results in lysosomal stress in the hemocytes both *in vitro* and *in vivo*, in bacterial growth in the hemolymph of adult mussels challenged *in vivo*, and in malformations in early embryos. Recent data indicate that *in vivo* challenge of the New Zealand Greenshell Mussel *Perna canaliculus* with a *V. coralliilyticus/neptunius*-like isolate induced perturbations of the immune system, oxidative stress, inflammation and metabolic changes at 6 days p.i [34]. Overall, these findings provide a further insight into the potential pathogenic effects of *V. coralliilyticus* in mussels.

In a global warming scenario, an increase in the seawater temperature could promote the proliferation and the potential disease outbreaks associated with *Vibrio* pathogens also in mussels. This is of particular concern in temperate regions such as the Mediterranean sea, where the relative increase in seawater temperature seems to be higher than in tropical areas [31]. Mediterranean strains of *V. coralliilyticus* have been isolated from diseased *P. clavata* colonies collected at Tavolara island (Sardinia, Italy) [16]. Among these, the most virulent strain is TAV24, recently identified as a new genotype of *V. coralliilyticus* by MLST and *vcpA* gene sequencing analyses [35]. The results here reported indicate that the *in vitro* effects of the TAV24 strain on hemocyte lysosomal membrane stability were comparable with those of the reference strain. The responses of *M. galloprovincialis* to challenge with the highly virulent Mediterranean strain require further investigation. Despite the fact that *V. coralliilyticus* appears to be a global bivalve pathogen, there is limited information about its pathogenicity, infection mechanism and/or disease mitigation. Further studies are needed of long term experimental infections of adult mussels to evaluate mortality records. These studies will contribute to understand the potential threat of this vibrio to bivalve aquaculture in the Mediterranean.

Acknowledgments

The authors wish to thank Dr. Rita Fabbri for her invaluable technical assistance and Dr. Giovanni Tassistro for bacterial cultures.

References

[1] L. Canesi, M. Gavioli, C. Pruzzo, G. Gallo, Bacteria-hemocyte interactions and phagocytosis in marine bivalves, Microsc. Res. Tech. 57 (2002) 469–476.
[2] L. Canesi, C. Pruzzo, Specificity of innate immunity in bivalves: a lesson from bacteria, in: L. Ballarin, M. Cammarata (Eds.), Lessons in Immunity: from Single-cell Organisms to Mammals, Elsevier Inc, 2016, pp. 79–91.
[3] C. Paillard, F. Le Roux, J.J. Borrego, Bacterial disease in marine bivalves, a review of recent studies: trends and evolution, Aquat. Living Resour. 17 (2004) 477–498.
[4] R. Beaz-Hidalgo, S. Balboa, J.L. Romalde, M.J. Figueras, Diversity and pathogenecity of *Vibrio* species in cultured bivalve molluscs, Environ. Microbiol. Rep. 2 (2010) 34–43.
[5] M.A. Travers, K. Boettcher Miller, A. Roque, C.S. Friedman, Bacterial diseases in marine bivalves, J. Invertebr. Pathol. 131 (2015) 11–31.
[6] J. Dubert, J.L. Barja, J.L. Romalde, New insights into pathogenic *Vibrios* affecting bivalves in hatcheries: present and future prospects, Front. Microbiol. 8 (2017) 762.
[7] Y. Ben-Haim, E. Rosenberg, A novel *Vibrio* sp. pathogen of the coral *Pocillopora damicornis*, Mar. Biol. 141 (2002) 47–55.
[8] M. Sussman, B.L. Willis, S. Victor, D.G. Bourne, Coral pathogens identified for white syndrome (WS) epizootics in the Indo-Pacific, PloS One 3 (2008) e2393.
[9] Y. Ben-Haim, M. Zicherman-Keren, E. Rosenberg, Temperature-regulated bleaching and lysis of the coral *Pocillopora damicornis* by the novel pathogen *Vibrio coralliilyticus*, Appl. Environ. Microbiol. 69 (2003) 4236–4242.
[10] E. de Oliveira Santos, N. Alves Jr., G.M. Dias, A.M. Mazotto, A. Vermelho, G.J. Vora, B. Wilson, V.H. Beltran, D.G. Bourne, F. Le Roux, F.L. Thompson, Genomic and proteomic analyses of the coral pathogen *Vibrio coralliilyticus* reveal a diverse virulence repertoire, ISME J. 5 (2011) 1471–1483.
[11] N. Alves Jr., O.S. Neto, B.S. Silva, R.L. De Moura, R.B. Francini-Filho, C. Barreira e Castro, R. Paranhos, B.C. Bitner-Mathé, R.H. Kruger, A.C. Vicente, C.C. Thompson, F.L. Thompson, Diversity and pathogenic potential of vibrios isolated from Abrolhos Bank corals, Environ. Microbiol. Rep. 2 (2010) 90–95.
[12] B. Austin, D. Austin, R. Sutherland, F. Thompson, J. Swings, Pathogenicity of vibrios to rainbow trout (*Oncorhynchus mykiss*, Walbaum) and *Artemia* nauplii, Environ. Microbiol. 7 (2005) 1488–1495.
[13] A. Kesarcodi-Watson, P. Miner, J.L. Nicolas, R. Robert, Protective effect of four potential probiotics against pathogen-challenge of the larvae of three bivalves: Pacific oyster (*Crassostrea gigas*), flat oyster (*Ostrea edulis*) and scallop (*Pecten maximus*), Aquaculture 344–349 (2012) 29–34.
[14] B. Genard, P. Miner, J.L. Nicolas, D. Moraga, P. Boudry, F. Pernet, R. Tremblay, Integrative study of physiological changes associated with bacterial infection in Pacific oyster larvae, PloS One 8 (2013) e64534.
[15] G.P. Richards, M.A. Watson, D.S. Needleman, K.M. Church, C.C. Häse, Mortalities of Eastern and Pacific oyster larvae caused by the pathogens *Vibrio coralliilyticus* and *Vibrio tubiashii*, Appl. Environ. Microbiol. 81 (2015) 292–297.
[16] L. Vezzulli, M. Previati, C. Pruzzo, A. Marchese, D.G. Bourne, C. Cerrano, The VibrioSea Consortium, *Vibrio* infections triggering mass mortality events in a warming Mediterranean Sea, Environ. Microbiol. 12 (2010) 2007–2019.
[17] C. Ciacci, A. Manti, B. Canonico, R. Campana, G. Camisassi, W. Baffone, L. Canesi, Responses of *Mytilus galloprovincialis* hemocytes to environmental strains of *Vibrio parahaemolyticus, Vibrio alginolyticus, Vibrio vulnificus*, Fish Shellfish Immunol. 65 (2017) 80–87.
[18] T. Balbi, K. Cortese, C. Ciacci, G. Bellese, L. Vezzulli, C. Pruzzo, L. Canesi, Autophagic processes in *Mytilus galloprovincialis* hemocytes: effects of *Vibrio tapetis*, Fish Shellfish Immunol. 73 (2018) 66–74.
[19] C. Anguiano-Beltrán, M.L. Lizárraga-Partida, R. Searcy-Bernal, Effect of *Vibrio alginolyticus* on larval survival of the blue mussel *Mytilus galloprovincialis*, Dis. Aquat. Org. 59 (2004) 119–123.
[20] T. Balbi, R. Fabbri, K. Cortese, A. Smerilli, C. Ciacci, C. Grande, L. Vezzulli, C. Pruzzo, L. Canesi, Interactions between *Mytilus galloprovincialis* hemocytes and the bivalve pathogens *Vibrio aestuarianus* 01/032 and *Vibrio splendidus* LGP32, Fish Shellfish Immunol. 35 (2013) 1906–1915.
[21] L. Canesi, C. Pruzzo, R. Tarsi, G. Gallo, Surface interactions between *Escherichia coli* and hemocytes of the mediterranean mussel *Mytilus galloprovincialis* Lam. leading to efficient bacterial clearance, Appl. Environ. Microbiol. 67 (2001) 464–468.
[22] ASTM, Standard guide for conducting static acute toxicity tests starting with embryos of four species of saltwater bivalve molluscs, https://doi.org/10.1520/E0724-98, (2004).
[23] R. Fabbri, M. Montagna, T. Balbi, E. Raffo, F. Palumbo, L. Canesi, Adaptation of the bivalve embryotoxicity assay for the high throughput screening of emerging contaminants in *Mytilus galloprovincialis*, Mar. Environ. Res. 99 (2014) 1–8.
[24] S. Prado, J.L. Romalde, J. Montes, J.L. Barja, Pathogenic bacteria isolated from

disease outbreaks in shellfish hatcheries. First description of *Vibrio neptunius* as an oyster pathogen, Dis. Aquat. Org. 67 (2005) 209–215.
[25] R. Rojas, C.D. Miranda, R. Opazo, J. Romero, Characterization and pathogenicity of *Vibrio splendidus* strains associated with massive mortalities of commercial hatchery-reared larvae of scallop *Argopecten purpuratus* (Lamarck, 1819), J. Invertebr. Pathol. 124 (2015) 61–69.
[26] P. Balseiro, R. Moreira, R. Chamorro, A. Figueras, B. Novoa, Immune responses during the larval stages of *Mytilus galloprovincialis*: metamorphosis alters immunocompetence, body shape and behavior, Fish Shellfish Immunol. 3 (2013) 438–447.
[27] M.H. Kothary, R.B. Delston, S.K. Curtis, B.A. McCardell, B.D. Tall, Purification and characterization of vulnificolysin-like cytolysin produced by *Vibrio tubiashii*, Appl. Environ. Microbiol. 67 (2001) 3707–3711.
[28] R.B. Delston, M.H. Kothary, K.A. Shangraw, B.D. Tall, Isolation and characterization of zinc-containing metalloprotease expressed by *Vibrio tubiashii*, Can. J. Microbiol. 49 (2003) 525–529.
[29] H. Hasegawa, E.J. Lind, M.A. Boin, C.C. Häse, The extracellular metalloprotease of *Vibrio tubiashii* is a major virulence factor for Pacific oyster (*Crassostrea gigas*) larvae, Appl. Environ. Microbiol. 74 (2008) 4101–4110.
[30] H. Hasegawa, C.C. Häse, TetR-type transcriptional regulator VtpR functions as a global regulator in *Vibrio tubiashii*, Appl. Environ. Microbiol. 75 (2009) 7602–7609.
[31] E. Rubio-Portillo, J.F. Gago, M. Martínez-García, L. Vezzulli, R. Rosselló-Móra, J. Antón, A.A. Ramos-Esplá, *Vibrio* communities in scleractinian corals differ according to health status and geographic location in the Mediterranean Sea, Syst. Appl. Microbiol. 41 (2018) 131–138.
[32] N.E. Kimes, C.J. Grim, W.R. Johnson, N.A. Hasan, B.D. Tall, M.H. Kothary, H. Kiss, A.C. Munk, R. Tapia, L. Green, C. Detter, D.C. Bruce, T.S. Brettin, R.R. Colwell, P.J. Morris, Temperature regulation of virulence factors in the pathogen *Vibrio coralliilyticus*, ISME J. 6 (2012) 835–846.
[33] J. Tout, N. Siboni, L.F. Messer, M. Garren, R. Stocker, N.S. Webster, P.J. Ralph, J.R. Seymour, Increased seawater temperature increases the abundance and alters the structure of natural *Vibrio* populations associated with the coral *Pocillopora damicornis*, Front. Microbiol. 6 (2015) 432.
[34] T.V. Nguyen, A.C. Alfaro, T. Young, S. Ravi, F. Merien, Metabolomics study of immune responses of New Zealand Greenshell™ mussels (*Perna canaliculus*) infected with pathogenic *Vibrio* sp, Mar. Biotechnol. 20 (2018) 396–409.
[35] B. Wilson, A. Muirhead, M. Bazanella, C. Huete-Stauffer, L. Vezzulli, D.G. Bourne, An improved detection and quantification method for the coral pathogen *Vibrio coralliilyticus*, PloS One 812 (2013) e81800.

frontiers in Immunology

ORIGINAL RESEARCH
published: 15 April 2020
doi: 10.3389/fimmu.2020.00426

Shift in Immune Parameters After Repeated Exposure to Nanoplastics in the Marine Bivalve *Mytilus*

Manon Auguste[1]*, *Teresa Balbi*[1], *Caterina Ciacci*[2], *Barbara Canonico*[2], *Stefano Papa*[2], *Alessio Borello*[1], *Luigi Vezzulli*[1] and *Laura Canesi*[1]*

[1] Department of Earth, Environment and Life Sciences (DISTAV), University of Genoa, Genoa, Italy, [2] Department of Biomolecular Sciences (DIBS), University of Urbino, Urbino, Italy

Bivalves are widespread in coastal environments subjected to a wide range of environmental fluctuations: however, the rapidly occurring changes due to several anthropogenic factors can represent a significant threat to bivalve immunity. The mussel *Mytilus* spp. has extremely powerful immune defenses toward different potential pathogens and contaminant stressors. In particular, the mussel immune system represents a significant target for different types of nanoparticles (NPs), including amino-modified nanopolystyrene (PS-NH_2) as a model of nanoplastics. In this work, the effects of repeated exposure to PS-NH_2 on immune responses of *Mytilus galloprovincialis* were investigated after a first exposure (10 μg/L; 24 h), followed by a resting period (72-h depuration) and a second exposure (10 μg/L; 24 h). Functional parameters were measured in hemocytes, serum, and whole hemolymph samples. In hemocytes, transcription of selected genes involved in proliferation/apoptosis and immune response was evaluated by qPCR. First exposure to PS-NH_2 significantly affected hemocyte mitochondrial and lysosomal parameters, serum lysozyme activity, and transcription of proliferation/apoptosis markers; significant upregulation of extrapallial protein precursor (EPp) and downregulation of lysozyme and mytilin B were observed. The results of functional hemocyte parameters indicate the occurrence of stress conditions that did not however result in changes in the overall bactericidal activity. After the second exposure, a shift in hemocyte subpopulations, together with reestablishment of basal functional parameters and of proliferation/apoptotic markers, was observed. Moreover, hemolymph bactericidal activity, as well as transcription of five out of six immune-related genes, all codifying for secreted proteins, was significantly increased. The results indicate an overall shift in immune parameters that may act as compensatory mechanisms to maintain immune homeostasis after a second encounter with PS-NH_2.

Keywords: mussel, innate immunity, amino modified polystyrene, nanoplastics, immune training

OPEN ACCESS

Edited by:
Geert Wiegertjes, Wageningen University and Research, Netherlands

Reviewed by:
Viswanath Kiron, Nord University, Norway
Nerea Roher, Autonomous University of Barcelona, Spain

***Correspondence:**
Manon Auguste
manon.auguste@edu.unige.it
Laura Canesi
laura.canesi@unige.it

Specialty section:
This article was submitted to Comparative Immunology, a section of the journal Frontiers in Immunology

Received: *09 October 2019*
Accepted: *25 February 2020*
Published: *15 April 2020*

Citation:
Auguste M, Balbi T, Ciacci C, Canonico B, Papa S, Borello A, Vezzulli L and Canesi L (2020) Shift in Immune Parameters After Repeated Exposure to Nanoplastics in the Marine Bivalve Mytilus. Front. Immunol. 11:426. doi: 10.3389/fimmu.2020.00426

INTRODUCTION

Invertebrates represent more than 95% of animal diversity and are found in virtually any ecosystem, and the different species rely on its innate immune system to adapt and survive in its ecological niche. The mechanisms involved in "immune specificity" (sophisticated recognition systems for a wide variety of nonself material), as well as in "immune training/priming" (the capacity to

mount a faster and more effective response upon reexposure to a stimulus), are therefore central to the capacity of invertebrates to survive in diverse environments (1–5). However, the rapid environmental changes induced by several anthropogenic factors can represent a significant threat to invertebrate immune defenses. This in particular applies to marine species, which encounter challenges associated with climate changes such as increased water temperature that may favor the growth of some pathogens (6), as well as pollution caused by a number of emerging contaminants, including nanoparticles (NPs) and plastic debris (microplastics and nanoplastics) (7, 8).

Bivalve mollusks (mussels, oysters, and clams) are widespread in coastal environments characterized by a wide range of environmental fluctuations. In bivalves, both cellular and humoral components of the immune system cooperate in the process of recognition and elimination of microbial and other nonself particles [reviewed in (8–10)]. Among bivalves, the mussel *Mytilus* spp. is particularly resistant to infection; they are able to cope with a large variety of potential pathogens, as well as contaminants. Taking advantage of the robust immune defenses of mussels, they have been employed as a model organism for studying the effects of different types of NPs (11–14).

Nanoplastics can be derived from fragmentation of microplastics and larger plastic debris (15–17). Amino-modified nanopolystyrene (PS-NH_2) has been recently used as a model to study the effects of nanoplastics on marine invertebrates (18–23). The effects of PS-NH_2 (50 nm) have been investigated on *Mytilus galloprovincialis* hemocytes *in vitro* (24 and references quoted therein). The results showed lysosomal stress and activation of immune parameters [lysozyme release, extracellular reactive oxygen species (ROS), and NO production]. Moreover, the formation of a stable biomolecular corona around PS-NH_2 was identified in hemolymph serum (HS), whose unique component was represented by the extrapallial protein precursor (EPp), an immune-related, cation binding protein (24). The results underlined that the *in vitro* immunomodulatory properties of PS-NH_2 were mediated by specific interactions with both humoral and cellular components of the mussel immune system.

In this work, the *in vivo* effects of PS-NH_2 on the immune function of *M. galloprovincialis* were investigated. In particular, we evaluated the impact of nanoplastics on immune parameters after an acute exposure event to PS-NH_2 (10 μg/L, 24 h; Expo1), the possible recovery after 72-h depuration (Resting), and the response to a second acute exposure (10 μg/L, 24 h; Expo2). Controls (unexposed mussels) were run in parallel. At each time point, several functional parameters were measured in hemocytes, serum, and whole hemolymph from exposed and control mussels. In hemocytes, transcription of genes related to proliferation and apoptosis, as well as a set of immune-related genes, was evaluated by qPCR.

MATERIALS AND METHODS

Characterization of PS-NH_2

Primary characterization of 50-nm nonfluorescent amino polystyrene NPs PS-NH_2, purchased from Bangs Laboratories Inc. (Fishers, IN, USA), and analysis of their behavior in different aqueous media were carried out by a combination of analytical techniques as previously described (18, 24, 25). Average size, polydispersity index, and zeta potential of PS-NH_2 suspensions (50 μg/L) in Milli-Q water, artificial seawater (ASW), and *Mytilus* hemolymph serum (HS) were evaluated by dynamic light scattering (DLS) (18, 24, 25). Since agglomeration and surface charge in different media were shown to play a key role in determining the interactions of this type of PS-NH_2 with mussel hemocytes, these results are summarized in **Table S1**.

Animals and Treatments

Mussels (*M. galloprovincialis* Lam.), 4–5 cm long, purchased from an aquaculture farm (Arborea, OR, Italy) in July 2018, were transferred to the laboratory and acclimatized for 24 h in static tanks containing aerated ASW, pH 7.9–8.1, 36 ppt salinity (1 L per animal), at 16 ± 1°C.

Stock suspension of PS-NH_2 (25 mg/ml in water) was suitably diluted in Milli-Q water, quickly vortexed but not sonicated, and immediately spiked in the tanks in order to reach the final desired concentration of 10 μg/L per mussel (nominal concentration level).

Mussels were first exposed to PS-NH_2 (Expo1) at 10 μg/L for 24 h, followed by depuration in clean ASW for 72 h (Resting) and by a second exposure to PS-NH_2 (10 μg/L for 24 h) (Expo 2). A parallel group of control (untreated) mussels was kept in clean ASW throughout the exposure time (see **Figure 1** for details of the experimental setup). Seawater was changed daily. Animals were not fed during the experiments. At each time point (Expo1, Resting, and Expo2), hemolymph was extracted from the posterior adductor muscle of five mussels (from both control and exposed conditions), filtered through sterile gauze, and pooled in tubes at 16°C. Four independent experiments were performed ($n = 4$). Aliquots of whole hemolymph (from 50 to 200 μl, depending on the assay) were utilized for determination of different parameters. The remaining hemolymph was centrifuged at 100 × *g* for 10 min at 4°C, and the resulting supernatant was utilized for determination of serum lysozyme activity. The hemocyte pellet was resuspended in TRIzol reagent (Sigma, Milan, Italy) and stored at −80°C for gene expression analysis. All measurements were performed in triplicate.

Hemocyte Counts

Flow cytometry (FC) was utilized to determine total hemocyte counts (THCs) and various cell types in mussel hemolymph from control and PS-NH_2-exposed mussels in different experimental conditions, as previously described (26). Aliquots (50 μl) from the fresh hemocyte suspensions were added to 250 μl of PBS-NaCl (2 mM KH_2HPO_4, 10 mM Na_2HPO_4, 3 mM KCl, and 500 mM NaCl in distilled water, pH 7.4). Samples were analyzed by flow cytometry (FACSCalibur, BD Becton Dickinson, San Jose, CA, USA). Data acquisition and analysis were performed with the BD CellQuest software using the parameters of relative size (FSC) and granularity (SSC). Counting beads (DakoCytoCount™) were added in a volume of 50 μl to each tube. Five gates were set up to identify cell subpopulations, as well as spermatozoa, cell debris, and aggregates, which were not considered for further analysis. A representative 2D plot of control samples showing the

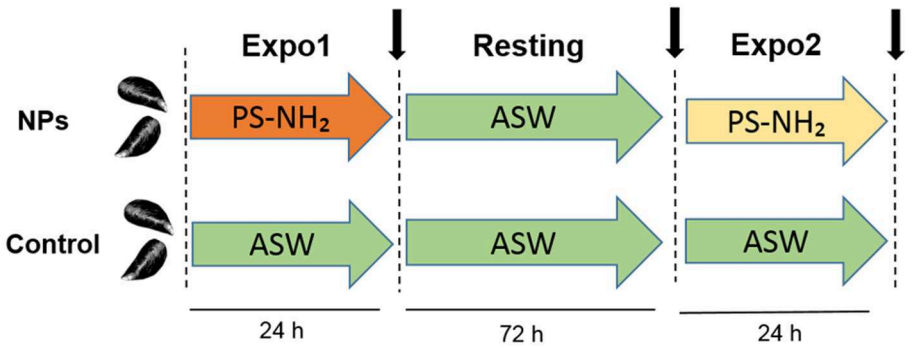

FIGURE 1 | Schematic representation of the *in vivo* experiment on *Mytilus galloprovincialis* upon repeated exposure to PS-NH_2 used in the present study. First exposure (Expo1): PS-NH_2, 10 μg/L, 24 h; resting period: clean ASW, 72 h; and second exposure (Expo2): PS-NH_2, 10 μg/L, 24 h. A control group of unexposed mussels was kept in clean ASW for the whole experiment time. For both conditions (control and PS-NH_2-exposed mussels), sampling times are indicated (black arrows). Four independent experiments were performed ($n = 4$).

three hemocyte subpopulations [R1: hyalinocytes (HY), R2: small granulocytes (SG), and R3: large granulocytes (LG)] is reported in **Figure S1**. Hemocyte viability was checked by propidium iodide (PI) staining as previously described (26), indicating >95% cell viability in samples from all experimental conditions (not shown).

Evaluation of Hemocyte Functional Parameters

Lysosomal membrane stability (LMS) was evaluated by the neutral red retention time (NRRT) assay as previously described (27–29). Hemocyte monolayers on glass slides were incubated with 20 μl of neutral red (NR) solution (final concentration 40 μg/ml from a stock solution of NR 40 mg/ml in DMSO); after 15 min, excess dye was washed out and 20 μl of ASW was added. Every 15 min, slides were examined under an optical microscope, and the percentage of cells showing loss of the dye from lysosomes in each field was evaluated. For each time point, 10 fields were randomly observed, each containing 8–10 cells. The end point of the assay was defined as the time at which 50% of the cells showed signs of lysosomal leaking (the cytosol becoming red and the cells being rounded). In control mussels, no significant changes in LMS were observed throughout the experiment, with average high NRRT values of >120 min. Data ($n = 4$) are expressed as percentage of control values.

For confocal laser scanning microscopy (CLSM) analyses, hemocytes were fixed with paraformaldehyde at 4% for 10 min, washed two times for 2 min with TBS (0.05 M Tris-HCl buffer, pH 7.8), and permeabilized with 0.05% NP-40 (Nonidet-40) for 10 min as previously described (25, 30, 31). Mitochondrial membrane potential (MMP, $\Delta\psi_m$) was evaluated by the fluorescent dye tetramethylrhodamine ethyl ester perchlorate (TMRE). TMRE is a quantitative marker for the maintenance of the MMP, and it is accumulated within the mitochondrial matrix in accordance to the Nernst equation. TMRE exclusively stains the mitochondria and is not retained in cells upon collapse of the $\Delta\psi_m$. Hemocytes were incubated with 40 nM TMRE for 10 min and observed by confocal microscopy.

Dynamic changes and functions of the lysosomes were evaluated in hemocytes loaded with 125 nM of LysoSensor™ Green DND-189 for 45 min. The LysoSensor™ dye accumulates inside acidic vesicles and exhibits an increase in fluorescence intensity which is proportional to acidification (32).

Fluorescence of TMRE (excitation 568 nm, emission 590–630 nm) and LysoSensor™ Green DND-189 (excitation 443 nm, emission 505 nm) was detected using a Leica TCS SP5 confocal setup mounted on a Leica DMI6000 CS inverted microscope (Leica Microsystems, Heidelberg, Germany) using a 63 × 1.4 oil objective (HCX PL APO 63.0-1.40 OIL UV). Images were analyzed by the Leica Application Suite Advanced Fluorescence (LASAF) and ImageJ Software (Wayne Rasband, Bethesda, MA). TMRE and LysoSensor fluorescence intensities were measured as integrated fluorescence density (arbitrary units) per cell area in at least 12 different fields of each sample. Data ($n = 4$) are reported as percentage of control values.

Serum Lysozyme Activity

Lysozyme activity in aliquots of hemolymph serum was determined spectrophotometrically at 450 nm utilizing *Micrococcus lysodeikticus* as previously described (29). Hen egg white (HEW) Lyso was used as a concentration reference, and lysozyme activity was expressed as HEW Lyso equivalents (U/ml/mg protein). Protein content was determined according to the bicinchoninic acid (BCA) method, using bovine serum albumin (BSA) as a standard. In control mussels, no significant changes in serum lysozyme activity were observed throughout the experiment, with overall average values of 50 ± 6 U/ml/mg of protein. Data ($n = 4$) are expressed as percentage of control values.

Bacterial Cultures and Evaluation of Bactericidal Activity of Whole Hemolymph Samples

The sensitivity of *Vibrio aestuarianus* 01/032 to the bactericidal activity of mussel hemolymph was evaluated *in vitro* as previously described (33, 34). *V. aestuarianus* 01/032 was

cultured in Zobell medium at 20°C under static conditions; after overnight growth, cells were harvested by centrifugation (4,500 × *g*, 10 min), washed three times with phosphate-buffered saline (PBS-NaCl: 0.1 M KH_2PO_4, 0.1 M K_2HPO_4, and 0.15 M NaCl, pH 7.2–7.4), and resuspended to obtain a concentration about 10^9 CFU/ml (determined spectrophotometrically as $Abs_{600} = 1$).

Aliquots (1 ml) of whole hemolymph were incubated with a bacterial suspension of *V. aestuarianus* 01/032 containing 1×10^9 CFU/ml, diluted in order to obtain a nominal concentration of 4×10^7 CFU/ml, at 16°C for different periods of time. Triplicate preparations were made for each sampling time. Immediately after the inoculum ($T = 0$) and after 60 and 90 min of incubation, aliquots (0.1 ml) of hemolymph samples were placed in a tube containing 9.9 ml of ASW supplemented with 0.05% Triton X-100 and vortexed for 10 s to lyse the hemocytes. Tenfold serial dilutions in ASW of the lysate were plated onto Luria-Bertani (LB) agar 3% NaCl. After overnight incubation at 24°C, the number of colony-forming units (CFUs) was determined. Percentages of killing were compared with values obtained at zero time ($n = 4$). The number of CFUs in control samples never exceeded 0.1% of those of exposed samples.

RNA Extraction and qPCR

Total RNA was extracted from hemocytes obtained from each condition ($n = 4$) using TRIzol reagent (Sigma, Milan, Italy) following the manufacturer's protocol. RNA concentration and quality were verified using the Qubit RNA assay (Thermo Fisher, Milan, Italy) and by electrophoresis using a 1.5% agarose gel under denaturing conditions. A first-strand cDNA for each sample was synthesized from 1 μg of total RNA (29). Gene transcription was evaluated in four independent RNA samples. Primer pairs employed for qPCR analysis were used as reported in previous studies (**Table S2**). qPCRs were performed in triplicate in a final volume of 15 μl containing 7.5 μl iTaq universal master mix with ROX (Bio-Rad Laboratories, Milan, Italy), 5 μl diluted cDNA, and 0.3 μM specific primers (**Table S2**). A control lacking a cDNA template (no-template) was included in the qPCR analysis to determine the specificity of target cDNA amplification. Amplifications were performed in a CFX96™ Real-Time PCR System (Bio-Rad Italy, Segrate, Milan) using a standard "fast mode" thermal protocol. For each target mRNA, melting curves were utilized to verify the specificity of the amplified products and the absence of artifacts. Relative quantification of each mRNA transcript was calculated by the comparative C_T method (35). Expression of the genes of interest was normalized using the expression levels of EF-α1 as a reference gene, and the normalized expression was then reported as relative quantity of mRNA (relative expression) with respect to control samples.

Statistical Analysis

Data are the mean ± SD of four independent experiments ($n = 4$), with each assay performed in triplicate. Data of functional parameters and hemocyte counts were analyzed by two-way ANOVA followed by Tukey's test at 95% confidence intervals ($P \leq 0.05$). For bactericidal activity and gene transcription, statistical differences were evaluated by the Mann–Whitney *U* test ($P < 0.05$). All statistical calculations were performed using the PRISM 7 GraphPad software.

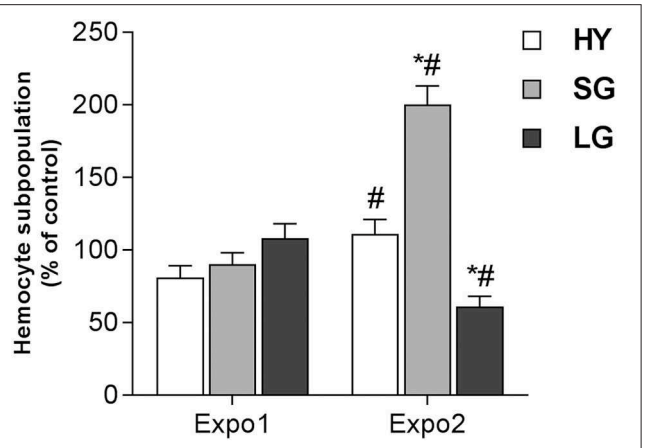

FIGURE 2 | Effect of PS-NH_2 on hemocyte subpopulations in *Mytilus galloprovincialis* hemolymph after first (Expo1) and second exposure (Expo2). HY = hyalinocytes, SG = small granulocytes, LG = large granulocytes. Data, expressed as percent values with respect to each control group, are the mean ± SD of four experiments. *all Expo. *versus* controls; #Expo1. vs. Expo2. $P \leq 0.05$ (ANOVA followed by Tukey's test).

RESULTS

Flow Cytometry

In control hemolymph, THCs were about $1.2 \pm 0.3 \times 10^6$/ml. No significant changes were observed in control samples throughout the experiments; moreover, THCs were unaffected by either Expo1 or Expo2 to PS-NH_2 (not shown). Based on particle size and granularity, three hemocyte subpopulations were identified, namely, HY, SG, and LG (**Figure S1**) as previously described (26, 36), with the sum of SG + LG accounting for more than 80% of total hemocytes in all experimental conditions. After Expo1 to PS-NH_2, no significant changes in hemocyte subpopulations were observed (**Figure 2**). However, after Expo2, a large increase was observed in the percentage of SG (about +100% with respect to controls and Expo1; $P \leq 0.05$); in contrast, the proportion of LG was significantly decreased (about −40% with respect to controls and Expo1). The percentage of HY was similar to controls but significantly higher (+30%; $P \leq 0.05$) than that observed after Expo1 to PS-NH_2.

Measurement of Hemocyte Mitochondrial and Lysosomal Parameters by CLSM

The effects of PS-NH_2 on hemocyte mitochondria were evaluated by cell staining with TMRE, an indicator of MMP $\Delta\psi_m$, and representative CLSM images are reported in **Figure 3**, together with the quantification of the TMRE fluorescence signal. After Expo1, a net decrease in $\Delta\psi_m$ was observed (**Figures 3A**,**B**), as shown by the significant reduction in TMRE fluorescence (−50%

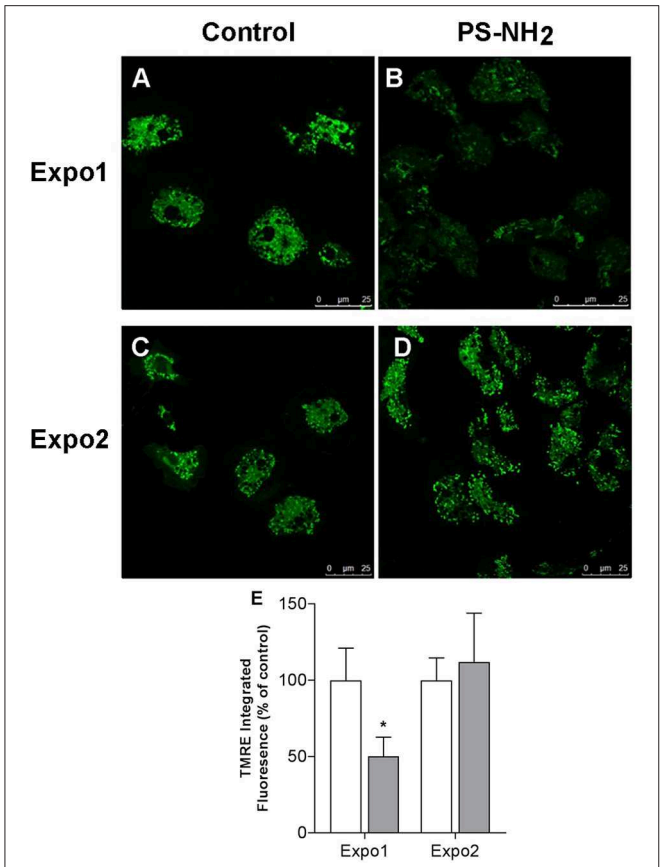

FIGURE 3 | Confocal fluorescence microscopy: effects of exposure of *Mytilus galloprovincialis* to PS-NH_2 on hemocyte mitochondrial membrane potential ($\Delta\Psi_m$) evaluated by TMRE fluorescence. Hemocytes from control and exposed mussels were loaded with TMRE, and representative images are reported (568 excitation/590–630 emission). Expo1: **(A)** Control and **(B)** PS-NH_2 exposed. Expo2: **(C)** Control and **(D)** PS-NH_2 exposed. **(E)** Quantification of the TMRE fluorescence signal in hemocytes from control and PS-NH_2-exposed mussels at each exposure. Data, expressed as percentage of integrated fluorescence density/cell area with respect to each control group, are the mean ± SD of four experiments. *$P \leq 0.05$ (ANOVA followed by Tukey's test). Scale bars: 25 μm.

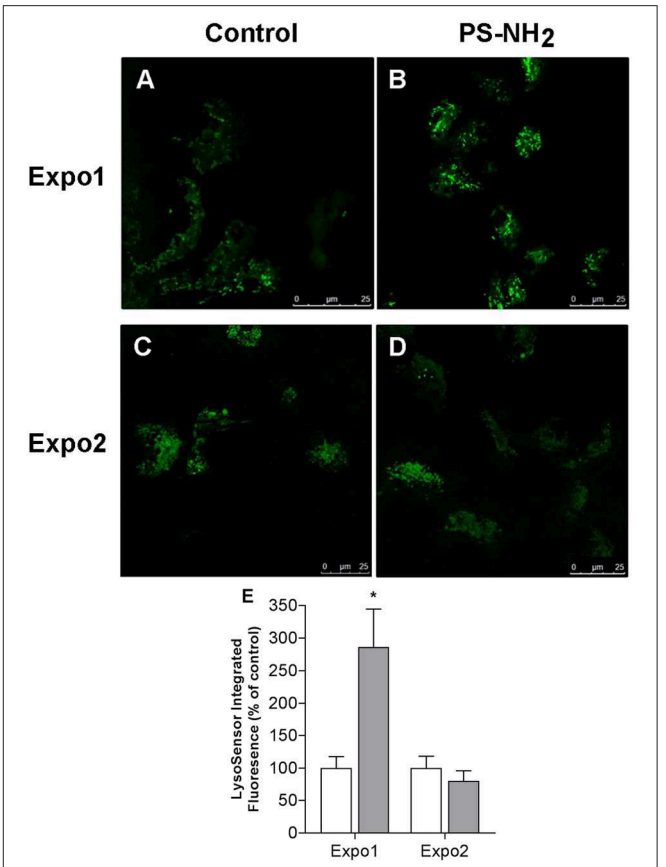

FIGURE 4 | Confocal fluorescence microscopy: effects of exposure of *Mytilus galloprovincialis* to PS-NH_2 on hemocyte lysosomal compartment evaluated by LysoSensor™ fluorescence and representative images (443 nm excitation/505 nm emission) are reported. Upper panel: hemocytes after Expo1, control **(A)** and PS-NH_2 exposed **(B)**; lower panel: hemocytes after Expo2, control **(C)** and PS-NH_2 exposed **(D)**. **(E)** Quantification of the LysoSensor fluorescence signal in hemocytes from control and PS-NH_2-exposed mussels after each exposure. Data, expressed as percentage of integrated fluorescence density/cell area with respect to each control group, are the mean ± SD of four experiments. *$P \leq 0.05$ (ANOVA followed by Tukey's test). Scale bars: 25 μm.

with respect to control; $P \leq 0.05$; **Figure 3E**). However, upon Expo2, no differences in fluorescence were recorded with respect to controls (**Figures 3C**,**D**).

Similarly, the effect on hemocyte lysosomal compartments was evaluated using the fluorescent dye LysoSensor™, which becomes more fluorescent in acidic environments, and representative images are reported in **Figure 4**. Expo1 induced a clear increase in the LysoSensor signal (**Figures 4A**,**B**) (+186% with respect to controls; $P \leq 0.05$; **Figure 4E**), whereas no effects were observed after Expo2 (**Figures 4C**,**D**).

Functional Immune Parameters

The effects of PS-NH_2 exposure on hemocyte and hemolymph immune functional parameters were evaluated, and the results are reported in **Figure 5**. LMS was first evaluated as a functional marker of the lysosomal function related to cellular stress and immune response. Expo1 resulted in a significant drop in LMS (about −50% with respect to control, $P \leq 0.05$). However, after Expo2, a smaller effect was observed (−30% with respect to control, $P \leq 0.05$) (**Figure 5A**). Expo1 also induced a large increase in serum lysozyme activity (+150% with respect to controls, $P \leq 0.05$) (**Figure 5B**), whereas no effects were observed after Expo2. In contrast, other immune parameters (phagocytic activity and extracellular ROS production) were not affected in any experimental condition (**Figure S2**). In order to assess possible recovery of functional parameters, hemocyte LMS, and $\Delta\psi_m$ and hemolymph lysozyme activity were evaluated after a 72-h resting period, as representative parameters of hemocytes and hemolymph serum, respectively. All parameters showed full recovery after depuration (**Figure S3**).

The overall immune function was evaluated in whole hemolymph samples challenged *in vitro* with *V. aestuarianus*

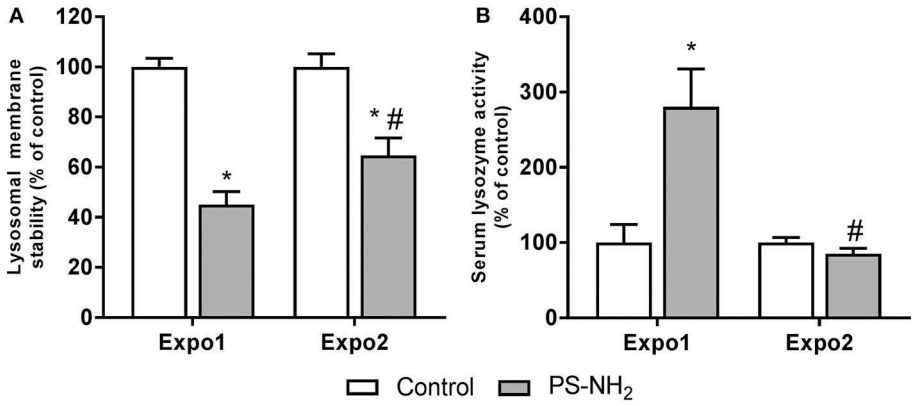

FIGURE 5 | Effects of PS-NH_2 exposure (10 μg/L) on *Mytilus galloprovincialis* hemocytes. **(A)** Lysosomal membrane stability (LMS); **(B)** serum lysozyme activity. Data, expressed as percent values with each respective control group, are the mean ± SD of four experiments. *all Expo. vs. controls; #Expo1. vs. Expo.; $P \leq 0.05$ (ANOVA followed by Tukey's test).

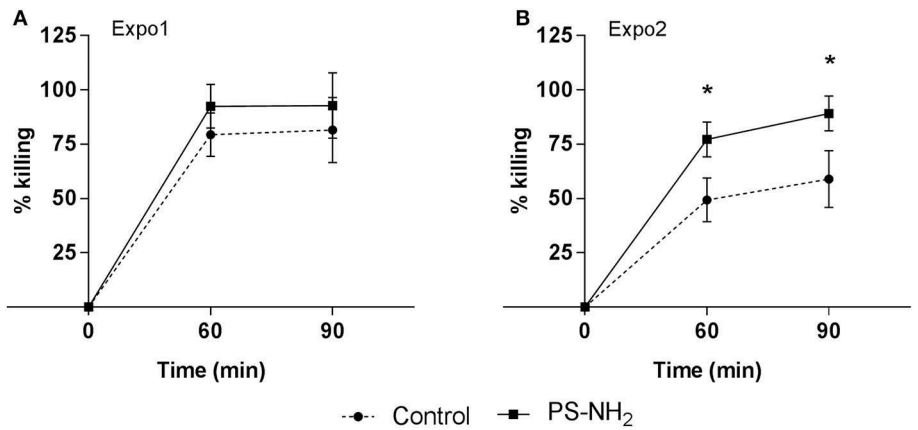

FIGURE 6 | Effects of PS-NH_2 exposure on *Mytilus galloprovincialis* hemolymph bactericidal activity. *In vitro* bactericidal activity toward *Vibrio aestuarianus* 01/032 of whole hemolymph samples from control (dotted line) and PS-NH_2-exposed mussels (black line), **(A)** after Expo1 and **(B)** after Expo2. Hemolymph was incubated with *V. aestuarianus* for 60 and 90 min as described in section Materials and Methods. Percentages of killing were determined in comparison to values obtained at zero time. Data, expressed as percent values with each respective control group, are the mean ± SD of four experiments (*$P < 0.05$) (Mann–Whitney's *U* test).

01/032 for 60 and 90 min. Data, expressed as percentage of killing activity, are presented in **Figure 6**. In control samples of Expo1, bactericidal activity at 60 min (**Figure 6A**) was higher with respect to that of controls of Expo2 (**Figure 6B**), whereas similar values were observed at 90 min; however, all data fell within the range of killing of this vibrio strain by mussel hemocytes (34). The first exposure to PS-NH_2 did not affect the bactericidal activity toward *V. aestuarianus* 01/032 with respect to controls at both times of incubation (**Figure 6A**). However, after Expo2, a significant increase was observed in samples from PS-NH_2-exposed mussels at both 60 and 90 min (+51% and +56%, respectively, $P \leq 0.05$) compared to control samples (**Figure 6B**). When the bactericidal activity of hemocytes alone (in the presence of ASW and absence of hemolymph serum) was evaluated, no killing of *V. aestuarianus* 01/032 was observed in any experimental condition as previously described (34).

Effects on Hemocyte Gene Expression

Transcription of a set of selected genes involved in cell proliferation and apoptosis [proliferating cell nuclear antigen (PCNA) and tumor suppression protein 53 (p53), respectively] and in immune response [Extrapallial protein precursor (EPp), Lyso, Toll-like receptor i isoform (TLR-i), mytilin B (MytB), myticin B (MytC), and fibrinogen-related protein (FREP)] was evaluated by qPCR. Data on relative expression of each transcript (fold changes with respect to control) are reported in **Figures 7A**,**B**.

The results show that Expo1 induced a significant decrease in mRNA levels for both PCNA and p53 (about −50% with respect to controls, $P \leq 0.05$). In contrast, after Expo2, transcription of both genes was similar in hemocytes from control and treated samples. Expo1 significantly affected transcription of three out of six immune-related genes (**Figure 7A**). The expression of EPp was upregulated (+88%, $P \leq 0.05$), whereas that of Lyso

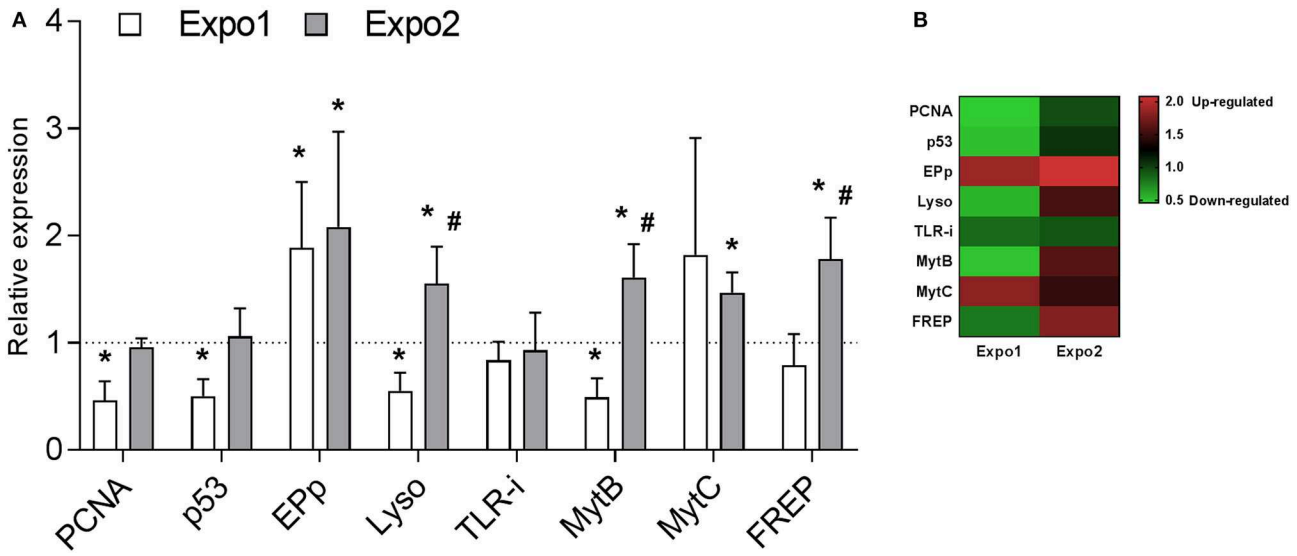

FIGURE 7 | Effect of PS-NH_2 exposure on gene transcription in *Mytilus galloprovincialis* hemocytes evaluated by qPCR. **(A)** Relative expression of proliferating cell nuclear antigen (PCNA), tumor suppression protein 53 (p53), extrapallial protein precursor (EPp), lysozyme (Lyso), Toll-like receptor i isoform (TLR-i), mytilin B (MytB), myticin B (MytC), and fibrinogen-related proteins (FREPs) after Expo1 (white bars) and Expo2 (gray bars). Data, reported as relative expression with respect to each control group, are the mean ± SD of four independent RNA samples. *all Expo. vs. controls; #Expo1. vs. Expo2. $P < 0.05$ (Mann–Whitney's *U* test). **(B)** Heatmap of eight differentially expressed genes was generated in each sample.

and MytB was downregulated (−45% and −51%, respectively, $P \leq 0.05$). After Expo2, a distinct gene expression pattern was observed. Five genes were upregulated with respect to controls: EPp (+107%, $P \leq 0.05$), Lyso (+54%, $P \leq 0.05$), the antimicrobial peptides (AMPs) MytB and MytC (+60 and +46%, respectively; $P \leq 0.05$), and FREP (+78%, $P \leq 0.05$). TLR-i expression was unaffected in either exposure condition. Data are summarized in the heatmap reported in **Figure 7B**.

DISCUSSION

Previous data showed that short-term *in vitro* exposure to PS-NH_2 significantly affected immune parameters of *M. galloprovincialis* hemocytes (24, 25). In the present study, the *in vivo* effects of PS-NH_2 were evaluated. The main aims of the work were (i) to gather information on the impact of acute (24 h) exposure to PS-NH_2 on functional immune parameters; (ii) to investigate the responses induced by repeated exposure to PS-NH_2 on the overall immune function; and (iii) to gain a first insight on the possible molecular mechanisms involved by evaluating the transcription of a set of selected genes.

The results show that Expo1 to PS-NH_2 significantly affected functional parameters of circulating hemocytes in terms of MMP, lysosomal acidification, and membrane destabilization and also increased lysozyme release in the hemolymph, indicating degranulation (**Figures 3**–**5**). No changes in THCs and hemocyte subpopulations (**Figure 2**) or in hemocyte phagocytic activity and ROS production (**Figure S2**) were observed. However, transcription of PCNA and p53 was affected, suggesting modulation of proliferation/apoptotic processes (**Figure 7**). The results confirm previous *in vitro* data obtained with PS-NH_2 (24, 25) and underline the occurrence of stress conditions in the hemocytes, which did not however result in significant changes in the overall hemolymph bactericidal activity. Accordingly, after 72-h depuration, key functional parameters in hemocytes and serum (lysosomal stability, MMP, and lysozyme activity, respectively) showed full recovery (**Figure S3**). This is in line with the observation that, in bivalve tissues, nanopolystyrene particles of similar size are rapidly depurated within three days (20).

Upon Expo2 to PS-NH_2, a distinct pattern of responses was observed. Hemocyte MMP and lysosomal acidification, as well as serum lysozyme activity, were similar in control and exposed mussels (**Figures 3**, **4**, **5B**). Moreover, a significantly smaller lysosomal membrane destabilization in hemocytes was recorded with respect to that induced by Expo1 (**Figure 5A**), corresponding to minor cellular stress (37, 38). Although THCs were unaffected, a shift in hemocyte subpopulations was observed (**Figure 2**), with a decrease in LG, which represent the fully mature phagocytes (39, 40). This may be the result of massive cell degranulation indicated by the large increase of lysozyme release after Expo1. A parallel increase in the percentage of SG was detected (**Figure 2**): since hemocyte subpopulations represent the progressive maturation stages of a single cell type (39), this indicates a maturation process of granular phagocytic cells. Such a homeostatic process is also suggested by the complete recovery of mRNA levels of genes involved in proliferation/apoptosis in the whole hemocyte population. In particular, with regard to apoptotic processes, a decrease in mitochondrial membrane depolarization, which represents a pre-apoptotic signal, was observed only after Expo1, and not after resting or Expo2 (**Figure S3**); accordingly, FC data on annexin/PI staining did not show significant changes in different experimental conditions (not shown).

Although phagocytosis of PS-NH_2 was not evaluated, preliminary FC data were obtained using fluorescently labeled PS-NH_2 of similar size (blue PS-NH_2, 45–55 nm, Sigma Aldrich).

This type of NPs showed the same agglomeration in exposure media as nonfluorescent PS-NH_2, as well as comparable effects on mussel immune parameters (data not shown). The results indicate that after Expo1, uptake of nanoplastics occurred in about 34% of total cells (with over 90% represented by granulocytes, SG + LG). In contrast, a much smaller uptake was observed after Expo2 (about 7%). However, these results were only indicative, due to the low fluorescence signal of the particles utilized (data not shown).

On the basis of these data, though not conclusive, it is likely that mussels are able to establish tolerance mechanisms in immune defenses upon repeated, acute exposure to nanoplastics; in this light, these results are in line with those recently obtained in *M. galloprovincialis* after repeated, long-term exposure to polyethylene microplastics (18 days' first exposure; 28 days' depuration; 18 days' second exposure) to simulate the temporal variability of microplastics concentrations (41). Whole-transcriptome profiling at the tissue level revealed that, despite the physiological impairment triggered by the first exposure to microplastics, after the second exposure a decrease of stress- and immune-related gene expression was observed, indicating the establishment of compensatory mechanisms (41). It was suggested that mussels may be able to establish a stress memory upon microplastics exposure.

However, the results of the present work also show that after Expo2 to nanoplastics, the bactericidal activity of whole hemolymph was significantly increased, demonstrating a stimulation of the overall immune capacity. When expression of immune-related genes was evaluated, a distinct pattern was observed after the first or second exposure to PS-NH_2 (**Figure 7**). Such a shift was evident for three genes that, after Expo1, showed downregulation (Lyso and MytB) or no changes (FREP) but that were upregulated after Expo2. Moreover, transcription of EPp and MytC was generally upregulated in both exposure conditions. Expression of the TLR-i was not affected in any experimental condition. Interestingly, the five genes that were upregulated after Expo2 to PS-NH_2 codify for hemocyte-secreted proteins: activation of the molecular machinery involved in the synthesis and release of immune effectors may partly explain the mechanisms underlying the stimulation of hemolymph bactericidal activity observed upon repeated exposure to nanoplastics. In fact, bactericidal activity of *V. aestuarianus* 01/032 could be observed only in the presence of hemolymph serum, indicating a key role for soluble components as previously described (34). However, due to the variety of secreted immune proteins, the exact components responsible for the increase in bactericidal activity induced by Expo2 cannot be identified. Some of them may participate in direct bacterial killing, others in bacterial recognition and binding. In particular, upregulation of EPp, also known as the MgC1q6 isoform, observed at both times of exposure, may represent a specific effect of this type of nanoplastics. EPp, the most abundant serum protein in *M. galloprovincialis*, is an acidic, histidine-rich, cation binding glycoprotein; it has a complex and anomalous N-glycan structure and contains a conserved C1q complement domain. Due to its peculiar composition, EPp is involved in multiple functions, from shell formation to immune response (42–44). This protein has been shown to play a key role in specific recognition of both selected bacterial strains and NP types. EPp promotes mannose-sensitive interactions between *Mytilus* hemocytes and different bacterial strains of *V. aestuarianus* and *Vibrio cholerae* expressing mannose-sensitive hemagglutinin (MSHA) and *Escherichia coli* MG1655, carrying type 1 fimbriae, leading to activation of the immune response (34, 45). Moreover, EPp represents the unique protein component of the stable biomolecular corona formed around PS-NH_2 in mussel hemolymph serum, which mediates specific recognition of this NP type by hemocytes and consequent immune response *in vitro* (18, 46). The persistent upregulation of EPp mRNA levels induced by PS-NH_2 at both exposure times may result in increased levels of the protein in the hemolymph. Due to the multiple roles of this protein, this would contribute to the formation of the specific EPp-PS-NH_2 corona in the hemolymph, affecting the interactions of PS-NH_2 with hemocytes and consequent responses. Moreover, since EPp acts as a specific opsonin toward *V. aestuarianus* 01/032, its upregulation may lead to increased bactericidal activity of whole hemolymph samples toward this strain. Overall, the results indicate that mussel hemocytes are able to mount a distinct and more efficient immune response upon repeated exposure to PS-NH_2. However, more experimental data, including measurements of immune responses after *in vivo* infection with *V. aestuarianus* 01/032, as well as with other vibrios, are needed to support this hypothesis. Preliminary data were obtained in mussels subjected to Expo1 conditions as in the present work and then challenged *in vivo* for 24 h with different vibrios. The results indicate that pre-exposure to PS-NH_2 increased the hemolymph bactericidal activity toward *V. aestuarianus* 01/032, but not toward *Vibrio tasmaniensis* LGP32 (not shown), suggesting a specific response to this vibrio strain.

The concept of innate immune memory is now fairly accepted due to accumulating evidence in literature (47, 48). Innate immune memory can be defined as the ability of the immune system to store or simply use the information on a previously encountered antigen or parasite upon a secondary exposure (1). Three main mechanisms have been identified: the first is called recall or trained response, expressed as potentiation (with parameters showing enhanced response/activity upon the second exposure); the second is represented by a sustained, unique response which corresponds to the maintenance of a high response between exposures; and the last is characterized by an immune shift, a change in the response observed between several exposures (2, 3). However, evidence for epigenetic reprograming of immune cells (i.e., histone acetylation/deacetylation and DNA methylation) leading to changes in gene expression, which represent the characteristic hallmark of immune training or memory, has not been provided yet in most invertebrate groups, including bivalve mollusks (2–4).

On the other hand, evidence for immune stimulation induced by repeated challenge with natural pathogens is available in clams and oysters (49–55). In the mussel *M. galloprovincialis*, increased bactericidal activity was observed after *in vivo* and subsequent *in vitro* challenge with *Vibrio anguillarum* (26). Recent transcriptomics data obtained in *M. galloprovincialis*

hemocytes after repeated challenge with *Vibrio splendidus* demonstrated a shift from a pro-inflammatory response to an anti-inflammatory and probably regenerative phenotype, indicating the existence of a secondary immune response in mussels oriented to tolerate infection (56).

Induction of innate memory mechanisms by NPs has been recently suggested for human monocytes primed with gold NPs (57). With the knowledge that NPs are able to modulate and induce immune responses similarly as natural pathogens do, in bivalves, they might at least contribute to mount a faster and/or stronger response upon a second display. Overall, repeated exposure of mussels to PS-NH_2 resulted in a shift in granular hemocyte subpopulations, together with reestablishment of basal functional parameters and expression of proliferation/apoptotic markers, stimulation of bactericidal activity, and upregulation of immune gene transcription. These data indicate that both tolerance and potentiation may represent compensatory mechanisms to maintain immune homeostasis after a second encounter with PS-NH_2. Experiments are in progress to investigate this possibility in more detail.

Bivalves express a wide range of inducible immune-related genes codifying for extracellular recognition and effector proteins, including lectins, peptidoglycan recognition proteins, lipopolysaccharide and β1,3-glucan-binding proteins, FREPs, and AMPs (58). The sequencing of the *Mytilus* genome reveals a very complex organization with high heterozygosity, abundant repetitive sequences, and extreme intraspecific sequence diversity among individuals (58–61). This complex machinery would be responsible for the high capacity of mussels to cope with microbial infection and environmental stress.

The present study demonstrates that NPs differentially stimulate the immune responses of *Mytilus*, and this species could serve as a model to explore the impact of nanoplastics on marine invertebrates, that respresents a major environmental concern.

DATA AVAILABILITY STATEMENT

The raw data supporting the conclusions of this article will be made available by the authors, without undue reservation, to any qualified researcher.

ETHICS STATEMENT

The Mediterranean mussel, *M. galloprovincialis*, is not considered an endangered or protected species in any international species catalog, including the CITES list (www.cites.org), and not included in the list of species regulated by EC Directive 2010/63/EU. Therefore, no specific authorization is required to work on mussel samples.

AUTHOR CONTRIBUTIONS

MA, TB, and LC conceived and designed the study. MA, TB, CC, BC, and AB performed the experiments. CC, SP, and LV wrote sections of the manuscript. MA, TB, and LC wrote the manuscript. All authors contributed to manuscript revision, read, and approved the submitted version.

FUNDING

This project has received funding from the European Union's Horizon 2020 research and innovation program under the Marie Skłodowska-Curie grant agreement PANDORA no. 671881 (Probing safety of nano-objects by defining immune responses of environmental organisms) and from the Italian Antarctic Research Program PNRA 16_00075 NANOPANTA (Nano-Polymers in the Antarctic mariNe environmenT and biotA).

ACKNOWLEDGMENTS

We want to thank Rita Fabbri and Michele Montagna for their invaluable technical assistance and Angelica Miglioli for designing qPCR primers.

SUPPLEMENTARY MATERIAL

The Supplementary Material for this article can be found online at: https://www.frontiersin.org/articles/10.3389/fimmu.2020.00426/full#supplementary-material

REFERENCES

1. Milutinović B, Kurtz J. Immune memory in invertebrates. *Semin Immunol.* (2016) 28:328–42. doi: 10.1016/j.smim.2016.05.004
2. Gourbal B, Pinaud S, Beckers GJM, Van Der Meer JWM, Conrath U, Netea MG. Innate immune memory: an evolutionary perspective. *Immunol Rev.* (2018) 283:21–40. doi: 10.1111/imr.12647
3. Melillo D, Marino R, Italiani P, Boraschi D. Innate immune memory in invertebrate metazoans: a critical appraisal. *Front Immunol.* (2018) 9:1915. doi: 10.3389/fimmu.2018.01915
4. Pradeu T, Du Pasquier L. Immunological memory: what's in a name? *Immunol Rev.* (2018) 283:7–20. doi: 10.1111/imr.12652
5. Cooper, E. *Advances in Comparative Immunology*. Cham: Springer (2018). p. 1063.
6. Vezzulli L, Grande C, Reid PC, Hélaouët P, Edwards M, Höfle MG, et al. Climate influence on *Vibrio* and associated human diseases during the past half-century in the coastal North Atlantic. *Proc Natl Acad Sci USA.* (2016) 113:E5062–E71. doi: 10.1073/pnas.1609157113
7. Avio CG, Gorbi S, Regoli F. Plastics and microplastics in the oceans: from emerging pollutants to emerged threat. *Mar Environ Res.* (2017) 128:2–11. doi: 10.1016/j.marenvres.2016.05.012
8. Wagner S, Reemtsma T. Things we know and don't know about nanoplastic in the environment. *Nat Nanotechnol.* (2019) 14:300–1. doi: 10.1038/s41565-019-0424-z
9. Canesi L, Pruzzo C. Specificity of innate immunity in bivalves: a lesson from bacteria. In: Ballarin L, Cammarata M, editors. *Lessons in Immunity: From Single-Cell Organisms to Mammals*. Academic Press (2016). p. 79–92.
10. Allam B, Raftos D. Immune responses to infectious diseases in bivalves. *J Invertebr Pathol.* (2015) 131:121–36. doi: 10.1016/j.jip.2015.05.005

11. Canesi L, Ciacci C, Fabbri R, Marcomini A, Pojana G, Gallo G. Bivalve molluscs as a unique target group for nanoparticle toxicity. *Mar Environ Res.* (2012) 76:16–21. doi: 10.1016/j.marenvres.2011.06.005
12. Canesi L, Procházková P. The invertebrate immune system as a model for investigating the environmental impact of nanoparticles. In: Boraschi D, Duschl A, editors. *Nanoparticles and the Immune System Safety and Effects*. Academic Press (2014). p. 91–112.
13. Canesi L, Ciacci C, Balbi T. Invertebrate models for investigating the impact of nanomaterials on innate immunity: the example of the marine mussel *Mytilus* spp. *Curr Bionanotechnol.* (2017) 2:77–83. doi: 10.2174/2213529402666160601102529
14. Canesi L, Auguste M, Bebianno MJ. Sublethal effects of nanoparticles on aquatic invertebrates, from molecular to organism level. In: Blasco J, Corsi I, editors. *Ecotoxicology of Nanoparticles in Aquatic Systems*. Boca Raton, FL: CRC Press (2019). p. 38–61.
15. Lambert S, Wagner M. Characterisation of nanoplastics during the degradation of polystyrene. *Chemosphere.* (2016) 145:265–8. doi: 10.1016/j.chemosphere.2015.11.078
16. ter Halle A, Ladirat L, Gendre X, Goudouneche D, Pusineri C, Routaboul C, et al. Understanding the fragmentation pattern of marine plastic debris. *Environ Sci Technol.* (2016) 50:5668–75. doi: 10.1021/acs.est.6b00594
17. Gigault J, Halle A ter, Baudrimont M, Pascal P-Y, Gauffre F, Phi T-L, et al. Current opinion: what is a nanoplastic? *Environ Pollut.* (2018) 235:1030–4. doi: 10.1016/j.envpol.2018.01.024
18. Balbi T, Camisassi G, Montagna M, Fabbri R, Franzellitti S, Carbone C, et al. Impact of cationic polystyrene nanoparticles (PS-NH2) on early embryo development of *Mytilus galloprovincialis*: Effects on shell formation. *Chemosphere.* (2017) 186:1–9. doi: 10.1016/j.chemosphere.2017.07.120
19. Manfra L, Rotini A, Bergami E, Grassi G, Faleri C, Corsi I. Comparative ecotoxicity of polystyrene nanoparticles in natural seawater and reconstituted seawater using the rotifer *Brachionus plicatilis*. *Ecotoxicol Environ Saf.* (2017) 145:557–63. doi: 10.1016/j.ecoenv.2017.07.068
20. Al-Sid-Cheikh M, Rowland SJ, Stevenson K, Rouleau C, Henry TB, Thompson RC. Uptake, whole-body distribution, and depuration of nanoplastics by the scallop *Pecten maximus* at environmentally realistic concentrations. *Environ Sci Technol.* (2018) 52:14480–6. doi: 10.1021/acs.est.8b05266
21. Brandts I, Teles M, Gonçalves AP, Barreto A, Franco-Martinez L, Tvarijonaviciute A, et al. Effects of nanoplastics on *Mytilus galloprovincialis* after individual and combined exposure with carbamazepine. *Sci Total Environ.* (2018) 643:775–84. doi: 10.1016/j.scitotenv.2018.06.257
22. Bergami E, Krupinski Emerenciano A, González-Aravena M, Cárdenas CA, Hernández P, Silva JRMC, et al. Polystyrene nanoparticles affect the innate immune system of the Antarctic sea urchin *Sterechinus neumayeri*. *Polar Biol.* (2019) 42:743–57. doi: 10.1007/s00300-019-02468-6
23. Marques-Santos LF, Grassi G, Bergami E, Faleri C, Balbi T, Salis A, et al. Cationic polystyrene nanoparticle and the sea urchin immune system: biocorona formation, cell toxicity, and multixenobiotic resistance phenotype. *Nanotoxicology.* (2018) 12:847–67. doi: 10.1080/17435390.2018.1482378
24. Canesi L, Ciacci C, Fabbri R, Balbi T, Salis A, Damonte G, et al. Interactions of cationic polystyrene nanoparticles with marine bivalve hemocytes in a physiological environment: Role of soluble hemolymph proteins. *Environ Res.* (2016) 150:73–81. doi: 10.1016/j.envres.2016.05.045
25. Canesi L, Ciacci C, Bergami E, Monopoli MP, Dawson KA, Papa S, et al. Evidence for immunomodulation and apoptotic processes induced by cationic polystyrene nanoparticles in the hemocytes of the marine bivalve *Mytilus*. *Mar Environ Res.* (2015) 111:34–40. doi: 10.1016/j.marenvres.2015.06.008
26. Ciacci C, Citterio B, Betti M, Canonico B, Roch P, Canesi L. Functional differential immune responses of *Mytilus galloprovincialis* to bacterial challenge. *Comp Biochem Physiol B Biochem Mol Biol.* (2009) 153:365–71. doi: 10.1016/j.cbpb.2009.04.007
27. Canesi L, Fabbri R, Gallo G, Vallotto D, Marcomini A, Pojana G. Biomarkers in *Mytilus galloprovincialis* exposed to suspensions of selected nanoparticles (Nano carbon black, C60 fullerene, Nano-TiO2, Nano-SiO2). *Aquat Toxicol.* (2010) 100:168–77. doi: 10.1016/j.aquatox.2010.04.009
28. Barmo C, Ciacci C, Canonico B, Fabbri R, Cortese K, Balbi T, et al. *In vivo* effects of n-TiO2 on digestive gland and immune function of the marine bivalve *Mytilus galloprovincialis*. *Aquat Toxicol.* (2013) 132:9–18. doi: 10.1016/j.aquatox.2013.01.014
29. Balbi T, Smerilli A, Fabbri R, Ciacci C, Montagna M, Grasselli E, et al. Co-exposure to n-TiO2 and Cd2+ results in interactive effects on biomarker responses but not in increased toxicity in the marine bivalve *M. galloprovincialis*. *Sci Total Environ.* (2014) 493:355–64. doi: 10.1016/j.scitotenv.2014.05.146
30. Canesi L, Ciacci C, Betti M, Fabbri R, Canonico B, Fantinati A, et al. Immunotoxicity of carbon black nanoparticles to blue mussel hemocytes. *Environ Int.* (2008) 34:1114–9. doi: 10.1016/j.envint.2008.04.002
31. Ciacci C, Canonico B, Bilanicovă D, Fabbri R, Cortese K, Gallo G, et al. Immunomodulation by different types of N-oxides in the hemocytes of the marine bivalve *Mytilus galloprovincialis*. *PLoS ONE.* (2012) 7:e36937. doi: 10.1371/journal.pone.0036937
32. Lu S, Sung T, Lin N, Abraham RT, Jessen BA. Lysosomal adaptation: how cells respond to lysosomotropic compounds. *PLoS ONE.* (2017) 12:e0173771. doi: 10.1371/journal.pone.0173771
33. Balbi T, Fabbri R, Cortese K, Smerilli A, Ciacci C, Grande C, et al. Interactions between *Mytilus galloprovincialis* hemocytes and the bivalve pathogens *Vibrio aestuarianus* 01/032 and *Vibrio splendidus* LGP32. *Fish Shellfish Immunol.* (2013) 35:1906–1915. doi: 10.1016/j.fsi.2013.09.027
34. Pezzati E, Canesi L, Damonte G, Salis A, Marsano F, Grande C, et al. Susceptibility of *Vibrio aestuarianus* 01/032 to the antibacterial activity of *Mytilus* haemolymph: identification of a serum opsonin involved in mannose-sensitive interactions. *Environ Microbiol.* (2015) 17:4271–9. doi: 10.1111/1462-2920.12750
35. Pfaffl MW. A new mathematical model for relative quantification in real-time RT-PCR. *Nucleic Acids Res.* (2001) 29:45e−45. doi: 10.1093/nar/29.9.e45
36. Parisi M-G, Li H, Jouvet LBP, Dyrynda EA, Parrinello N, Cammarata M, et al. Differential involvement of mussel hemocyte sub-populations in the clearance of bacteria. *Fish Shellfish Immunol.* (2008) 25:834–40. doi: 10.1016/j.fsi.2008.09.005
37. OSPAR Commission. *Background Documents and Technical Annexes for Biological Effects Monitoring.* (2013). p. 239. Available online at: www.ospar.org
38. Balbi T, Fabbri R, Montagna M, Camisassi G, Canesi L. Seasonal variability of different biomarkers in mussels (*Mytilus galloprovincialis*) farmed at different sites of the Gulf of La Spezia, Ligurian sea, Italy. *Mar Pollut Bull.* (2017) 116:348–56. doi: 10.1016/j.marpolbul.2017.01.035
39. Ottaviani E, Franchini A, Barbieri D, Kletsas D. Comparative and morphofunctional studies on *Mytilus galloprovincialis* hemocytes: presence of two aging-related hemocyte stages. *Ital J Zool.* (1998) 65:349–54. doi: 10.1080/11250009809386772
40. García-García E, Prado-Álvarez M, Novoa B, Figueras A, Rosales C. Immune responses of mussel hemocyte subpopulations are differentially regulated by enzymes of the PI 3-K, PKC, and ERK kinase families. *Dev Comp Immunol.* (2008) 32:637–53. doi: 10.1016/j.dci.2007.10.004
41. Détrée C, Gallardo-Escárate C. Single and repetitive microplastics exposures induce immune system modulation and homeostasis alteration in the edible mussel *Mytilus galloprovincialis*. *Fish Shellfish Immunol.* (2018) 83:52–60. doi: 10.1016/j.fsi.2018.09.018
42. Oliveri C, Peric L, Sforzini S, Banni M, Viarengo A, Cavaletto M, et al. Biochemical and proteomic characterisation of haemolymph serum reveals the origin of the alkali-labile phosphate (ALP) in mussel (*Mytilus galloprovincialis*). *Comp Biochem Physiol Part D Genomics Proteomics.* (2014) 11:29–36. doi: 10.1016/j.cbd.2014.07.003
43. Campos A, Apraiz I, da Fonseca RR, Cristobal S. Shotgun analysis of the marine mussel *Mytilus edulis* hemolymph proteome and mapping the innate immunity elements. *Proteomics.* (2015) 15:4021–9. doi: 10.1002/pmic.201500118
44. Balbi T, Franzellitti S, Fabbri R, Montagna M, Fabbri E, Canesi L. Impact of bisphenol A (BPA) on early embryo development in the marine mussel *Mytilus galloprovincialis* : effects on gene transcription. *Environ Pollut.* (2016) 218:996–1004. doi: 10.1016/j.envpol.2016.08.050
45. Canesi L, Grande C, Pezzati E, Balbi T, Vezzulli L, Pruzzo C. Killing of *Vibrio cholerae* and *Escherichia coli* strains carrying D-mannose-sensitive ligands by *Mytilus* hemocytes is promoted by a multifunctional hemolymph serum protein. *Microb Ecol.* (2016) 72:759–62. doi: 10.1007/s00248-016-0757-1

46. Canesi L, Balbi T, Fabbri R, Salis A, Damonte G, Volland M, et al. Biomolecular coronas in invertebrate species: implications in the environmental impact of nanoparticles. *NanoImpact.* (2017) 8:89–98. doi: 10.1016/j.impact.2017.08.001
47. Pinaud S, Portet A, Allienne J-F, Belmudes L, Saint-Beat C, Arancibia N, et al. Molecular characterisation of immunological memory following homologous or heterologous challenges in the schistosomiasis vector snail, *Biomphalaria glabrata*. *Dev Comp Immunol.* (2019) 92:238–52. doi: 10.1016/j.dci.2018.12.001
48. Netea MG, Schlitzer A, Placek K, Joosten LAB, Schultze JL. Innate and adaptive immune memory: an evolutionary continuum in the host's response to pathogens. *Cell Host Microbe.* (2019) 25:13–26. doi: 10.1016/j.chom.2018.12.006
49. Cong M, Song L, Wang L, Zhao J, Qiu L, Li L, et al. The enhanced immune protection of Zhikong scallop *Chlamys farreri* on the secondary encounter with *Listonella anguillarum*. *Comp Biochem Physiol B Biochem Mol Biol.* (2008) 151:191–6. doi: 10.1016/j.cbpb.2008.06.014
50. Wang J, Wang L, Yang C, Jiang Q, Zhang H, Yue F, et al. The response of mRNA expression upon secondary challenge with *Vibrio anguillarum* suggests the involvement of C-lectins in the immune priming of scallop *Chlamys farreri*. *Dev Comp Immunol.* (2013) 40:142–7. doi: 10.1016/j.dci.2013.02.003
51. Zhang T, Qiu L, Sun Z, Wang L, Zhou Z, Liu R, et al. The specifically enhanced cellular immune responses in Pacific oyster (*Crassostrea gigas*) against secondary challenge with *Vibrio splendidus*. *Dev Comp Immunol.* (2014) 45:141–50. doi: 10.1016/j.dci.2014.02.015
52. Liu C, Zhang T, Wang L, Wang M, Wang W, Jia Z, et al. The modulation of extracellular superoxide dismutase in the specifically enhanced cellular immune response against secondary challenge of *Vibrio splendidus* in Pacific oyster (*Crassostrea gigas*). *Dev Comp Immunol.* (2016) 63:163–70. doi: 10.1016/j.dci.2016.06.002
53. Li Y, Song X, Wang W, Wang L, Yi Q, Jiang S, et al. The hematopoiesis in gill and its role in the immune response of Pacific oyster *Crassostrea gigas* against secondary challenge with *Vibrio splendidus*. *Dev Comp Immunol.* (2017) 71:59–69. doi: 10.1016/j.dci.2017.01.024
54. Lafont M, Petton B, Vergnes A, Pauletto M, Segarra A, Gourbal B, et al. Long-lasting antiviral innate immune priming in the Lophotrochozoan Pacific oyster, *Crassostrea gigas*. *Sci Rep.* (2017) 7:13143. doi: 10.1038/s41598-017-13564-0
55. Green T, Speck P. Antiviral defense and innate immune memory in the oyster. *Viruses.* (2018) 10:133. doi: 10.3390/v10030133
56. Rey-Campos M, Moreira R, Gerdol M, Pallavicini A, Novoa B, Figueras A. Immune tolerance in *Mytilus galloprovincialis* hemocytes after repeated contact with *Vibrio splendidus*. *Front Immunol.* (2019) 10:1894. doi: 10.3389/fimmu.2019.01894
57. Italiani P, Boraschi D. Induction of innate immune memory by engineered nanoparticles: a hypothesis that may become true. *Front Immunol.* (2017) 8:734. doi: 10.3389/fimmu.2017.00734
58. Gerdol M, Gomez-Chiari M, Castillo MG, Figueras A, Fiorito G, Moreira R, et al. Immunity in molluscs: recognition and effector mechanisms, with a focus on bivalvia. In: Cooper E, editor. *Advances in Comparative Immunology*. Springer (2018). p. 225–342.
59. Gerdol M, Venier P. An updated molecular basis for mussel immunity. *Fish Shellfish Immunol.* (2015) 46:17–38. doi: 10.1016/j.fsi.2015.02.013
60. Murgarella M, Puiu D, Novoa B, Figueras A, Posada D, Canchaya C. A first insight into the genome of the filter-feeder mussel *Mytilus galloprovincialis*. *PLOS ONE.* (2016) 11:e0151561. doi: 10.1371/journal.pone.0151561
61. Figueras A, Moreira R, Sendra M, Novoa B. Genomics and immunity of the Mediterranean mussel *Mytilus galloprovincialis* in a changing environment. *Fish Shellfish Immunol.* (2019) 90:440–445. doi: 10.1016/j.fsi.2019.04.064

Conflict of Interest: The authors declare that the research was conducted in the absence of any commercial or financial relationships that could be construed as a potential conflict of interest.

environmental microbiology
environmental microbiology reports

A deep-sea bacterium related to coastal marine pathogens

Journal:	*Environmental Microbiology and Environmental Microbiology Reports*
Manuscript ID	EMI-2021-0670.R1
Journal:	Environmental Microbiology
Manuscript Type:	EMI - Research article
Date Submitted by the Author:	n/a
Complete List of Authors:	Lasa González, Aide; DISTAV, Dipartimento di Microbiologia; University of Santiago de Compostela, Microbiología y Parasitología Auguste, Manon; Universita degli Studi di Genova, Dipartimento di Scienze della Terra, dell'Ambiente e della Vita (DISTAV) Lema, Alberto; Universidade de Santiago de Compostela, Department of Microbiology and Parasitology Oliveri, Caterina; Università degli Studi di Genova, Dipartimento di Scienze della Terra, dell'Ambiente e della Vita (DISTAV) Borello, Alessio; Università degli Studi di Genova, Dipartimento di Scienze della Terra, dell'Ambiente e della Vita (DISTAV) Taviani, Elisa; Università degli Studi di Genova, Dipartimento di Scienze della Terra, dell'Ambiente e della Vita (DISTAV) Bonello, Guido; Università degli Studi di Genova, Dipartimento di Scienze della Terra, dell'Ambiente e della Vita (DISTAV) Doni, Lapo; Università degli Studi di Genova, Dipartimento di Scienze della Terra, dell'Ambiente e della Vita (DISTAV) Millard , Andrew; University of Leicester, Genetics and Genome biology Bruto, Maxime; Université LYON1, Microbial ecology Romalde, Jesús; Universidad de Santiago de Compostela, Microbiologia y Parasitologia Yakimov, Michail; National Research Council, Istituto per la Ricerca e l'Innovazione Biomedica (CNR-IRIB) Balbi, Teresa; Università degli Studi di Genova, Dipartimento di Scienze della Terra, dell'Ambiente e della Vita (DISTAV) Pruzzo, Carla; Università degli Studi di Genova, Dipartimento di Scienze della Terra, dell'Ambiente e della Vita (DISTAV) Canesi, Laura; University of Genova, DISTAV Vezzulli, Luigi; Università degli Studi di Genova, Dipartimento di Scienze della Terra, dell'Ambiente e della Vita (DISTAV)
Keywords:	pathogen ecology, Vibrio, Deep Sea, Bivalve, Mediterranean Sea

A deep-sea bacterium related to coastal marine pathogens

REVISED

Aide Lasa[1,2], Manon Auguste[1], Alberto Lema[2], Caterina Oliveri[1], Alessio Borello[1], Elisa Taviani[1], Guido Bonello[1], Lapo Doni[1], Andrew D. Millard[3], Maxime Bruto[4], Jesus L Romalde[2], Michail Yakimov[5], Teresa Balbi[1], Carla Pruzzo[1], Laura Canesi[1], Luigi Vezzulli[1]*

[1]Department of Earth, Environmental and Life Sciences (DISTAV), University of Genoa, Corso Europa 26, 16132 Genoa, Italy.

[2]Department of Microbiology and Parasitology, CIBUS-Facultade de Bioloxía & Institute CRETUS, Universidade de Santiago de Compostela, Santiago de Compostela, 15782, Spain.

[3]Department of Genetics and Genome Biology, University of Leicester, University Road, Leicester, United Kingdom

[4]Sorbonne Universités, UPMC Paris 06, CNRS, UMR 8227, Integrative Biology of Marine Models, Station Biologique de Roscoff, CS 90074, Roscoff cedex, F-29688, France

[5] Institute of Biological Resources and Marine Biotechnology, National Research Council (IRBIM-CNR),98122 Messina, Italy

* Luigi Vezzulli

Email: luigi.vezzulli@unige.it

Significant statement

A novel *Vibrio* species *Vibrio bathopelagicus* sp. nov. was isolated from warm bathypelagic waters (3309m depth) of the Mediterranean Sea showing strong phylogenetic relationship with coastal bacterial strains pathogenic for farmed bivalves. Genomic analyses revealed genomic features related to adaptation to the deep-sea environment but also the presence of virulence traits commonly associated with microbial infections and mortality in marine shellfish. Functional *in vitro* assays on mussel and oyster immunocytes as well as early larval development assay in *Mytilus* support strong toxicity of *V. bathopelagicus* sp. nov. towards bivalves. *V. bathopelagicus* sp. nov., is an example of a planktonic marine bacterium with genotypic and phenotypic traits associated with animal pathogenicity, that might have played an evolutionary role in the origin of coastal marine pathogens.

Abstract

Evolution of virulence traits from adaptation to environmental niches other than the host is probably a common feature of marine microbial pathogens, whose knowledge might be crucial to understand their emergence and pathogenetic potential. Here we report genome sequence analysis of a novel marine bacterial species, *Vibrio bathopelagicus* sp. nov., isolated from warm bathypelagic waters (3309m depth) of the Mediterranean Sea. Interestingly, *V. bathopelagicus* sp. nov. is closely related to coastal *Vibrio* strains pathogenic to marine bivalves. *V. bathopelagicus* sp. nov. genome encodes genes involved in environmental adaptations to the deep-sea but also in virulence, such as the R5.7 element, MARTX toxin cluster, Type VI secretion system and zinc-metalloprotease, previously associated with *Vibrio* infection in farmed oysters. The results of functional *in vitro* assays on immunocytes (hemocytes) of the Mediterranean mussel *Mytilus galloprovincialis* and the Pacific oyster *Crassostrea gigas,* and of the early larval development assay in *Mytilus* support strong toxicity of *V. bathopelagicus* sp. nov. towards bivalves. *V. bathopelagicus* sp. nov., isolated from a remote Mediterranean bathypelagic site, is an example of a planktonic marine bacterium with genotypic and phenotypic traits associated with animal pathogenicity, that might have played an evolutionary role in the origin of coastal marine pathogens.

Introduction

Understanding the emergence of bacterial pathogens as well as the origin and evolution of their pathogenicity potential is of great importance for the comprehension of infectious diseases epidemiology affecting humans and animals. It has been long believed that the complex interactions occurring between pathogens and the infected hosts are the primary driving forces that determine the strategies used by microorganisms to counter host defence. However, new evidence suggests that the external (non-host) environment might play a greater role in the evolution of certain pathogens and their virulence traits than previously thought (Nakagawa *et al*., 2007; Vezzulli *et al*., 2008; Hasan *et al*., 2015). This holds particularly true for non-obligatory parasite that spend a substantial part of their life cycle outside hosts, but once introduced into the host cause disease with measurable frequency (Gerba, 2015).

The naturally occurring gram-negative bacteria belonging to the genus *Vibrio* comprise several species pathogenic to humans and animals and are widespread in the marine environment. They are more common in warmer coastal waters, especially above 17°C, and depending on the species, they tolerate a range of salinities (5 to 25 ppt) (Ceccherelli *et al*.,

2019). Several *Vibrio* species have been associated with diseases in marine invertebrates (Wilson *et al*., 2013), including oyster spat and/or larvae (Destoumieux-Garzón *et al*., 2020), and are associated with mortality outbreaks affecting the production of the Pacific oyster *Crassostrea gigas* worldwide (Lemire *et al*., 2015; Vezzulli *et al*., 2015; Bruto *et al*., 2017, 2018; Rubio *et al*., 2019; Oyanedel *et al*., 2020). In particular, *Vibrio* species belonging to the Splendidus clade have been repeatedly isolated from oysters suffering the 'summer mortality syndrome' and experimentally showed to cause death when injected to bivalves (Le Roux *et al*., 2007). A number of virulence factors have been reported to cause disease, including cytolisin and secreted metalloproteases, many of them shared by phylogenetically coherent virulent population (Lemire *et al*., 2015; Bruto *et al*., 2017). Interestingly, it was recently reported that virulence potential in *Vibrio* populations may derive from the acquisition of ancestral genes such as the case of the R5.7 exported conserved protein within the Splendidus clade and the MARTX toxin cluster in *Vibrio splendidus* (Bruto *et al*., 2018; Oyanedel *et al*., 2020). According to the coincidental selection hypothesis factors responsible for virulence may have resulted from adaptation to other ecological niches other than the host. Coincidental selection is well exemplified by *Vibrio cholerae* virulence factors involved in resistance to protozoan grazing in the marine environment (Van der Henst *et al* 2018). Studies on pathogenicity of environmental vibrios and other related microbial pathogens also provided evidence that some virulence factors (also named "Dual Role Virulence Factors-DRVFs") used by pathogens during human and animal infection may have primary evolved for survival in the aquatic habitat and later coincidentally adapted to host infection (Nakagawa *et al*., 2007; Vezzulli *et al*., 2008). The existence of DRVFs suggests that the ability to use the same structure(s) to interact with different substrates (e.g. in the environment and in the host) may be a common property of pathogenic bacteria having environmental reservoirs and that this may represent a discriminating feature between the harmless and the potentially pathogenic environmental bacteria. Ultimately, DRVFs may also represent good targets for developing novel prophylactic or therapeutic interventions that not only affect the success of an infection (e.g. pathogen–host interaction) but also the ecological fitness of the microbial pathogen in the external environment (Vezzulli *et al*., 2008).

Deep-Sea Mediterranean basins, dating to about five million years ago, are remote, pristine and stable environments offering a peculiar evolutionary context for microbes, well separated to conditions found in coastal marine areas (Martin-Cuadrado *et al*., 2007). Notably, deep Mediterranean water mass never gets below 13.5°C, representing a unique relatively warm deep habitat suitable for the isolation of vibrios, thus offering a great

opportunity to study the origin and evolution of environmental microbial pathogens and the identification of new DRVFs.

In this study we report the isolation, characterization and full genome sequence analysis of a novel *Vibrio* species, *Vibrio bathopelagicus* sp. nov., isolated from warm bathypelagic Mediterranean waters, which is phylogenetically closed and shows genomic virulence traits similar to those found in coastal *Vibrio* strains pathogenic to bivalves. The results of in vitro challenge assays carried out in immune cells (hemocytes) of the Mediterranean mussel *Mytilus galloprovincialis* and the Pacific oyster *Crassostrea gigas* and of the 48 h larval toxicity assay in mussels support toxicity of this species towards bivalves. *Vibrio bathopelagicus* sp. nov. provides evidence on roots of bacterial virulence that may have contributed to the emergence and evolution of coastal bacterial strains pathogenic for bivalves.

Results and Discussion

Strain identification and taxonomy

A Gram-negative, motile and bacillar shape bacteria was isolated from the Ionian station Sal10^T in the Mediterranean Sea at the depth of 3309 m (Supplementary Figure 1). The strain was sucrose negative in thiosulfate-citrate-bile salts-sucrose agar (TCBS) media, and oxidase and catalase positive. Growth in the presence of NaCl was observed in the range of 1-50 ‰ and in the presence of sea salts from 1 to 45 ‰. The isolate grew well in a wide range of pH (3-12), and growth was observed at temperatures in the range of 4-30 ºC.

Identification of the isolate was preliminary performed through the analysis of 16S rRNA gene sequences which were retrieved from the genome, resulting in a total of 15 sequences, 14 in chromosome I (C-I) and 1 in chromosome II (C-II). It is well known that the number of rRNA operons varies among bacterial genomes from 1 to 15 copies (Pei *et al*., 2010) and over 80% bacterial genomes sequenced possess more than one operon. Multiple rRNA copies would result in a selective pressure to maintain and rapidly increase high ribosome content that would enable rapid adaptation to nutritional upshift or favourable temperature change (Klappenbach *et al*., 2000; Roller *et al*., 2016), even though multiple rRNA operons are not essential. Accordingly, deep sea bacteria are known to harbour a high ratio of rRNA operon copies per genome (Lauro and Bartlett, 2008).

Phylogenetic analysis of 16S rRNA gene combined with multilocus sequence analysis (MLSA), including 5 housekeeping genes (*atp*A, *pyr*H, *rec*A, *rpo*A and *rpo*D) showed that Sal10^T strain branched with the Splendidus clade species (Figure 1). This result was

confirmed when a RAxML phylogenetic tree was constructed based on 100 housekeeping genes obtained from all the Splendidus clade species genomes present in the databases (Supplementary Figure 2). The evolutionary tree fully resolved the phylogeny, placing Sal10^T and *Vibrio lentus* in a monophyletic branch that corroborated the results of the MLSA based on 5 housekeeping genes. Species delineation was determined by Average Nucleotide Identity (OrthoANI) and *in silico* DNA-DNA hybridization (*is*DDH) between Sal10^T isolate and the closest relatives, with highest OrthoANI and *is*DDH values with *V. lentus*, 91.16% and 43.70% respectively, both of which are under the species delineation threshold values. Sal10^T strain can be differentiated from its closest relatives by several phenotypic features, such as the inability to hydrolyse arginine, to grow at 6% NaCl, acetoin production (Voges-Proskauer reaction), utilization of glucuronic acid, maltose, D-galactose and aesculin hydrolysis (Supplementary Table 1). Together, these findings confirm separate species demarcation for Sal10^T strain for which the species name *V. bathopelagicus* sp. nov. is proposed.

Description of V. bathopelagicus sp. nov. (ba.tho.pe. la'gi.cus. Gr. adj. bathos deep; L. masc. adj. pelagicus, from the sea; N.L. masc. adj. bathpelagicus, belonging to the deep sea).
Cells are Gram-stain-negative, rod-shaped and motile. Colonies were circular with irregular edges and cream coloured in MA medium after 24 h at 24ºC. The strain was sucrose negative in TCBS, oxidase and catalase positive, and susceptible to O/129 (10 µg and 150 µg per disc). Bacteria grow at 4-30 ºC and in the presence of 1-5% (w/v) NaCl and in the presence of 1-4.5% of Sea Salts (w/v). The isolate grew well from pH 3 to 12. Nitrates are reduced to nitrites. Indole is not produced and hydrolysis of esculin, gelatine and starch are observed. Decarboxylation of arginine, lysine and ornithine is not produced, urease reaction is negative, whereas citrate and gas glucose are positive. Enzymatic activity is observed for alkaline phosphatase, esterase lipase (C8), leucine arylamidase, valine arylamidase, trypsin, acid phosphatase, Naphthol-AS-BI-phosphohydrolase and N-acetyl-beta-glucosaminidase, but no activity for esterase (C4), lipase (C8), cystine arylamidase, alpha-chymotrypsin, alpha-galactosidase, beta-galactosidase, beta-glucuronidase, alpha-glucosidase, beta-glucosidase, alpha-mannosidase and alpha-fucosidase. Use as sole carbon source of citric acid, fumaric acid, glucuronic acid, malic acid, piruvic acid, succinic acid, sodium acetate, D-galactose, D-gluconate, glycerol, glycine, glucose, histamine, maltose, mannitol, ribose, sucrose, serine, tyrosine and threonine are positive, while use of alpha-ketoglutaric acid, galacturonic acid, glutamic acid, hydroxybutyric acid, propionic acid, saccharic acid, trans-aconitic acid, amygdaline, arabinose, citrulline, phenylacetate,

phenylalanine, lactose, leucine, lysine, melibiose, myo-inositol, N-acetyl glucosamine, ornithine, salicine, sarcosine and xylose are is observed.

The type strain, Sal10^T (= CECT30197^T = LMG 32069^T), was isolated from the water column of Sal10 station in the Ionian Sea at a depth of 3309m. The DNA G+C content (genome) of the type strain is 44.05 mol%. The assembled genome sequence of strain Sal10^T is deposited at DDBJ/ENA/GenBank under the accession CP062500-CP062501 and 16S rRNA consensus sequence under the accession MW195017.

Genomic features

Completion of Sal10^T genome was achieved by combining different sequencing technologies and obtaining a hybrid assembly that comprised two chromosomes (Figure 2, Supplementary Table 2). The larger chromosome (C-I) was 3,649,238 bp in length with a 44.18% GC content, while smaller chromosome (C-II) was 2,018,969 bp in length and a 43.92% GC content. Annotation of both chromosomes detected 3,255 genes (2,589 coding sequences with functional assignment) and 161 RNAs (118 tRNAs and 43 rRNAs) in C-I, whilst C-II harboured 1,797 genes (1,271 coding sequences with functional assignment) and 19 RNAs (16 tRNAs and 3 rRNAs). Gene content distribution across chromosomes displayed a similar pattern to that observed in other Vibrios, with C-I containing mainly genes associated to viability and growth and C-II including genes related to environmental adaptation. The Sal10^T genome encoded a total of 50 genomic islands (GIs) including 627 genes, 45 GIs were allocated in C-I and 5 GIs in C-II. Genes related to toxins, modification-restriction systems, antibiotic resistance, LPS modification, metabolism, and other putative proteins with unknown functions were found in the GIs. For example, a two-component regulatory system PhoP/PhoQ was present in C-I, known to regulate the expression of genes involved in virulence, adaptation to acidic and low Mg^{2+} environments and resistance to host defence antimicrobial peptides, or a leukotoxin that plays an important role in immune evasion. Genes encoding biosynthetic pathways responsible for the production of secondary metabolites were found in C-I and six different gene clusters of secondary metabolites synthesis were predicted by antiSMASH and summarized in Supplementary Table 3. The assembled completed genome sequence of strain Sal10^T is deposited at DDBJ/ENA/GenBank under the accession CP062500-CP062501 and 16S rRNA consensus sequence under the accession MW195017.

Deep-sea adaptation

The genome of Sal10^T harboured a number of genes that were previously predicted to protect bacteria under the extreme conditions of the deep-sea environment that are summarized in Table 1. (Vezzi *et al*., 2005; Goudenège *et al*., 2014; Hasan *et al*., 2015) Functions annotated in the genome included different systems of protection against O_2 reactive species, such as Cytochrome C_{551} peroxidase or KatE catalase, both detoxify H_2O_2, an alkyl hydroperoxide reductase that scavenge endogenous hydrogen peroxide and genes encoding different superoxide dismutase for tolerating high O_2 concentrations. These genes have been previously found in *Vibrio antiquarius* EX25 a deep-sea hydrothermal vent strain (Hasan *et al*., 2015). Methionine-(R)-sulfoxide reductase (MrsA and MrsB) have been shown to play an important role in response to oxidative stress by repairing methionine residues oxidation preventing protein oxidative damage (Singh *et al*., 2018).

High hydrostatic pressure (HHP) adaptation involves different metabolic systems, such as Trimethylamine-N-oxide (TMAO) reductase system that is present in Sal10^T genome (Table 1). TMAO can be produced through oxidation of TMA by a variety of marine bacteria, including *Vibrio fluvialis*, *V. cholerae*, *Photobacterium phosphoreum* or different deep-sea *Shewanella* species (Wang *et al*., 2008; Aono *et al*., 2010; Zang *et al*. 2016), and serves to protect against osmotic stress, adverse effects of low temperature, high concentration of urea or HHP but also as an electron acceptor of anaerobic respiration. It has been suggested that TMAO may provide the bacterial cell an alternative source of energy when oxygen concentration decreases and HHP induces the expression of TMAO reductase system.

Genome of Sal10^T strain also contains genes for fatty acid unsaturation synthesis, including Δ-9 fatty acid desaturase or polyketide synthase, which are essential for growth under HHP by increasing membrane fluidity (Lauro and Bartlett, 2008). Two different classes of Mg^{2+} transporters have been identified, MgeT and CorC (Table 1), responsible for the maintenance of a correct Mg^{2+} homeostasis for fundamental cell functioning. Additionally, betaine-choline-carnitine transporter genes family were detected. Many halophilic bacteria adjust their cell turgor pressure through the acquisition of different osmoprotectants from the surroundings, such as ectoine, betaine, carnitine or choline, or by the synthesis from their precursors (Oren, 2008; Zeaiter *et al*., 2019). The presence of these transporters may contribute to the accumulation of these osmoprotectants inside the bacterial cell favouring the adaptation to high hydrostatic pressure.

Sensing of environmental cues represents a key factor that favours microbe survival and allows them to move away from toxic compounds. Methyl-accepting chemotaxis proteins (MCPs) are the main chemoreceptors in bacteria involved in regulation of diverse aspects of cellular activities including biofilm formation, flagellum biosynthesis, degradation of

xenobiotic compounds, encystment and fruiting body formation, exopolysaccharide and toxins production and pathogenicity (Berleman *et al*., 2005; Hickman *et al*., 2005; Kirby, 2009; Nishiyama *et al*., 2016). The hunt for dissolved and particulate organic matter makes MCPs proteins (usually found in high number) a peculiar genomic feature characterising bacterial strains indigenous to hadal and abyssal environments (Lauro and Bartlett, 2008). Accordingly, MCPs has been detected in large number in the genome of Sal10^T strain (Figure 2).

Other quorum sensing and biofilm formation systems (*Lux* operon) and flagellar cluster present in the deep bathytype Sal10^T strain, may reflect its ability to survive and adapt under harsh environmental conditions. Response to small concentrations of nutrients may also led the bacteria into a low metabolic activity by forming persister cells promoting cell downsizing, thus reducing cell surface, mediated by different systems including autoinducer-2 (AI-2), ribosome modulation factor (*rmf*) and cell division inhibitor (*sulA)* genes (Hasan *et al*., 2015; Song *et al*., 2020). Interestingly, the photolyase gene (*phr*), involved in cyclobutene pyrimidine dimers repair in UV irradiated DNA, has been found in Sal10^T strain, as well as in several deep-sea bacterial isolates (Lauro and Bartlett, 2008). In particular, the *phr* gene was found in other deep-sea Vibrio (e.g. *V. antiquarius* and *V. diabolicus*) (Goudenège *et al*., 2014; Hasan *et al*., 2015) as well as in piezosensitive *Photobacterium profundum* strain 3TCK (Zhang *et al*., 2016). It is suggested that these strains might be in an early stage of their adaptation to the deep biosphere and the vestigial *phr* gene functioning in euphotic bacteria was not yet lost.

Virulence

In silico genome analysis revealed a wide range of features associated with bacterial virulence with a potential role in environmental adaptation. In particular, a vibriolysin metalloprotease showing 94% nucleotide sequence similarity to the metalloprotease Vsm secreted by the oyster pathogen *Vibrio tasmaniensis* LGP32 strain (Le Roux, 2007) was found in C-I of Sal10^T genome. Vsm is an essential determinant of oyster lethality in extracellular products of *V. tasmaniensis* LGP32 and *Vibrio aestuarianus* (Binesse *et al*., 2008, Labreuche *et al*., 2010). Nevertheless, the main physiological function of bacterial extracellular metalloproteases is to degrade environmental proteins and peptides for bacterial heterotrophic nutrition (Wu and Chen, 2011)

rtxACHBDE gene cluster was also annotated within the genome containing a putative RTX toxin in C-I (encoded by the gene *rtx*A) and an acyltransferase (*rtx*C), the determinant A Ca^{2+} binding protein (*rtx*H) and a putative type-I secretion system (*rtx*BDE) in C-II. So far, in

the Splendidus clade, the *rtxACHBDE* gene cluster has been only found in *V. splendidus*, although it is present in other *Vibrio* spp. such as *Vibrio vulnificus* and *V. cholerae*. In *V. vulnificus* MARTX toxin could protect bacteria from predation by amoebae, which would increase bacterial survival outside the host and would explain the fitness of this species in the marine environment (Lee *et al*. 2013). Resistance to protozoan grazing is also a common mechanism fostering coincidental selection of virulence factors in *Vibrio* species (Erken *et al* 2013; Van der Henst *et al* 2018). In *V. splendidus*, the MARTX toxin cluster has been associated with virulence in marine invertebrates, especially oysters, by possibly impairing the host innate immune response. In this study, the identified rtxA toxin (7878 bp) showed low sequence similarity, both nucleotide (72%) and aminoacidic (53.96%), with chromosomic regions of distantly related *Vibrionaceae* bacteria. MARTX toxins are a heterogeneous group of toxins, composed of conserved repeat regions, an autoprocessing protease domain and several effector domains that varies through bacterial species or even from different strains (Kim, 2018). Functional analysis and domain prediction of the protein identified two multifunctional-autoprocessing repeats-in-toxin domains, together with several tandem repeat domains, also identified as Cadherin-like domains. Besides, an actin cross-linking domain (ACD) was identified, an effector that is responsible for cytoskeleton disruption (Sheahan *et al*., 2004) (Supplementary Figure 3). More data is required to study the phylogeny of the toxin and further analysis on the protein structure would help to fully characterize this new rtxA toxin. Together with the RTX toxin, three different loci of a T1SS secreted agglutinin RTX were identified in C-I, two of which are phylogenetically related to other species of the Splendidus clade and the third one, with a total length of 20,082 nucleotides, with homology with species of the Splendidus clade (96%) but also with *V. cholerae* (80%) on their nucleotide sequence.

The ancestral virulence trait R5.7, present in all Splendidus clade virulent populations implicated in oyster mortalities (Bruto *et al*., 2018), has been found within Sal10^{T} genome (Supplementary Figure 3). This gene has been demonstrated to be necessary but not sufficient for virulence and, therefore, it has been suggested that additional virulence determinants might be involved in virulence of Splendidus populations, such as the MARTX toxin (Bruto *et al*., 2018).

Other genes potentially involved in virulence are also present, including type IV pilin (C-I), *pil*A, which encodes proteins expressed during human infection. Type VI secretion system (T6SS), which is present in Sal10^{T} C-I, has been demonstrated to be important in virulence being related to anti hemocyte activity in oyster (Rubio *et al*., 2019). A role of T6SSs in environmental fitness of *Vibrio* was also recently suggested (Salomon *et al*., 2013). In

contrast, Sal10^T does not contain a type III secretion system (T3SS), responsible for the injection of effector proteins into target host cells. Sal10^T genome also encodes different hemolysin genes, including a thermolabile hemolysin precursor in C-II with sequence similarity to that in other Splendidus clade species (*V. crassostreae*, *V. tasmaniensis*, *V. chagassi* and *V. splendidus*) and *V. alginolyticus*. C-I includes other putative genes that are predicted to encode hemolysins, along with homologs to ToxR and ToxS, a family of regulator which role in virulence has been showed in *V. cholerae*. Aquatic environments contain limited amount of nutrients and it has been proposed that hemolysins might play a role in environmental adaptation of *Vibrio* species by acquiring nutrients through damage to cells of marine organisms (Matz *et al*., 2011).

The genome also contains two prophages of 27.3 Kb in C-I (52 proteins) and 35.7 Kb in C-II (46 proteins), respectively. Prophage in C-I, identified as CTX-prophage, may be ascribed to Zot-enconding prophages by the presence of the Zona occludens toxin (*zot*), accessory cholera enterotoxin (*ace*), and other core genes such as RstA phage-related protein, RstB phage-related integrase and RstR phage-related transcriptional repressor. *Zot* and *Ace* toxin gene sequences were similar to that in *V. splendidus* with 94.55% and 92.75% nucleotide sequence similarities respectively, however its function and role in virulence remains untested. Additionally, insertion of another bacteriophage gene was noted with 85.87% identity to bacteriophage f237 of *Vibrio parahaemolyticus*. Although displaying similar genomic structure on the prophage core genes, the identified prophage exceeds the average length of such *Zot*-encoding prophages, ranging from 5 kb to 10 kb, probably due to the presence of concatamers upstream. These *Zot*-encoding prophages have been previously found in several non-cholerae strains (*V. vulnificus, Vibrio maritimus, Vibrio azureus, Vibrio splendidus, Vibrio crassostreae, Vibrio diabolicus* EX25, *Vibrio diazotrophicus* and *Vibrio halioticoli*), including deep-sea strains (Hasan *et al*. 2015; Castillo *et al*., 2018), pointing out that these elements are widespread in environmental *Vibrio* species. Conversely, prophage in C-II, identified as a *Vibrio* phage, only contained genes encoding phage core proteins, such as integrase, tail and assembly proteins, lysozyme, head and capsid proteins, scaffolding proteins and terminase, together with unknown proteins.

Overall, most of the virulence related traits here described which are present in the Sal10T genome are likely to play a role in environmental survival of the bacterium suggesting that the marine ecosystem might foster the selection of strains with pathogenic potential. Knowledge of these traits and their ecological drivers is of pivotal importance to fully understand the emergence of virulence in coastal *Vibrio* pathogens.

Antibiotic resistance

Sequence analysis using the "Comprehensive Antibiotic Resistance Database" (CARD, Alcock *et al*. 2020) identify five different drug resistance classes in the Sal10^T genome including resistance to macrolids, quinolones, tetracycline, beta-lactams and sulphonamides. Phenotypic resistance was confirmed for tetracycline while phenotypic intermediate susceptibility was observed for ciprofloxacin and ampicillin. Resistance to antibiotics of *V. bathopelagicus* sp nov. support the role of the marine environment as a reservoir of antibiotic resistance genes, encompassing resistances to both natural and synthetic antimicrobials, possibly having a natural origin (D'Costa *et al*., 2011). Interestingly, genes associated with resistance to toxic compounds such as copper homeostasis, cobalt-zinc-cadmium, arsenic and chromium were also found in Sal10^T genome.

V. bathopelagicus sp. nov. interactions with mussel and oyster hemocytes

Potential toxigenicity of *V. bathopelagicus* sp. nov. toward bivalves was investigated in model organisms by *in vitro* challenge of mussel and oyster immune cells (hemocytes). Incubation of *V. bathopelagicus* sp. nov. (10^7 CFU ml^{-1}) with mussel hemocytes induced a large decrease of lysosomal membrane stability (LMS) a marker of cellular stress (-70% with respect to controls treated with ASW only) (Figure 3A). By comparison, the bivalve pathogen *Vibrio tasmaniensis* LGP32 induced a comparable effect only at a concentration ten times higher (10^8 CFU ml^{-1}). Data on bactericidal activity show that mussel cells retained a significant and sustained ability to kill *V. bathopelagicus* over time (up to 60% of cells were killed after 60 min) (Figure 3B).

In oysters the effects of *V. bathopelagicus* sp. nov. on LMS were similar to those observed in mussel hemocytes, however, *V. tasmaniensis* LGP32 caused a stronger lysosomal destabilization (-95% with respect to controls) (Figure 3C). Oyster hemocytes showed a lower and transient bactericidal activity against *V. bathopelagicus* sp. nov. and an inability to kill *V. tasmaniensis* LGP32 (Figure 3D). The results obtained for LMS suggest that *V. bathopelagicus* sp. nov. is toxigenic for both mussel and oyster hemocytes. The effects are stronger than those of the bivalve pathogen *V. tasmaniensis* LGP32 in mussels (this work, Balbi *et al*., 2013), and comparable to that of the marine pathogen *V. coralliilyticus* (Balbi *et al*., 2018a). The effects of *V. bathopelagicus* sp. nov. on oyster hemocytes were noticeable as observed with *V. tasmaniensis* LGP32, a known pathogen responsible for oyster mortality. However, despite bacterial recognition and fast induction of cellular responses, the immune response of bivalve hemocytes depends on activation of intra and extracellular

pathways leading to both cell-mediated and humoral effectors, whose activity does not always necessarily lead to successful elimination of pathogens. In this light, mussel hemocytes, despite the initial stress conditions, showed an efficient bactericidal activity towards *V. bathopelagicus* sp. nov. over time, indicating substantial recovery. In contrast, oyster hemocytes display a low ability to overcome the stress conditions induced by *V. bathopelagicus* sp. nov., as shown by the low bactericidal activity. This suggests a higher toxigenicity for oyster compared to mussels. This is a known general trait, with oysters more susceptible to *Vibrio* pathogens and subject to mortality, and mussels rather more resistant to similar infections (Destourmieux-Garzon *et al*., 2020).

V. bathopelagicus sp. nov. effects on *M. galloprovincialis* larval development

The possible effects of *V. bathopelagicus* were also evaluated on early larval development of mussels by the standard 48 h embryotoxicity assay, and the results are reported in Figure 4. *V. bathopelagicus* induced a dramatic decrease in the percentage of normal D-larvae at concentrations as low as 10^6 CFU/mL(Figure 4A), indicating that early larval stages of mussels are highly sensitive to the toxicity of this species. A comparable effect was induced by the same concentration of *V. tasmaniensis* LGP32. When the effects of both Vibrios on larval phenotypes were evaluated (see representative images of control and exposed larvae in Figure 4, B-C), *V. bathopelagicus* induced larval death (Figure 4C), whereas exposure to *V. tasmaniensis* resulted in arrested larval development (Figure 4C), as previously observed with *V. aestuarianus* and *V. corallilyticus* (Balbi *et al*., 2019). The results suggest that distinct mechanisms may be involved in the pathogenicity towards mussel larvae of *V. bathopelagicus* sp. nov., with respect to those of other common marine vibrios.

Conclusions

Virulence is a complex phenotype that requires a susceptible host. In environmental pathogens, defined as microorganisms that usually spend a substantial part of their life cycle outside the host, virulence is believed to arise not only from selection pressures imposed by the interaction with the host, but also from the adaptation of traits that play a more fundamental role for bacterial life outside the host. In marine bacterial pathogens such as vibrios, virulence factors may have an ancestral origin and play a significant role for bacterial life in aquatic habitats.

The deep sea presents peculiar physical-chemical parameters such as high hydrostatic pressure, very low nutrient content and physical separation of water masses that likely preclude significant interaction between deep sea microbes with coastal and shallow-water

marine organisms. Accordingly, environmental adaptation rather than interaction with the bivalve host is likely a primary driver that led to the origin of virulence traits in Sal10^T deep-sea strain. Association with an animal host (e.g. free living protozoa or zooplankton organisms) in the deep-sea environment cannot be excluded and may also have played a role in coincidental selection of virulence factors responsible of the pathogenicity of this strain towards bivalve molluscs.

Overall, *V. bathopelagicus* Sal10^T strain isolated from a remote Mediterranean bathypelagic site, is an example of a planktonic marine bacterium with genotypic and phenotypic traits associated with animal pathogenicity, that might have played an evolutionary role in the origin of coastal marine pathogens.

Experimental procedures

Sample collection and Sal10^T strain isolation

Sampling was conducted at Sal10 station in the Ionian Sea from the R/V Urania during SALINE2014 (October–November 2014) cruise. Seawater samples were collected from the top of aphotic water column (200 m depth) down to the seabed (30 m above the bottom) using 12-L Niskin bottles housed on a rosette (General Oceanics, Miami, FL, USA). To measure conductivity, temperature, pressure and oxygen, a calibrated Seabird SBE9/11+CTD was employed.

All 12-L Niskin bottles were equipped with silicone rubber closure and tubing that had been carefully cleaned to avoid introducing contaminants during sampling. Water samples were collected in sterile glass bottles and filtered on 0.2 µm pore size membrane filters with a sterile syringe. The membrane was subsequently transferred in a 50 ml Falcon vial containing Alkaline Peptone Water (APW) culture medium and placed at environmental temperature for 48 h. 100 µl of the resulting solution were then plated on Thiosulfate-citrate-bile salts-sucrose (TCBS) agar plates and the microbial growth was monitored every 12 hours. Sal10^T colonies were isolated via stripping, re-cultured and subsequently transferred in glycerol (10%) and deep frozen (-80°C).

Genomic DNA isolation and whole genome sequencing

An overnight cell culture of Sal10^T strain was prepared for genomic DNA extraction and High Pure PCR Template Preparation Kit (Roche Diagnostics) was used, following manufacturer's protocol, for genomic DNA isolation. DNA concentration and quality were determined fluorimetrically with QuantiFluorTM dsDNA System using a QuantiFluorTM

fluorometer (Promega Italia srl, Milano, Italy). The genome of Sal10^T strain was sequenced combining short-read Illumina technology with long-read MinION sequencing. Illumina sequencing was performed on a MiSeq platform (2 x 250 bp). Libraries were prepared using the NexteraXT library kit following the manufactures instructions, with the following modifications, 2/5th of the recommended reagent volume was used, with 1.4 ng of input DNA. The library amplification parameters were adjusted to: 16 cycles of denaturation at 97°C for 10 s, annealing at 55 °C for 30 s and extension at 65 °C for 60 s. All other parameters were kept the same. Long reads were obtained on a MinION sequencing device (Oxford Nanopore Technologies) using one-dimensional (1D) genomic DNA sequencing kit SQK-LSK109 according to Oxford Nanopore Technologies instructions (Version: GDE_9063_v109_revC_23May2018).

Briefly, purified genomic DNA was repaired with NEBNext FFPE repair mix (New England Biolabs). A NEBNext End repair / dA-tailing Module was utilized to phosphorylate 5' ends and add dAMP to the 3' ends of the repaired DNA. Adapter Mix (Oxford Nanopore Technologies) was ligated to the DNA using NEBNext Quick T4 DNA ligase (New England Biolabs). The DNA was purified with AMPureXP beads (Beckman Coulter, Inc., Danvers, MA) following each enzymatic reaction. Purified, adapted DNA was sequenced on an MK1B (MIN-101B) MinION platform with a FLO-min 106 (SpotON) R9.4 flow cell using MinKNOW software version 1.7.14 (Oxford Nanopore Technologies). After sequencing, Fast5 files were base-called using Albacore version 2.1.7 (Oxford Nanopore) on a laptop with a 3.3 GHz Intel Core i7 processor. The genome of *V. lentus* CECT 5110^T was also sequenced in this study in order to include this species of the Splendidus clade in the phylogenomic analysis, using the paired-end chemistry in an Illumina MiSeq 2x250 platform.

Genome assembly and analysis

Bacterial genome assembly was conducted with Unicycler v0.4.7 pipeline, selecting the bold mode for assembly, by generating a hybrid sequence between short Illumina reads and long MinION reads (Wick *et al*., 2017).

Protein-encoding sequences (CDS) were annotated using the PATRIC server v3.6.3 (Wattam *et al*., 2017) and general features were searched within the genome together with genes involved in deep-sea adaptation, in order to predict the biology of Sal10^T strain in such environment. Virulence genes were searched by BLASTn analysis with default parameters using the Virulence Factors of Pathogenic Bacteria Database (VFDB) (Chen *et al*., 2012), Victors Database (University of Michigan, USA) and PATRIC_VF (Wattam *et al*., 2017). Antibiotic resistance genes (ARGs) and heavy metal resistance genes (HMRGs)

were searched using the Antibiotic Resistance Database (ARDB) (Liu and Pop, 2009) and the Comprehensive Antibiotic Resistance Database (CARD) (Jia *et al*., 2017). The five mentioned databases are included at the Specialty Genes tool available at the PATRIC server (Wattam *et al*., 2017). Search of specific virulence factors within the genome were performed manually using the Blast service. Additionally, annotation was performed using Prokka v1.13 software (Seemann, 2014) and Prodigal v2.6.3 (Hyatt *et al*., 2010).

Presence of mobile genetic elements and putative Genomic Islands were predicted on IslandViewer 4 (Bertelli *et al*., 2017) and prophage-like elements were identified by running each bacterial chromosome in PHASTER (Arndt *et al*., 2016). The detection of secondary metabolite biosynthesis gene clusters was determined using anti-SMASH 5.0 database (Blin *et al*., 2019).

Protein function and domain prediction was performed using both BLASTP 2.11.0+ (Stephen *et al*., 1997) and InterPro database (Blum *et al*., 2021).

Phylogenetics and *phenotypic characterization*

Sequence similarity of 16S rRNA was determined using the EzTaxon-e server (https://www.ezbiocloud.net) (Yoon *et al*., 2017), and the relatedness of Sal10^T strain and closely related Splendidus clade species was inferred by the analysis of the 16S rRNA gene sequence and a Multilocus Sequence Analysis (MLSA) based on five housekeeping genes (*atp*A, *pyr*H, *rec*A, *rpo*A, *rpo*D). Genes were aligned using CLUSTALW (Larkin *et al*., 2007) implemented in MEGA X software (Kumar *et al*., 2018). The same software was used for the phylogenetic analysis using both Neighbor-Joining (NJ) and Maximum Likelihood algorithm (Kumar *et al*. 2018), and the bootstrap support for individual nodes was calculated with 1,000 replicates. Additionally, a phylogenetic analysis of Sal10^T and 11 Splendidus clade species (*V. toranzoniae* CECT 7225^T, *V. splendidus* DSM 19640^T, *V. gigantis* LGP13^T, *V. celticus* CECT 7224^T, *V. crassostreae* LGP7^T, *V. atlanticus* CECT 7223^T, *V. tasmaniensis* LGP32^T, *V. coraliirubri* Corallo1^T, *V. kanaloae* CCUG 56968^T, *V. lentus* CEC 5110^T and *V. gallaecicus* DSM 23502^T) was carried out using the Maximum Likelihood estimation using RAxML (Stamatakis, 2014), with the pipeline implemented in the PATRIC server (Wattam *et al*., 2017), based on 100 housekeeping genes. Besides, genome similarity was calculated using the Average Nucleotide Identity (ANI) and the *in silico* DNA-DNA hybridization (*is*DDH) indices using OrthoANI (Lee *et al*., 2016) and Genome-to-Genome Distance Calculator implementation (Meier-Kolthoff *et al*., 2013), respectively.

The deep-sea isolate was subjected to the following phenotypic tests (MacFaddin, 2006): cell morphology and motility, Gram stain, oxidase, catalase, oxidation/fermentation test, gas

and acid production from glucose, indole, methyl red, Voges–Proskauer reaction, utilization of citrate, Thornley´s arginine dihydrolase test, Moeller´s decarboxylases for arginine, lysine and ornithine, nitrate reduction, hydrolysis of gelatine, Tween 80, amylase and aesculin. Salt tolerance test was performed on Basal medium agar (BMA, neopeptone [4 g/l], yeast extract [1 g/l], bacteriological agar [15 g/l]) supplemented with 1, 2, 3, 4, 5, 6, 7, 8, 9, 10, 12, 15 % NaCl and with 0.5 1, 2, 3, 4, 4.5, 5, 6, 7, 8, 9, 10, 12, 15 % Sea Salts. Growth at different temperatures (4, 20, 25, 30, 37 and 44 ºC) and pH (1-12) were also determined. Phenotypic characterization was complemented by using commercial miniaturized tests API 20NE and API ZYM. The following substrates were tested: ribose, arabinose, xylose, glucose, D-galactose, maltose, lactose, melibiose, salicin, amygdalin, mannitol, myo-inositol, glycerol, sodium acetate, propionic acid, citric acid, lactic acid, trans-aconitic acid, succinic acid, glycine, leucine, serine, threonine, glutamic acid, tyrosine, ornithine, citrulline, lysine , alpha-ketoglutaric acid, galacturonic acid, glucuronic acid, pyruvic acid, D-gluconate, phenylacetate, phenylalanine, histamine, sarcosine, 3-hydroxybutyric acid, N-acetyl-D-glucosamine, fumaric acid, malic acid and saccharic acid.

Antibiotic sensitivity assay

Antimicrobial susceptibility testing (AST) was performed by disk diffusion according to the European Committee on Antimicrobial Susceptibility testing (EUCAST, 2020a). Based on genomic information Sal 10 isolate was tested against a panel of 5 antimicrobial agents using antibiotic disks (Oxoid, UK) on Mueller-Hinton agar (MH) (Oxoid, UK). The following agents were included: ciprofloxacin (CIP, 5 µg), chloramphenicol (C, 30 µg), tetracycline (TE, 15 µg), trimethoprim + sulfamethoxazole (SXT 1,25-23,75 µg), ampicillin (AMP, 10 µg). E. coli ATCC 25922 was included as quality control. The isolates were classified as sensitive (S), intermediate susceptible, increased exposure (I) or resistant (R) according to EUCAST breakpoints for Enterobacterales [EUCAST, 2020b]. Breakpoints were unavailable for TET and no inhibition zone was the criterion used for classifying the isolate as resistant.

Animals, hemolymph sampling, hemocyte monolayers

Mussels (*Mytilus galloprovincialis*), 4–5 cm long, were purchased from an aquaculture farm (La Spezia, Italy) in November 2020 and acclimated for 24 h in static tanks containing aerated artificial sea water (ASW), 35 ppt salinity (1 L/mussel) at 18 °C. Oysters (*Crassostrea gigas*), 8-10 cm long, were purchased from an aquaculture farm (Bretagne, France) at the same time of the year and acclimated in the same conditions at lower salinity (23 ppt). Hemolymph was extracted from the posterior adductor muscle of 4-6 individuals

as previously described (Balbi *et al*., 2013, 2018a,b) filtered through a sterile gauze and pooled. Hemocyte monolayers from mussels and oysters were prepared on glass slides as previously described (Balbi *et al*., 2013, 2018a,b).

Bacterial cultures

V. *bathopelagicus* Sal10^T and *V. tasmaniensis* LGP32 were cultured in Zobell medium at 20°C and 23°C degree respectively, under static conditions. After overnight growth, cells were harvested by centrifugation (4500 x g, 10 min), washed three times with artificial sea water (ASW), salinity 35 ppt and resuspended to an A_{600}=1 (about 10^9 CFU/ml). Thiosulfate citrate bile salt sucrose (TCBS) agar (Scharlau Microbiology, Italy) was used for culturing both strains.

In vitro challenge of bivalve hemocytes with V. bathopelagicus sp. nov.

Hemocyte monolayers were incubated for 30 min at 18°C with suspensions of *V. bathopelagicus* Sal10^T, 10^7 CFU/mL in ASW (35 and 23 ppt salinity for mussel and oysters, respectively). Control hemocyte samples were run in parallel. Lysosomal membrane stability (LMS) was evaluated as a marker of cellular stress by the Neutral Red Retention Time (NRRT) assay as previously described (Balbi *et al*., 2013, 2018 a,b). After incubation with bacteria, the medium was removed and cells were incubated with a neutral red (NR) solution in ASW (final concentration 40 µg/mL from a stock solution of NR 40 mg/mL in DMSO); after 15 min excess dye was washed out and 20 µL of ASW were added. For oyster hemocytes, ASW at 23 ppt salinity was utilized and assay conditions were optimized (NR final concentration 20 µg/mL, incubation time 7 min). Every 15 min, slides were examined under optical microscope and the percentage of cells showing loss of dye from lysosomes in each field was evaluated. For each time point, 10 fields were randomly observed (8–10 cells each). The endpoint of the assay was defined as the time at which 50% of the cells showed sign of lysosomal leaking, i.e. the cytosol becoming red and the cells rounded. All incubations were carried out at 18 °C. For comparison, in mussel hemocytes parallel experiments were carried out with the bivalve pathogen *V. tasmaniensis* LGP32.

Bactericidal activity

Bactericidal activity of hemocyte monolayers was evaluated as previously described (Balbi *et al*., 2013, 2018a). Hemocyte monolayers were incubated with *V. bathopelagicus* Sal10^T 10^7 CFU/mL, at 18 °C. Immediately after the inoculum (T=0) and after 60 and 90 min of incubation, supernatants were collected and hemocytes were lysed by adding 0.5 ml of filter

sterilized ASW added with 0.05% Triton X-100 and by 10 s agitation. The collected supernatants and hemocyte lysates were pooled and tenfold serial diluted in ASW. Diluted samples (10 µL drop) were plated onto TCBS Agar in triplicate. After overnight incubation at 20 °C, the number of colony-forming units (CFU) per mL was determined. Percentages of killing were determined in comparison to values obtained at T=0. The number of CFU in control hemocytes never exceeded 0.1% of those enumerated in experimental samples. Same procedure was used for *V. tasmaniensis* LGP32, but diluted samples were plated onto LB agar 3% NaCl.

Mytilus early larval development assay

The 48 h larval toxicity assay was carried out in 96-microwell plates as described in Balbi *et al*. (2019). Aliquots of 20 µL of suspensions of *V. bathopelagicus* (obtained from a 10^7 CFU/mL stock suspension), suitably diluted in ASW, were added to fertilized eggs in each microwell to reach tenfold nominal final concentrations (from 10^1 to 10^6 CFU/mL) in a 200 µL volume. For comparison, similar experiments were carried out with *V. tasmaniensis* LGP32. At each dilution step, all suspensions were immediately vortexed prior to use. Microplates were gently stirred for 1 minute, and then incubated at 18 ± 1°C for 48 hours, with a 16 hours:8 hours light:dark photoperiod. All the following procedures were carried out following ASTM (2004). Samples were fixed with buffered formalin (4%) and all larvae in each well were examined by optical microscopy using an inverted Olympus IX53 microscope (Olympus, Milano, Italy) at 40X, equipped with a CCD UC30 camera and a digital image acquisition software (cellSens Entry). The acceptability of test results was based on controls for a percentage of normal D-shell stage larvae >75% (ASTM 2004).

Data analysis

Data are the mean ± SD of at least 4 independent experiments with each assay performed in triplicate. Statistical analyses were performed by Mann-Whitney U test using the GraphPad Prism 5 software.

Acknowledgements

We greatly thank Dr. Andrea Di Cesare for his precious help with antibiotic resistance assays. This work was funded by the Italian Ministry of University and Research (MUR), PRIN 2017 “Emergence of virulence and antibiotic-resistance vectors in coastal and deep-sea marine environments and analysis of the mechanisms and conditions underlying their spread and evolution”, code: 201728ZA49_002. Andrew Millard was supported by Medical

Research Council [MR/L015080/1]. A. Lasa acknowledge Xunta de Galicia for the Posdoctoral fellowship (ED481B 2017/054) of the “Axudas da movilidade A de apoio á etapa posdoutoral 2017”. The authors declare that they have no competing interests.

References

Alcock, B.P., Raphenya, A.R., Lau, T.T.Y., Tsang, K.K., Bouchard, M., Edalatmand, A., *et al*. (2020) CARD 2020: antibiotic resistome surveillance with the Comprehensive Antibiotic Resistance Database. *Nucleic Acids Res* **48**: D517-D525.

Aono, E., Baba, T., Ara, T., Nishi, T., Nakamichi, T., Inamoto, E., *et al*. (2010) Complete genome sequence and comparative analysis of *Shewanella violacea*, a psychrophilic and piezophilic bacterium from deep sea floor sediments. *Mol Biosyst* **6**: 1216–1226.

Arndt, D., Grant, J., Marcu, A., Sajed, T., Pon, A., Liang, Y. and Wishart, D.S. (2016) PHASTER: a better, faster version of the PHAST phage search tool. *Nucleic Acids Res* **44**: 16-21.

ASTM, Standard guide for conducting static acute toxicity tests starting with embryos of four species of saltwater bivalve molluscs, http://dx.doi.org/10.1520/E0724-98, 2004.

Balbi, T., Auguste, M., Cortese, K., Montagna, M., Borello, A., Pruzzo, C., *et al.* (2018a) Responses of *Mytilus galloprovincialis* to challenge with the emerging marine pathogen *Vibrio coralliilyticus*. *Fish Shellfish Immunol* **84**: 352–360.

Balbi, T., Cortese, K., Ciacci, C., Bellese, G., Vezzulli, L., Pruzzo, C., *et al.* (2018b) Autophagic processes in *Mytilus galloprovincialis* hemocytes: effects of *Vibrio tapetis*. *Fish Shellfish Immunol* **73**: 66–74.

Balbi, T., Fabbri, R., Cortese, K., Smerilli, A., Ciacci, C., Grande, C., *et al.* (2013) Interactions between *Mytilus galloprovincialis* hemocytes and the bivalve pathogens *Vibrio aestuarianus* 01/032 and *Vibrio splendidus* LGP32. *Fish Shellfish Immunol* **35**: 1906–1915.

Balbi, T., Auguste, M., Cortese, K., Montagna, M., Borello, A., Pruzzo, C., *et al.* (2019) Responses of *Mytilus galloprovincialis* to challenge with the emerging marine pathogen *Vibrio coralliilyticus*. *Fish Shellfish Immunol* **84**: 352-360.

Berleman, J.E., and Bauer, C.E. (2005) Involvement of a Che-like signal transduction cascade in regulating cyst cell development in *Rhodospirillum centenum*. *Mol Microbiol* **56**:1457–1466.

Bertelli, C., Laird, M.R., Williams, K.P., Simon Fraser University Research Computing Group, Lau, B.Y., Hoad, G., *et al*. (2017) IslandViewer 4: Expanded prediction of genomic islands for larger-scale datasets. *Nucleic Acids Res* **45**: 30-35.

664 Binesse, J., Delsert, C., Saulnier, D., Champomier-Vergès, M.C., Zagorec, M., Munier-
665 Lehmann, H., *et al*. (2008) Metalloprotease *vsm* is the major determinant of toxicity for
666 extracellular products of *Vibrio splendidus*. *Appl Environ Microbiol* **74**: 7108–7117.
667 Blin, K., Shaw, S., Steinke, K., Villebro, R., Ziemert, N., Lee, S.Y., *et al*. (2019) antiSMASH 5.0:
668 updates to the secondary metabolite genome mining pipeline. *Nucleic Acids Res* **47**(W1):
669 W81-W87.
670 Blum, M., Chang, H.Y., Chuguransky, S., Grego, T., Kandasaamy, S., Mitchell, A., *et al*. (2021)
671 The InterPro protein families and domains database: 20 years on. *Nucleic Acids Res* **49**(D1):
672 D344-D354.
673 Bruto, M., James, A., Petton, B., Labreuche, Y, Chenivesse, S, Alunno-Bruscia, M., *et al.*
674 (2017) *Vibrio crassostreae*, a benign oyster colonizer turned into a pathogen after plasmid
675 acquisition. *ISME Journal* **11**(4): 1043–1052.
676 Bruto, M., Labreuche, Y., James, A., Piel, D,. Chenivesse, S., Petton, B., *et al.* (2018) Ancestral
677 gene acquisition as the key to virulence potential in environmental *Vibrio* populations. *ISME*
678 *J* **12**: 2954–2966.
679 Castillo, D., Kauffman, K., Hussain, F., Kalatzis, P., Rørb, N., Polz, M., *et al.* (2018) Widespread
680 distribution of prophage-encoded virulence factors in marine *Vibrio* communities. *Sci Rep* **8**:
681 9973.
682 Ceccarelli, D., Amaro, C., Romalde, J.L., Suffredini, E., and Vezzulli, L. (2019) *Vibrio* species.
683 Food Microbiology: Fundamentals and Frontiers, 5th Ed. Editors: M. P. Doyle, F. Diez-
684 Gonzalez, and C. Hill ©2019 ASM Press, Washington, DC
685 doi:10.1128/9781555819972.ch13
686 Chen, L., Xiong, Z., Sun, L., Yang, J., and Jin, Q. (2012) VFDB 2012 update: Toward the
687 genetic diversity and molecular evolution of bacterial virulence factors. *Nucleic Acids Res*
688 **40**: D641–D645.
689 D'Costa, V.M., King, C.E., Kalan, L., Morar, M., Sung, W.W.L., Schwarz, C., *et al*. (2011)
690 Antibiotic resistance is ancient. *Nature* **477**: 457–46.
691 Destoumieux-Garzón, D., Canesi, L., Oyanedel, D., Travers, M.A., Charrière, G.M., Pruzzo, C.
692 *et al*. (2020) Vibrio–bivalve interactions in health and disease. *Environ Microbiol* **22**(10):
693 4323–4341.
694 Erken, M., Lutz, C., and McDougald, D. (2013) The Rise of Pathogens: Predation as a Factor
695 Driving the Evolution of Human Pathogens in the Environment. *Microb Ecol* **65**(4): 860–868.
696 EUCAST (2020a). Antimicrobial Susceptibility Testing-EUCAST Disk Diffusion Method.
697 Available online: https://www.eucast.org (accessed on 9 January 2020).

EUCAST (2020b). Breakpoint Tables for Interpretation of MICs and Zone Diameters. Available online: https://www.eucast.org/(accessed on 10 July 2020).

Gerba, C. (2015) Environmentally Transmitted Pathogens in I.L. Pepper, C.P. Gerba, T.J. Gentry: Environmental Microbiology, Third edition. DOI: http://dx.doi.org/10.1016/B978-0-12-394626-3.00022-3 © 2015 Elsevier Inc.

Goudenège, D., Boursicot, V., Versigny, T., Bonnetot, S., Ratiskol, J., Sinquin, C, *et al*. (2014) Genome sequence of *Vibrio diabolicus* and identification of the exopolysaccharide HE800 biosynthesis locus. *Appl Microbiol Biotechnol* **98**(24): 10165-10176.

Hasan, N.A., Grim, C.J., Lipp, E.K., Rivera, I.N., Chun, J., Haley, B.J., *et al*. (2015) Deep-sea hydrothermal vent bacteria related to human pathogenic *Vibrio* species. *Proc Natl Acad Sci USA* **112**(21): E2813-9.

Hickman, J.W., Tifrea, D.F. and Harwood, C.S. (2005) A chemosensory system that regulates biofilm formation through modulation of cyclic diguanylate levels. *Proc Nat Acad Sci USA* **102**: 14422–14427.

Hyatt, D., Chen, G.L., Locascio, P.F., Land, M.L., Larimer, F.W. and Hauser, L.J. (2010) Prodigal: prokaryotic gene recognition and translation initiation site identification. *BMC Bioinformatics* **11**:119.

Jia, B., Raphenya, A.R., Alcock, B., Waglechner, N., Guo, P., Tsang, K.K., *et al.* (2017) "CARD 2017: expansion and model-centric curation of the comprehensive antibiotic resistance database". *Nucleic Acids Res* **45**: D566–D573.

Kim, B.S. (2018) The Modes of Action of MARTX Toxin Effector Domains. *Toxins* (Basel). **10**(12): 507.

Kirby, J.R. (2009) Chemotaxis-like regulatory systems: unique roles in diverse bacteria. *Annu Rev Microbiol* **63**:45–59.

Klappenbach, J.A., Dunbar, J.M., and Schmidt, T.M. (2000) rRNA operon copy number reflects ecological strategies of bacteria. *Appl Environ Microbiol* **66**: 1328–1333.

Kumar, S., Stecher, G., Li, M., Knyaz, C. and Tamura, K. (2018) MEGA X: Molecular Evolutionary Genetics Analysis across computing platforms. *Mol Biol Evol* **35**: 1547-1549.

Labreuche, Y., Le Roux, F., Henry, J., Zatylny, C., Huvet, A., Lambert, C., *et al*. (2010) *Vibrio aestuarianus* zinc metalloprotease causes lethality in the Pacific oyster *Crassostrea gigas* and impairs the host cellular immune defenses. *Fish Shellfish Immunol* **29**(5): 753-758.

Larkin, M.A., Blackshields, G., Brown, N.P., Chenna, R., McGettigan, P.A., McWilliam, H., *et al*. (2007). ClustalWand Clustal X version 2.0. *Bioinformatics* **23**: 2947–2948.

Lauro, F.M. and Bartlett, D.H. (2008) Prokaryotic lifestyles in deep sea habitats. *Extremophiles* **12**(1): 15-25.

733 Lee, C.T., Pajuelo, D., Llorens, A., Chen, Y.H., Leiro, J.M., Padrós, F. *et al* (2013) MARTX of
734 Vibrio vulnificus biotype 2 is a virulence and survival factor. *Environ Microbiol* **15**(2): 419-
735 432.
736 Lee, I., Ouk Kim, Y., Park, S.C., and Chun, J. (2016). OrthoANI: an improved algorithm and
737 software for calculating average nucleotide identity. *Int J Syst Evol Microbiol* **66**: 1100–1103.
738 Lemire, A., Goudenege, D., Versigny, T., Petton, B., Calteau, A., Labreuche, Y., *et al.* (2015)
739 Populations, not clones, are the unit of vibrio pathogenesis in naturally infected oysters.
740 *ISME J* **9**: 1523–1531.
741 Le Roux, F., Binesse, J., Saulnier, D., and Mazel, D. (2007) Construction of a *Vibrio splendidus*
742 mutant lacking the metalloprotease gene *vsm* by use of a novel counterselectable suicide
743 vector. *Appl Environ Microbiol* **73**(3): 777–784.
744 Liu, B., and Pop, M. (2009) ARDB--antibiotic resistance genes database. *Nucleic Acids Res*
745 **37**: D443–447.
746 Mac Faddin, J.F. (2006) Pruebas bioquímicas para la identificación de bacterias de
747 importancia clínica. t.1. 3ed. La Habana: Editorial Ciencias Médicas.
748 Martın-Cuadrado, A.B., Lopez-Garcıa, P., Alba, J.C., Moreira, D., Monticelli, L., Strittmatter, A.,
749 *et al*. (2007). Metagenomics of the Deep Mediterranean, a Warm Bathypelagic Habitat.
750 *PLoS ONE* **9**: e914.
751 Matz, C., Nouri, B., McCarter, L., and Martinez-Urtaza, J. (2011). Acquired type III secretion
752 system determines environmental fitness of epidemic *Vibrio parahaemolyticus* in the
753 interaction with bacterivorous protists. *PLoS ONE* **6**: e20275.
754 Meier-Kolthoff, J.P., Auch, A.F., Klenk, H.P., and Göker, M. (2013) Genome sequence-based
755 species delimitation with confidence intervals and improved distance functions. *BMC*
756 *Bioinformatics* **14**: 60.
757 Nakagawa, S., Takaki, Y., Shimamura, S., Reysenbach, A.L., Takai, K., and Horikoshi, K.
758 (2007) Deep-sea vent epsilon-proteobacterial genomes provide insights into emergence of
759 pathogens. *Proc Natl Acad Sci USA* **104**: 12146-12150.
760 Nishiyama S., Takahashi Y., Yamamoto K., Suzuki D., Itoh Y., Sumita K., *et al*. (2016)
761 Identification of a *Vibrio cholerae* chemoreceptor that senses taurine and amino acids as
762 attractants. *Sci Rep* **6**: 20866.
763 Oren, A. (2008) Microbial life at high salt concentrations: phylogenetic and metabolic diversity.
764 *Saline Syst* **15**: 2.
765 Oyanedel, D., Labreuche, Y., Bruto, M., Amraoui, H., Robino, E., Haffner, P., *et al.* (2020).
766 *Vibrio splendidus* O-antigen structure: a trade-off between virulence to oysters and
767 resistance to grazers. *Environ Microbiol* **22**(10): 4264–4278.

768 Pei, A.Y., Oberdorf, W.E., Nossa, C.W., Agarwal, A., Chokshi, P., Gerz, E.A., *et al*. (2010).
769 Diversity of 16S rRNA genes within individual prokaryotic genomes. *Appl Environ Microbiol*
770 **76**: 3886–3897.
771 Roller, B.R.K., Stoddard, S.F. and Schmidt, T.M. (2016) Exploiting rRNA operon copy number
772 to investigate bacterial reproductive strategies. *Nat Microbiol* **1**: 16160.
773 Rubio, T., Oyanedel, D., Labreuche, Y., Toulza, E, Luo, X, and Bruto, M. (2019) Species-
774 specific mechanisms of cytotoxicity toward immune cells determine the successful outcome
775 of Vibrio infections. *P Natl Acad Sci USA* **116**(28): 14238–14247.
776 Seemann, T. (2014). Prokka: rapid prokaryotic genome annotation. *Bioinformatics* **30**: 2068–
777 2069.
778 Sheahan, K.L., Cordero, C.L. and Satchell, K.J. (2004) Identification of a domain within the
779 multifunctional *Vibrio cholerae* RTX toxin that covalently cross-links actin. *Proc Natl Acad*
780 *Sci USA* **101**: 9798–9803.
781 Singh, V.K., Singh, K., and Baum, K. (2018) The Role of Methionine Sulfoxide Reductases in
782 Oxidative Stress Tolerance and Virulence of *Staphylococcus aureus* and Other Bacteria.
783 *Antioxidants* **7**(10): 128.
784 Salomon, D., Gonzalez, H., Updegraff, B. L., and Orth, K. (2013). *Vibrio parahaemolyticus* type
785 VI secretion system 1 is activated in marine conditions to target bacteria, and is differentially
786 regulated from system 2. *PLoS ONE* **8**: 61086.
787 Song, S., and Wood, T.K. (2020) ppGpp ribosome dimerization model for bacterial persister
788 formation and resuscitation. *Biochem Biophys Res Commun* **523**(2): 281-286.
789 Stamatakis, A. (2014) RAxML version 8: a tool for phylogenetic analysis and post-analysis of
790 large phylogenies. *Bioinformatics* **30**: 1312–1313.
791 Stephen, F., Altschul, S.F., Madden, T.L., Schäffer, A.A., Zhang, J., Zhang, Z. *et al* (1997)
792 Gapped BLAST and PSI-BLAST: a new generation of protein database search programs.
793 *Nucleic Acids Res* **25**(17): 3389-3402.
794 Van der Henst, C., Vanhove, A.S., Drebes Dörr, N.C., Stutzmann, S., Stoudmann, C., Clerc,
795 S., *et al.* (2018). Molecular insights into *Vibrio cholerae*'s intra-amoebal host-pathogen
796 interactions. *Nat Commun* **9**: 3460.
797 Vezzi, A., Campanaro, S., D'Angelo, M., Simonato, F., Vitulo, N., Lauro, F.M., *et al*. (2005) Life
798 at depth: *Photobacterium profundum* genome sequence and expression analysis. *Science*
799 **307**(5714): 1459-1461.
800 Vezzulli, L., Guzmán, C.A., Colwell, R.R., and Pruzzo, C. (2008) Dual role colonization factors
801 connecting Vibrio cholerae's lifestyles in human and aquatic environments open new
802 perspectives for combating infectious diseases. *Curr Opin Biotech* **19**: 254–259.

803 Vezzulli, L., Pezzati, E., Brettar, I., Höfle, M. and Pruzzo, C. (2015) Effects of Global Warming
804 on *Vibrio* Ecology. *Microbiol Spectr* **3**(3): VE-0004-2014.
805 Wang, F.P., Wang, J.B., Jian, H.H., Zhang, B., Li, S.K., Wang, F., *et al*. (2008) Environmental
806 adaptation: genomic analysis of the piezotolerant and psychrotolerant deep-sea iron
807 reducing bacterium *Shewanella piezotolerans* WP3. *PLoS ONE* **3**: e1937.
808 Wattam, A.R., Davis, J.J., Assaf, R., Boisvert, S., Brettin, T., Bun, C., *et al*. (2017)
809 Improvements to PATRIC, the all-bacterial Bioinformatics Database and Analysis Resource
810 Center. *Nucleic Acids Res* **45**: D535-D542.
811 Wick, R.R., Judd, L.M., Gorrie, C.L. and Holt, K.E. (2017) Unicycler: resolving bacterial genome
812 assemblies from short and long sequencing reads. *PLoS Comput Biol* **13**(6): e1005595.
813 Wilson, B., Muirhead, A., Bazanella, M., Huete-Stauffer, C., Vezzulli, L., and Bourne, D.G.
814 (2013) An improved detection and quantification method for the coral pathogen *Vibrio*
815 *coralliilyticus*. *PLoS ONE* **8**(12): e81800.
816 Wu, J.W., and Chen, X.L. (2011) Extracellular metalloproteases from bacteria. *Appl Microbiol*
817 *Biotechnol* **92**(2): 253-262.
818 Yoon, S.H., Ha, S.M., Kwon, S., Lim, J., Kim, Y., Seo, H. *et al.* (2017) Introducing EzBioCloud:
819 A taxonomically united database of 16S rRNA and whole genome assemblies. *Int J Syst*
820 *Evol Microbiol* **67**:1613-1617.
821 Zeaiter, Z., Marasco, R., Booth, J.M., Prosdocimi, E.M., Mapelli, F., Callegari, M., *et al*. (2019)
822 Phenomics and Genomics Reveal Adaptation of *Virgibacillus dokdonensis* Strain 21D to Its
823 Origin of Isolation, the Seawater-Brine Interface of the Mediterranean Sea Deep Hypersaline
824 Anoxic Basin Discovery. *Front Microbiol* **10**:1304.
825 Zhang, S.D., Santini, C.L., Zhang, W.J., Barbe, V., Mangenot, S., Guyomar, C., *et al*. (2016).
826 Genomic and physiological analysis reveals versatile metabolic capacity of deep-sea
827 *Photobacterium phosphoreum* ANT-2200. *Extremophiles* **20**: 301–310.
828
829
830
831
832

Table 1. Predicted deep-sea adaptation characteristics of Sal10T genome

Predicted biology	Chromosome (ocurrence)	Function
Response to environment		
Cytochrome c551 peroxidase	C-I, C-II (2)	Protection against O_2 and H_2O_2
Catalase KatE	C-II (2)	
Superoxide dismutase (Fe), (Mn), (Cu-Zn)	C-I (2), C-II	
Alkyl hydroperoxide reductase	C-I	Scavenge endogenous hydrogen peroxide
Methionine-(R)-sulfoxide reductase (MrsA, MrsB, free reductase)	C-I (2), C-II	Oxidative damage repair
Trimethylamine-N-oxide reductase system torA,C,D,E,R	C-I	TMAO respiration involved in High Hydrostatic Pressure adaptation
Trimethylamine-N-oxide reductase system S,T	C-II	
Δ-9 fatty acid desaturase	C-II	Fatty acid unsaturation, essential for growth under high pressure
Other fatty acid desaturases	C-I (2), C-II	
Polyketide synthase	C-I (2)	Synthesis of polyunsaturated fatty acids
Zinc carboxypeptidase	C-I	Functioning in high concentrations of HM
Magnessium transporters (MgeT, CorC)	C-I	Growth at high $MgCl_2$ concentrations
Betaine-choline-carnitine transporter (BCCT) family	C-I, C-II (2)	Acquisition of different osmoprotectants
Cell sensing system		
Lux S	C-I	Autoinducer-2 (AI-2) mediated QS, biofilm formation, virulence, other metabolic functions
Lux P,Q,N	C-II	
Methyl-accepting chemotaxis proteins (MCPs)	C-I, C-II	Signal transducing proteins, respond to gradients of chemicals in the environment. Maximize productivity and growth in low nutrients environments
Biofilm-related pathways		
Arginine decarboxylase	C-I	Polyamine biosynthesis
c-di-GMP phosphodiesterase mbaA	C-I, C-II	Norspermidine
Syp gene cluster	C-I	Gene clusters mediating biofilm formation
Flagellar cluster	C-I	
Others		
rmf and sulA	C-I	Persister cells
Multicopper oxidase	C-I	Mn(II) oxidation
Universal stress protein family	C-I	

Figure captions

Figure 1. Maximum-Likelihood (GTR+G+I parameters) phylogenetic tree based on concatenated sequences of *atpA*, *pyrH*, *recA*, *rpoA* and *rpoD* genes. Only bootstrap values (1000 replications) above 50 % are shown. *Vibrio cholerae* CECT 514^T=ATCC 14035^T was used as an outgroup. Black circles: *Vibrio* species found in association with oysters; white circles: *Vibrio* species found in association with other marine bivalves (Lemire *et al*., 2015; Destoumieux-Garzón *et al*., 2020).

Figure 2 Full genome map of Sal10^T indicating the adaptation features (orange color), putative virulence factors and prophage (blue color) position on each chromosome.

Figure 3. *In vitro* effects of *V. bathopelagicus sp. nov.* on hemocyte lysosomal membrane stability (LMS) and bactericidal activity in the *M. galloprovincialis* (upper panel) and *C. gigas* (lower panel).
Upper panel: A) LMS: mussel hemocytes were treated with *V. bathopelagicus* (V.b.) 10^7 CFU/mL. For comparison, data obtained with *V. tasmaniensis* LGP32 (V.t) at 10^7 and 10^8 CFU/ml are reported; Controls hemocytes (C) were treated with Artificial Sea Water (ASW). B) Bactericidal activity: hemocytes were incubated for different periods of time (60–90 min) with *V. bathopelagicus sp. nov.* at the same concentration utilized in the LMS assay, and the number of viable, cultivable bacteria (CFU) per monolayer was evaluated. Percentages of killing were determined in comparison to values obtained at zero time.
Lower panel: oyster hemocytes treated with *V. bathopelagicus* (V.b.) 10^7 CFU/mL. C) LMS; D) bactericidal activity. Data obtained with *V. tasmaniensis* LGP32 (V.t) at 10^7 CFU/ml are also reported. * = $p < 0.05$, Mann-Whitney U test.

Figure 4. Effects of *V. bathopelagicus sp. nov*. (V.b.) and *V. tasmaniensis* LGP32 (V.t) (10^6 CFU/mL) on *M. galloprovincialis* larval development in the 48 h embryotoxicity assay.
A) Percentage of normal D-shaped larvae at 48 hpf. Data represent the mean ± SD of 4 experiments carried out in 96-multiwell plates (6 replicate wells for each sample). * = $p < 0.01$, Mann-Whitney U test.
B-D) Representative images of control (B) and vibrio-exposed larvae (C,D). Scale bars = 100 µm. B) normal D-veligers, characterized by regular shells with straight hinge; C) *V. bathopelagicus* induced larval death, as shown by open shells and release of soft tissues.

C) *V. tasmaniensis* resulted in arrested development, as shown by the presence of larvae witheld at the trocophora stage.

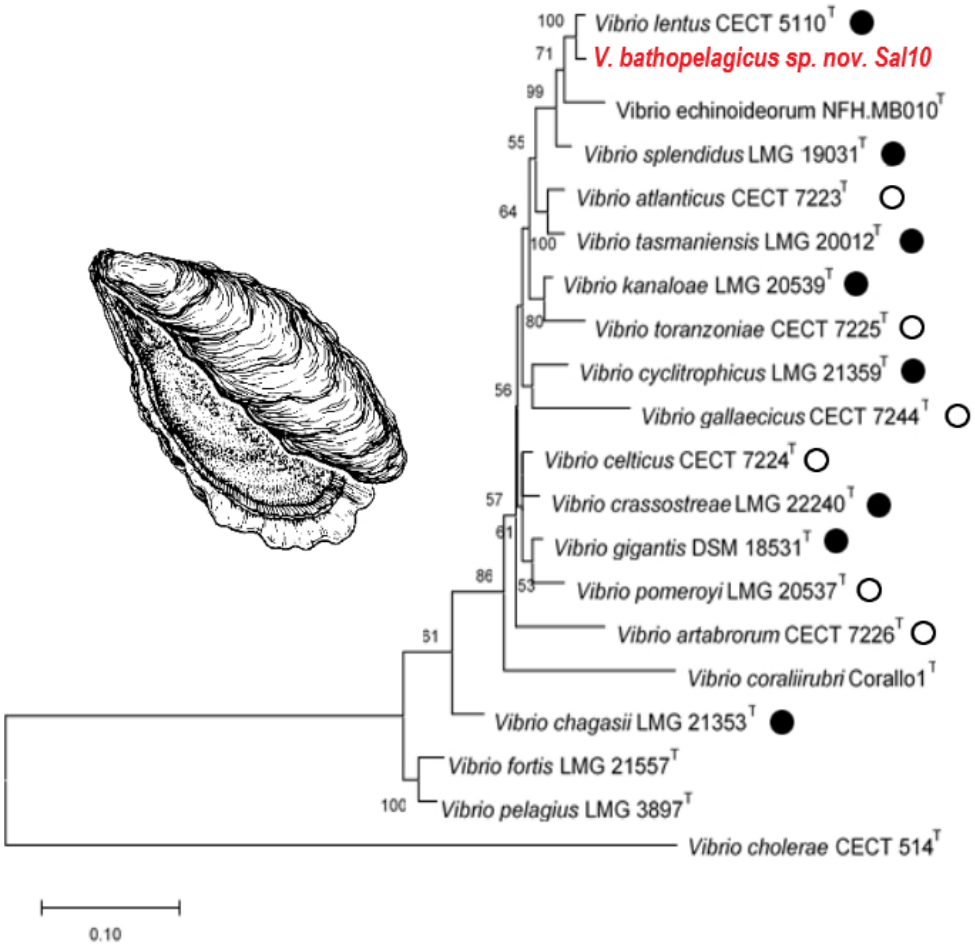

Figure 1. Maximum-Likelihood (GTR+G+I parameters) phylogenetic tree based on concatenated sequences of atpA, pyrH, recA, rpoA and rpoD genes. Only bootstrap values (1000 replications) above 50 % are shown. Vibrio cholerae CECT 514T=ATCC 14035T was used as an outgroup. Black circles: Vibrio species found in association with oysters; white circles: Vibrio species found in association with other marine bivalves (Lemire et al., 2015; Destoumieux-Garzón et al., 2020).

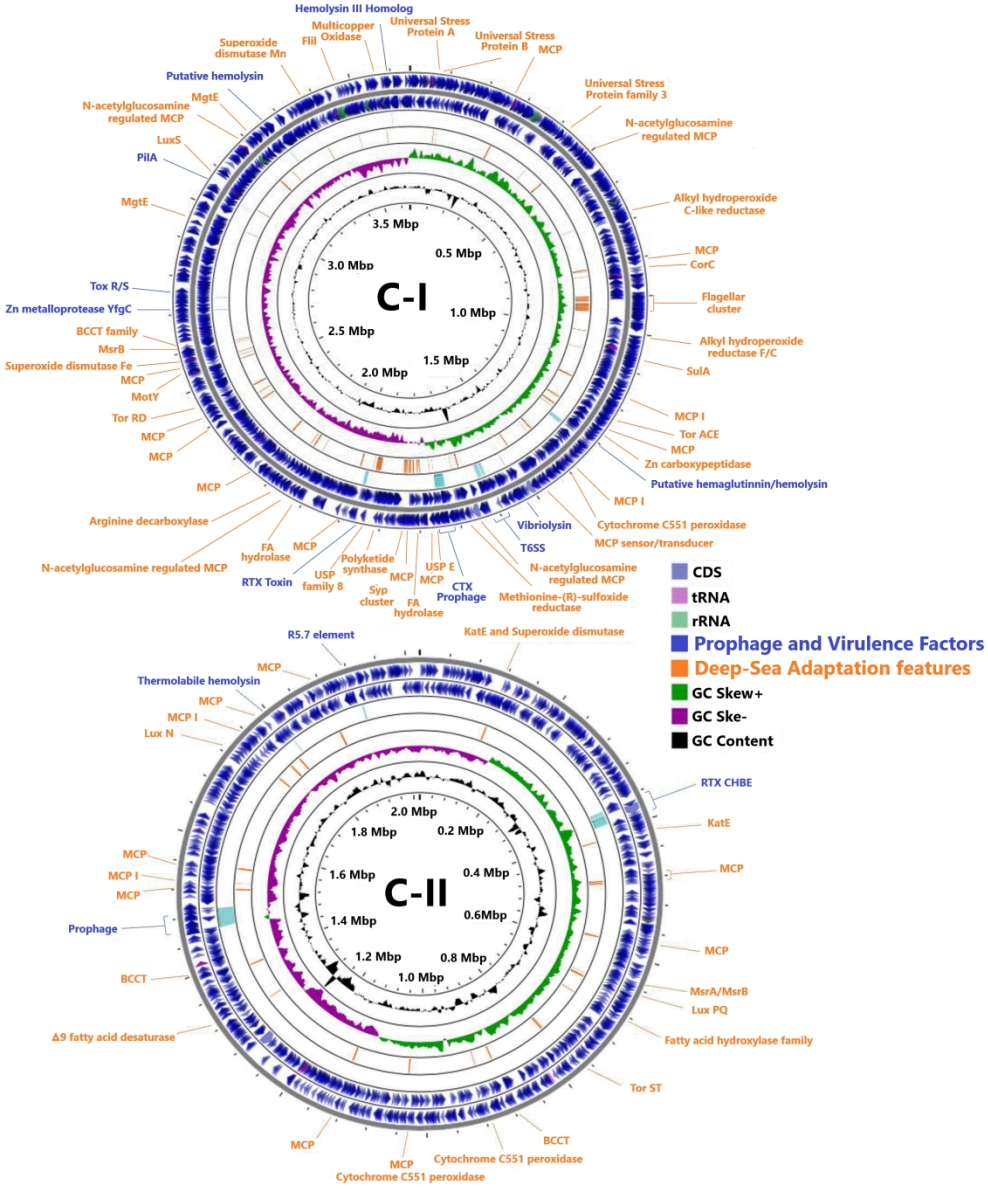

Figure 2 Full genome map of Sal10T indicating the adaptation features (orange color), putative virulence factors and prophage (blue color) position on each chromosome.

866x1040mm (72 x 72 DPI)

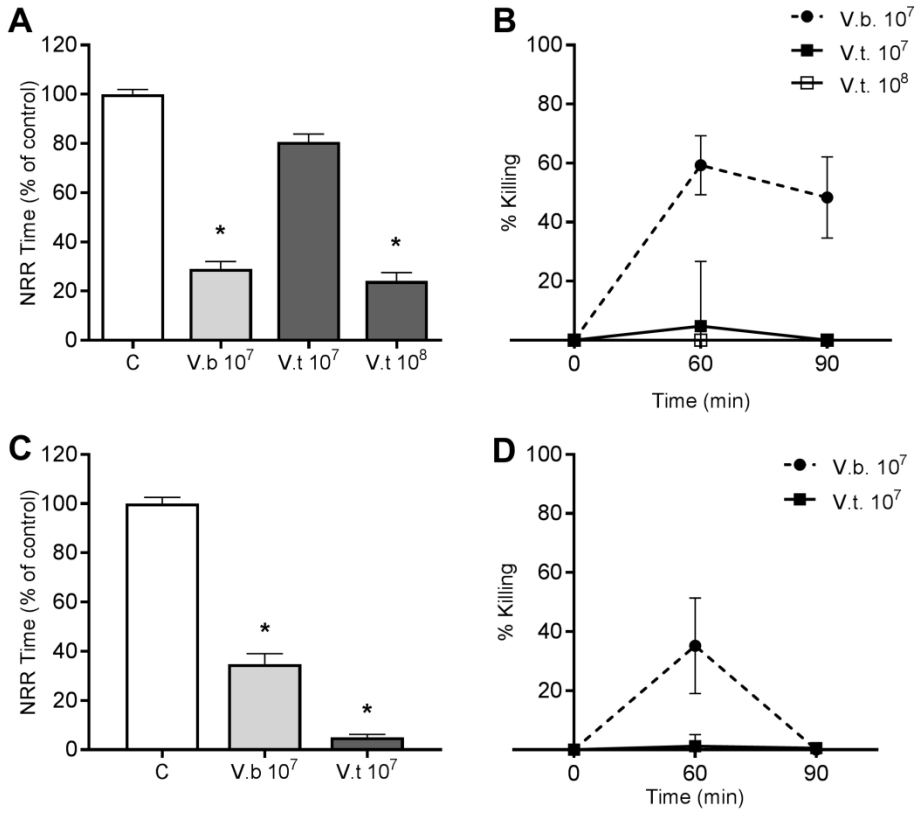

Figure 3. In vitro effects of V. bathopelagicus sp. nov. on hemocyte lysosomal membrane stability (LMS) and bactericidal activity in the M. galloprovincialis (upper panel) and C. gigas (lower panel).
Upper panel: A) LMS: mussel hemocytes were treated with V. bathopelagicus (V.b.) 107 CFU/mL. For comparison, data obtained with V. tasmaniensis LGP32 (V.t) at 107 and 108 CFU/ml are reported; Controls hemocytes (C) were treated with Artificial Sea Water (ASW). B) Bactericidal activity: hemocytes were incubated for different periods of time (60–90 min) with V. bathopelagicus sp. nov. at the same concentration utilized in the LMS assay, and the number of viable, cultivable bacteria (CFU) per monolayer was evaluated. Percentages of killing were determined in comparison to values obtained at zero time.
Lower panel: oyster hemocytes treated with V. bathopelagicus (V.b.) 107 CFU/mL. C) LMS; D) bactericidal activity. Data obtained with V. tasmaniensis LGP32 (V.t) at 107 CFU/ml are also reported. * = $p < 0.05$, Mann-Whitney U test.

206x181mm (300 x 300 DPI)

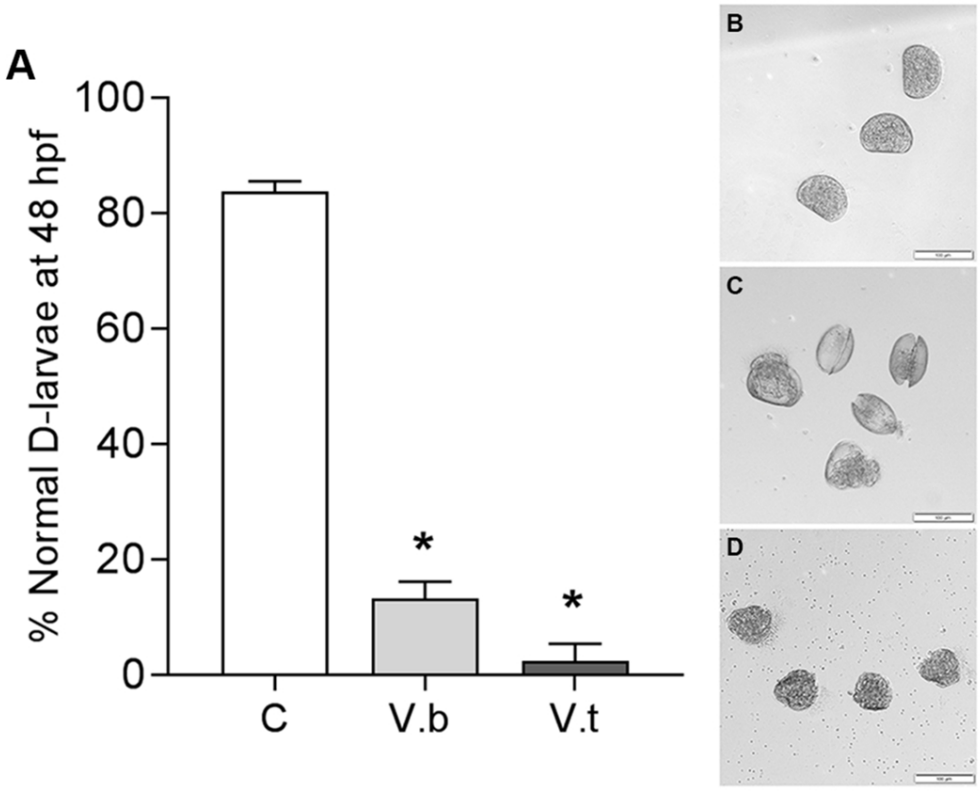

Figure 4. Effects of V. bathopelagicus sp. nov. (V.b.) and V. tasmaniensis LGP32 (V.t) (106 CFU/mL) on M. galloprovincialis larval development in the 48 h embryotoxicity assay.
A) Percentage of normal D-shaped larvae at 48 hpf. Data represent the mean ± SD of 4 experiments carried out in 96-multiwell plates (6 replicate wells for each sample). * = $p < 0.01$, Mann-Whitney U test. B-D) Representative images of control (B) and vibrio-exposed larvae (C,D). Scale bars = 100 µm. B) normal D-veligers, characterized by regular shells with straight hinge; C) V. bathopelagicus induced larval death, as shown by open shells and release of soft tissues. C) V. tasmaniensis resulted in arrested development, as shown by the presence of larvae witheld at the trocophora stage.

ISME

www.nature.com/ismecomms

BRIEF COMMUNICATION OPEN

Check for updates

Aquatic reservoir of *Vibrio cholerae* in an African Great Lake assessed by large scale plankton sampling and ultrasensitive molecular methods

Luigi Vezzulli[1✉], Caterina Oliveri[1], Alessio Borello[1], Lance Gregory[2], Ismael Kimirei[3], Martina Brunetta[2], Rowena Stern[2], Simona Coco[4], Luca Longo[4], Elisa Taviani[1], Andrès Santos[5], Jaime Martinez-Urtaza[6], William H. Wilson[2], Rita R. Colwell[7,8], Carla Pruzzo[1] and Pierre-Denis Plisnier[9]

The significance of large tropical lakes as environmental reservoirs of *Vibrio cholerae* in cholera endemic countries has yet to be established. By combining large scale plankton sampling, microbial culture and ultrasensitive molecular methods, namely Droplet Digital PCR (ddPCR) and targeted genomics, the presence of *Vibrio cholerae* was investigated in a 96,600 L volume of surface water collected on a 322 nautical mile (596 km) transect in Lake Tanganyika. *V. cholerae* was detected and identified in a large area of the lake. In contrast, toxigenic strains of V. cholerae O1 or O139 were not detected in plankton samples possibly in relation to environmental conditions of the lake ecosystem, namely very low salinity compared to marine brackish and coastal environments. This represents to our knowledge, the largest environmental study to determine the role of tropical lakes as a reservoir of *V. cholerae*.

ISME Communications (2021)1:20 ; https://doi.org/10.1038/s43705-021-00023-1

Cholera is an acute life-threatening diarrheal disease caused by *Vibrio cholerae* serogroups O1 and O139[1]. Today, Africa is most affected by the disease, with over 41% of worldwide cholera cases and deaths reported from this continent[2]. In particular, the African Great Lake (AGL) region has suffered endemic cholera since the late 1970s, with outbreaks occurring regularly in specific districts bordering the lakes and rivers of the region[3].

Cholera epidemiology of the AGL has been linked to introduction of toxigenic *V. cholerae* by fecal contamination of water or concurrently from environmental reservoirs of the bacteria in lake water and rivers[4,5]. The latter hypothesis, the cholera paradigm, gained attention following pioneering studies in the Bay of Bengal where the presence of *V. cholerae* in that coastal and brackish aquatic environment was linked to the incidence of cholera in neighboring villages. A strong association of the bacterium with zooplankton, namely copepods, was observed as had been demonstrated earlier in the Chesapeake Bay of the United States[6]. *V. cholerae* has been shown to require Na+ to maintain structural integrity and growth[7,8]. Nevertheless, the incidence and distribution of *V. cholerae* in tropical lake ecosystems has not been studied despite the fact that they constitute a major "hotspot" of cholera infections globally[3]. In addition, studies to date that investigated large aquatic systems as potential reservoirs of *V. cholerae* were limited in geographic extension or involved analysis of small volumes of water collected at individual point sites, hence not capturing the ecological factors associated with the disease[3]. Remarkably since these tropical areas are located in remote regions of low-income countries, accessibility to sampling sites and deployment of technologies needed to detect the presence of pathogenic bacteria in their natural reservoirs are challenging.

In this study, large scale sampling was accomplished in Lake Tanganyika and both standard bacteriological and ultrasensitive molecular methods were used to test the samples for *V. cholerae*. In total a path of 322 nautical miles (596 km) was sampled at the beginning of the short rainy season (cholera season), and 96,600 L of lake water were analysed (Fig. 1a). Sampling was conducted with the Continuous Plankton Recorder (CPR), a high-speed plankton sampler designed to be towed from ships of opportunity over long distances[9,10] (Figs. S1 and S2). Each CPR sample represents ten nautical miles of tow (ca. 3 m^3 of filtered water) and was previously shown to capture a substantial fraction of the plankton associated *Vibrio* community[10].

From October 22 to 26th 2018, six CPR tows were conducted across Lake Tanganyika (Fig. 1a–c). A total of eighteen non-formalin fixed CPR samples were collected along routes 4ALT, 5ALT and 6ALT, corresponding to ~180 nautical miles. In total ca. 54,000 L of water were analysed for the presence of *V. cholerae* by conventional culture methods[11] (Figs. 1b and S3). A total of 27 presumptive *V. cholerae*

[1]Department of Earth, Environmental and Life Sciences (DISTAV), University of Genoa, Genoa, Italy. [2]The Marine Biological Association the Laboratory, Citadel Hill Plymouth, Devon, UK. [3]Tanzania Fisheries Research Institute (TAFIRI), Kunduchi, Dar es Salaam, Tanzania. [4]Lung Cancer Unit, IRCCS Ospedale Policlinico San Martino, Genova, Italy. [5]Universidad de la Frontera, Temuco, Araucanía, Chile. [6]Department of Genetics and Microbiology, Facultat de Biociéncies, Universitat Autònoma de Barcelona (UAB), Bellaterra, Barcelona, Spain. [7]Maryland Pathogen Research Institute and Center of Bioinformatics and Computational Biology, University of Maryland, College Park, MD, USA. [8]Johns Hopkins Bloomberg School of Public Health, Baltimore, MD, USA. [9]Chemical Oceanography Unit, Institut de Physique (B5A), University of Liège, Liège, Belgium. ✉email: luigi.vezzulli@unige.it

Received: 26 February 2021 Revised: 11 May 2021 Accepted: 25 May 2021
Published online: 07 June 2021

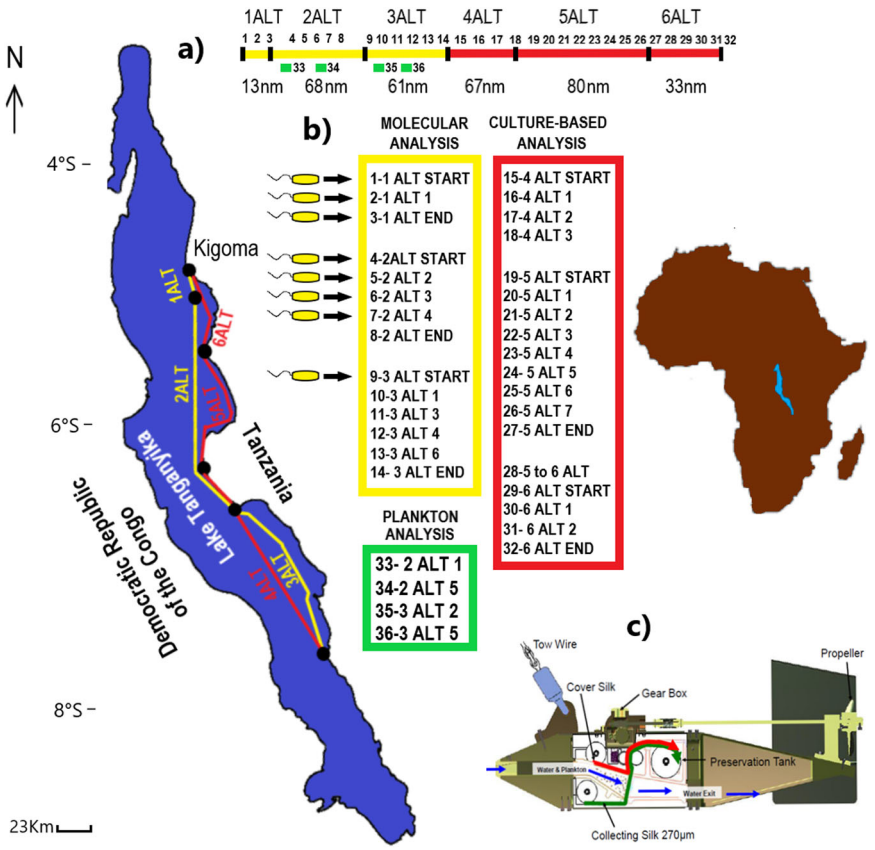

Fig. 1 Continuous Plankton Recorder sampling in Lake Tanganyika. The sampling tows (**a**) and samples (**b**) collected in Lake Tanganyika using the Continuous Plankton Recorder (**c**). A transect of 322 nautical miles (nm) was towed October 22–26, 2018 at the beginning of the short rainy season (cholera season) with a lake water sample of 96,600 L collected and analyzed. Samples name (e.g., 1 ALT START) and number (from 1 to 36) are reported. Yellow color indicates tows and samples analyzed by molecular microbiological analysis. Red color indicates tows and samples analyzed by culture-based microbiological analysis. Green color indicate samples that were analyzed microscopically for plankton according to standard CPR procedures. Black arrows indicate samples where V. cholerae was detected using an ultrasensitive ddPCR protocol.

colonies were isolated on TCBS Cholera medium and screened by *V. cholerae*-specific PCR testing and partial sequencing of the *rpoA* gene[12]. None were confirmed as *V. cholerae* (Table S1).

Since *V. cholerae* cells can be present in a viable but nonculturable (VBNC) state in environmental water, molecular analysis of the *Vibrio* community was performed on fourteen formalin fixed CPR samples collected along the 1ALT, 2ALT and 3ALT transects, corresponding to approximately 142 nautical miles, with ca. 42.000 L lake water sample collected (Fig. 1b, Fig. S4).

To detect *V. cholerae* cells with high efficiency, an ultrasensitive Droplet Digital PCR (ddPCR) protocol was developed showing a high sensitivity and robustness in detecting few genomes of *V. cholerae* (6 on ~13,000 genomes analyzed). Samples scoring positive by ddPCR were further investigated by capillary quantitative PCR assay targeting the *gpbA* (control), *ctxA, tcpA, rfbN, wbfR* genes, specifically to detect toxigenic strains[13].

Results of the PCR analysis showed that *V. cholerae* was present in eight of the fourteen CPR samples collected over a large area of the lake (Fig. 1b) confirming that *V. cholerae* is likely present in the VBNC state in lake water (Table S2). This finding is consistent with previous reports that *V. cholerae* occurs as VBNC cells within the planktonic copepod community[14,15]. Accordingly, calanoid copepods, predominantly *Tropodiaptomus simplex*, accounted for nearly 60% of the lake plankton community (Fig. S5). Nevertheless, toxigenic *V. cholerae* O1 and O139 strains were not found. Toxigenic strains are thus lacking in pelagic waters of the lake or likely represent a very small portion of the *V. cholerae* population[15].

To investigate the bacterial genotypes identified in the samples genome-wide enrichment of *V. cholerae* DNA from selected CPR samples (2ALTstart, 2 ALT2, and 2ALT3) was performed using hybridization-based capture employing target specific biotinylated probes (whole genome enrichment), as previously described[16] (Fig. S4). The applied enrichment was estimated to be ca. 2500 times more effective than shotgun sequencing alone to retrieve and sequence the *V. cholerae* metagenome from complex aquatic samples[16]. By combining the targeted and shotgun metagenomic analyses, a total of 351,222,423 sequence reads (NCBI-SRA accession: PRJNA679303) were produced from the CPR samples, of which 19,886,000 reads specifically mapped against *V. cholerae* N16961 reference sequence. Taxonomic profiling and K-mer analysis of the metagenomic reads against a reference database of 466 *V. cholerae* genome sequences allowed identification of at least 10 genomic signatures belonging to non-epidemic *V. cholerae* strains (Fig. 2b). In addition, phylogenetic analysis of a reconstructed 1,017,718 nucleotide (nt) region of the metagenome-assembled genome (MAG) specifically assigned to *V. cholerae* by taxonomic binning also substantiated the presence of non-toxigenic *V. cholerae* in the samples (Fig. 2a,b), i.e., major virulence genes (e.g., *ctxAB*, *tcpA*) and epidemic markers (O1*rfb*, O139*rfb*) were not detected (Fig. 2c) (see supplementary material for more information on methods and data produced in this study).

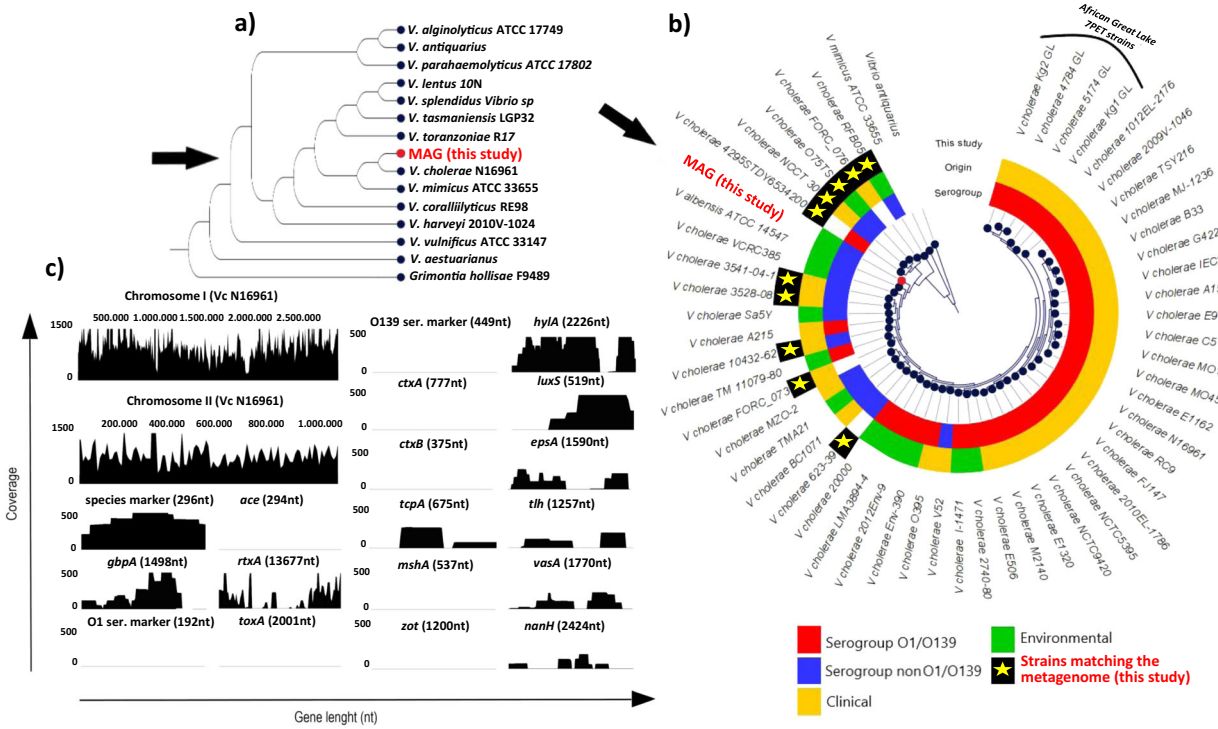

Fig. 2 Metagenomic analysis of CPR samples. Phylogenetic analysis (**a**, **b**) of the reconstructed V. cholerae metagenome-assembled genome (MAG) sequence (indicated by arrows) based on average nucleotide identity with Vibrio reference genomes. Strain genomes (**b**) matching a 351,222,423 read sequence metagenome obtained by targeted and shotgun metagenomic analysis of CPR samples are shown (matches are indicated by yellow stars and defined by taxonomic profiling analysis of the metagenome against 466 V. cholerae genomes). **c** Read mapping analysis of the produced metagenome against the virulence factor database (http://www.mgc.ac.cn/VFs/). Only those reads uniquely mapping at a reference position were included in the analysis and further checked for specificity using BLAST against nucleotide collection (nr/nt) and RefSeq Genome databases.

In conclusion, extensive data from this study do not support the role of Lake Tanganyika pelagic water and plankton as a reservoir of *V. cholerae* strains responsible for epidemic cholera in contrast to what observed in coastal marine water and estuaries in other endemic cholera regions[6]. These findings are nevertheless consistent with studies investigating V. cholerae's reservoirs in other freshwater bodies in Africa[17,18]. Interestingly, *V. cholerae* was detected in pelagic areas of the lake, the epidemiological relevance of which and the potential of emergence of pathogenic strains needs to be assessed[19]. That *V. cholerae* O1 or O139 toxigenic strains were not isolated appear to be linked to the different environmental conditions of Lake Tanganyika water, in particular the very low salinity (<0.4 ‰). Accordingly, a salinity of 25‰ is required for optimum growth of *V. cholerae* O1, higher than required for *V. cholerae* non O1[7]. Ecological niches for toxigenic *V cholerae* may thus only establish in confined local settings i.e. very near to the shore linked to human pollution, coastal upwelling, or episodic planktonic blooms.

REFERENCES

1. Mutreja, A. et al. Evidence for several waves of global transmission in the seventh cholera pandemic. *Nature* **477**, 462–465 (2011).
2. Ali, M., Nelson, A. R., Lopez, A. L. & Sack, D. A. Updated global burden of cholera in endemic countries. *PLoS Negl. Trop. Dis.* **9**, e0003832 (2015).
3. Bompangue, D. N. et al. Lakes as source of cholera outbreaks, Democratic Republic of Congo. *Emerg. Infect. Dis.* **14**, 798–800 (2008).
4. Weill, F. X. et al. Genomic history of the seventh pandemic of cholera in Africa. *Science* **358**, 785–789 (2017).
5. Hounmanou, Y. M. G. et al. Genomic insights into *Vibrio cholerae* O1 responsible for cholera epidemics in Tanzania between 1993 and 2017. *PLoS Neglect Trop. D.* **13**, e0007934 (2019).
6. Colwell, R. R. Global climate and infectious disease: the cholera paradigm. *Science* **274**, 2025–2031 (1996).
7. Singleton, F., Attwell, R., Jangi, M. & Colwell, R. Influence of salinity and organic nutrient concentration on survival and growth of Vibrio choleraein aquatic microcosms. *Appl. Environ. Microbiol.* **43**, 1080–1085 (1982).
8. Kirschner, A. K. T. et al. Rapid growth of planktonic *Vibrio cholerae* non-O1/non-O139 strains in a large alkaline lake in Austria: Dependence on temperature and dissolved organic carbon quality. *Appl. Environ. Microb.* **74**, 2004–2015 (2008).
9. Reid, P. C. et al. The continuous plankton recorder: concepts and history, from Plankton Indicator to undulating recorders. *Prog. Oceanogr.* **57**, 117–173 (2003).
10. Vezzulli, L. et al. Climate influence on *Vibrio* and associated human diseases during the past half-century in the coastal North Atlantic. *Proc. Natl. Acad. Sci. USA.* **113**, E5062–E5071 (2016).
11. Huq, A. et al. Detection, isolation, and identification of *Vibrio cholerae* from the environment. *Curr. Protoc. Microbiol.* https://doi.org/10.1002/9780471729259.mc06a05s26 (2012).
12. Thompson, F. L. et al. Phylogeny and molecular identification of vibrios on the basis of multilocus sequence analysis. *Appl. Environ. Microb.* **71**, 5107–5115 (2005).
13. Vezzulli, L. et al. GbpA as a novel qPCR target for the species-specific detection of *Vibrio cholerae* O1, O139, Non-O1/Non-O139 in environmental, stool, and historical continuous plankton recorder samples. s. *PLoS ONE* **10**, e0123983 (2015).
14. Alam, M. et al. Toxigenic *Vibrio cholerae* in the aquatic environment of Mathbaria, Bangladesh. *Appl. Environ. Microb.* **72**, 2849–2855 (2006).
15. Senoh, M. et al. Isolation of viable but nonculturable *Vibrio cholerae* O1 from environmental water samples in Kolkata, India, in a culturable state. *Microbiol. Open* **3**, 239–246 (2014).
16. Vezzulli, L. et al. Whole-genome enrichment provides deep insights into vibrio cholerae metagenome from an African river. *Microb. Ecol.* **73**, 734–738 (2017).
17. Kaboré, S. et al. Occurrence of Vibrio cholerae in water reservoirs of Burkina Faso. *Res Microbiol* **169**, 1–10 (2018).
18. Bwire, G. et al. Environmental surveillance of *Vibrio cholerae* O1/O139 in the five African Great Lakes and other major surface water sources in Uganda. *Front. Microbiol.* **9**, 1560 (2018).
19. Vezzulli, L., Baker-Austin, C., Kirschner, A., Pruzzo, C. & Martinez-Urtaza, J. Global emergence of environmental non-O1/O139 *Vibrio cholerae* infections linked with climate change: a neglected research field? *Environ. Microbiol.* **22**, 4342–4355 (2020).

ACKNOWLEDGEMENTS

We thank and gratefully acknowledge Dr. George Graham, Dr. David Johns, and Dr. Andrea Di Cesare for their help with CTDs, plankton, and microbiological analysis. All staff at the Tanzania Fisheries Research Institute (TAFIRI), with the help of Bombi Kakogozo (CRH-Congo), Mupape Mukali and the crew of the Mama Benita boat are acknowledged for their most appreciated contribution to the sampling cruise in Lake Tanganyika that made this work possible. The sampling expedition was funded by the National Geographic Society (USA), Grant number: NGS-167R-18.

AUTHOR CONTRIBUTIONS

L.V., P.D.P., L.G., W.W., J.M.U. and C.P. designed research. L.V., C.O., A.B., L.G., I.K., M.B., R.S., S.C., L.L., E.T., A.S., J.M.U. and P.D.P. performed research. L.V., P.D.P., L.G., W.W., J.M.U., R.R.C. and C.P. wrote the paper.

COMPETING INTERESTS

The authors declare no competing interests.

ADDITIONAL INFORMATION

Supplementary information The online version contains supplementary material available at https://doi.org/10.1038/s43705-021-00023-1.

Correspondence and requests for materials should be addressed to L.V.

Supplementary Information for

Aquatic reservoir of *Vibrio cholerae* in an African Great Lake assessed by large scale plankton sampling and ultrasensitive molecular methods

Luigi Vezzulli[1]*, Caterina Oliveri[1], Alessio Borello[1], Lance Gregory[2], Ismael Kimirei[3], Martina Brunetta[2], Rowena Stern[2], Simona Coco[4], Luca Longo[4], Elisa Taviani[1], Andrès Santos[5], Jaime Martinez-Urtaza[6], William Wilson[2], Rita R Colwell[7,8], Carla Pruzzo[1], Pierre-Denis Plisnier[9]

[1]Department of Earth, Environmental and Life Sciences (DISTAV), University of Genoa, Corso Europa 26, 16132 Genoa, Italy.
[2] The Marine Biological Association the Laboratory, Citadel Hill Plymouth, Devon PL1 2PB, UK
[3] Tanzania Fisheries Research Institute (TAFIRI), Ugweno Street, P.O.BOX 9750, Kunduchi, Dar es Salaam, Tanzania
[4] Lung Cancer Unit, IRCCS Ospedale Policlinico San Martino, Largo Rosanna Benzi, 10, 16132 Genova, Italy
[5] Universidad de la Frontera, Francisco Salazar 1145, Temuco, Araucanía, Cile
[6] Department of Genetics and Microbiology, Facultat de Biociéncies, Universitat Autònoma de Barcelona (UAB), 08193 Bellaterra, Barcelona, Spain.
[7]Maryland Pathogen Research Institute and Center of Bioinformatics and Computational Biology, University of Maryland, College Park, MD 20742
[8]Johns Hopkins Bloomberg School of Public Health, Baltimore, MD 21205
[9] Chemical Oceanography Unit, Institut de Physique (B5A), University of Liège, B-4000 Liège, Belgium

* Luigi Vezzulli
Email: luigi.vezzulli@unige.it

This PDF file includes:

Supplementary text
SI References
Supplementary Figures
Supplementary Tables

Supplementary Information Text

Material and Methods

Study area

Lake Tanganyika is situated in the western branch of the East African Rift Valley between the latitudes of 3° 30′ and 8° 50′ S and the longitudes of 29°05′ and 31°15′ E. With an approximate surface area of 32,600 km^2, Lake Tanganyika is the longest (673 km) and second deepest (1470 m) freshwater lake in the world. The volume of the lake waters (18,900 km^3) represents 17% of the Earth's surface free fresh water (1). It is shared by four countries: the Democratic Republic of the Congo (DRC), Tanzania, Zambia and Burundi. Lake Tanganyika is meromictic and oligotrophic (1,2). There is a general clockwise current in the lake (1). Meteorological conditions and particularly wind and heat exchange drive important hydrodynamics in Lake Tanganyika strongly impacting primary production (3). Some years, dense cyanobacteria blooms have been observed (4,5). Coastal planktonic blooms have also been observed from remote sensing (6). The lake waters are alkaline with a surface pH close from 9 (7) and salinity <0.5 ‰. Mean water temperature is 25°C.

In the last decades, climate change including warming and decreased winds have been noted with apparent impacts on the thermic stratification, oxygenation and primary production patterns of Lake Tanganyika (8-10).
Cholera outbreaks have occurred at Lake Tanganyika as in the East African region almost every year since 1977–1978. It has been noted that epidemics often started near the lake shores (11-12). During lull periods, persistence of cholera near the Great African lakes was explained by outbreak dynamics, which suggested a metapopulation pattern, and by endemic foci around the lakes (12). Cross analyses have indicated correlation between phytoplankton blooms and cholera outbreaks at Lake Tanganyika (13). Moore et al. (14) indicate that isolates from the African Great Lakes Region (DRC and Zambia) formed a closely related group. They also found that certain MLVA types collected in the DRC persisted in the country for several years, occasionally giving rise to expansive epidemics.

Large scale Continuous Plankton Recorder sampling in Lake Tanganyika
The CPR is a robust mechanical plankton-sampling device that has been used extensively by large merchant vessels in the oceans across the globe for more than 80 years (15) (Figure S1). For the present study, the CPR was mounted on a small transport vessel Maman Benita KAL 2271 for sampling across Lake Tanganyika. Six tows of 13 (1ALT), 68 (2ALT), 61 (3ALT), 67 (4ALT), 80 (5ALT) and 33 (6ALT) nautical miles were conducted between Kigoma and Kiranda on the eastern part of Lake Tanganyika at the beginning the short rainy season (cholera season) from 22nd to 26th October 2018. 18 standard formalin-fixed CPR samples were collected along routes 1ALT, 2ALT and 3ALT for molecular and plankton analysis. In addition, 18 non-formalin fixed CPR samples (viable-CPR protocol) were collected along routes 4ALT, 5ALT and 6ALT for culture-based microbiological studies. Sampling took place in the surface layer (~7 meters) and plankton was collected on a band of silk (mesh-size 270 µm) moving across the sampling aperture at a rate proportional to the speed of the towing ship. The CPR mesh width of 270 µm retains larger zooplankton with a high efficiency, but also collects small planktonic organisms such as nauplii, microzooplankton and phytoplankton. On return to the laboratory, the silk was removed from the device and divided into individual samples that were stored in sterile plastic boxes with or without 4% buffered formalin. Each sample represented 10 nautical miles of tow ($3m^3$ of filtered seawater) and was previously shown to capture a substantial fraction of the plankton associated *Vibrio* community (16) (Figure S1). A conductivity-temperature depth (CTD) sensor was mounted on the CPR to record surface water temperature and conductivity along the tows (Figure S2).
A key element of the CPR methodology is its ability to obtain large amounts of information from remote areas at low cost by using merchant ships of opportunity freely towing the sampling machine. The costs involved, other than for purchase of equipment, are largely for subsequent laboratory analysis of the bacteria and plankton. All samples collected during the cruise were shipped to Europe and analyzed within 14 days from collection.

***V. cholerae* culture-based studies**
Laboratory tests were initially conducted to assess recovery and culturability of *V. cholerae* strains on CPR silk under conditions mimicking those found in Lake Tanganyika environment (Figure S3). Briefly 1 ml of bacterial suspension corresponding to 10^6 cells of *V. cholerae* N16961 (ATCC 39315) strain were inoculated on $1cm^2$ sterilized CPR silk section. Silks were incubated in 5ml Eppendorf tubes containing 3ml of Artificial Seawater (ASW) or Phosphate-buffered saline (PBS) or Alkaline peptone water (APW) or unsterilized Lake water (LW) at different temperatures (+4°C and room temperature). Each condition was run in triplicate. Culturability was then assessed by conventional APW enrichment and Thiosulfate-citrate-bile salts-sucrose agar (TCBS) plating of the bacterial suspension at different time intervals of 7, 15, 28, 365 and 730 days, respectively (results showed that V. cholerae could be cultivated up to 12 weeks at room temperature on the CPR silk under all tested conditions, Figure S3).
Isolation of *V. cholerae* from CPR samples collected by the viable-CPR protocol (no formalin fixation of the CPR samples) was accomplished by employing APW enrichment of the silk (static incubation for 16h at 30 to 35°C overnight) followed by selective culture on Thiosulfate-citrate-bile salts-sucrose agar (TCBS) (incubation at 30°C to 35°C for 24 ± 2 h) as described in Huq *et al*. (17).

The silk used for enrichment corresponds to ca 3000 L of filtered lake water. Colonies grown onto TCBS agar were inspected and sucrose fermenting (yellow) colonies that have different sizes and morphologies were picked off the agar and isolated as pure cultures onto the same medium. A PCR assay (18) and partial sequencing of the *rpoA* gene (19) was used to determine if each colony belonged to the species *V. cholerae.* Table S1.

Nucleic acid extraction

For each CPR sample, the filtering silk was cut into strip sections (1x10 cm) and DNA was extracted and purified from each section using the methodology described in Vezzulli *et al*. (16, 18). The amount of DNA extracted from the CPR samples was determined fluorimetrically with PicoGreen using a NanoDrop® ND-3300 fluorometer (NanoDrop Technologies, Wilmington, DE, USA). Sizing of genomic DNA was also conducted in an Agilent Bioanalyzer 2100 (Agilent, Palo Alto, CA) using the High Sensitivity DNA kit (Agilent Technologies).

Droplet Digital Polymerase Chain Reaction (ddPCR) studies

Preliminary screening of CPR samples was carried out by ultrasensitive QX200 Droplet Digital PCR System (Bio-Rad Laboratories, Hercules, CA, USA) ddPCR to target the *V. cholerae* O1, O139, Non-O1, and Non-O139 specific *gbpA* marker gene (18). ddPCR is a third generation of PCR that allows absolute quantification of DNA copies by partitioning DNA single molecule into approximately 20,000 droplets based on the Poisson distribution, and then counting the number of positive and negative droplets (20). In order to estimate the ddPCR limit of detection (LoD) for detecting *V. cholerae* genomes into a sample, we firstly determined the genome mass of the pathogen using the formula m = (n) (1.096 x 10E-21 g/bp) where “m” is the genome mass in grams (1g =1E+12 pg) and n is the genome size in base pairs (bp). Therefore, since *V. cholerae* N16961 reference genome is made up of 4,033,464 bp, one haploid genome weighs 0.004421 pg. Then, we used this value to define the minimum amount of *V. cholerae* DNA that could be detected. Specifically, we made 10-fold serial dilutions starting from 0.06 ng containing only *V. cholerae* DNA to 0.00006 ng of V. *cholerae* DNA mixed with a DNA from *V. aestuarianus*, a phylogenetically close bacteria with a comparable genome size (4,837,307 bp). Briefly, DNA was mixed with Supermix no d-UTP (Bio-Rad Laboratories) and 0.4 µM primers and 0.2 µM FAM-labeled TaqMan Probe (1) in a final volume of 22 µl. Then, PCR mix was partitioned in at least 10,000 droplets by droplet generator (Bio-Rad Laboratories) and amplified in a Mastercycler nexus gradient thermal cycler (Eppendorf, Hamburg, Germany). The PCR program was as follows: enzyme activation at 95°C for 10 min followed by 40 cycles of denaturation at 94°C for 30 sec and annealing/extension at 57°C for 1 min followed by a final step of enzyme deactivation at 98°C for 10 min. Finally, the droplets were acquired into the droplet reader (Bio-Rad Laboratories), and data analyzed using the QuantaSoft software (Bio-Rad Laboratories). Notably, at a quantity of 0.00006 ng we were able to detect a mean of 6 positive droplets (two replicates) of *V. cholerae* DNA, reaching a LoD of six haploid genomes on a total of ~13,000 analyzed. Since the DNA composition in our CPR samples was unknown, we assumed that each sample contained a mix of genomes from the major subgroups of life and viruses (average genome sizes: 3,95E-02 Mb viruses; 3,214 Mb prokaryotes; 31,874 Mb fungi; 59,529 Mb unicellular eukaryotes; 855,59 Mb algae; 4456 Mb animals; 5958 Mb plants) (21) with a theoretical mean genome size of approximately 1,623 Mb (1 genome ~ 1.78 pg). In light of these considerations we used an input of 10 ng of DNA for the ddPCR, running these samples in triplicate (total DNA: 30 ng) to reach an ideal sensitivity of approximately 3 *VC* positive droplets on ~17,000 analyzed genomes. Table S2.

Capillary quantitative Real-Time PCR (qPCR) studies

CPR samples that scored positive to ddPCR were further investigated by quantitative PCR using assays targeting *gbpA* (control), *ctxA, tcpA, rfbN and wbfR* genes as described in Vezzulli *et al.* (22). Briefly, with the exception of the *gbpA* protocol (18), the LightCycler-FastStart DNA Master SYBR Green I kit (Thermofisher Scientific) optimized for use with glass capillaries and containing a hot start polymerase was used as the master mix base for all reactions. Each reaction mixture contained 5.0 mmol of MgCl2 and 500 nmol of each primer in a final volume of 20 ml. The PCR programme used was as follows: initial denaturation at 95°C for 10 min, followed by 45 cycles of denaturation at 95°C for 10 sec, annealing at 59°C for 20 sec and elongation at 72°C for 4 sec,

followed by final elongation at 72°C for 10 min. PCR runs were analyzed directly in the LightCycler using melt-curve analysis and the software provided with the instrument. The correct size of the products was further confirmed by agarose gel electrophoresis. Presence of *V. cholerae* toxigenic strains was also evaluated by Real-Time PCR using the commercial VibChoTx MONODOSE dtec-qPCR Test (Genetic PCR Solutions™, Alicante, Spain). Table S2.

Metagenomic studies

Selected CPR samples (2ALTstart, 2 ALT2 and 2ALT3) were analyzed by shotgun metagenomic and targeted metagenomic techniques (Whole Genome Enrichment) following protocols described in Vezzulli *et al* (22) (Figure S4). Briefly, genomic DNA extracted from CPR samples was used for the production of an indexed library for next-generation sequencing on the Illumina platform (Illumina, Inc) using the KAPA HyperPlus Kit for Illumina (Roche Diagnostics, Mannheim, Germany). About 200 ng of the produced shotgun metagenomic library was used for target DNA capturing using biotinylated RNA baits (on average >100-mer). Baits were produced using the MYcroarray WGE proprietary technology (MYcroarray, Ann Arbor, MI, USA) and made out from genomic DNA extracted from different *V. cholerae* strains representative of the main pathotypes: *V. cholerae* N16961 (serogroup O1, biotype El Tor), *V. cholerae* O395 (serogroup O1, biotype classical), *V. cholerae* MO10 (serogroup O139) and *V. cholerae* TMA21 (serogroup non O1/O139). The DNA library was heat-denatured and hybridized to the RNA baits under stringent conditions. Hybridization was carried out at 65°C for 36 h. After hybridization, the biotinylated baits hybridized to captured material were pulled out of the solution with streptavidin-coated magnetic beads and the captured genomic DNA was released by chemical degradation of the RNA baits. Enriched libraries were amplified and sequenced by STAB VIDA, LDA company (Caparica, Portugal) on a MiSeq Illumina™ platform (V3 flow cell, 600 cycles, 25M reads 250bp pair ends). Shotgun metagenomic libraries (not enriched libraries) were also sequenced on a Illumina® HiSeq®2500 platform (PE150 on one lane with an output of ~600M reads). Sequence reads data were archived at NCBI sequence read archive (SRA) with Accession Number PRJNA679303.

Bioinformatics analysis

Pair-read sequences from both shotgun and targeted metagenomic analyses were quality trimmed to a minimum length (75bp), with quality scores (quality nucleotide limit 0.05 based on Phred scale) and the presence of ambiguous nucleotides (n=2). Sequencing adapters were also removed. Trimmed reads were mapped against reference *V. cholerae* N16961 sequence (Accession: AE003852/AE003853) using the mapping tool of the CLC Genomics Workbench (version 20.0.4) (QIAGEN, CLC Bio, Aarthas, Denmark). A length fraction of 0.5 and similarity fraction of 0.8 were employed in the analysis (e.g. 50% minimum read length matching the reference at >80% nucleotide identity). Masking of 16SrDNA encoding genes was applied. Mapped reads-pairs obtained from shotgun and targeted metagenomic analyses for all samples were then extracted and pooled for subsequent bioinformatic analysis. Taxonomic Profiling and Find Best Matches with K-mer Spectra (Microbial Genomics Module; CLC genomics workbench) against a reference database of 466 complete *V. cholerae* genome sequences were applied for strain identification (*V.cholerae* sequences used in this study are listed in a separate excel table as supplementary). Metagenome assembly was conducted using metaSPADES (version 3.14.1) (23) and metagenome-assembled genomes (MAGs) reconstruction was carried out using CONCOCT (version 1.1.0) (24). MAGs were then refined using the CheckM (v1.1.3) 'merge' and 'outliers' tools which merge MAGs with complementary sets of marker genes to improve completeness and remove contigs from MAGs which appear to be outliers (contaminants) relative to reference GC and tetranucleotide distributions (25). MAG's taxonomic assignment to *V. cholerae* N16961 reference sequence was determined by using Kraken2 (26).

Phylogenetic analysis was performed by annotating contigs based on core genes and assigning a mass-probability to their classification with Phylosift (27). A phylogenetic tree based on alignment of the conserved codons among the strains was created with Fastree (28). Whole genome alignment and calculation of average nucleotide identity (ANI) of the MAG region with *V. cholerae* reference genomes were also applied and a tree was created through a neighbor joining clustering method with the CLC software.

Assessment of virulence genes and epidemic markers was performed by mapping reads against selected nucleotide sequences: *V. cholerae* phylogenetic marker (VC_A0047), *ace* (VFG000110), *gbpA* (VFG043577), *rtxA* (VFG000983), O1 marker region (*rfb*_region AE003852), *toxA* (VFG043673), O139 marker region (AAKF03000001), *hylA* (VFG007038), *ctxA* (VFG000107), *luxS* (VFG018241), *ctxB* (VFG000108), *epsA* (VFG040945), *tcpA* (VFG000091), *tlh* (VFG007033), *mshA* (VFG006986), *vasA* (VFG002078), *zot* (VFG000109), *nanH* (VFG001117) retrieved from the virulence factor database (29) using the mapping tool of the CLC Genomics Workbench with same settings as described above. Specificity of reads matching reference sequences was assessed by running Blastn software (version 2.10.1+; http://blast.ncbi.nlm.nih.gov/Blast.cgi) on generated consensus sequences against the nucleotide collection (nr/nt) and RefSeq Genome (refseq_genomes) database.

Sample contamination

To avoid laboratory contamination of treated samples all the analyses including DNA extraction, DNA amplification and NGS library preparations were carried out in a separate laboratory (non-aquatic/non-microbiological laboratory) using a dedicated set of pipettes, reagents, and consumables.

Plankton analysis

Qualitative assessment of plankton organisms in CPR samples (2ALT1, 2 ALT5, 3ALT2, 3ALT5) was analyzed microscopically according to standard CPR procedures as described in Reid *et al.* (30) (Figure S5).

SI References

1. Coulter, G.W. (eds) *Lake Tanganyika and its life* (Natural History Museum Publications & Oxford University Press, 1991).
2. Beauchamp R.S.A. Hydrology of Lake Tanganyika. *Int. Rev. Gesamten. Hydrobiol.* **39**, 316-353 (1939)
3. Langenberg, V.T., Sarvala, J. & Roijackers R. Effect of Wind Induced Water Movements on Nutrients, Chlorophyll-a, and Primary Production in Lake Tanganyika. *Aquatic Ecosystem Health & Management.* **6**(3), 279-288 (2003).
4. Symoens, J.J. Observation d'une fleur d'eau à Cyanophycées au Lac Tanganyika. *Folia Scient. Afr. Centr.* **1** (3): 17 (1955).
5. Salonen, K. et al. Phytoplankton in Lake Tanganyika – vertical and horizontal distribution of in vivo fluorescence. *Hydrobiologia* **407**, 89–103 (1999)
6. Plisnier, P.D. et al. Limnological variability and pelagic fish abundance (Stolothrissa tanganicae and Lates stappersii) in Lake Tanganyika. *Hydrobiologia* **625**(1), 117-134 (2009)
7. Plisnier, P.D. et al. Limnological annual cycle inferred from physical-chemical fluctuations at three stations of Lake Tanganyika. *Hydrobiologia*, 407, 45-58 (1999).
8. Plisnier, P.D. Recent climate and limnology changes in lake Tanganyika. *Verh. Internat. Verein. Limnol.* **27**, 2670-2673 (2000).
9. O'Reilly C.M., Alin, S.R., Plisnier, P.D., Cohen, A.S. & and McKee, B.A. Climate change decreases aquatic ecosystem productivity of Lake Tanganyika, Africa. *Nature* **424**, 766-768 (2003).
10. Verburg, P., Hecky, R.E. & Kling, H. Ecological consequences of a century of warming in Lake Tanganyika. *Science* **301**, 505-507 (2003).
11. Birmingham, M. et al. Epidemic cholera in Burundi: patterns of transmission in the Great Rift Valley Lake region. *The Lancet* **349**(9057), 981-985 (1997).
12. Bompangue DN. et al. Dynamics of Cholera Outbreaks in Great Lakes Region of Africa, 1978–2008. Emerg. Infect. Dis. **17**(11), 2026-2034 (2011).
13. Plisnier, P.D. et al. Cholera outbreaks at Lake Tanganyika induced by Climate Change? - "CHOLTIC". Final Report. Brussels: Belgian Science Policy 117 p. (Research Programme Science for a Sustainable Development, 2015)

14. Moore, S. et al. Relationship between distinct African cholera epidemics revealed via MLVA haplotyping of 337 Vibrio cholerae isolates. *PLoS Negl. Trop. Dis.* **9**(6), e0003817 (2015)
15. Richardson, A.J. et al. Using continuous plankton recorder data. *Prog Oceanogr* **68**, 27–74 (2006).
16. Vezzulli, L. et al. Climate influence on Vibrio and associated human diseases during the past half-century in the coastal North Atlantic. *Proc. Natl. Acad. Sci. USA 2016* **113**, E5062–E5071 (2016).
17. Huq, A. et al. Detection, isolation, and identification of *Vibrio cholerae* from the environment. *Curr. Protoc. Microbiol.* CHAPTER: Unit6A.5. doi:10.1002/9780471729259.mc06a05s26 (2012).
18. Vezzulli, L. et al. GbpA as a novel qPCR target for the species-specific detection of *Vibrio cholerae* O1, O139, Non-O1/Non-O139 in environmental, stool, and historical continuous plankton recorder samples. s. *PLoS ONE* **10**(4), e0123983. doi:10.1371/journal.pone.0123983 (2015)
19. Thompson, F.L. et al. Phylogeny and molecular identification of vibrios on the basis of multilocus sequence analysis. *Appl. Environ. Microb.* 71: 5107–5115 (2005).
20. Hindson, B.J. et al. High-throughput droplet digital PCR system for absolute quantitation of DNA copy number. *Anal. Chem.* **83**, 8604–8610 (2011).
21. Landenmark, H.K.E., Forgan, D.H. & Cockell, C.S. An estimate of the total DNA in the biosphere. *PLoS Biol*. **13**, 1–10 (2015)
22. Vezzulli, L. et al. Whole-Genome Enrichment Provides Deep Insights into Vibrio cholerae Metagenome from an African River. *Microb Ecol.* **73**, 734–738 (2017).
23. Nurk, S., Meleshko, D., Korobeynikov, A. & Pevzner, P.A. MetaSPAdes: A new versatile metagenomic assembler. *Genome Res.* **27**: 824–834 (2017).
24. Alneberg, J. et al. Binning metagenomic contigs by coverage and composition. *Nat Methods* **11**, 1144–1146 (2014).
25. Parks, D.H. et al. CheckM: Assessing the quality of microbial genomes recovered from isolates, single cells, and metagenomes. Genome Res. **25**: 1043–1055 (2015).
26. Wood, D.E., Lu, J. & Langmead, B. Improved metagenomic analysis with Kraken 2. *Genome Biol.* **20,** 257 (2019).
27. Darling, A.E. PhyloSift: Phylogenetic analysis of genomes and metagenomes. PeerJ 2:e243 https://doi.org/10.7717/peerj.243 (2014)
28. Price, M.N., Dehal, P.S. & Arkin, A.P. FastTree 2 - Approximately maximum-likelihood trees for large alignments. PLoS ONE 5(3): e9490. https://doi.org/10.1371/journal.pone.0009490 (2010)
29. Chen, L., Xiong, Z., Sun, L., Yang, J. & Jin, Q. VFDB 2012 update: Toward the genetic diversity and molecular evolution of bacterial virulence factors. *Nucleic Acids Res.* **40**, D641–D645 (2012).
30. Reid, P.C. et al. The Continuous Plankton Recorder: Concepts and history, from Plankton Indicator to undulating recorders. *Progr Oceanogr.* **57**, 117–173 (2003).

Figure S1. The Continuous Plankton Recorder (CPR)

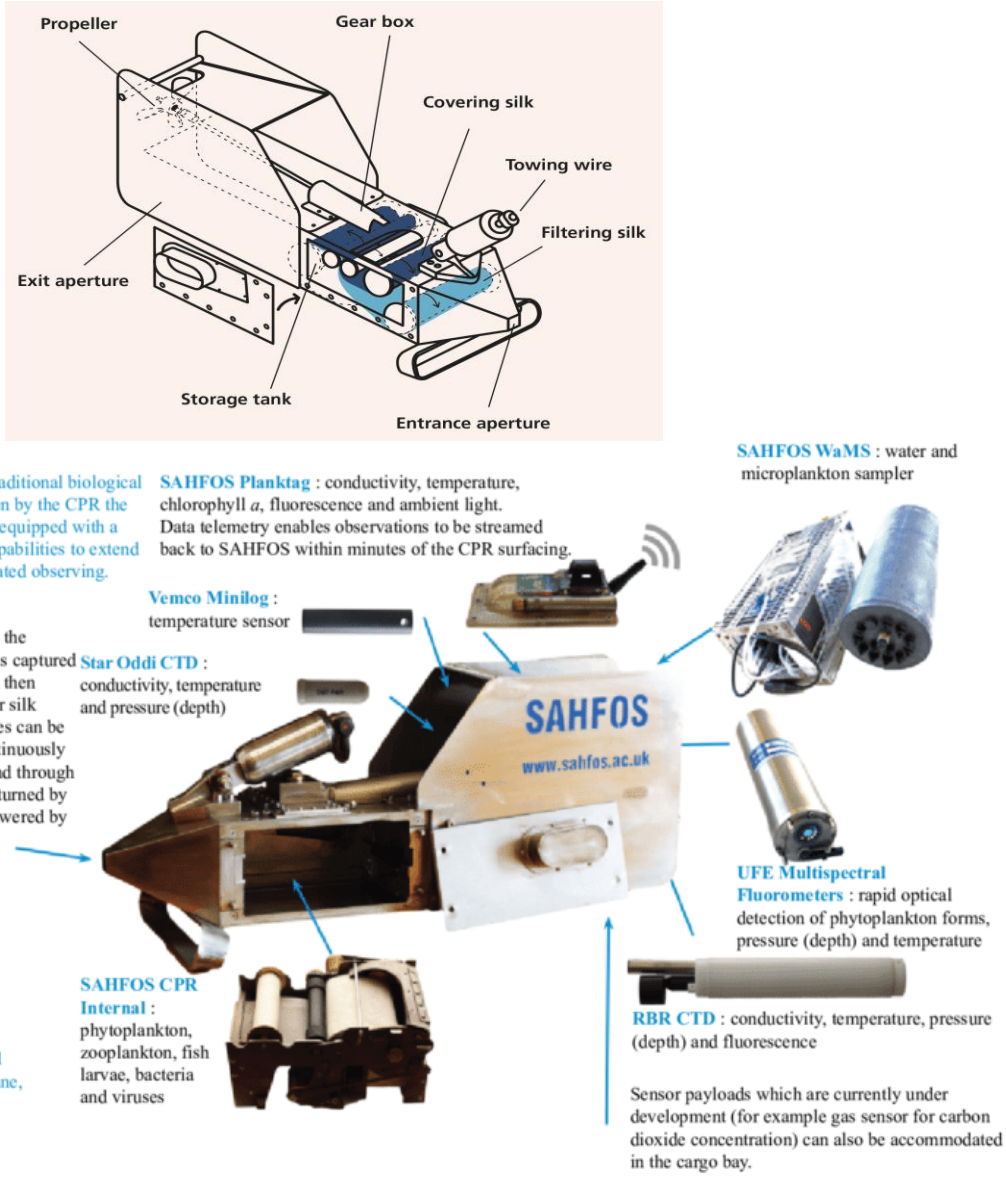

Figure S2. Water temperature profile measured by a CTD mounted on the CPR during the cruise.

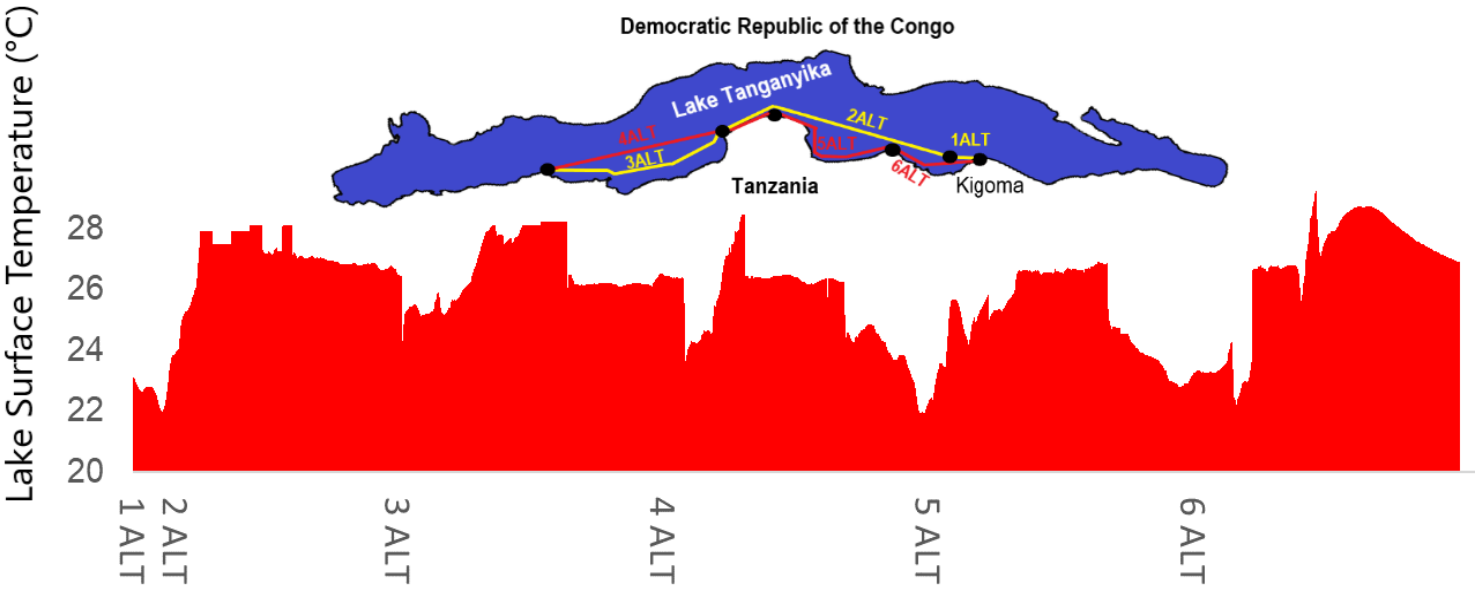

Figure S3 *V. cholerae* culturability test in CPR samples.

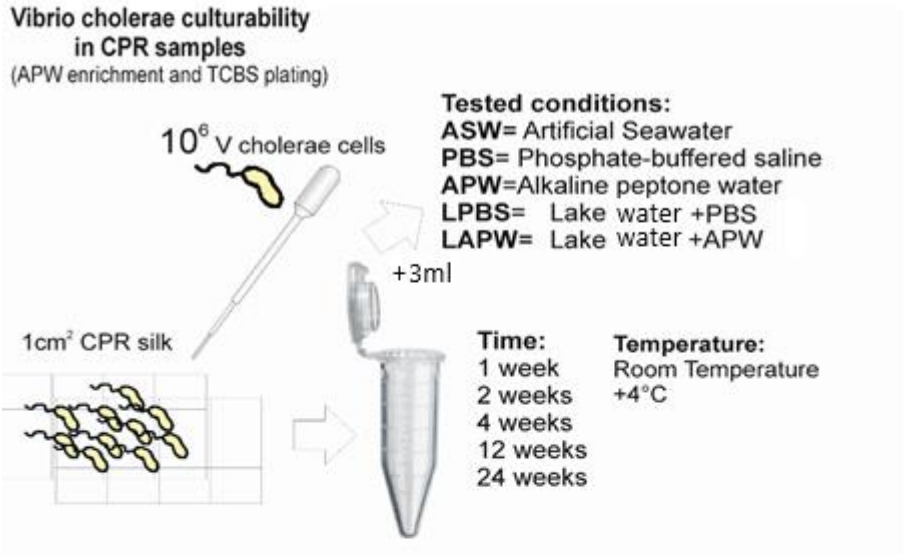

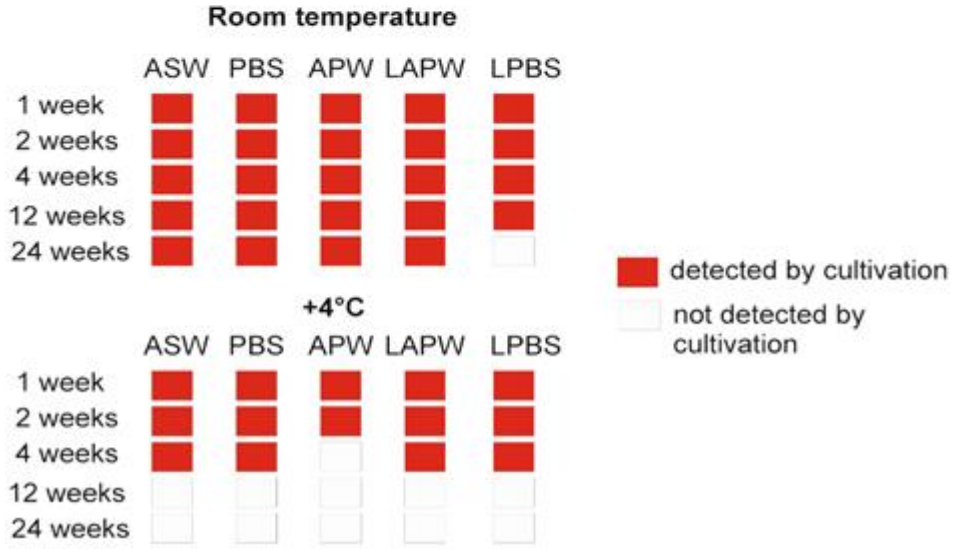

Figure S4. Metagenomic analysis workflow applied on CPR samples.

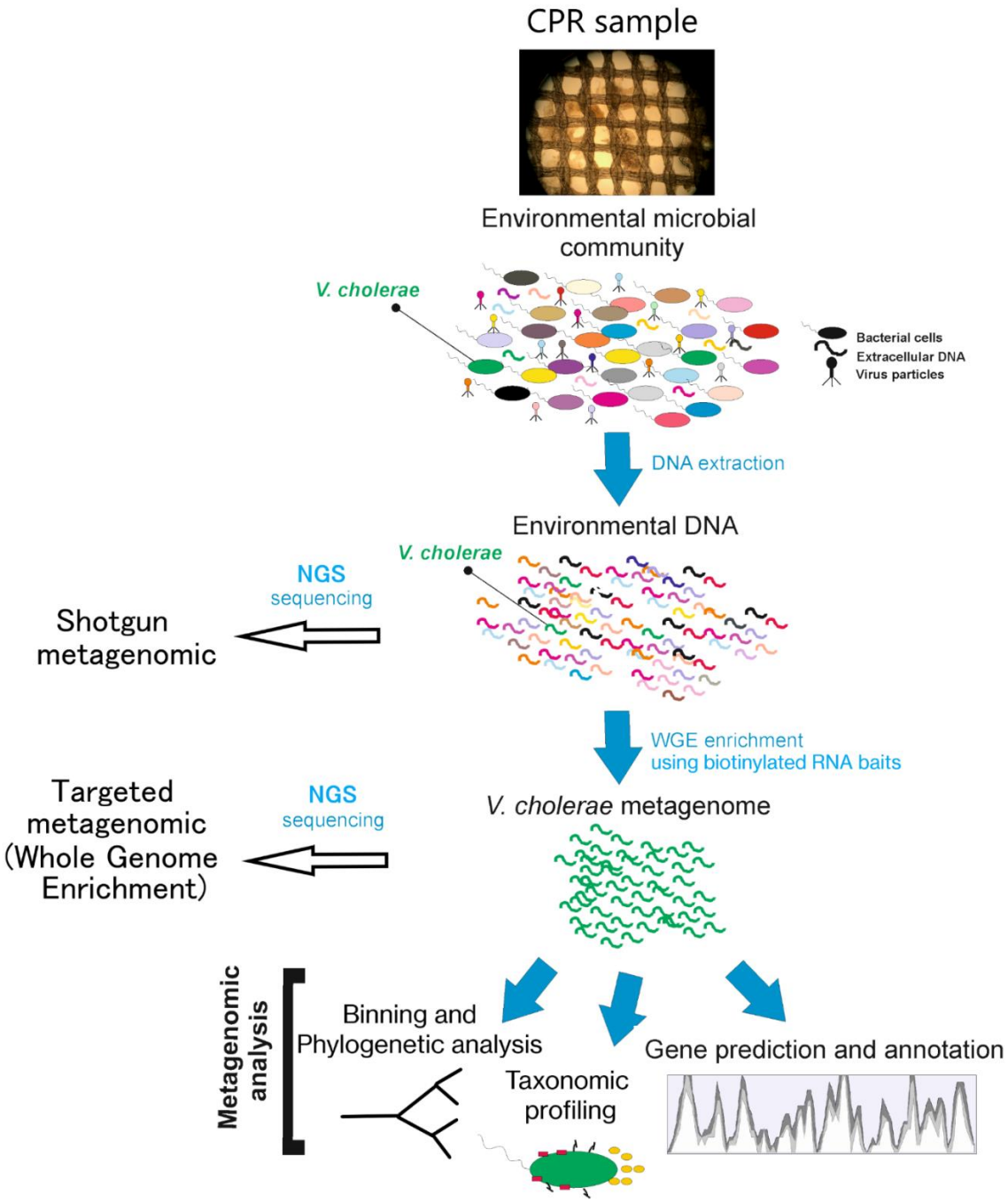

Figure S5. Average plankton composition of the collected CPR samples along routes 2ALT and 3ALT.

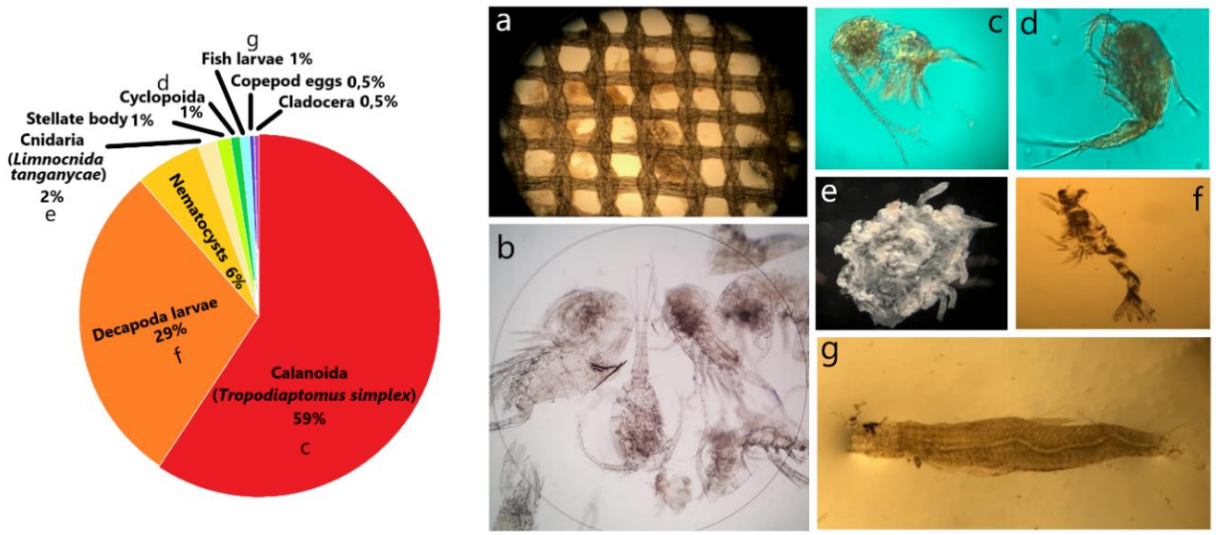

Table S1. Results of *V. cholerae* cultivation in APW and TCBS media from CPR samples collected in Lake Tanganyika

APW culture		TCBS culture					
Sample	V. cholerae PCR test	tow	morphotype	morphology	V. cholerae PCR test	rpoA sequencing Blast Best hit	rpoA sequencing Identity
4 ALT START	negative	4 ALT	1	green	negative	Leclercia sp.	100%
4 ALT 1	negative		2	small yellow	negative	Enterobacter hormaechei	100%
4 ALT 2	negative		3	yellow	negative	Enterobacter hormaechei	100%
4 ALT 3	negative						
5 ALT START	negative	5 ALT	4	yellow	negative	Aeromonas media	99,60%
5 ALT 1	negative		5	small yellow	negative	Enterobacter hormaechei	100%
5 ALT 2	negative		6	star yellow	negative	Enterobacter hormaechei	100%
5 ALT 3	negative		7	yellow with dark center	negative	Enterobacter hormaechei	100%
5 ALT 4	negative		8	yellow with salmon center	negative	Aeromonas media	99,40%
5 ALT 5	negative		9	star yellow	negative	Aeromonas hydrophila	98,50%
5 ALT 6	negative		10	salmon	negative	Aeromonas media	99,40%
5 ALT 7	negative		11	green	negative	Aeromonas veronii	98,10%
5 ALT END	negative		12	star yellow	negative	Enterobacter hormaechei	99,90%
			13	transparent yellow	negative	Enterobacter hormaechei	99,90%
			14	yellow with dark center	negative	Enterobacter hormaechei	99,70%
5 to 6 ALT	negative	6 ALT	15	star yellow	negative	Enterobacter hormaechei	99,60%
6 ALT START	negative		16	yellow with brown center	negative	Vibrio mimicus	99,80%
6 ALT 1	negative		17	yellow with dark center	negative	Vibrio mimicus	99,70%
6 ALT 2	negative		18	semitransparent yellow	negative	Enterobacter hormaechei	99,80%
6 ALT END	negative		19	yellow with salmon center	negative	Aeromonas media	99,60%
			20	yellow with dark center	negative	Enterobacter hormaechei	99,90%
			21	yellow with salmon center	negative	Aeromonas media	99,30%
			22	green	negative	Enterobacter cloacae	100%
			23	yellow	negative	Enterobacter hormaechei	99,60%
			24	yellow	negative	Enterobacter cloacae complex sp.	99,90%
			25	big yellow	negative	Enterobacter hormaechei	100%
			26	green	negative	Enterobacter cloacae complex sp.	99,90%
			27	salmon	negative	Vibrio mimicus	99,60%

Table S2 . Results of PCR and ddPCR test targeting *V. cholerae* in CPR samples collected in Lake Tanganyika (GU/rx=Genomic Unit/reaction)

Sample (positive samples)	DNA extraction (ng/ul)	Analysed DNA (ng)	n° replicate	V. cholerae qPCR (GU/rx)	Toxigenic V. cholerae qPCR (GU/rx)	V. cholerae ddPCR
1 ALT START	0,4	10	3	78,6±7,6	negative	positive
1 ALT 1	0,4	10	3	6,0±0,5	negative	positive
1 ALT END	1	10	3	5,6±0,4	negative	positive
2 ALT START	0,3	10	3	19,2±0,8	negative	positive
2 ALT 2	26,47	10	3	23,1±1,6	negative	positive
2 ALT 3	25,5	10	3	99,9±9	negative	positive
2 ALT 4	17,15	10	3	22,5±2,6	negative	positive
2 ALT END	27,42	10	3	negative	negative	negative
3 ALT START	0,5	10	3	negative	negative	positive
3 ALT 1	2,25	10	3	negative	negative	negative
3 ALT 3	5,2	10	3	negative	negative	negative
3 ALT 4	4,6	10	3	negative	negative	negative
3 ALT 6	5,33	10	3	negative	negative	negative
3 ALT END	1,55	10	3	negative	negative	negative
Control	0	10	3	negative	negative	negative